PREMIXED PREVAPORIZED COMBUSTOR TECHNOLOGY FORUM

JANUARY 9-10, 1979

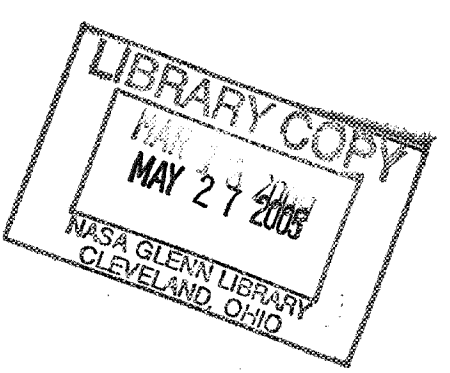

NASA
National Aeronautics and
Space Administration
Lewis Research Center
Cleveland, Ohio 44135

AGENDA

Premixed-Prevaporized Combustor Technology Forum

NASA- Lewis Research Center

Cleveland, Ohio

January 9 - 10, 1979

9 Jan 79 Tuesday AM		
8:00	Official Registration	
8:45	Welcome	Mr. W. Stewart, Director of Aeronautics, NASA - Lewis Research Center
9:00	Introductory Remarks	Dr. E. Mularz, Forum Chairman
9:15	Turbulence Characteristics of Compressor Discharge Flows	Mr. H. Grant Pratt & Whitney Aircraft
9:45	Turbulence Measurements in the Compressor Exit Flow of a General Electric CF6-50 Engine	Mr. J. Taylor General Electric
10:15	Beverage Break	
10:30	Fuel Spray Data with LDV	Dr. D. Rohy Solar, I. H. Corp.
11:00	Modeling of Premixing-Prevaporizing Fuel/Air Mixing Passages	Dr. O. Anderson United Technologies Research Center
11:30	Effect of Fuel Sprays on Emissions	Prof. A. Nichols U. of Michigan
12:00	Lunch	
Tuesday PM		
1:00	Performance of a Multiple Venturi Fuel-Air Preparation System	Mr. R. Tacina NASA LeRC
1:30	Autoignition of Fuels	Dr. L. Spadaccini United Technologies Research Center
2:00	Emissions Measurements for a Lean Premixed Propane/Air System at Pressures Up to 30 Atmospheres	Mr. G. Roffe General Applied Science Labs., Inc.

Tuesday PM (Conti.)

2:30	Beverage Break	
2:45	Effect of Degree of Fuel Vaporization Upon Emission for a Premixed-Prevaporized Combustor System	Dr. L. Cooper NASA LeRC
3:10	Effect of Fuel/Air Nonuniformity On Nitric Oxide Emissions	Ms. V. Lyons NASA LeRC
3:30	Effect of Flameholder Geometry on Emissions & Performance	Dr. K. Venkataramani General Applied Science Labs., Inc.
4:00	Effects of Flameholder Blockage on the Emissions and Performance of Lean Premixed-Prevaporized Combustors	Mr. R. Duerr NASA LeRC
4:30	Adjourn	
5:30	Social Hour (Cash Bar) and Dinner	

10 Jan 79
Wednesday AM

8:15	Reconvene	Dr. E. Mularz, Forum Chairman
8:30	Lean Stability Augmentation Study	Dr. J. McVey United Technologies Research Center
9:00	Modelling Turbulent Flame Ignition and Blowout	Dr. K. Radhakrishnan Massachusetts Institute of Technology
9:30	Stabilization of Premixed Combustors	Prof. A. Oppenheim U. of California (Berkeley)
10:00	Beverage Break	
10:15	Effect of Swirl on Premixed Combustion	Prof. F. Gouldin Cornell University
10:45	Advanced Low Emissions Catalytic Combustor Program	Mr. W. Dodds General Electric
11:15	Advanced Low Emissions Catalytic Combustor Program	Dr. G. Sturgess Pratt & Whitney Aircraft
11:45	Lunch	

Wednesday PM

1:00	Lean, Premixed Prevaporized Combustor Conceptual Design Study	Mr. A. Fiorentino Pratt & Whitney Aircraft
1:30	Lean, Premixed Prevaporized Combustor Design Study	Mr. E. Ekstedt General Electric
2:00	Closing Remarks	Dr. E. Mularz, Forum Chairman
2:15	Dismissal	

Introduction to the Premixed Prevaporized Combustor Technology Forum

by E. J. Mularz

Propulsion Lab., USARTL (AVRADCOM),

and

NASA Lewis Research Center

Cleveland, Ohio

An objective of the meeting (Figure 1) is to acquaint you with programs which are being sponsored by NASA to provide basic information required for demonstration of lean, premixed, prevaporized (LPP) combustors for aircraft gas turbine engine application. This meeting also provides an opportunity to discuss results of the programs among all the Forum participants.

Most of the programs which will be discussed during this meeting are part of the first phase of the Stratospheric Cruise Emission Reduction (SCERP) Program (Figure 2). This NASA program was created to evolve and demonstrate a combustion system for aircraft gas turbine application which achieves superior performance, promises good durability, and exhibits environmentally acceptable pollutant emissions. The LPP combustion technique has the potential to achieve these goals and to produce especially low NO_x emissions at engine cruise with minimum or no adverse effect on engine weight and complexity.

Since 1976 Lewis has been conducting studies (Figure 3) to increase our understanding of various aspects of LPP combustion through Phase I of the SCERP program. This forum will discuss the major results to date. Phase II of the SCERP Program will screen several candidate combustor concepts in test rings. Phase III will then refine the most promising concepts of Phase II. Finally, Phase IV will be an engine verification of the evolved combustor-control system from Phase III. These efforts will be conducted over several years with a schedule as shown in Figure 4.

Some of the expected results and benefits of the SCERP Program (Figure 5) are an improvement in the turbine nozzle temperature distribution, an increase in combustor liner life, and a combustion system which meets the current 1981 EPA Standards, and achieves very low NO_x emissions at engine cruise. This advanced technology could be applied to future aircraft engines for improved performance and durability; and if aircraft emissions are found to pose a threat to the composition of the earth's stratosphere, this technology could significantly reduce this threat.

All the activities under Phase I of the SCERP Program are shown in Figure 6. The programs that will be discussed at this meeting are so denoted by an asterisk. For your information a list of reports that have been published thus far are shown in Figure 7.

Another program which will be discussed at this meeting because of its similar requirements for basic information in premixed fuel and air systems is the NASA-sponsored Advanced Low Emissions Catalytic Combustor Program. The objective of this program (Figure 8) is to evolve the technology required for incorporating catalytic combustors into aircarft gas-turbine engines. Expected results of this program are lower NO_x emission levels and improved combustion stability while retaining customary safety and endurance qualities of current aircraft engines.

The schedule of the Advanced Low Emissions Catalytic Combustor Program is shown in Figure 9. The design studies are currently in progress and will be followed by combustor concept screening tests and combustor refinement of the most promising concepts. Tests will be conducted only in test rigs and not in an engine.

Other programs which will be discussed during this meeting are shown in Figure 10. Although these four programs are not directly associated with the Catalytic Combustor or SCERP programs, they all involve premixing fuel and air systems. The first three programs are NASA grants for basic research on combustion phenomena. The fourth program is an in-house activity here at Lewis to design improved fuel injectors for application to the automotive gas turbine.

FORUM OBJECTIVES

TO PRESENT AN OVERVIEW OF PROGRAMS WHICH ARE BEING SPONSORED BY NASA TO PROVIDE BASIC INFORMATION REQUIRED FOR DEMONSTRATION OF LEAN, PREMIXED, PREVAPORIZED (LPP) COMBUSTORS FOR GAS TURBINE ENGINE APPLICATION, &

TO PROVIDE AN ARENA FOR DISCUSSION OF RESULTS OF THESE PROGRAMS.

CS-78-3678

FIGURE 1

STRATOSPHERIC CRUISE EMISSION REDUCTION (SCERP) PROGRAM

OBJECTIVE:

TO EVOLVE & DEMONSTRATE A COMBUSTION SYSTEM WHICH ACHIEVES SUPERIOR PERFORMANCE, SHOWS PROMISE FOR GOOD DURABILITY, & EXHIBITS ENVIRONMENTALLY ACCEPTABLE POLLUTANT EMISSIONS, ESPECIALLY LOW NO_x EMISSIONS AT CRUISE, WITH MIN. ADVERSE EFFECT ON WEIGHT & COMPLEXITY.

MAJOR PROGRAM FOCUS:

LEAN, PREMIXED, PREVAPORIZED (LPP) COMBUSTION.

CS-78-3683

FIGURE 2

SCERP PROGRAM

APPROACH:

ESTABLISH A DATA BASE OF FUNDAMENTAL INFORMATION ON LEAN PREMIXED-PREVAPORIZED COMBUSTION.

CONDUCT CONCEPT SCREENING STUDIES TO IDENTIFY PROMISING CONCEPTS.

CONDUCT COMBUSTOR REFINEMENT TESTING ON MOST PROMISING CONCEPTS.

INTEGRATE COMBUSTOR WITH EXPERIMENTAL ENGINE & DETERMINE PERFORMANCE & EMISSIONS.

CS-78-3680

FIGURE 3

SCERP PROGRAM

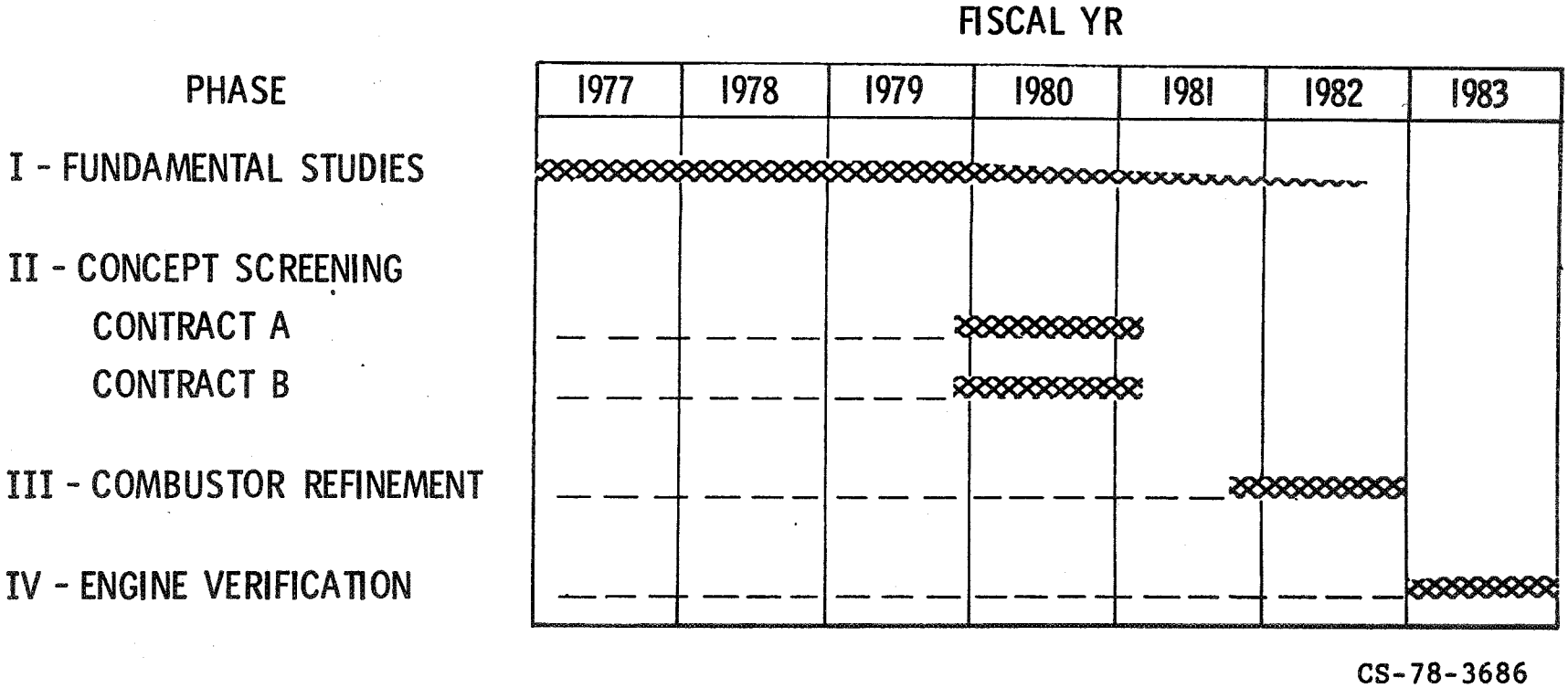

FIGURE 4

SCERP PROGRAM

EXPECTED RESULTS, BENEFITS:

MEETS EPA EMISSION STDS, ACHIEVES LOW NO_x EMISSION AT CRUISE
- DUE TO LEAN HOMOGENEOUS COMBUSTION

IMPROVED TURBINE NOZZLE TEMP DISTRIBUTION
- DUE TO UNIFORMITY OF FUEL & AIR MIXTURE BEFORE BURNING TAKES PLACE

INCREASED COMBUSTOR LINER LIFE
- DUE TO LOWER GAS TEMPS IN PRIMARY ZONE

IF DETERMINED NECESSARY, TECHNOLOGY DEMONSTRATED TO REDUCE IMPACT OF AIRCRAFT EMISSIONS ON STRATOSPHERE.

CS-78-3681

FIGURE 5

SCERP PROGRAM

PHASE I: FUNDAMENTAL STUDIES

PROGRAM ELEMENTS

A. LEAN COMBUSTION
- EFFECT OF CYCLE PRESSURE (GASL)*
- FLAMEHOLDER GEOMETRY STUDY (GASL)*
- LEAN STABILITY AUGMENTATION (UTRC)*
- SECONDARY AIR DILUTION (GASL)
- LPP CONCEPT STUDY (GE, P & WA)*
- FLAMEHOLDER BLOCKAGE STUDY (IH)*
- FUEL PREPARATION EFFECTS (IH)*
- LPP SECTOR TESTS (IH)

B. FUEL-AIR PREPARATION
- FUEL PREPARATION DATA (SOLAR)*
- FUEL PREPARATION MODEL (UTRC)*
- DROP-SIZE CHARACTERISTICS (PURDUE)
- SPRAY CHARACTERISTICS (MICHIGAN)*
- DROP-SIZE WITH LASER (IH)
- FUEL DISTRIBUTION STUDIES (IH)

C. AUTOIGNITION & FLASHBACK
- AUTOIGNITION OF FUELS (UTRC)*
- B-L AUTOIGNITION & FLASHBACK STUDIES (IH)

D. ENGINE INTERFACES
- COMPRESSOR DISCHARGE TURBULENCE (P & WA, GE)*
- ENGINE TRANSIENTS STUDY (IH)
- COMPRESSOR DISCHARGE DATA (IH)

*PARTICIPANT IN PPCT FORUM.

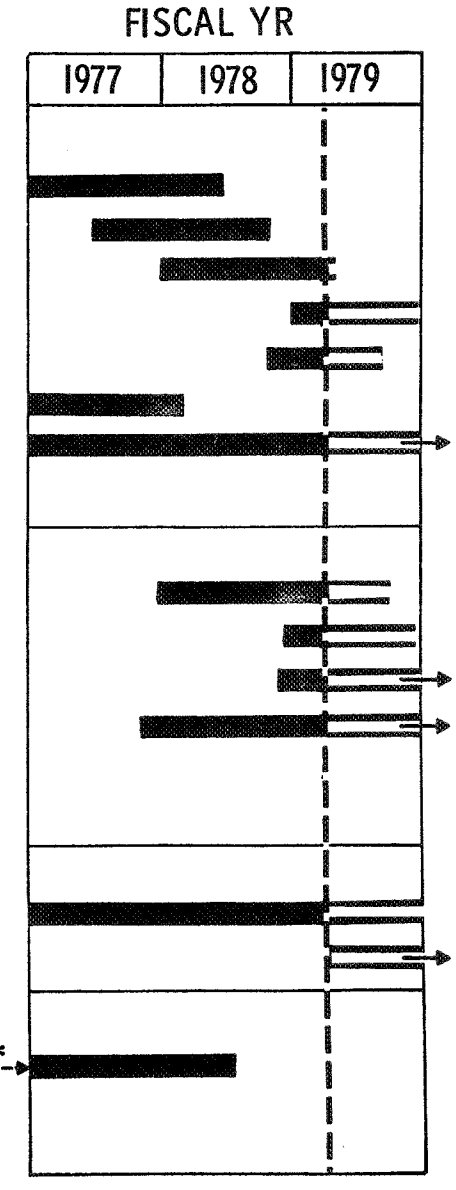

CS-78-3687

FIGURE 6

SCERP PROGRAM

PUBLICATIONS TO DATE

1. LEFEBVRE, A. H., EDITOR: LEAN PREMIXED/PREVAPORIZED COMBUSTION, NASA CP-2016, 1977.
2. FOLLANSBEE, P. S., & DILS, R. R.: EXPERIMENTAL CLEAN COMBUSTOR PROGRAM - TURBULENCE CHARACTERISTICS OF COMPRESSOR DISCHARGE FLOWS, NASA CR-135277, 1977.
3. SPADACCINI, L. J.: DEVELOPMENT OF AN EXPERIMENT FOR DETERMINING THE AUTOIGNITION CHARACTERISTICS OF AIRCRAFT - TYPE FUELS, NASA CR-135329, 1977.
4. ROFFE, G., & VENKATARAMINI, K. S.: EXPERIMENTAL STUDY OF THE EFFECTS OF FLAMEHOLDER GEOMETRY ON EMISSIONS & PERFORMANCE OF LEAN PREMIXED COMBUSTORS, NASA CR-135424, 1978.
5. ROFFE, G., & VENKATARAMINI, K. S.: EXPERIMENTAL STUDY OF THE EFFECT OF CYCLE PRESSURE ON LEAN COMBUSTION EMISSIONS, NASA CR-3032, 1978.
6. ROFFE, G., & VENKATARAMINI, K. S.: EMISSIONS MEASUREMENTS FOR A LEAN PREMIXED PROPANE/AIR SYSTEM AT PRESSURES UP TO 30 ATMOSPHERES, NASA CR-159421, 1978.
7. TAYLOR, J. R.: EXPERIMENTAL CLEAN COMBUSTOR PROGRAM - PHASE III TURBULENCE MEASUREMENT ADDENDUM FINAL REPORT, NASA CR-135422, 1978.

CS-78-3684

FIGURE 7

ADVANCED LOW EMISSIONS CATALYTIC COMBUSTOR PROGRAM

OBJECTIVE:

TO EVOLVE THE TECHNOLOGY REQUIRED FOR INCORPORATING CATALYTIC COMBUSTORS INTO ADVANCED AIRCRAFT GAS-TURBINE ENGINES.

LOWER NO_x EMISSION LEVELS.

IMPROVE COMBUSTION STABILITY.

RETAIN CUSTOMARY SAFETY & ENDURENCE QUALITIES OF CURRENT AIRCRAFT ENGINES.

CS-78-3682

FIGURE 8

SCHEDULE FOR ADVANCED LOW EMISSIONS CATALYTIC COMBUSTOR PROGRAM

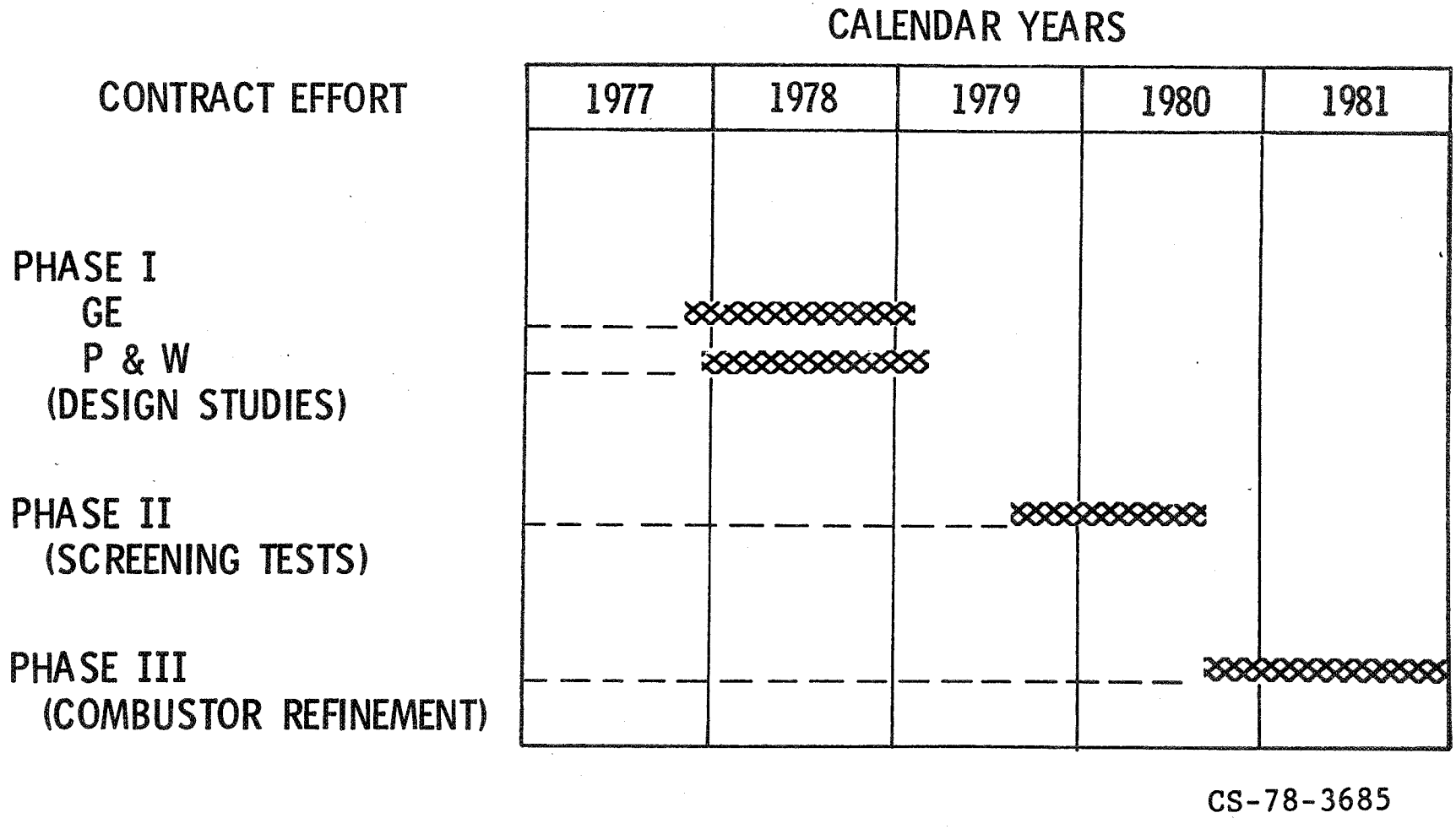

FIGURE 9

OTHER RELATED PROGRAMS

EFFECT OF SWIRL ON PREMIXED COMBUSTION (CORNELL U)

MODEL FOR FLAME IGNITION & BLOWOUT (MIT)

STABILIZATION OF PREMIXED COMBUSTORS (U OF CALIF)

FUEL INJECTOR DESIGNS FOR PREMIXED COMBUSTORS (I-H)

CS-78-3677

FIGURE 10

Presentation Prepared for the Premixed-Prevaporized
Combustor Technology (PPCT) Forum
NASA Lewis Research Center, Jan 9-10, 1978

Turbulence Characteristics of Compressor Discharge Flows

Howard P. Grant, P&WA CPD E. Hartford

Turbulence measurements were conducted in a large gas turbine engine (JT9D) at the entrance to the diffuser duct, joining the compressor discharge to the combustor inlet. Hot film probe and hot wire probe measurements were obtained at temperatures from 450K (350F) (idle) to 608K (635°F) (rich approach).

The work was conducted at P&WA in East Hartford in late 1976 under NASA LeRC Contract NAS3-19447 as part of the ECCP - Experimental Clean Combustor Program. The detailed results are presented in report No. NASA CR-135277.

At I.D. (25 percent span) and mid-span locations, the turbulence intensity increased slightly from 6 ±1 percent at idle condition to 7±1 percent at rich approach. AT O.D. (75 percent span) the turbulent intensity increased more rapidly, from 7.5± 0.5 percent at idle to 15±0.5 percent at rich approach. The spectra showed turbulent energy distributed uniformly over a 0.1 to 5 KHz bandwidth (down 3 db) at all operating conditions, corresponding to random turbulence with velocity wave lengths of 2 cm to 1 meter travelling at the mean velocity of 100 m/sec. Above 5 KHz the turbulent energy decreased at a rate proportional to $f^{-0.25 \pm 0.1}$ in all cases, with roll-off frequency not a strong function of engine operating point.

The turbulence near the diffuser O.D. is large enough in amplitude and scale to affect the flow to the front end sections of the burner. The origin of this high turbulence level requires further information on the turbulence development along the diffuser.

Velocity fluctuations at blade-passing frequency (about 10KHz) were identifiable at all spanwise positions, but the amplitude and scale were not large enough to affect the combustor flow.

Measurements at higher engine power levels are of course needed to determine whether shifts in amplitude or scale of turbulence occur. Laser Doppler anemometer optical instrumentation should be considered for these higher power studies, since the 608K temperature is the upper limit for state-of-the-art hot wire or hot film probes in the engine environment. Hot wires are capable of operation at stream temperatures to at least 800K (1000°F), but only in extremely clean air streams free of foreign matter. In fact all the hot wires tried in the engine failed in a matter of minutes. The hot film probes are orders of magnitude more durable and all but one survived the entire 3 day engine test. Films, however, can not be used at stream temperatures above 615K (650°F) because thermally induced stresses in the sensor head exceed the strength of the quartz insulating material.

Measurements of this kind in the compressor exit environment are difficult, requiring meticulous attention to preliminary calibration, data acquisition procedure, and automated data reduction procedures. The sensors are continuously threatened with destruction by foreign object damage in the engine, so operating time on the engine test stand must be used efficiently, and provision for quick change of probes must be included in the installation scheme used.

The engine, test cell, combustor cross section, and turbulence probe locations are shown in Figs 1 through 5. The probes used are described in Table 1 and Figs 6,7 and 8.

Note particularly in Fig 7 that each probe was equipped with a mounting boss with depth preset, and alignment with engine axis predetermined. Replacement probes could be inserted in a few minutes.

A series of special calibrations was carried out with each probe in the laboratory. The first calibration was sensor resistance vs. temperature (Fig 9) to determine the maximum safe operating resistance for each sensor. Next each sensor was inserted in a conventional commercial anemometer bridge circuit of the constant resistance type, in which a feedback circuit automatically varies the bridge voltage (i.e. sensor heating current) to mantain the sensor at the selected constant resistance. The bridge voltage was then measured as a function of gas temperature at zero flow (Fig 10) and as a function of gas velocity at room temperature (Figs 11 and 12). This provides all the information needed for calculation of d.c. velocity sensitivity at any combination of gas velocity and gas temperature. The equations are presented in the referenced report. The frequency response of each probe was then determined by comparison with a 6μ platinum wire probe (known to have flat response beyond 20 KHz) in a turbulent jet, and a transfer function (frequency response correction function) constructed for each probe. An example is shown in Fig 13. The transfer function was found not to be a strong function of Reynolds number.

The data acquisition system (magnetic tape) and playback system is shown in Fig 14. The key to success in playback is the use of the spectrum analyzer and the mini-computer programmed with the calibration equations that permitted calculation of the turbulence energy content of each of 399 frequency intervals 50 Hz wide, covering the 0.1 to 20 KHz frequency range. From this information the mimcomputer was able to output spectrum plots, turbulence intensity, integral scale, and microscale, using the Hinze turbulence relations.

The results are presented numerically in tables II, III, IV, V, and VI and graphically in Figures 15 through 26.

Figure 15 is a plot of all validated turbulence data, showing the trends already discussed.

Fig. 16 is a typical spectrum plot, showing the classical random turbulence spectrum, except that it is punctuated with spikes at blade passing frequency (about 10 KHz) and at twice blade passing frequency. The energy in these spikes is small. The weak peak at about 900Hz at 75% span (Figs 18,19) is unexplained, by the way. Rotor frequency was below 100 Hz.

Note again that the turbulent scale is quite large. 5 KHz component corresponds to an axial scale of about 2 cm.. Most of the random energy is contained in velocity wave lengths between 1.0 meter and 2 cm.

Finally it is interesting to note that the large turbulence level at O.D. may improve the performance of the diffuser by retarding separation.

The program illustrates well the capability of sophisticated anemometer instrumentatio to produce valuable data under extremely difficult conditions, when sufficient care an feeding is supplied.

TABLE I

PROBE TYPES AND LOCATIONS

Test No. 1 *Probe No.	Type	Angular Location	Spanwise Location (Percent)
1	370μ diameter Stainless Steel Wire Probes	323° 05′	25, 50, 75
2	TSI 949K Hot Film Probes	358° 22′	25, 50, 75
3	TSI 949K Hot Film Probes	17° 52′	25, 50, 75
4	TSI 949K Hot Film Probes	143° 04′	25, 50, 75
5	370μ diameter Stainless Steel Wire Probes	178° 18′	25, 50, 75
6	12μ Pt-Ir Wire Probes	217° 25′	25, 50, 75

Test No. 2 *Probe No.	Type	Angular Location	Spanwise Location (Percent)
1	370μ diameter Stainless Steel Wire Probes	323° 05′	25, 50, 75
2	370μ diameter Stainless Steel Wire Probes	358° 22′	25, 50, 75
3	370μ diameter Stainless Steel Wire Probes	17° 52′	25, 50, 75
4			
5	370μ diameter Stainless Steel Wire Probes	178° 18′	25, 50, 75
6	12μ Pt - Ir Wire Probes	217° 25′	25, 50, 75

Test No. 2 *Probe No.	Type	Angular Location	Spanwise Location (Percent)
1	TSI 949K Hot Film Probe	323° 05′	25, 50, 75
2	TSI 949K Hot Film Probe	358° 22′	25, 50, 75
3	TSI 949K Hot Film Probe	17° 52′	25, 50, 75
4	TSI 949K Hot Film Probe	143° 04′	25, 50, 75
5	TSI 949K Hot Film Probe	178° 18′	25, 50, 75
6	TSI 949K Hot Film Probe	217° 25′	25, 50, 75

*See Figure 5 for Probe Location

TABLE II

DEPENDENCE OF TURBULENT INTENSITY ON ENGINE OPERATION, TEST 1

Test Point	Designation	Probe 1 S.S. Wire 323° 5′ 50% Span		Probe 2 Hot Film 358° 22′ 50% Span		Probe 3 Hot Film 17° 52′ 25% Span		Probe 4 Hot Film 143° 04′ 75% Span		Probe 5 S.S. Wire 178° 18′ 50% Span		Probe 6 Pt.-Ir. Wire 217° 25′ 50% Span	
		T_4 K	$Tu/\bar{u}$ %	T_4 K	$Tu/\bar{u}$ %	T_4 K	$Tu/\bar{u}$ %	T_4 K	$Tu/\bar{u}$ %	T_4 K	$Tu/\bar{u}$ %	T_4 K	$Tu/\bar{u}$ %
1	Idle	Failed		450	7.0	454	4.76	Erratic		Erratic		Failed	
2	Flight Idle	Failed		516	8.16	Erratic		Erratic		Erratic		Failed	
3	Approach	Failed		591	7.64	597	6.65	Erratic		Erratic		Failed	
4	Idle	Failed		456	6.59	464	4.78	Erratic		Failed		Failed	
5	Rich Approach	Failed		608	7.96	616	5.42	Erratic		Failed		Failed	
6	Idle	Failed		455	5.22	455	4.81	Erratic		Failed		Failed	

TABLE III

DEPENDENCE OF TURBULENT INTENSITY ON ENGINE OPERATION, TEST 2

Test Point	Designation	Probe 1 S.S. Wire 323° 05′ 25% Span		Probe 2 S.S. Wire 358° 22′ 75% Span		Probe 3 S.S. Wire 17° 52′ 50% Span		Probe 4 None Installed		Probe 5 S.S. Wire 178° 18′ 50% Span		Probe 6 Pt-Ir Wire 217° 25′ 25% Span	
		T_4 K	$Tu/\bar{u}$ %	T_4 K	$Tu/\bar{u}$ %	T_4 K	$Tu/\bar{u}$ %	T_4 K	$Tu/\bar{u}$ %	T_4 K	$Tu/\bar{u}$ %	T_4 K	$Tu/\bar{u}$ %
1	Climb	Failed		Failed		Failed		—	—	Erratic		Failed	

TABLE IV

DEPENDENCE OF TURBULENT INTENSITY ON ENGINE OPERATION, TEST 3

Test Point	Designation	Probe 1 Hot Film 323° 05′ 25% Span		Probe 2 Hot Film 358° 22′ 75% Span		Probe 3 Hot Film 17° 52′ 50% Span		Probe 4 Hot Film 143° 4′ 75% Span		Probe 5 Hot Film 178° 18′ 50% Span		Probe 6 Hot Film 217° 25′ 25% Span	
		T_4 K	$Tu/\bar{u}$ %	T_4 K	$Tu/\bar{u}$ %	T_4 K	$Tu/\bar{u}$ %	T_4 K	$Tu/\bar{u}$ %	T_4 K	$Tu/\bar{u}$ %	T_4 K	$Tu/\bar{u}$ %
1	Idle	461	6.83	452	7.09	Erratic		450	7.93	Erratic		459	5.87
2	Flight Idle	536	7.70	525	10.56	Erratic		520	11.03	Erratic		519	6.14
3	Approach	611	7.09	602	16.17	Erratic		597	14.17	Erratic		602	5.68
4	Idle	461	6.88	450	7.05	Erratic		447	8.08	Erratic		452	6.18

TABLE V

ENGINE TEST CONDITIONS

	Test Pt.	Designation	T_{T4}* K	P_{T4}* 10^5 N/m^2	Average Velocity Calculated From P_{T4}/T_{T4} m/sec	F/A	N_2 RPM	Fn N
Test 1	1	Idle	450	3.71	109.3	0.0096	4941	14052
	2	Flight Idle	520	6.02	112.2	0.0106	5765	31471
	3	Approach	590	9.17	122.8	0.0140	6376	61759
	4	Idle	452	3.76	108.9	0.0095	4983	14470
	5	Rich Approach	609	9.91	128.1	0.0148	6499	70366
	6	Idle	446	3.63	107.1	0.0095	4913	13549
Test 2	1	Climb	732	18.2	139.3	0.0227	7206	169030
Test 3	1	Idle	454	3.88	110.1	0.0102	4830	16436
	2	Flight Idle	520	6.16	119.2	0.0118	5557	35177
	3	Approach	599	9.77	125.7	0.0152	6203	72284
	4	Idle	449	3.80	122.1	0.0103	4801	16018

*Measured

TABLE VI

TURBULENCE CHARACTERISTICS OF COMPRESSOR DISCHARGE FLOWS

Hot Film Probe						
Number	Percent Span	Angular Location	Tu (meters/sec)	Turbulent Intensity Tu/$\bar{u}$	Λ (Macro-scale In Meters)	λ (Micro-scale In Meters)
2	50	358° 22′	6.782	0.06998	0.0079	0.0051
			8.556	0.08160	0.0116	0.0097
			8.620	0.07644	0.0083	0.0104
			6.471	0.06593	0.0094	0.0078
			9.145	0.07958	0.0124	0.0093
			5.103	0.05216	0.0169	0.0079
3	25	17° 52′	4.645	0.04762	0.0153	0.0094
			7.560	0.06650	0.0109	0.0076
			4.723	0.04782	0.0111	0.0082
			6.273	0.05416	0.0107	0.0090
			4.710	0.04814	0.0121	0.0089
1	25	323° 05′	6.725	0.06831	0.0212	0.0087
			8.209	0.07695	0.0099	0.0089
			8.163	0.07085	0.0086	0.0076
			6.774	0.06880	0.0181	0.0077
2	75	358° 22′	6.890	0.07086	0.0082	0.0079
			11.166	0.10557	0.0063	0.0085
			18.482	0.16169	0.0100	0.0058
			6.834	0.07050	0.0161	0.0071
4	75	143° 04′	7.683	0.07927	0.0323	0.0064
			11.561	0.11026	0.0162	0.0064
			16.104	0.14165	0.0104	0.0090
			7.807	0.08080	0.0333	0.0086
6	25	217° 25′	5.747	0.05873	0.0104	0.0081
			6.453	0.06136	0.0095	0.0083
			6.489	0.05677	0.0088	0.0077
			6.007	0.06178	0.0290	0.0072

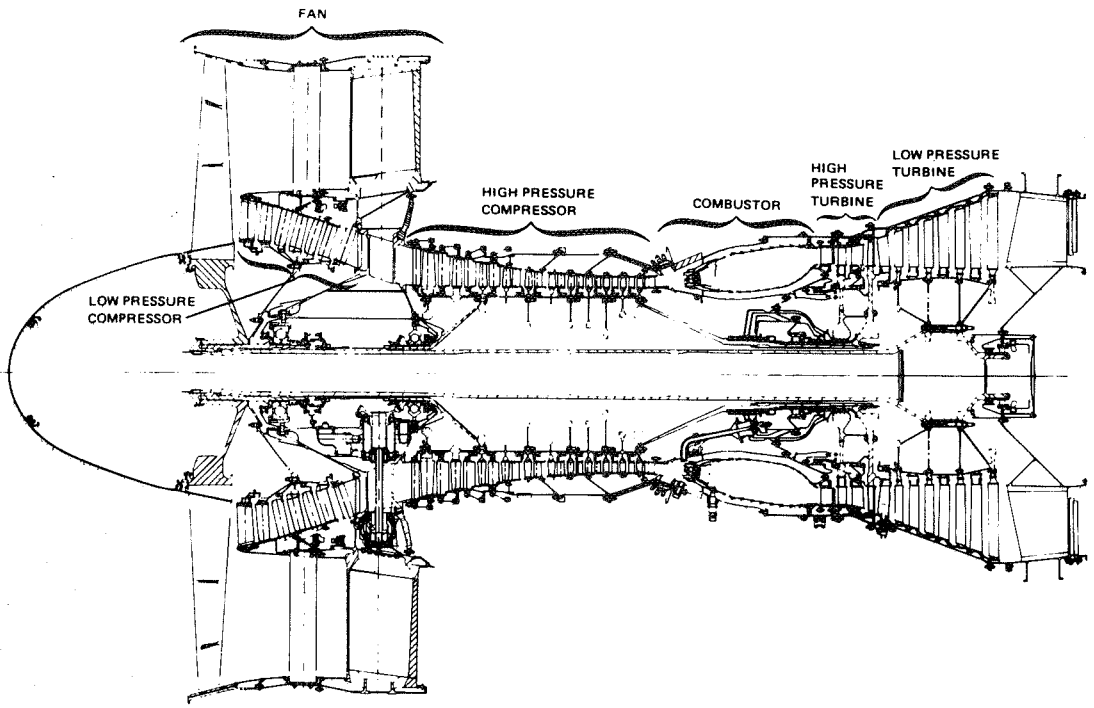

Figure 1 *Cross Sectional Schematic of the JT9D-7A Reference Engine*

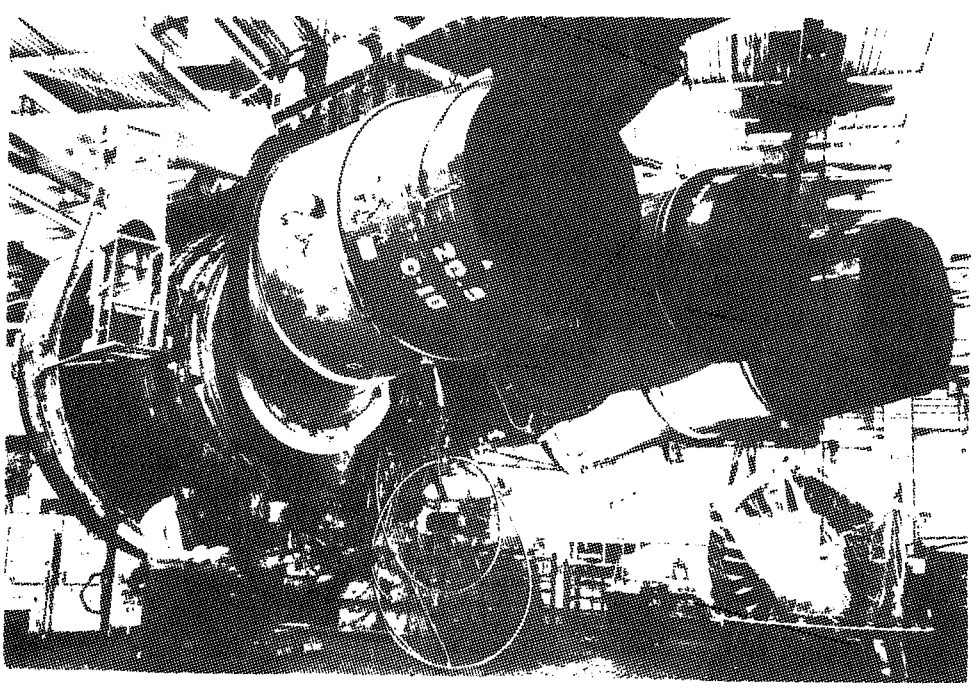

Figure 2 *Experimental Engine, X-686, With Bifurcated Ducts Installed* *(X-43208)*

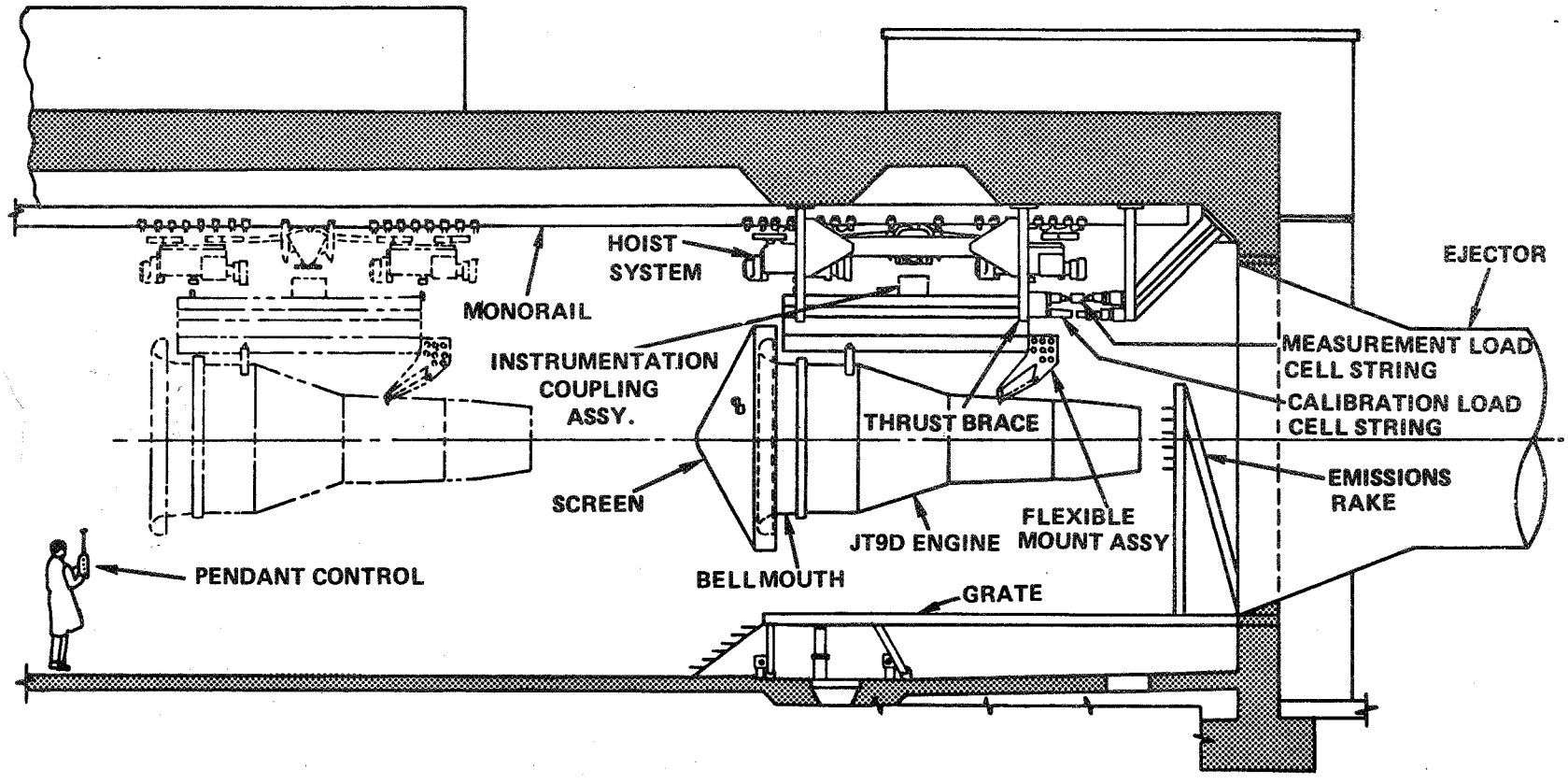

Figure 3 *P-6 Test Cell Layout*

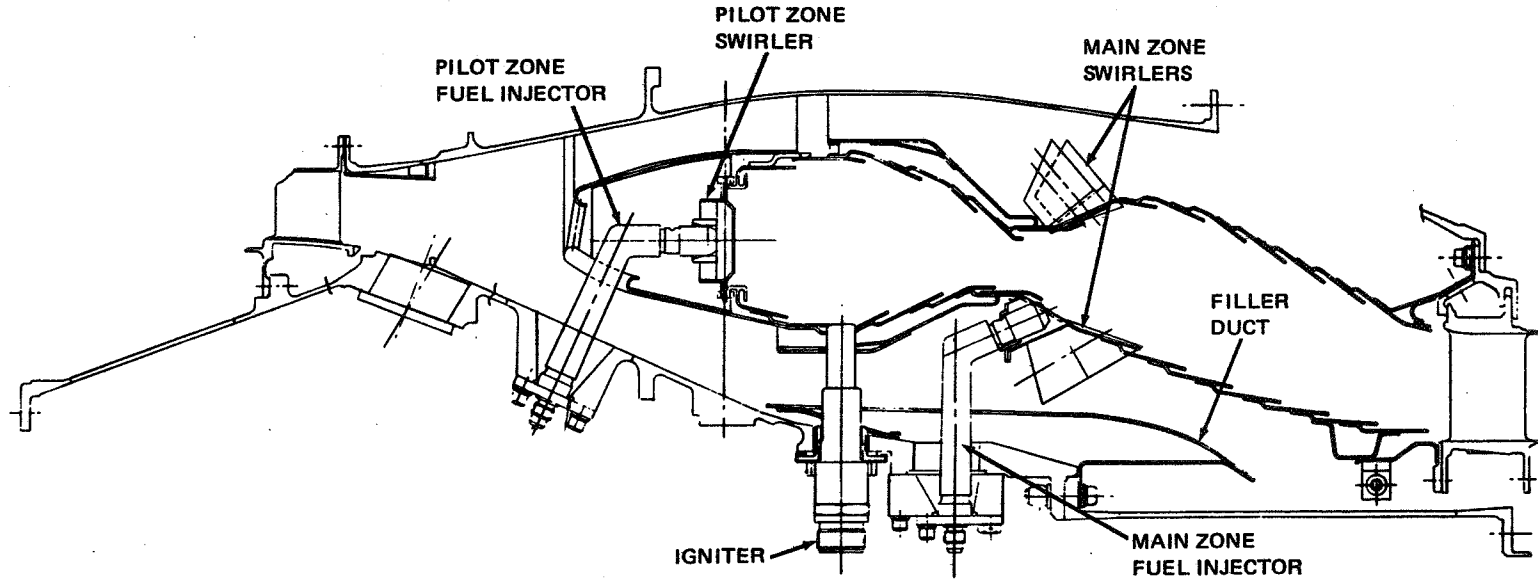

Figure 4 *Cross Section of Experimental Clean Combustor Program Phase III Vorbix Combustor*

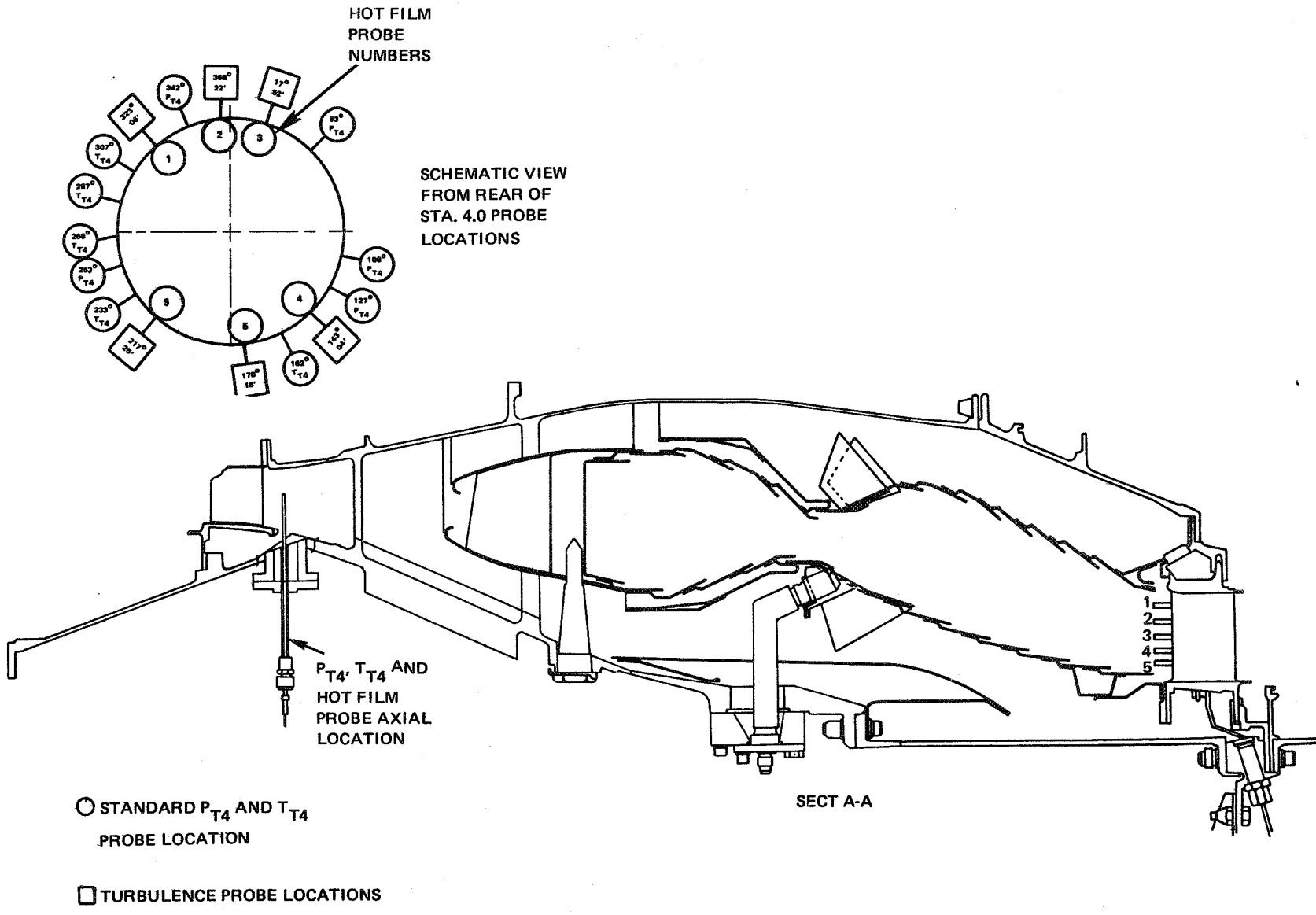

Figure 5 Location of Turbulence Probes

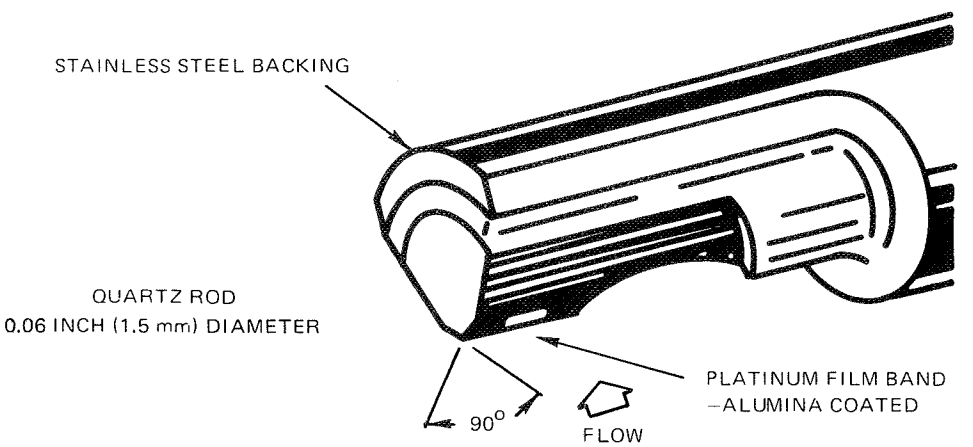

SENSING SIZE: TWO WEDGE SURFACES EACH 0.005 INCH (0.12 mm) WIDE BY 0.04 INCH (1.0 mm) LONG

(a)

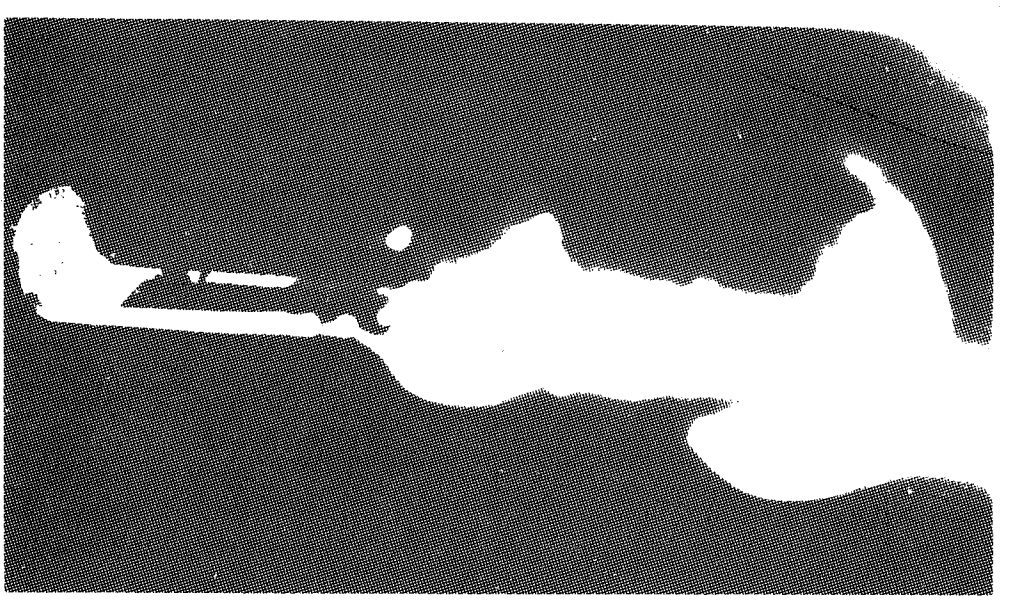

(b)

Figure 6 Wedge Type Probe (77-444-9004)

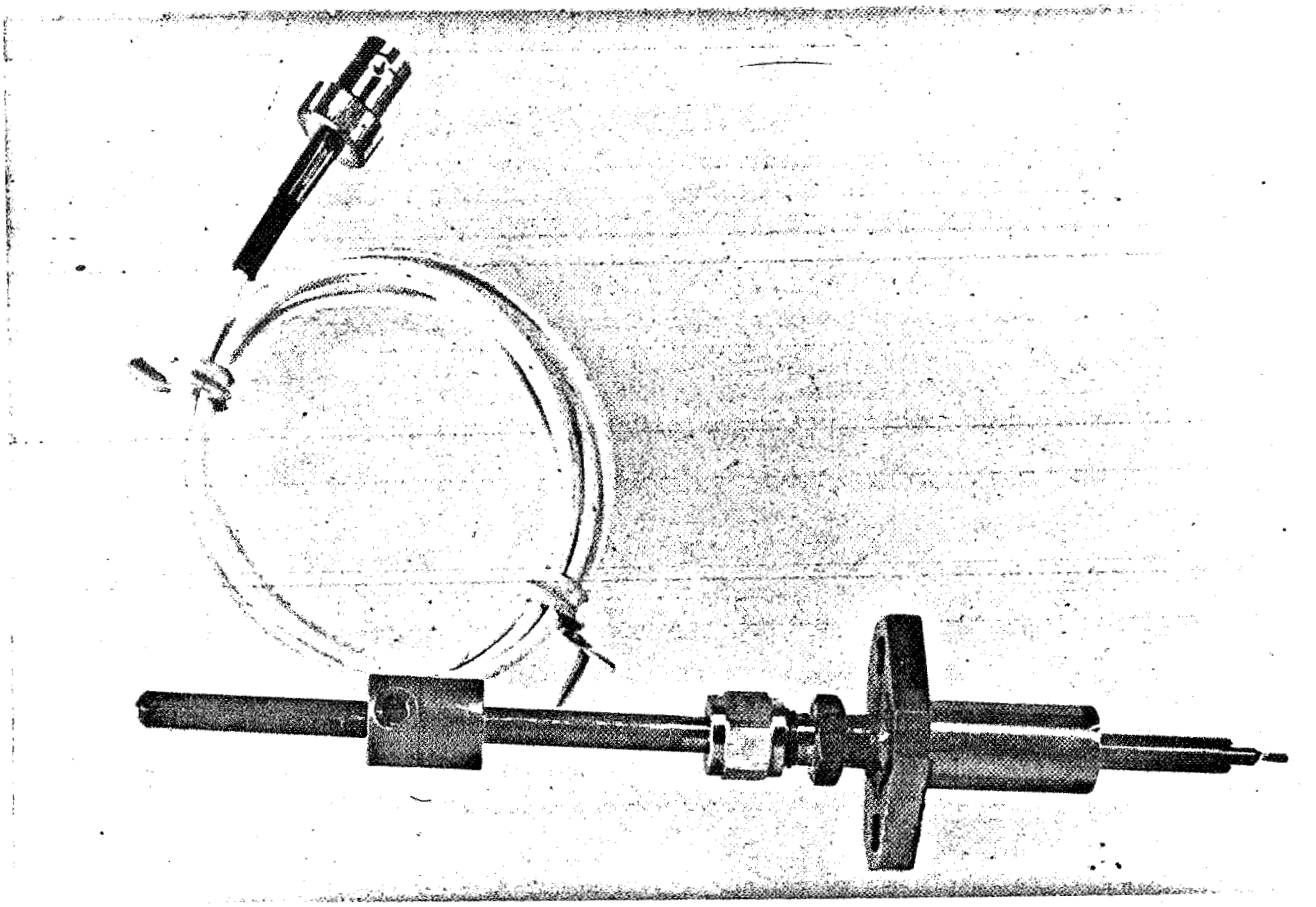

Figure 7 *Station 4 Probe Adaptor* *(77-441-9142)*

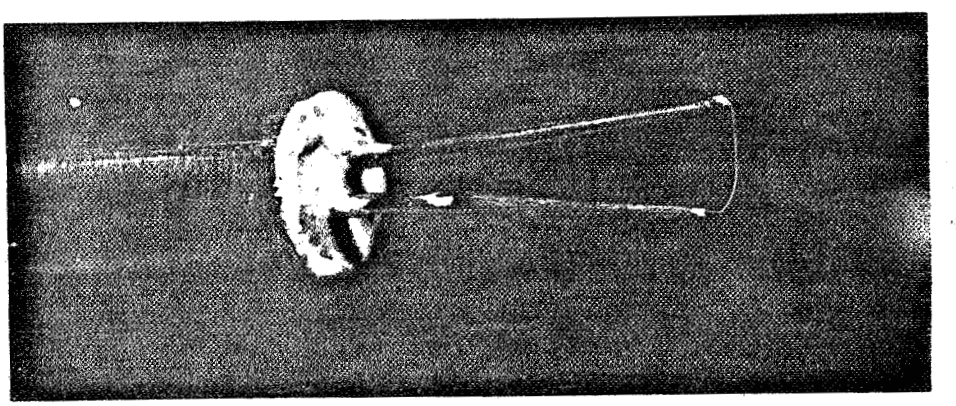

Figure 8 *Wire Probe* *(77-444-9002A)*

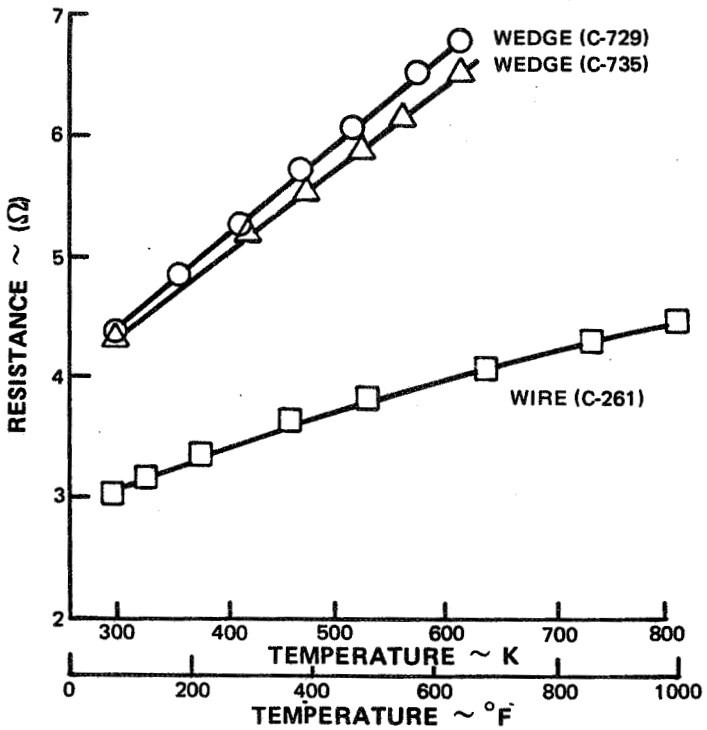

Figure 9 *Dependence of Probe Resistance on Temperature*

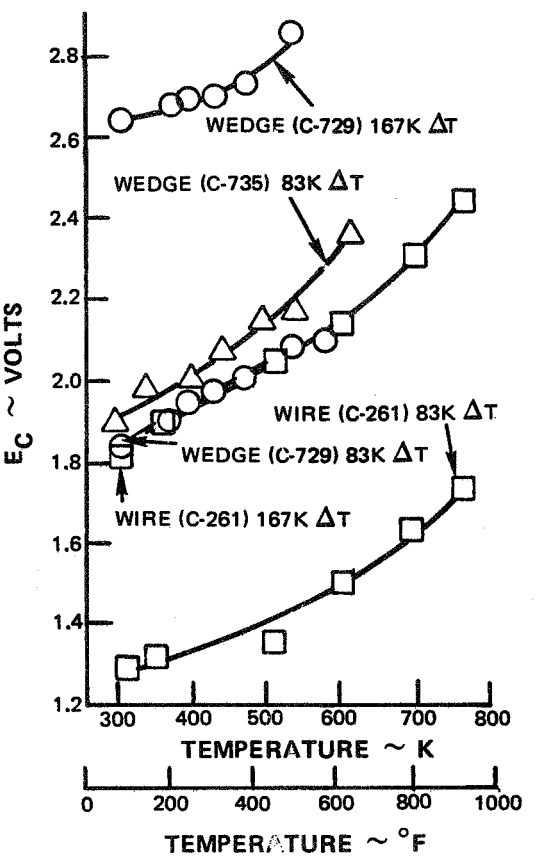

Figure 10 *Dependence of Quiescent Environment Bridge Voltage On Temperature*

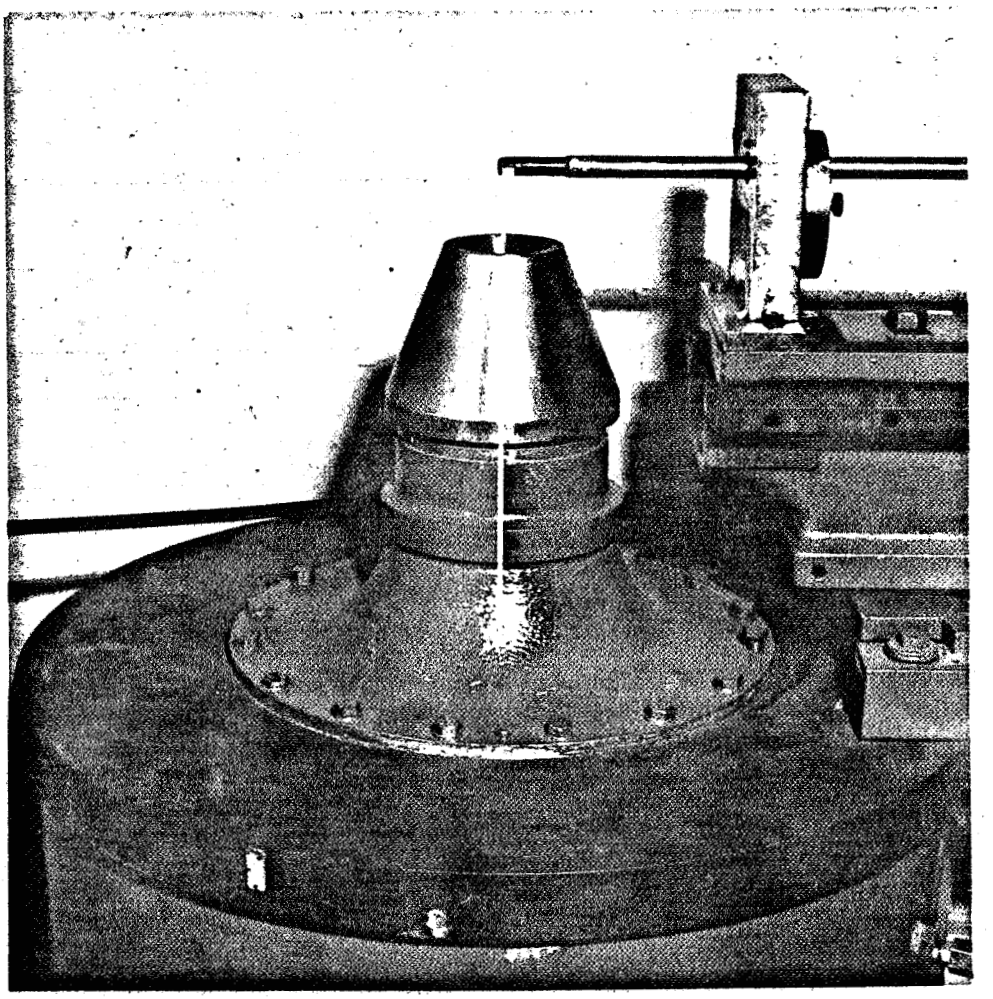

Figure 11 *Experimental Arrangement for Anemometer Velocity Calibrations* *(X-30941)*

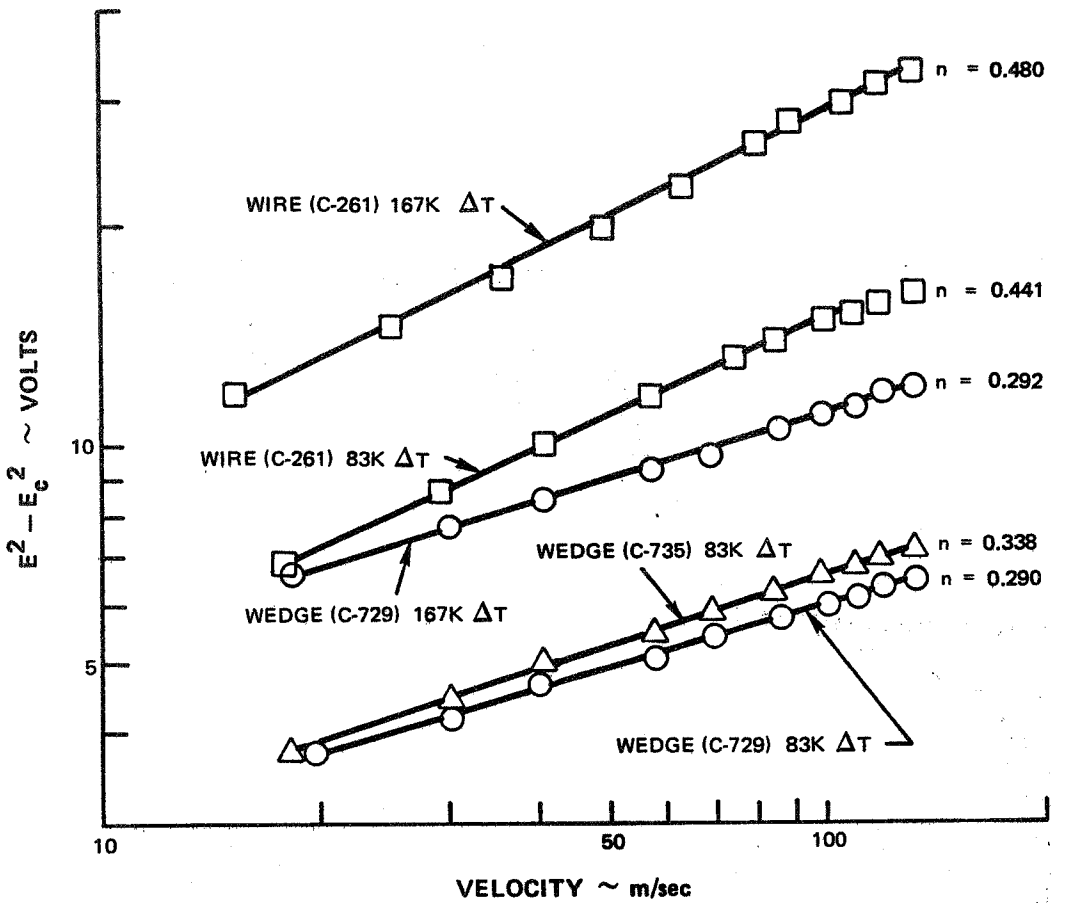

Figure 12 *Anemometry Probe Velocity Calibrations*

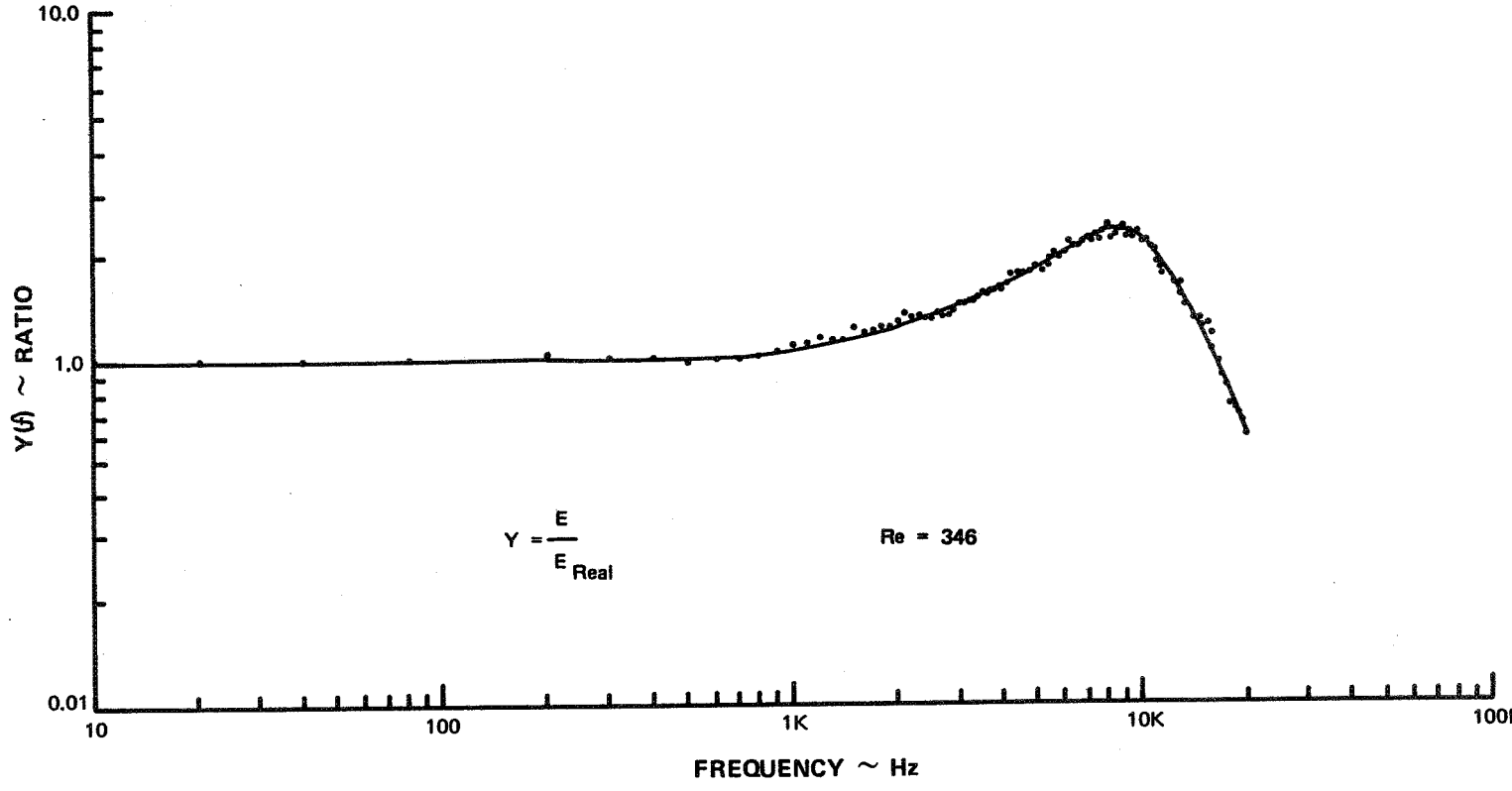

Figure 13 Wedge Probe Transfer Function

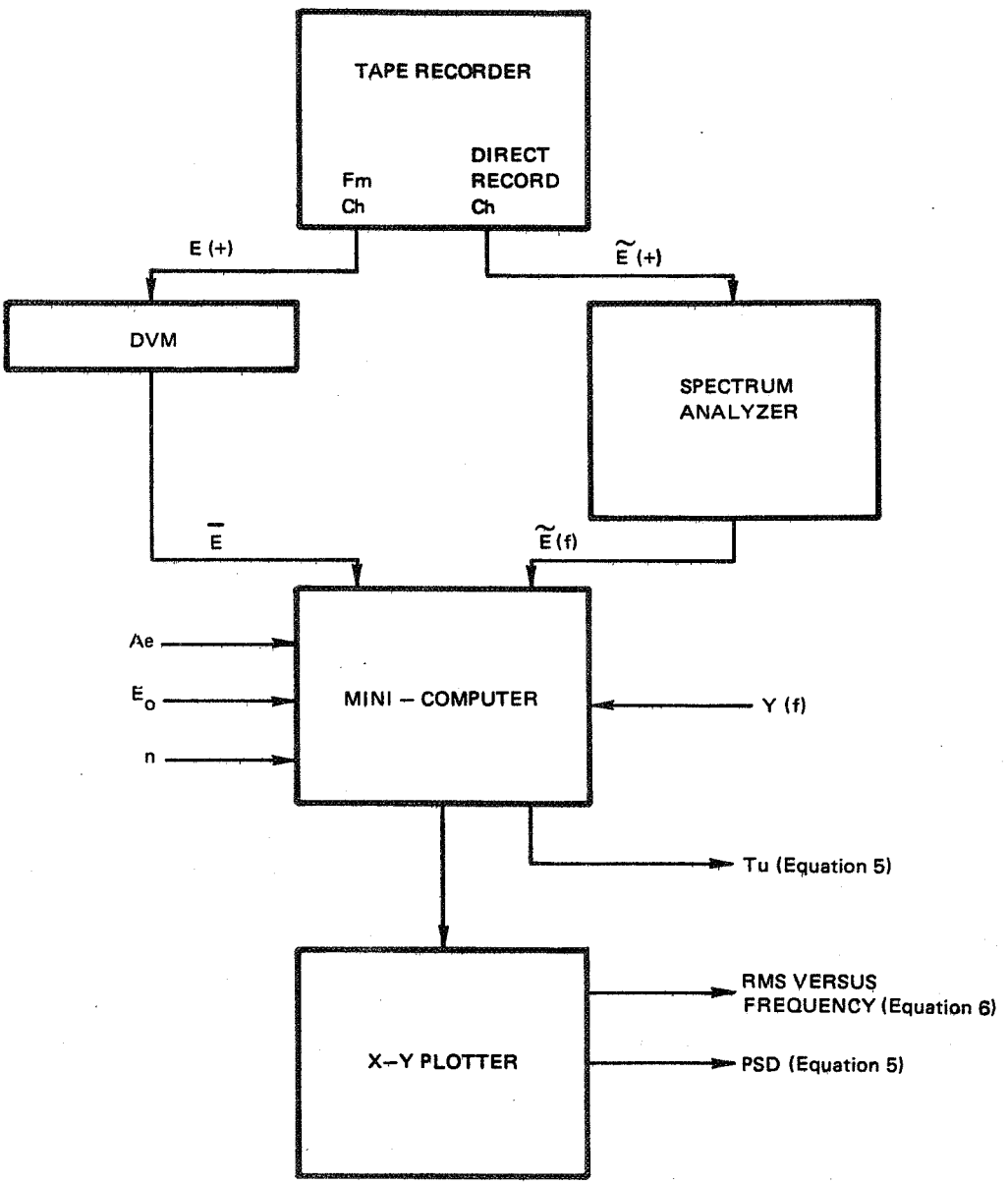

Figure 14 *Block Diagram of Data Reduction System*

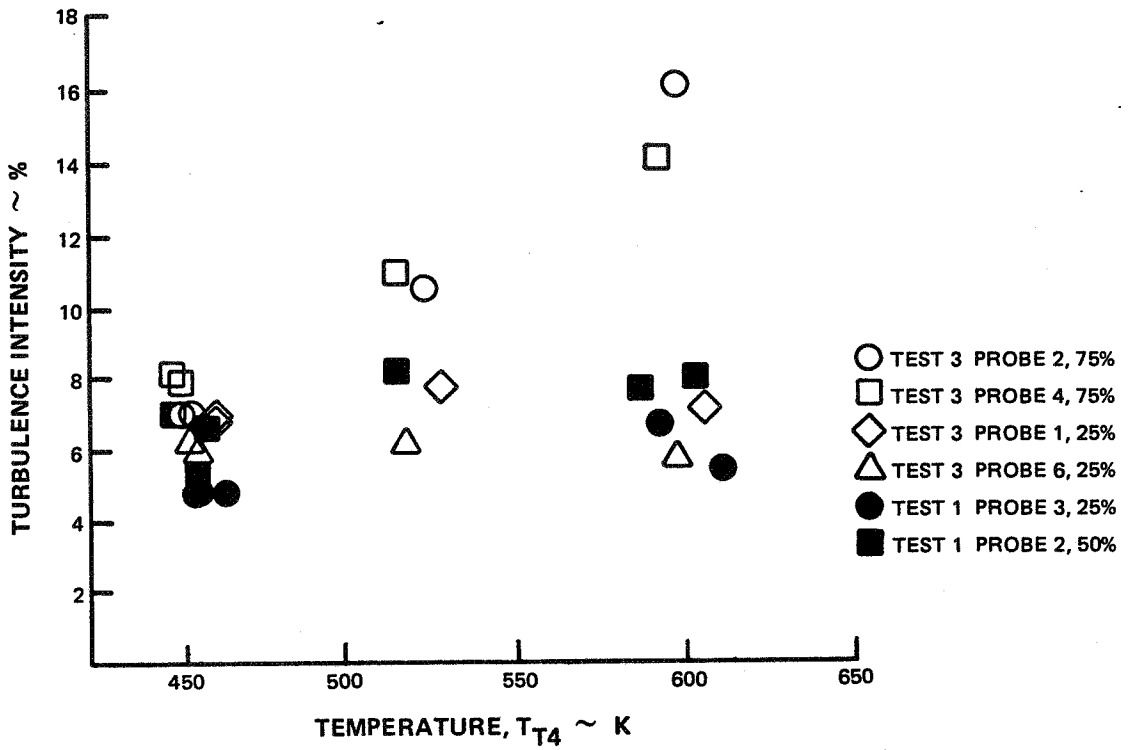

Figure 15 *Dependence of Turbulence on Engine Operation*

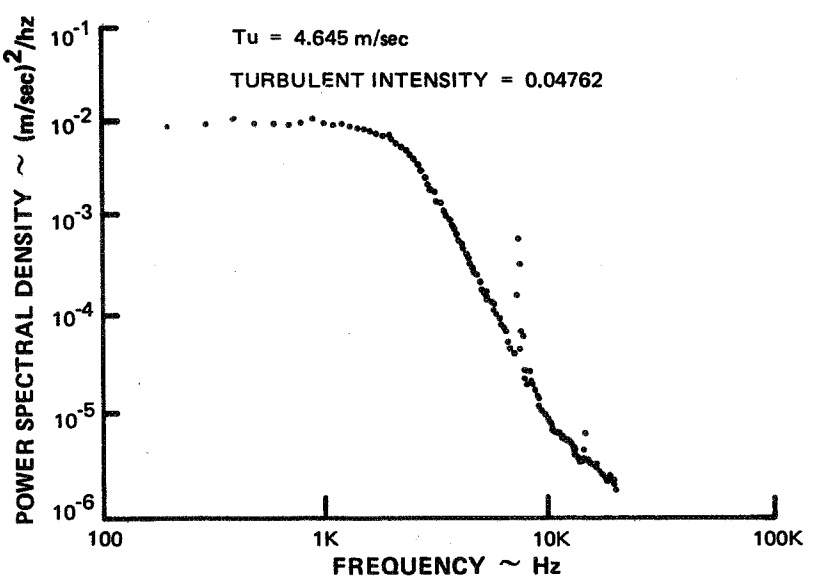

Figure 16 *Test 1, Probe 3 (Wedge Type) Power Spectral Density Function for Idle Condition at 25 Percent Span*

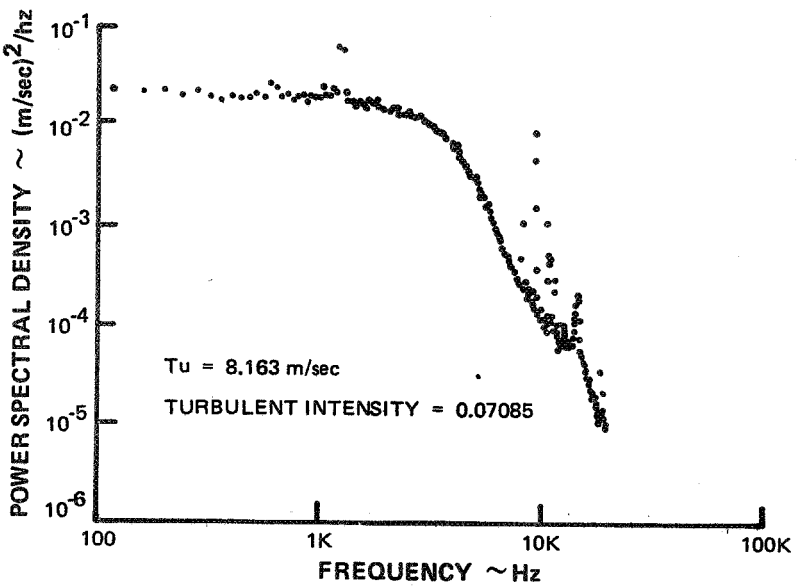

Figure 17 *Test 3, Probe 1 (Wedge Type) Power Spectral Density Function for Approach Power Condition at 25 Percent Span*

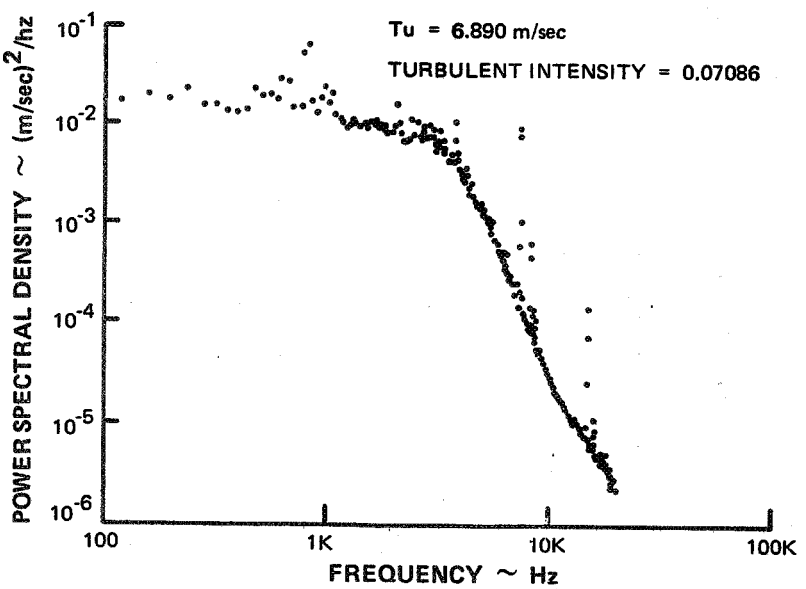

Figure 18 *Test 3, Probe 2 (Wedge Type) Power Spectral Density Function for Idle Condition at 75 Percent Span*

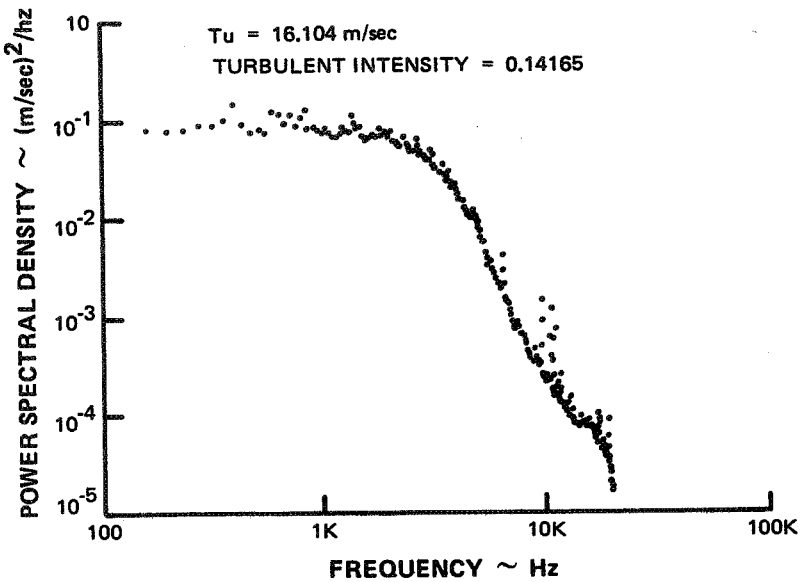

Figure 19 *Test 3, Probe 4 (Wedge Type) Power Spectral Density Function for Approach Power Condition at 75 Percent Span*

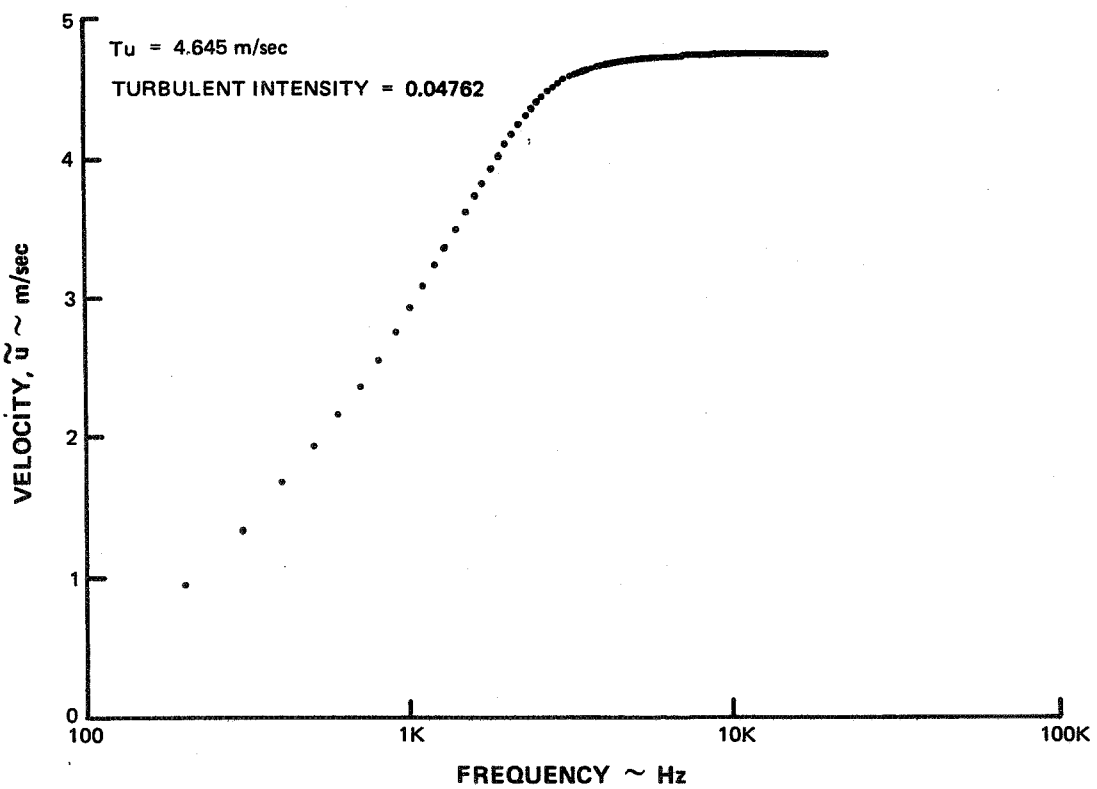

Figure 20 *Test 1, Probe 3 (Wedge Type) Spectral Distribution for Idle Condition at 25 Percent Span*

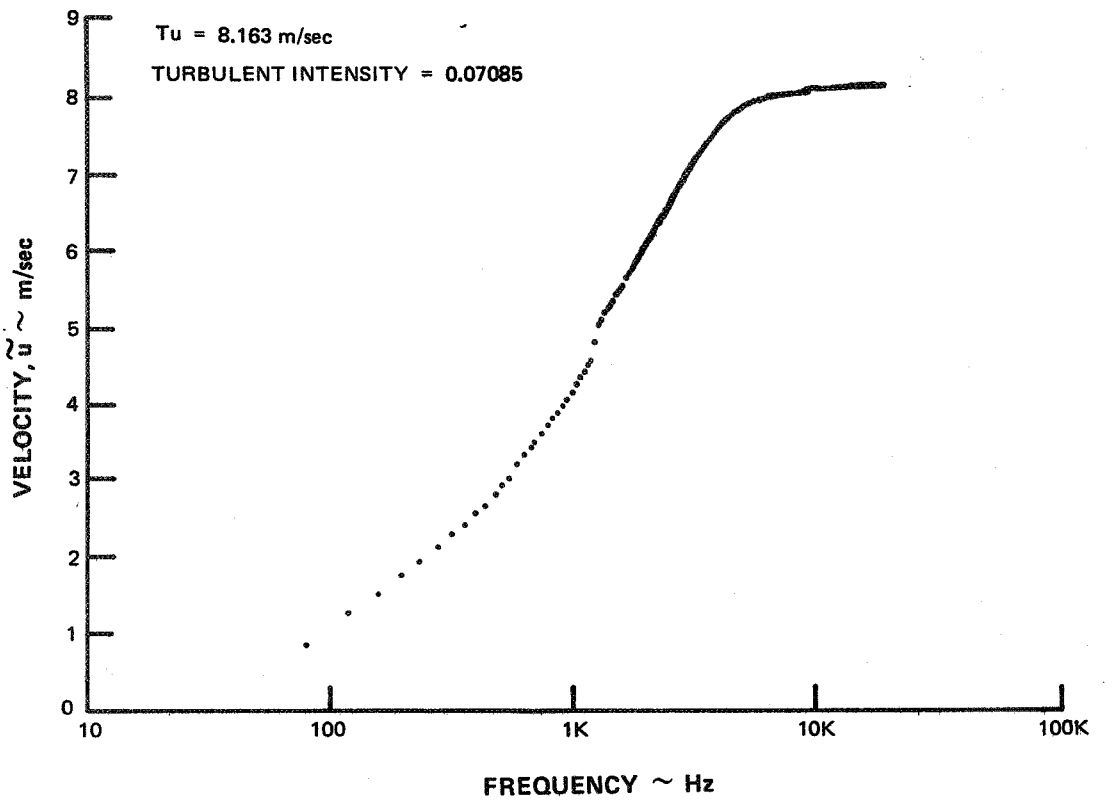

Figure 21 *Test 3, Probe 1 (Wedge Type) Spectral Distribution for Idle Condition at 25 Percent Span*

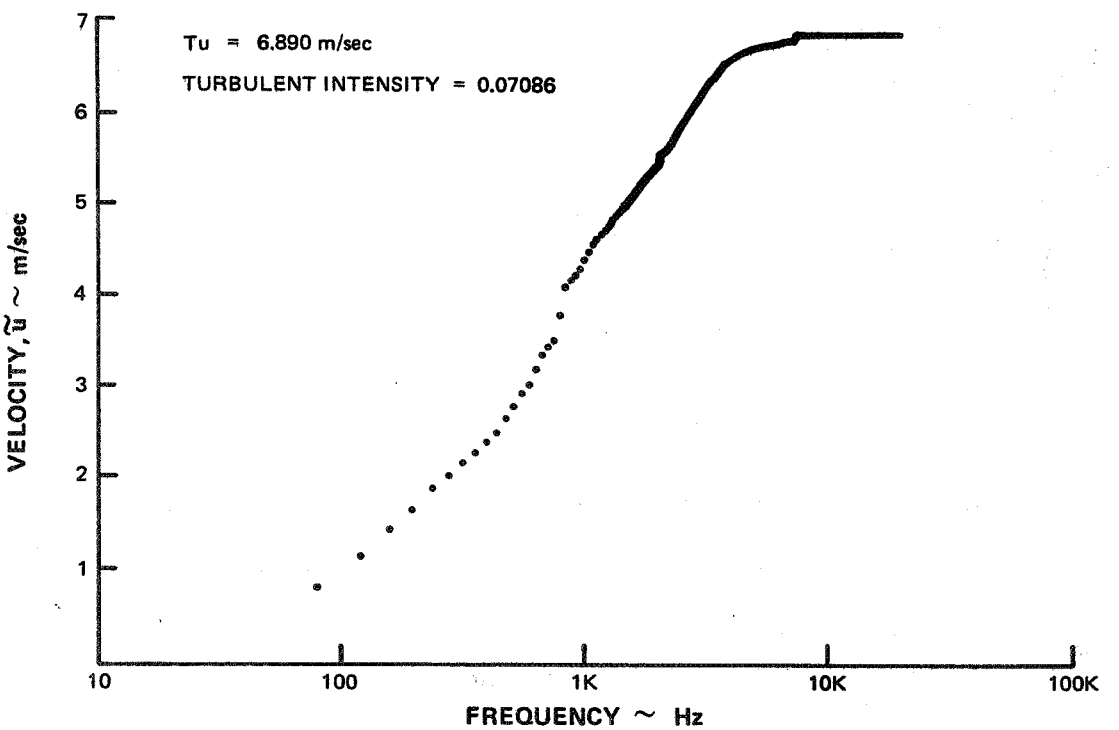

Figure 22 *Test 3, Probe 2 (Wedge Type) Spectral Distribution for Idle Condition at 75 Percent Span*

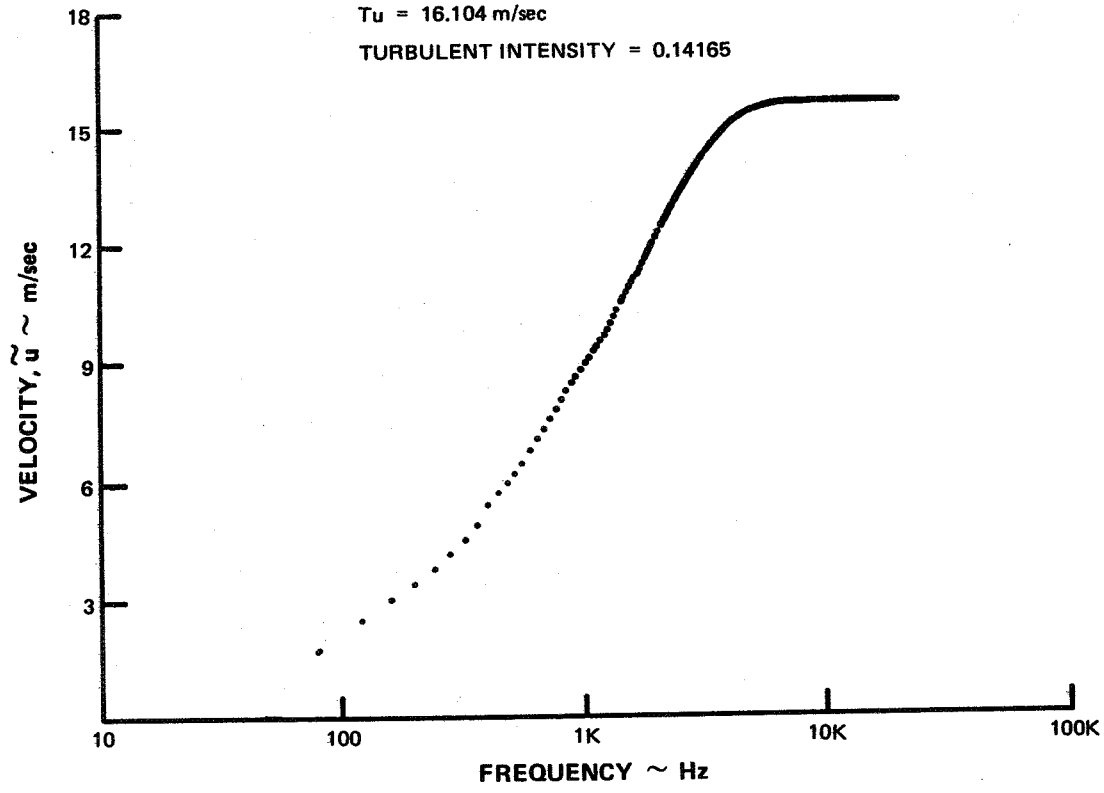

Figure 23 *Test 3, Probe 4 (Wedge Type) Spectral Distribution for Approach Power Condition at 75 Percent Span*

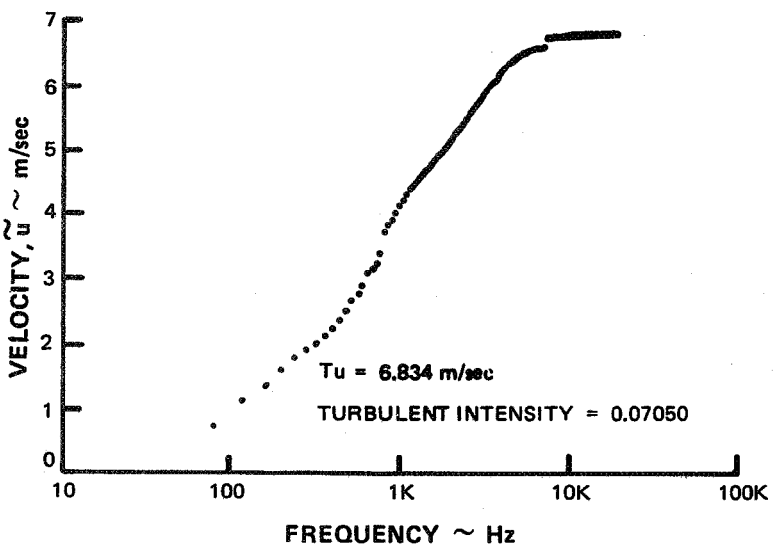

Figure 24 *Test 3, Probe 2 (Wedge Type) Spectral Distribution for Idle Condition at 75 Percent Span*

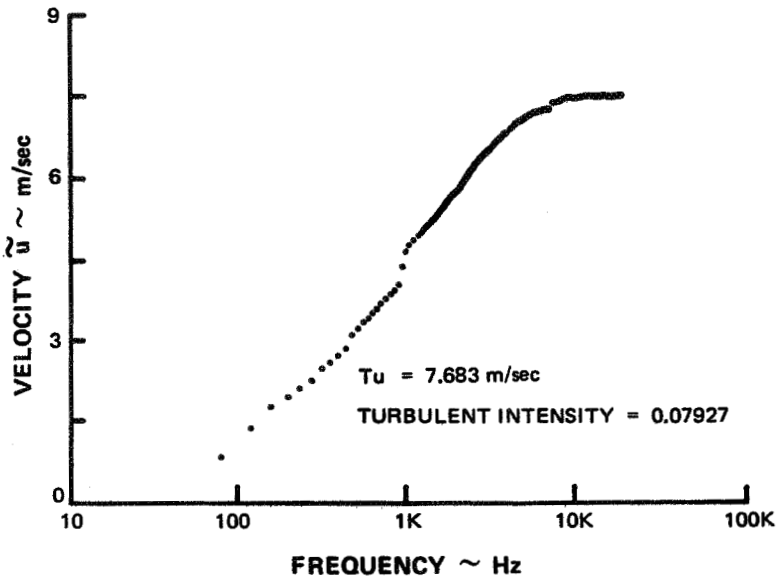

Figure 25 *Test 3, Probe 4 (Wedge Type) Spectral Distribution for Idle Condition at 75 Percent Span*

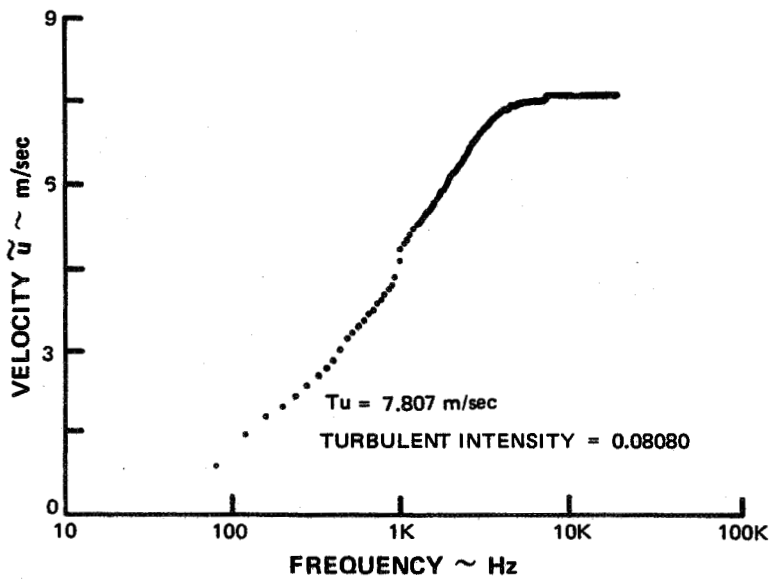

Figure 26 *Test 3, Probe 4 (Wedge Type) Spectral Distribution for Idle Condition at 75 Percent Span*

TURBULENCE MEASUREMENTS IN THE COMPRESSOR EXIT FLOW OF A GENERAL ELECTRIC CF6-50 ENGINE

by J. R. TAYLOR

The purpose of this program was to measure the turbulence intensity and scale in the compressor exit flow stream of an operating CF6-50 gas turbine engine. This program was conducted as an addendum to, and concurrently with, Phase III of the NASA/GE Experimental Clean Combustor Program (Contract NAS3-19736). Compressor exit turbulence data are required for the development of lean burning, premixed, prevaporized combustion systems that have low levels of nitrogen oxide (NO_x) emissions. The systematic development of very lean burning premixed, prevaporized combustion systems to the point of practical application to advanced gas turbine engines requires quantitative knowledge of compressor exit turbulence parameters and the effects of turbulence intensity and scale on fuel preparation, the premixing process and fuel droplet evaporation.

Prior to this program, compressor exit turbulence test data have not been available, probably because compressor exit flow conditions represent a very severe environment for turbulence measurement instrumentation. Flow velocities, temperatures and pressure levels are very high. Also, high vibration levels and solid particles in the air stream can destroy fragile instrumentation very quickly.

Ruggedized cooled film probes were used in this program to measure CF6-50 compressor exit turbulence properties at three different engine idle condition test points. Data were also obtained with this probe at the 30 percent and at the 85 percent engine power settings but, unfortunately, the quality of the data for these conditions was not acceptable. These measurements were made by using an electric motor-driven probe actuator to set three "equal area" radial immersions in the compressor exit diffuser flow stream at an axial location 15.5 cm downstream of the compressor exit plane. At each engine test condition, the sensing element of the probe was moved to

three radial immersion points in the compressor exit flowpath. Each immersion point was located at the center of one-third of the flowpath cross-sectional area.

The turbulence probe was coupled to a constant temperature anemometer and signal conditioning system. An on-line readout system connected to the anemometer was used to check the data as it was acquired. A well calibrated digital voltmeter displayed the signal DC level, a true RMS meter measured the AC level and a small oscilloscope was used to visually observe the signal output. A magnetic tape recorder made a permanent record of the data which was used for the data reduction analysis. A Time-Data Fast Fourier Transform (FFT) system was used for the data reduction and curve plotting procedures.

At engine idle conditions, the turbulence intensity ranged from 4.8 percent to 5.6 percent and the length scale ranged from 5.64 cm to 6.95 cm. The length scale values are somewhat larger than the passage height at the measurement plane (5.54 cm), which indicates that the shape of the turbulent eddies are elongated in the axial direction. The microscale values range from about 0.73 cm to about 0.98 cm.

Power spectral density distributions show that a large proportion of the turbulent energy at the measurement plane is concentrated at frequencies below one kilohertz.

These turbulence data can be used to help simulate compressor exit flow conditions in development test programs for advanced combustion systems. These results also demonstrate the feasibility of using ruggedized cooled film probes to make turbulence measurements in the high pressure, high temperature and high velocity environment of an operating gas turbine engine.

However, a considerable amount of probe development work will be required to develop turbulence measurement probes that can withstand the very severe environment encountered in the compressor exit flow of a gas turbine engine at high engine power operating conditions.

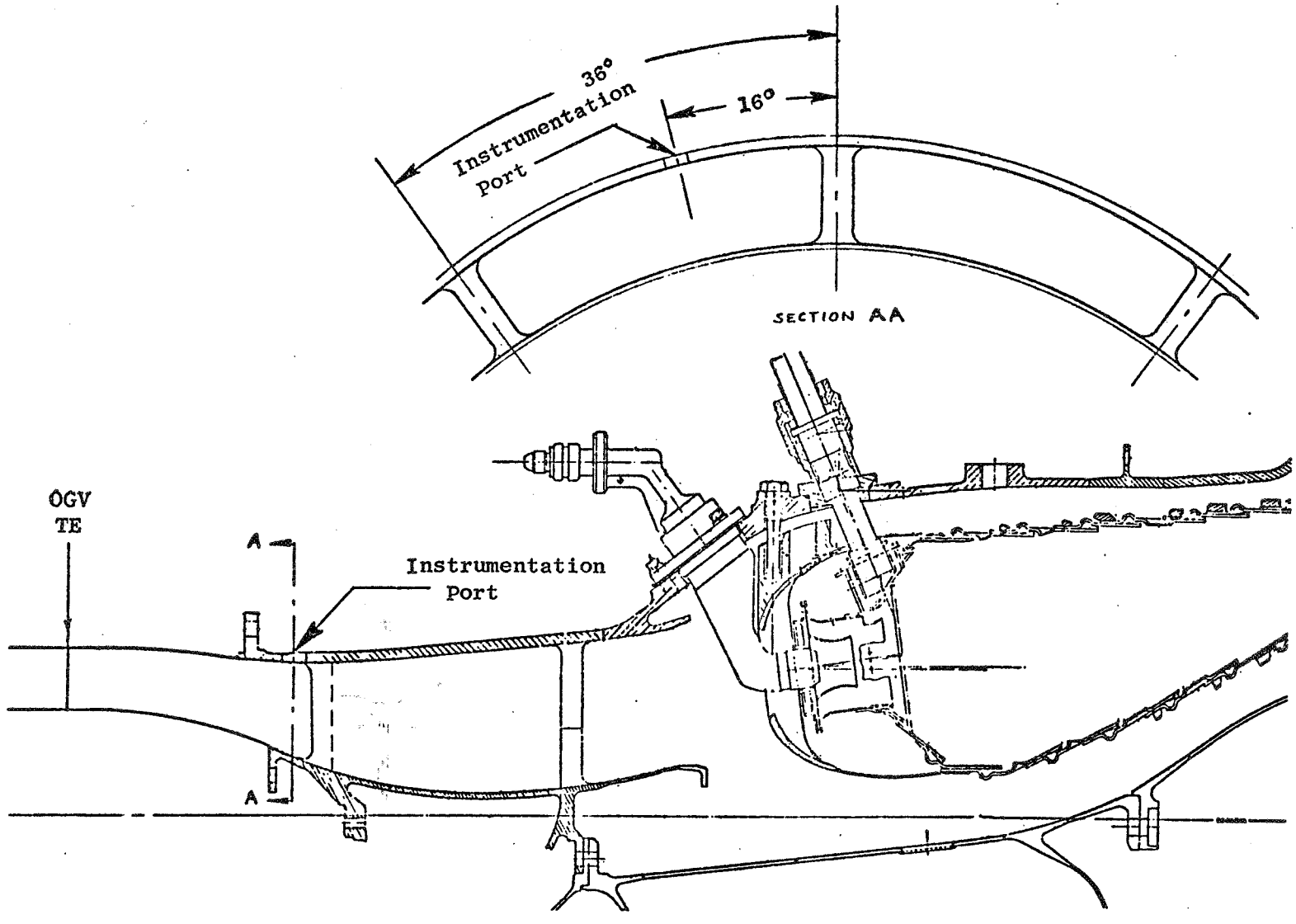

CF6-50 Frame Drawing Showing Instrumentation Port Location.

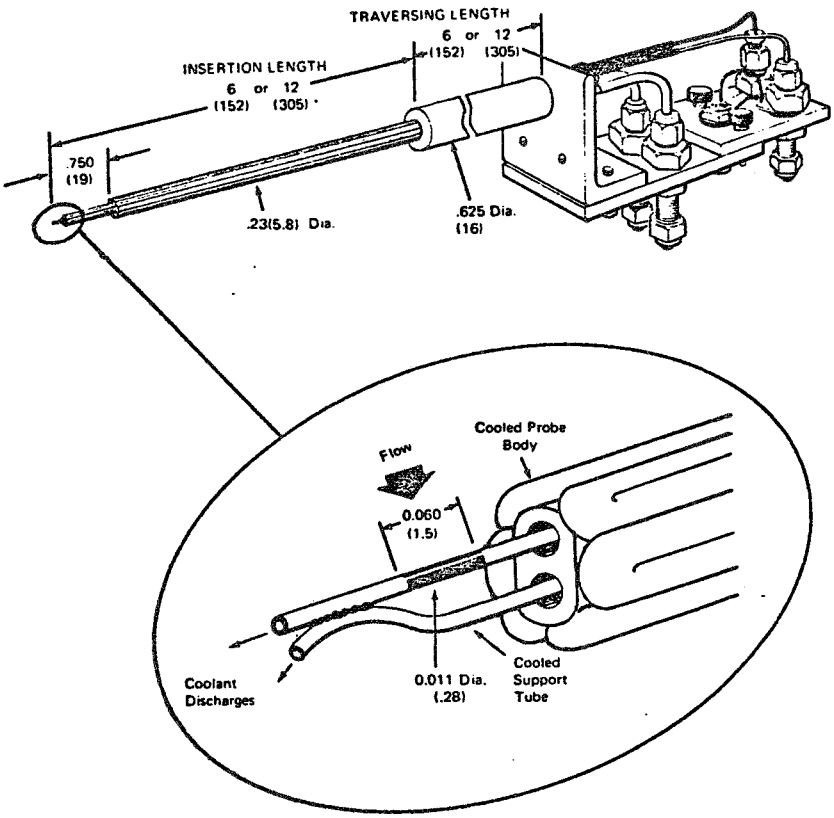

Water-Cooled Hot Film Probe

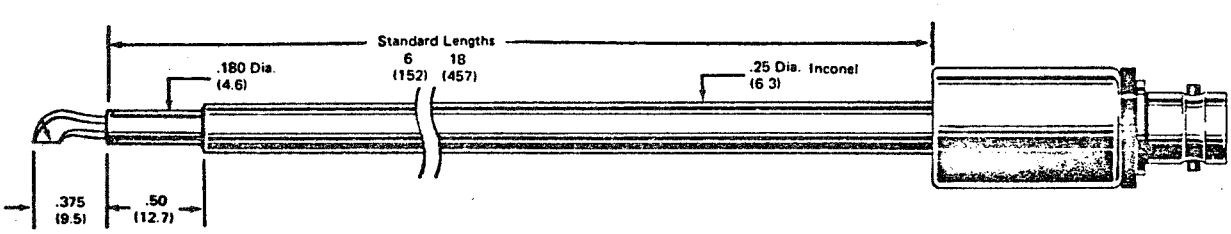

Hot Wire Probe

Turbulence Measurement Probes.

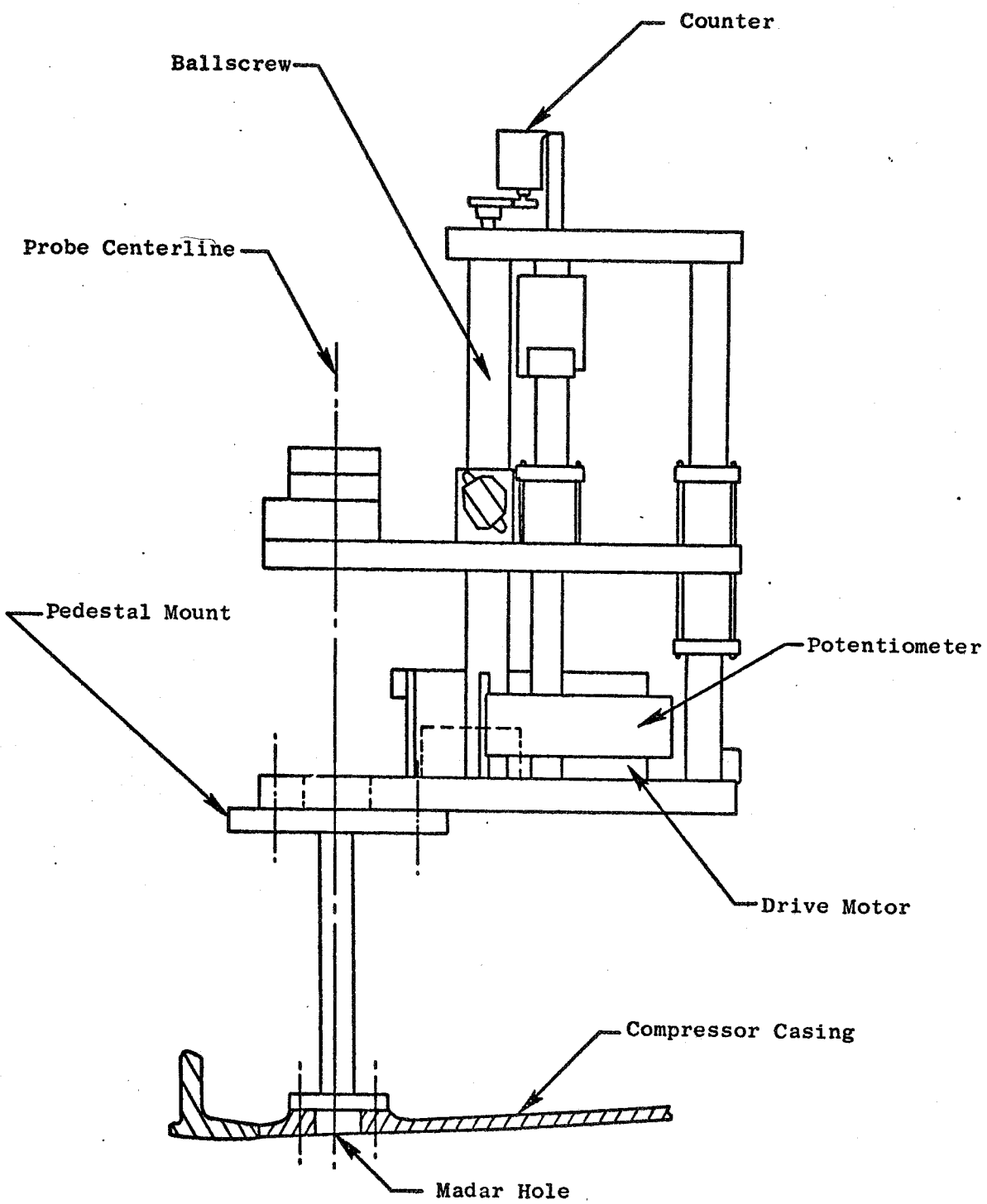

Turbulence Probe Actuator.

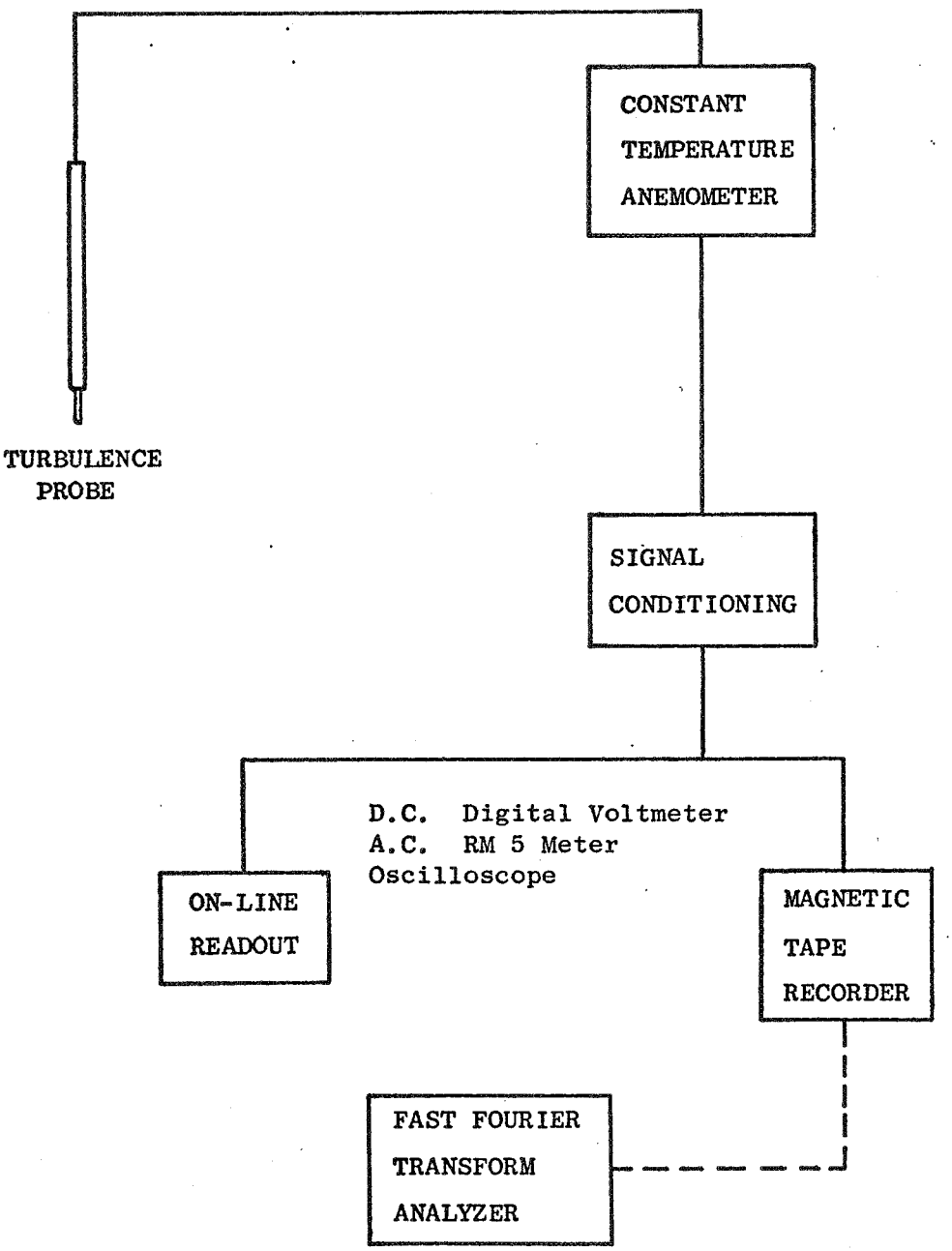

Data Acquisition and Reduction System.

TURBULENCE TEST DATA

DATA POINT NUMBER	95	106	106	106A	106A	106A
PROBE POSITION	INNER	INNER	OUTER	INNER	CENTER	OUTER
CALCULATED VELOCITY - m/sec	68.3	69.2	69.2	68.6	76.2	68.6
TURBULENCE - m/sec	3.26	3.66	3.44	3.60	4.27	3.84
TURBULENT INTENSITY - %	4.8	5.3	5.0	5.2	5.6	5.6
TURBULENT MISCOSCALE - cm	0.73	0.94	0.85	0.79	0.98	0.91
TURBULENT LENGTH SCALE - cm	6.58	6.04	5.73	5.64	6.95	5.97

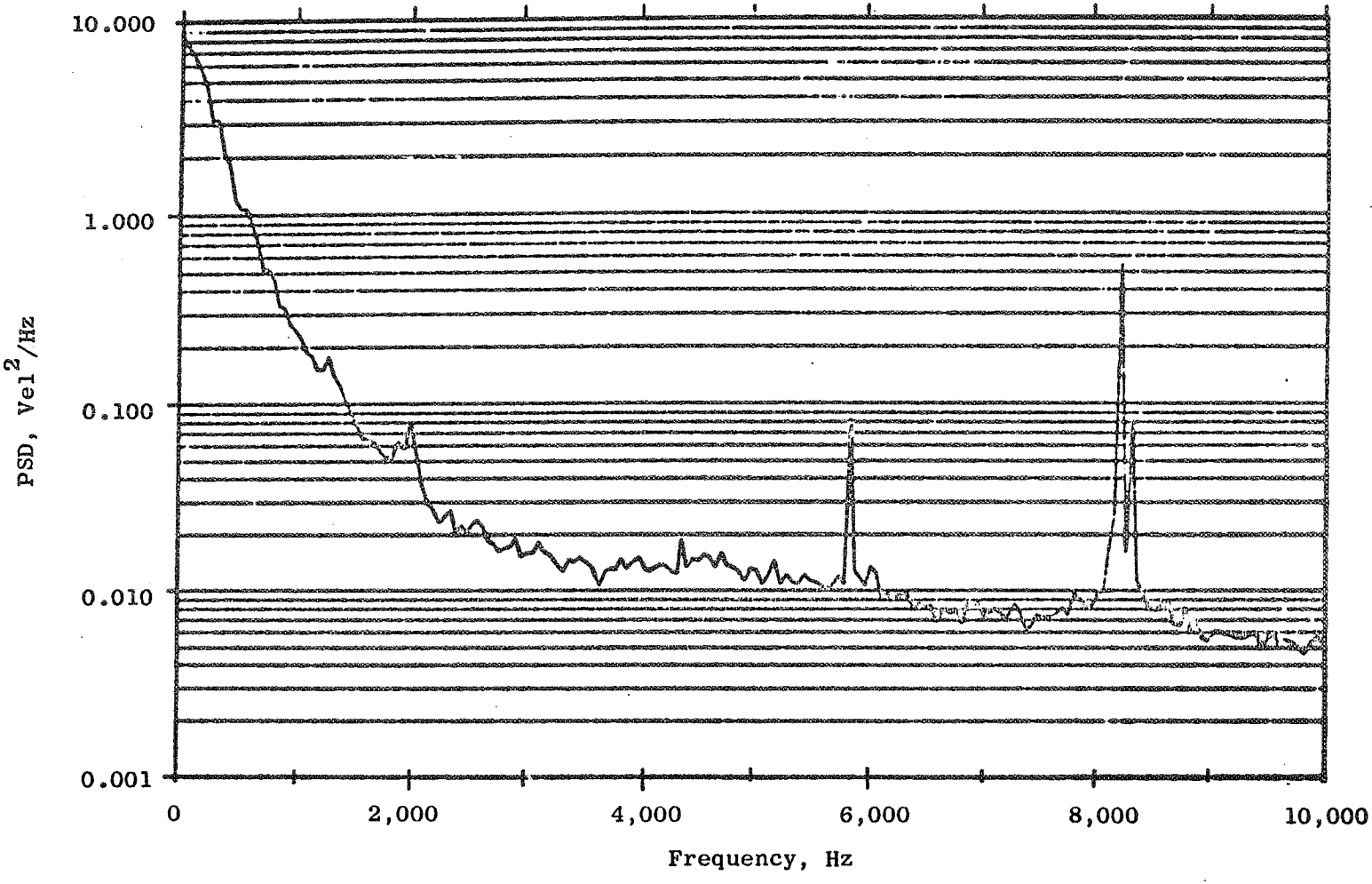

Power Spectral Density for Data Point 106A, Outer Probe Position.

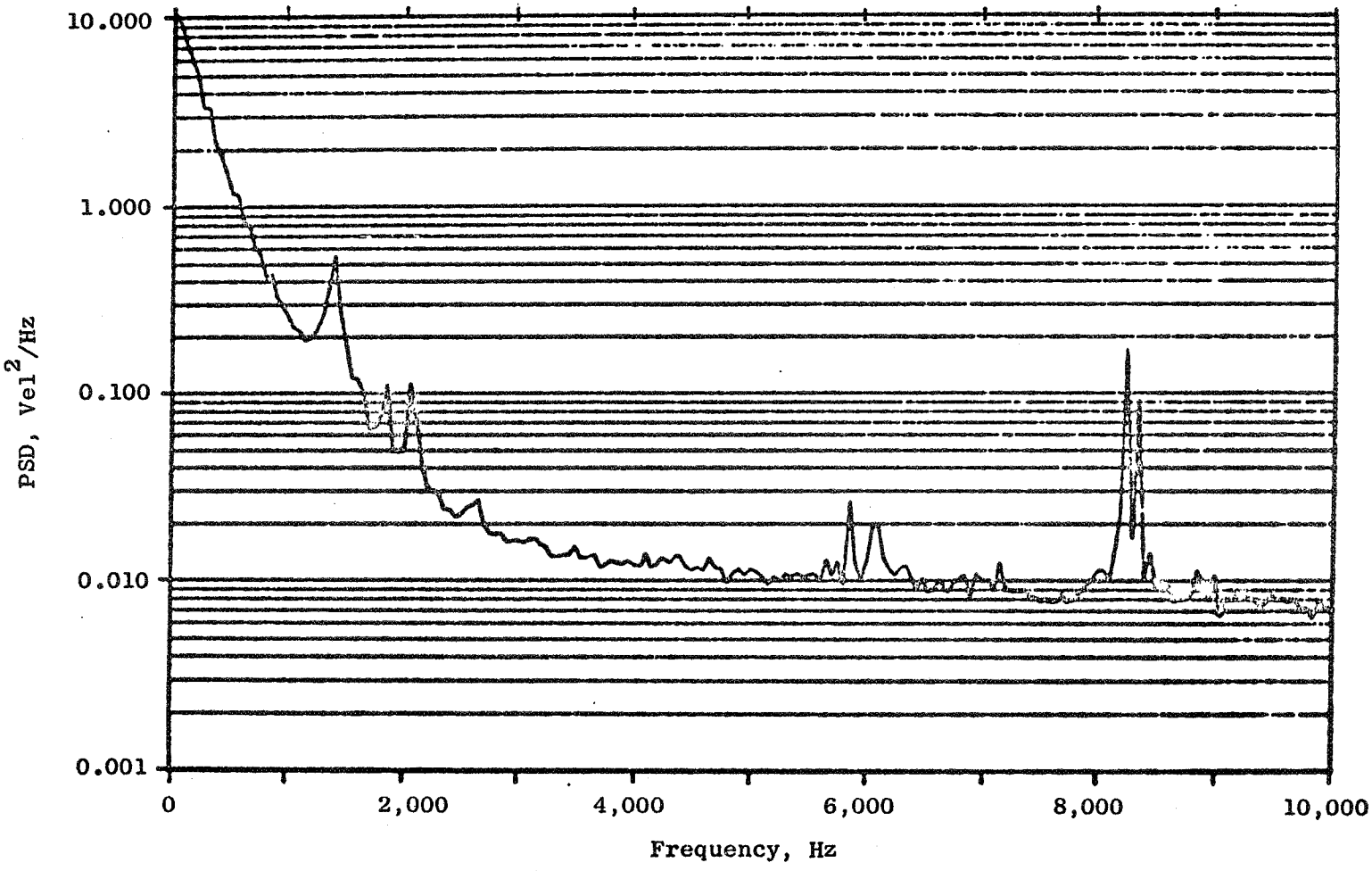

Power Spectral Density for Data Point 106A, Center Probe Position.

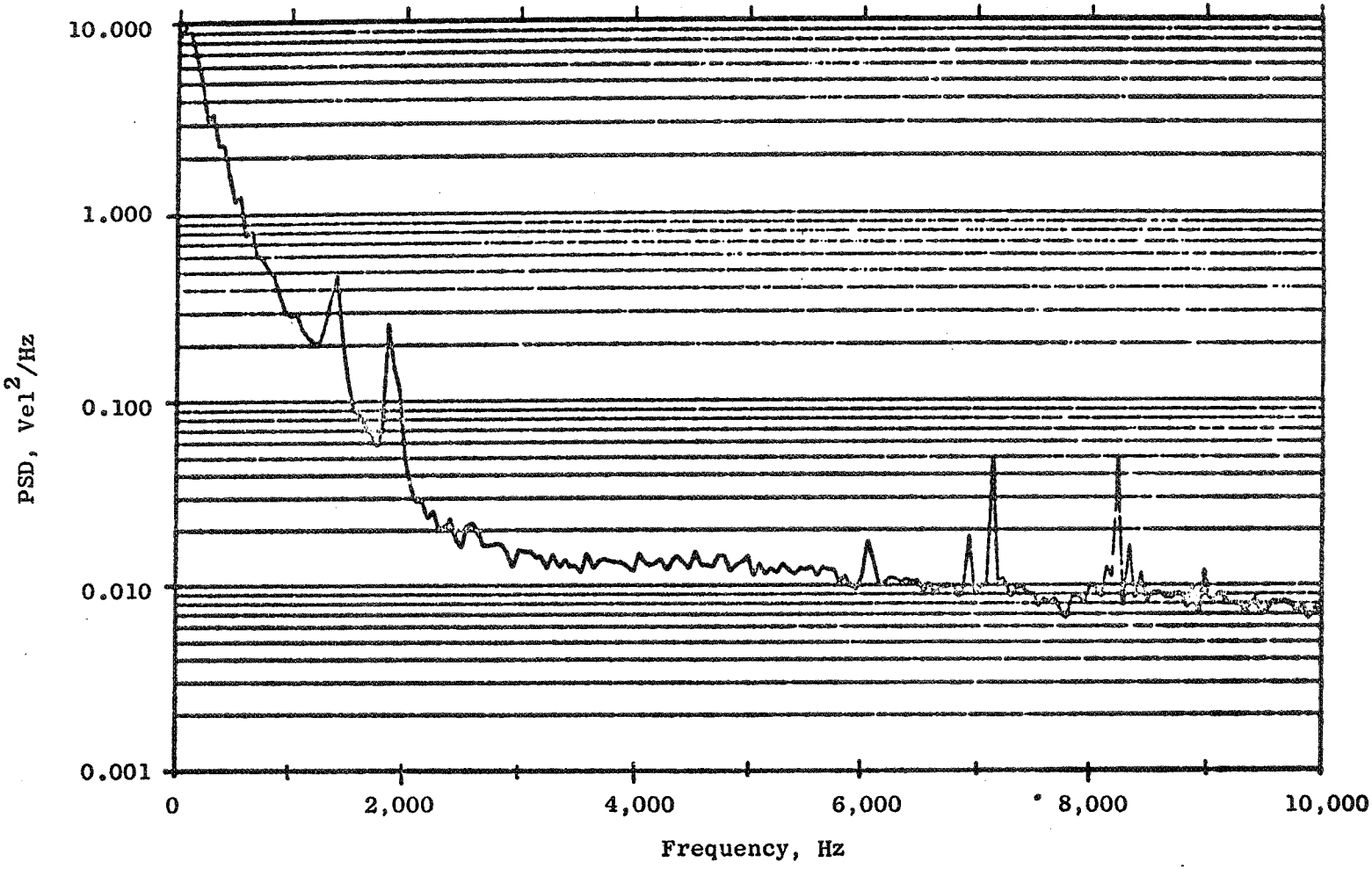

Power Spectral Density for Data Point 106A, Inner Probe Position.

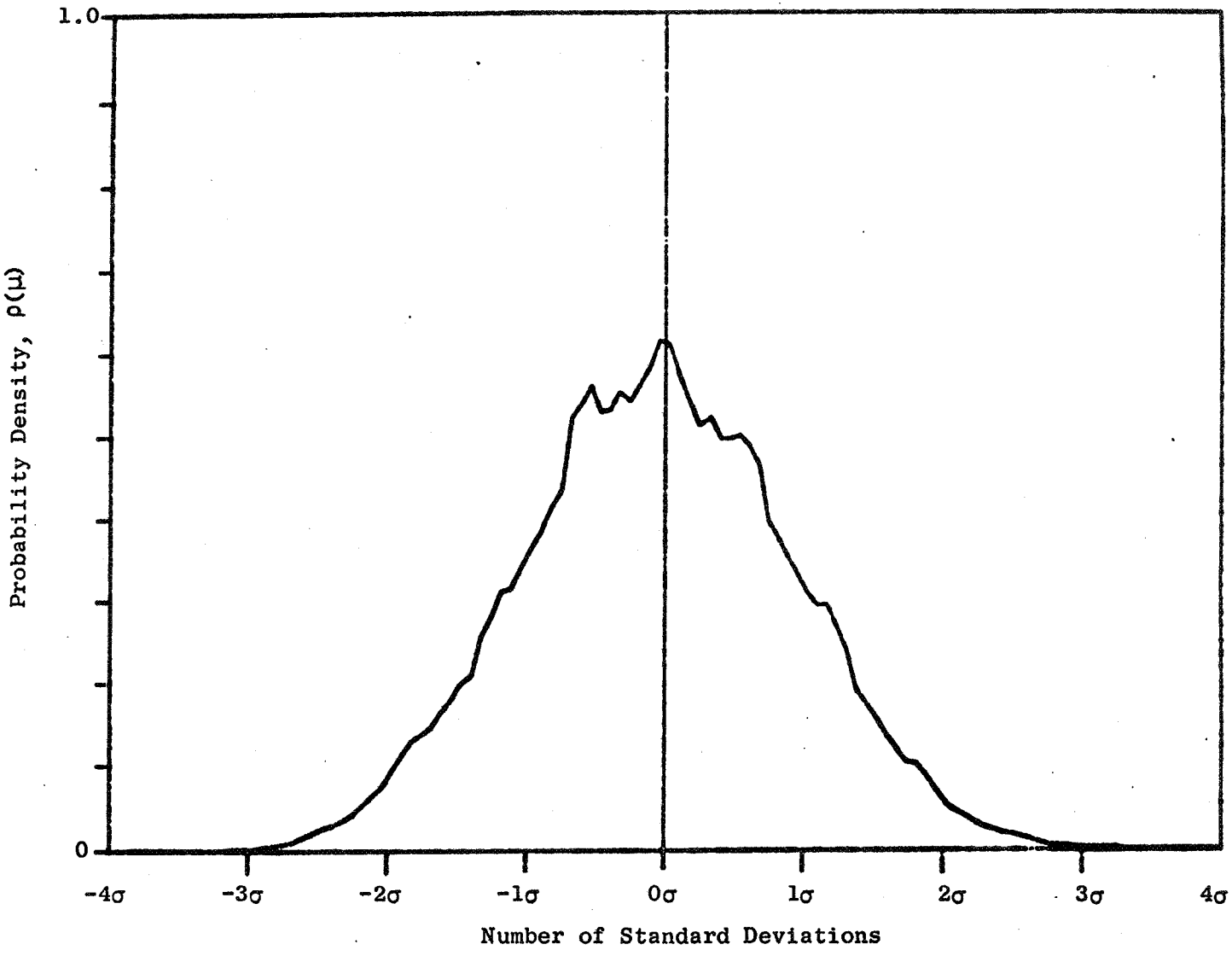

Probability Density for Data Point 106A, Center Probe Position.

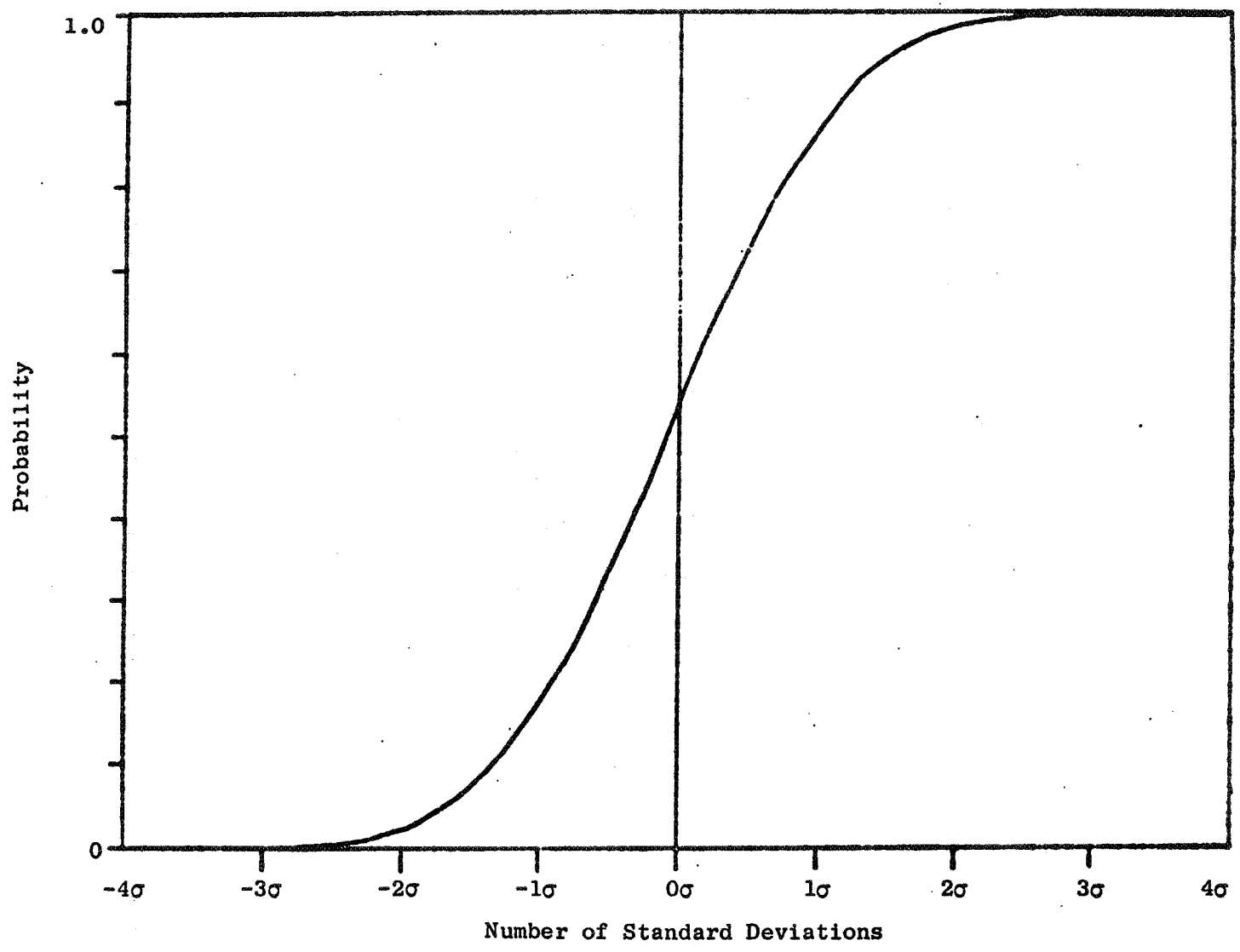

Probability Distribution for Data Point 106A, Center Probe Position.

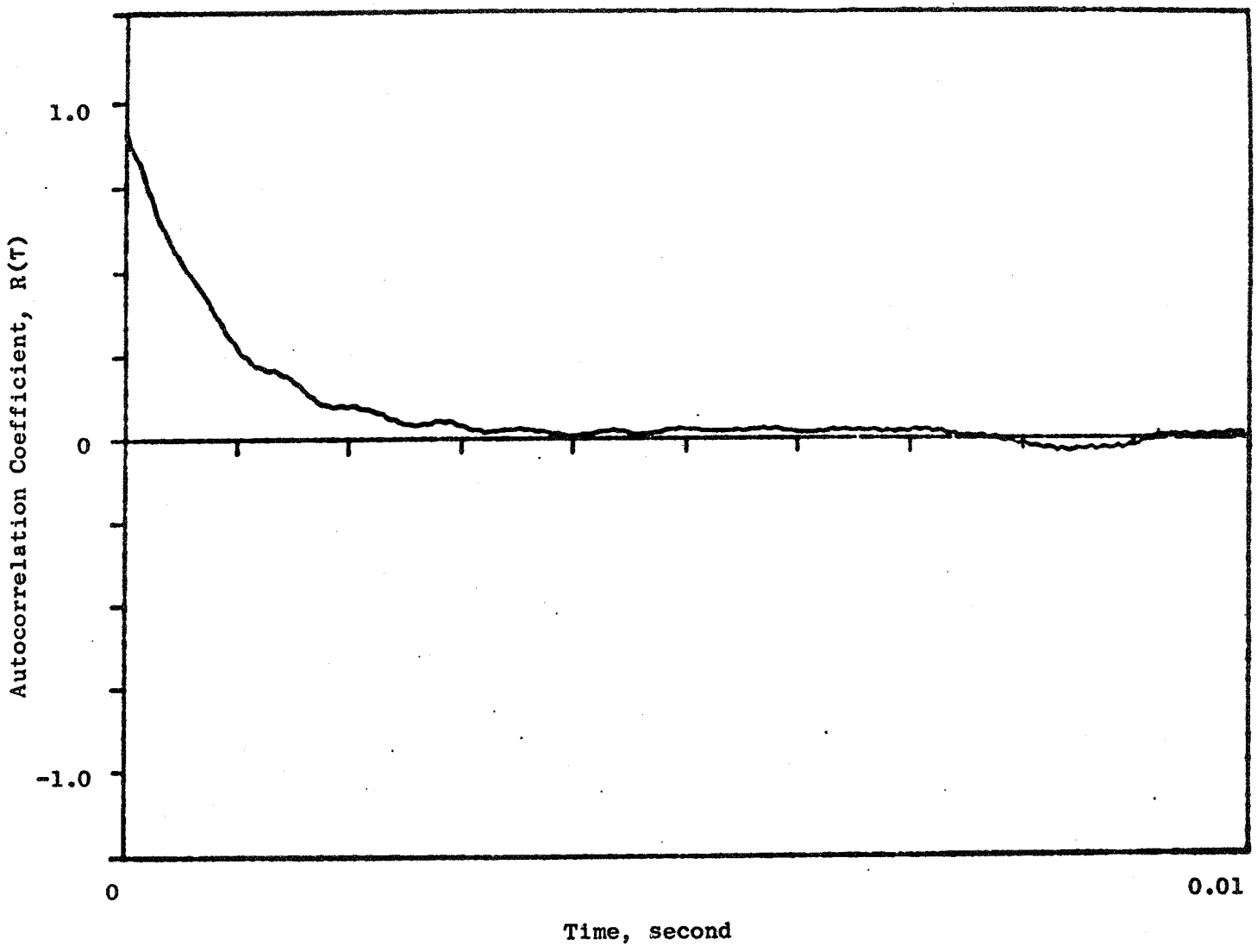

Autocorrelation Coefficient for Data Point 106A, Center Probe Position.

FUEL SPRAY DATA WITH LDV

CONTRACT NAS3-20662

David A. Rohy
John G. Meier
Solar Turbines International
P.O. Box 80966, San Diego, CA 92138

Successful application of the lean premixing-prevaporizing combustor concept requires an understanding of the operational characteristics of a fuel-air preparation section. The stability limits, efficiency, emissions, autoignition and flashback characteristics of premixing-prevaporizing combustors depends upon the mixing and distribution of fuel droplets, air and vapor, the degree of vaporization, the droplet size distribution and the gas flow properties.

The data obtained in the course of this contract will be used to calibrate and verify an analytical computer model of fuel/air preparation sections.

MEASUREMENT CAPABILITIES

Solar Turbines International sponsored the development of a special instrument for combustion research in gas turbine combustion systems at Spectron Development Laboratories. The instrument is unique in its capabilities of simultaneous measurement of droplet size and two component velocities in the severe environment of an operating gas turbine combustor system (Fig. 1). The instrument is referred to as the Solar Laser Morphokinetomer (SLM) and incorporates the following capabilities:

- Measurement of a true two-dimensional velocity vector with a range of $\pm$(0.01-200 m/sec)
- Measurement of particle size (range 5-300 μm) simulxaneously with the measurement of velocity
- Specification of probe volume position coordinates with a high degree of accuracy ($\pm$0.5 mm)
- Immediate on-line data checks
- Rapid computer storage of acquired data.

The optical system (Fig. 2) of the SLM was constructed based on proven designs and incorporates an ultrasonic beam splitter to allow the measurement of a true two-dimensional velocity vector simultaneously with particle size. The optical system is designed so the instrument can be used in the backscatter observation mode. An off-axis detector with coincidence circuits has been added to further reduce the probe volume size.

A microprocessor (Fig. 3) with a limited storage capability permits immediate analysis of test data in the test cell. A NOVA 2/10 minicomputer is used for on-line data retrieval, temporary storage and limited in-cell data analysis. The test data are then transferred onto magentic tape for later, statistical analysis on an IBM 370/158 computer.

Before measurements can be made on an atomizer or spray nozzle, the instrument must be calibrated. Four experiments have been devised to achieve calibration; a spinning disk, a monodispersed droplet generator, a nitrogen flow tunnel and a calibrated spray nozzle. Each is briefly described below.

Fringe spacing for different optical parameters will be verified using a reference velocity calibrator. This consists of a disc with a steel pin protruding from the edge is rotated through the probe volume at predetermined velocities.

The monodispersed droplet generator will be used to assess the particle size measurement uncertainty of the SLM using water drops with sizes over the range of 15 to 300 μm. Typical microphotographs are shown in Figures 4. Any factors, such as refractive index, which might contribute to sizing errors using Jet A will also be evaluated.

Simultaneous measurement of particle size and velocity will be evaluated in a laboratory experiment. Glass beads of different size ranges 15-37 μm, 53-63 μm, 88-105 μm, 125-145 μm, 177-210 μm, 250-297 μm will be suspended in nitrogen in a fluidized bed and injected into a nitrogen stream. The particle stream exiting the tunnel will be analyzed with the SLM.

A pressure atomizer purchased and calibrated to provide a mean droplet diameter of 75 microns (Sauter Mean Diameter) by the Delavan Corp. will be evaluated at the operating conditions used during manufacturer's calibration in a spray nozzle test stand.

Fuel Spray Rig. When these experimental calibration procedures are completed in early January 1979, the SLM will be employed on the primary contract goal - the characterization of several fuel injectors under varying conditions of air pressure, temperature and equivalence ratio. These injectors will be installed in a special rig built for this purpose. It is shown in Figure 5 and 6 and is the SLM test cell.

Fuel Spray Characterization. During an experiment all pertinent data on air and fuel flow, and wall conditions, will be monitored on a data logger system. Data from the SLM will be automatically screened for validity, counted and stored on magnetic tape for later reduction.

The signal processing system is equipped with a small data acquisition system. This microprocessor is used to acquire large amounts of data in a histogram format and has programs which allow the recording of various system parameters in addition to measured data. The data which can be acquired with this system include: velocity histograms covering four decades of velocity variation; and particle size histograms which are programmed in terms of signal visibility measurements and correlated directly with a library

function which relates signal visibility to particle size. Also included in these programs are weighting factors which allow the normalization of the histogram such that equal sample space volumes are compared for the particle number density measurements. The microprocessor indicates the number of "events" or attempted measurements by the signal processor and it records the total data acquisition time, or the acquisition time for each measurement.

The data tapes will be processed by an IBM 370/158. The steps in this processing are: read header data and perform unit conversion for fixed operating conditions; read data in blocks, screen data against preset conditions, perform engineering unit conversion, apply anti-bias skewing factors, arrange data in matrices for storage, and arrange data in preselected output formats.

PROGRAMS AND PLANS

Calibration experiments have been built and debugged. SLM calibration is underway with completion scheduled for mid January. Software for data acquisition and for data handling are essentially completed.

Instrument bias studies have been completed by Dr. Farmer. The rig has been built, instrumented and installed. First atomizer tests should begin in mid January 1979. Atomizer characterization tests will continue through several months of FY 79.

1. Two equal intensity, coherent light beams are mixed at an angle.

2. A well-defined set of equally spaced interference fringes is formed by interference of the two beams.

3. Light scattered by a particle traversing the fringe set is modulated according to size and position of the particle.

4. Particle size is determined from the ratio of the amplitudes of (1) the modulated scattered intensity to (2) the average scattered intensity.

5. Particle velocity is determined by measurement of the signal time period.

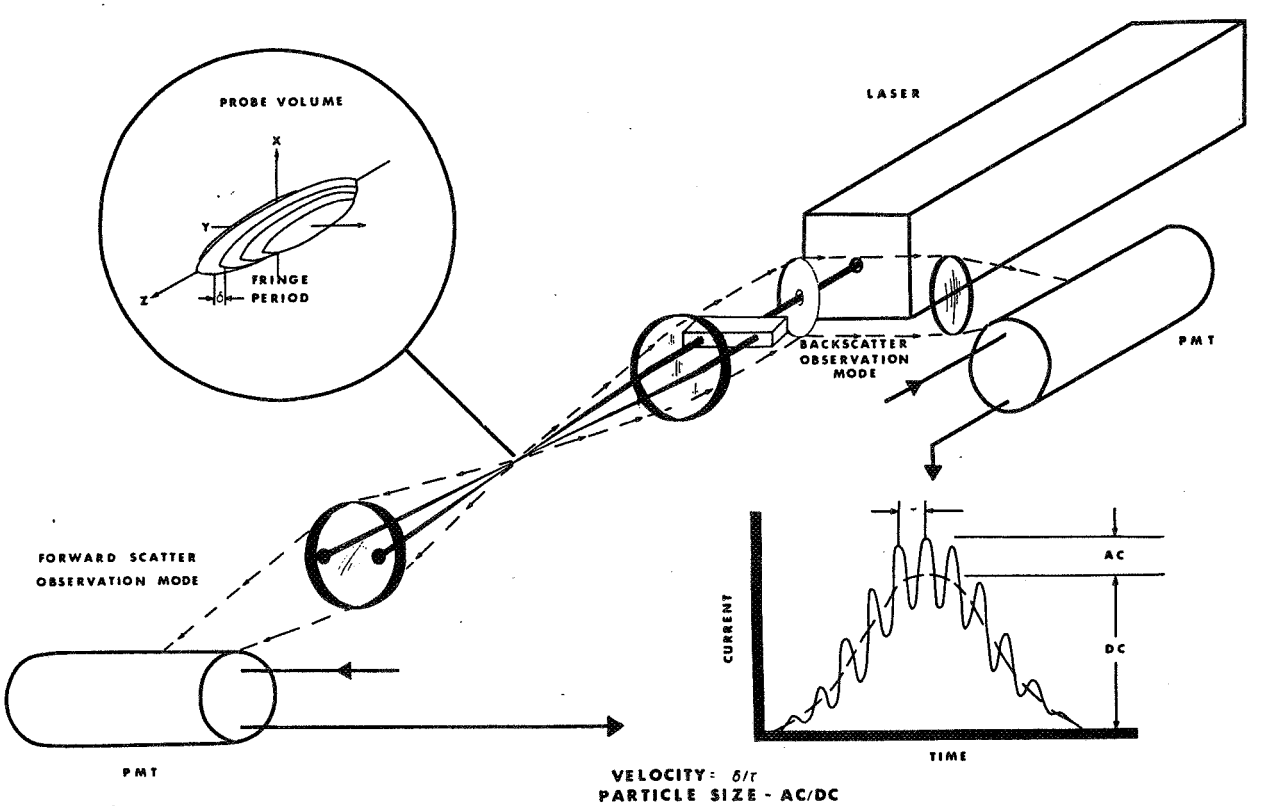

Figure 1. Interferometric Measurement of Velocity and Particle Size

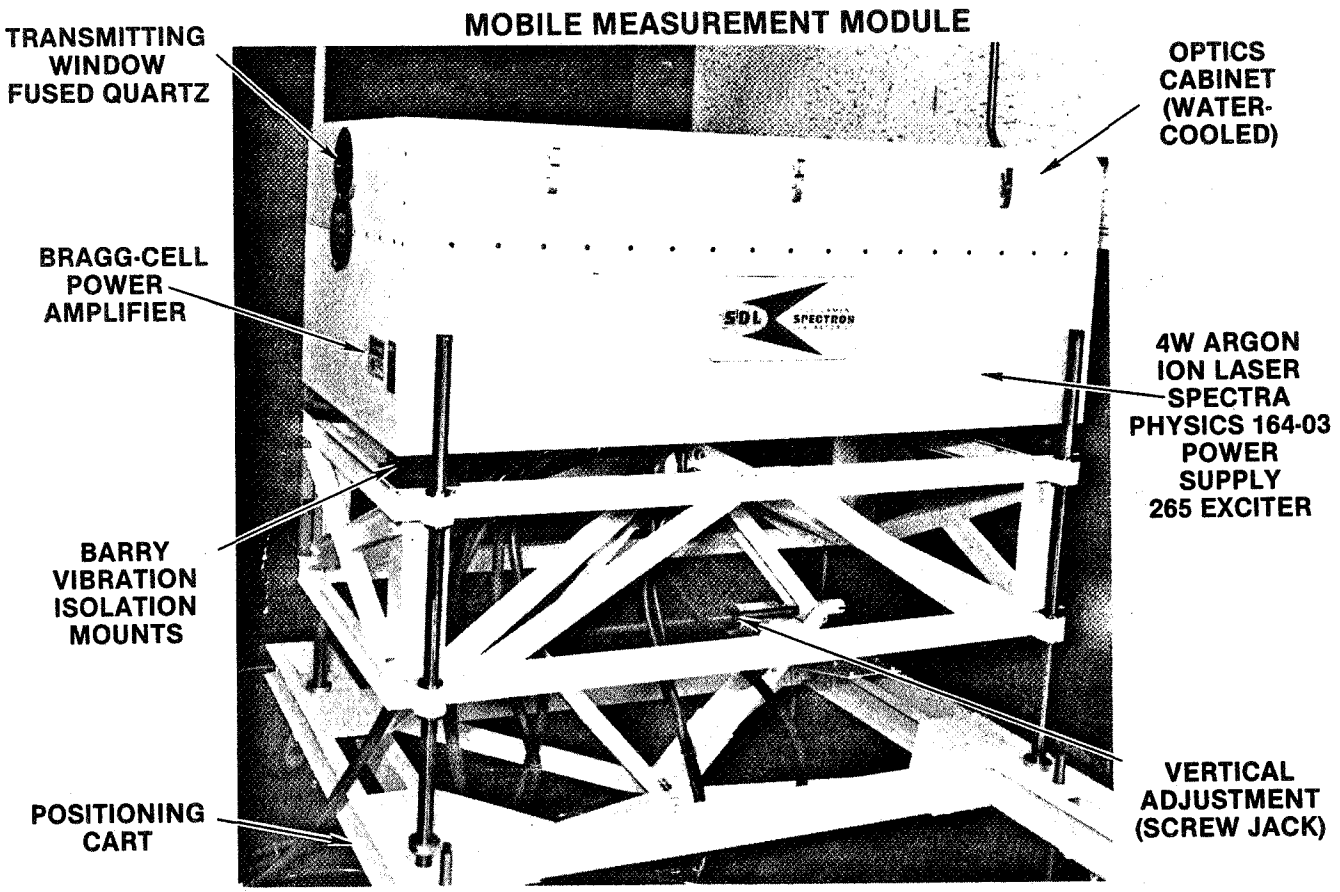

Figure 2. Mobile Measurement Module

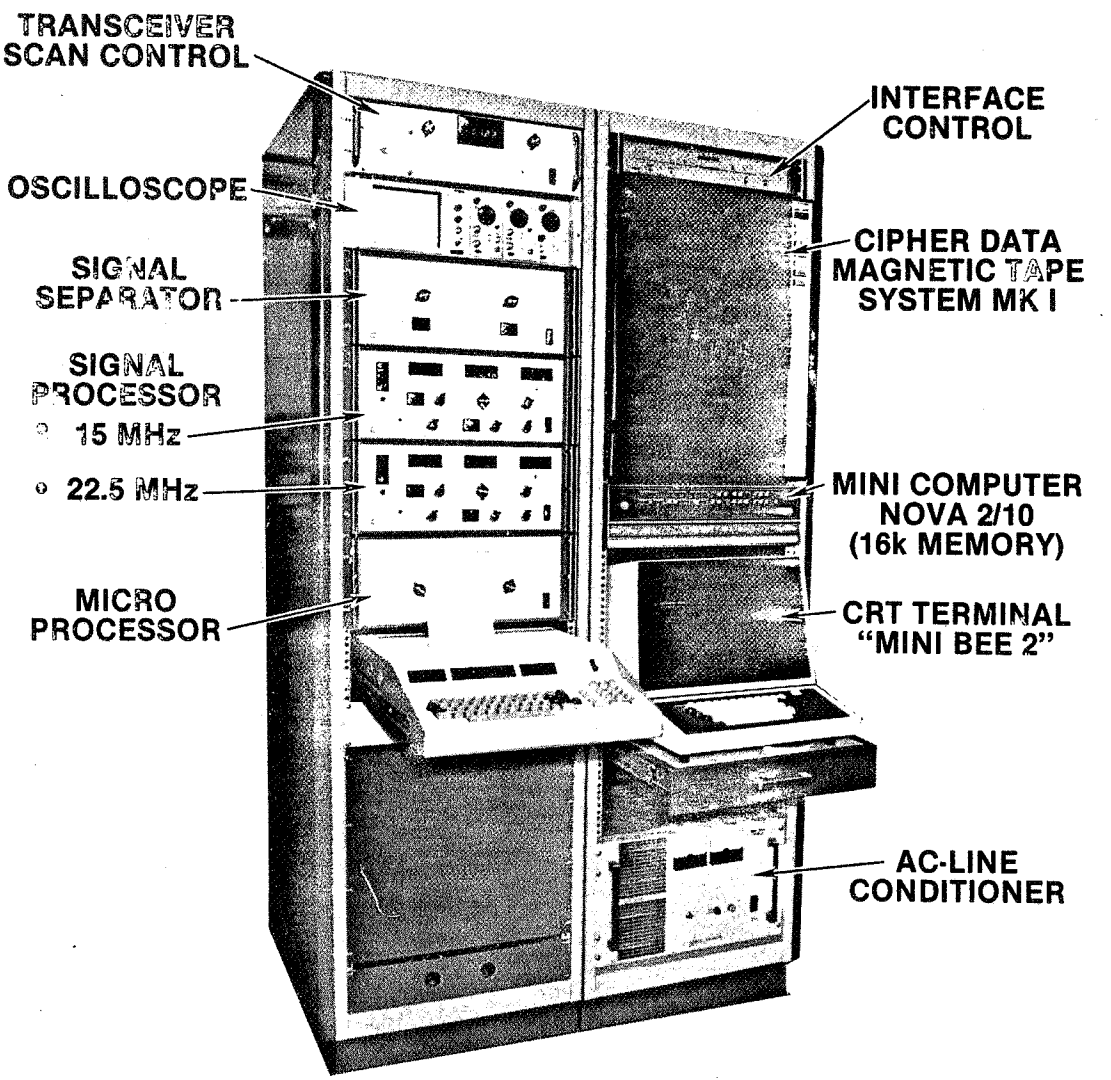

Figure 3. Signal Processing and Data Acquisition Module

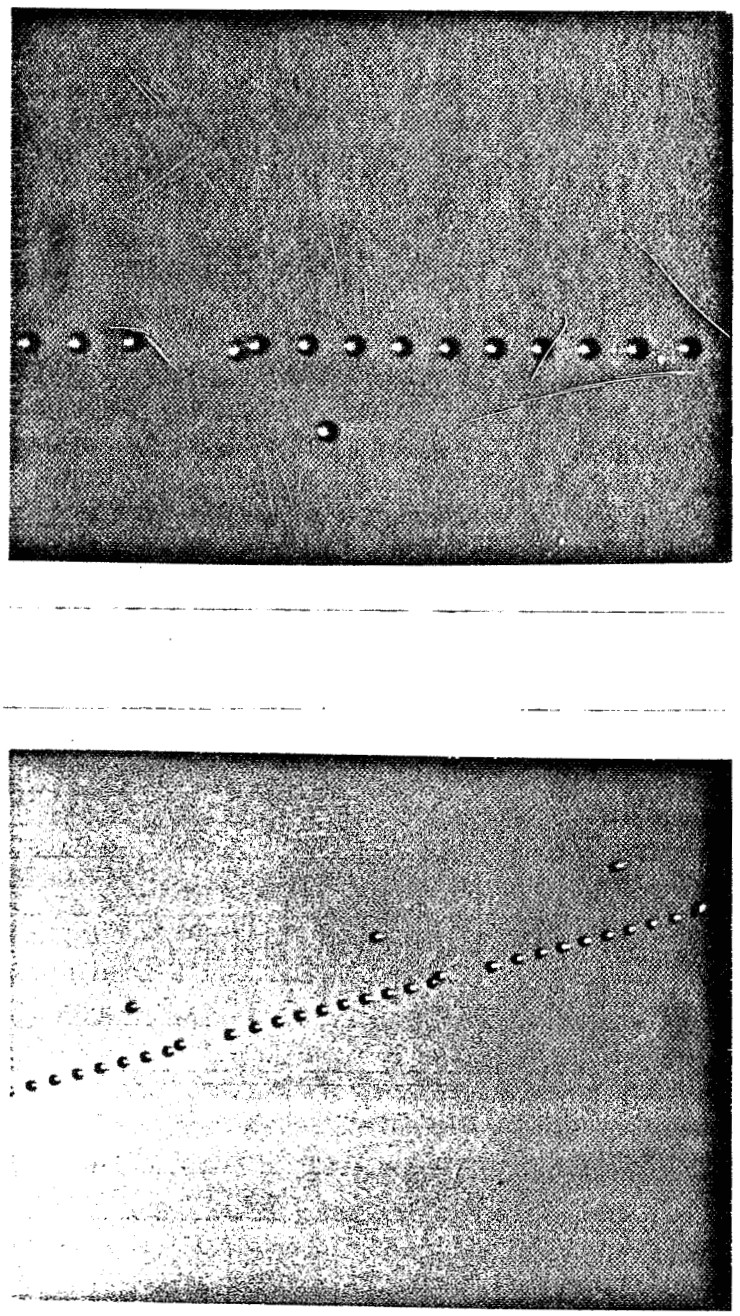

Figure 4. Droplets Produced by the Monodispersed Droplet Generator. An Electronic Deflecting Circuit Permits the Selection of a Small Number of Droplets for use in Calibration

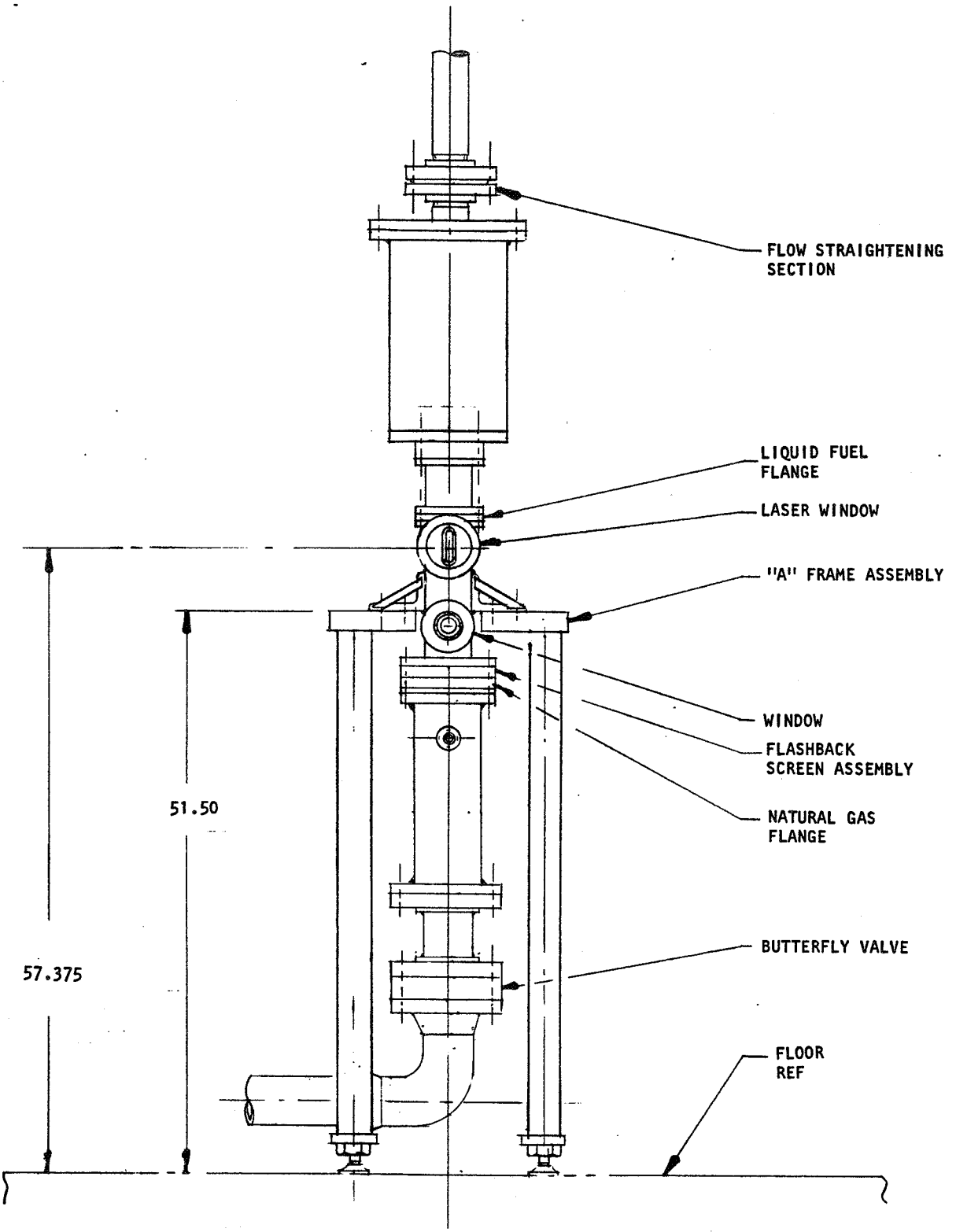

Figure 5. Fuel Atomization Rig Mounted on A-Frame

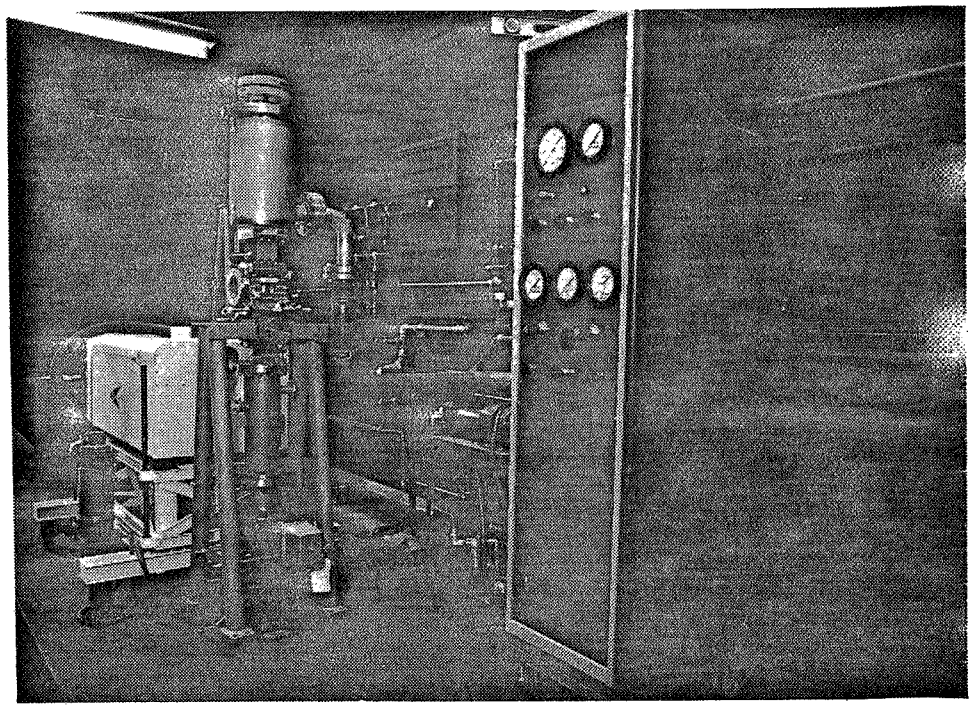

Figure 6. Fuel Spray Rig in Test Cell. SLM Optical System is in the Background

MODELING OF PREMIXING-PREVAPORIZING FUEL/AIR MIXING PASSAGES

NASA Contract NAS3-21269

O. L. Anderson
J. B. McVey
D. E. Edwards
L. M. Chiappetta

United Technologies Research Center
Silver Lane
East Hartford, Connecticut 06108

Introduction

One combustion control strategy for meeting governmental regulations on emissions of pollutants from internal combustion engines which has recently received considerable attention is the use of premixing, prevaporizing combustion concepts whereby uniform, homogeneous fuel-air mixtures are delivered to the combustion chamber in such proportions that the gas temperature-time history permits complete oxidation of the hydrocarbon fuel but does not permit significant production of oxides of nitrogen. Methods of achieving premixed prevaporized fuel-air mixtures include external vaporization schemes whereby the fuel is vaporized before being mixed with air and direct injection of a finely atomized spray into the airstream. The current program is concerned with the analytical prediction of the distribution of liquid and vapor fuel in the premixing-prevaporizing passage by the direct injection method.

Technical Program

The technical approach adopted for this program is to separate the problem into three parts each with its own computer code. These three parts are: calculation of the two-dimensional or axisymmetric air flow; calculation of the three-dimensional fuel droplet evaporation; and calculation of the fuel vapor diffusion. This method of approach is justified because premixing passages operate at lean equivalance ratios. Hence, a weak interaction assumption can be made wherein the air flow can effect the fuel droplet

behavior but the fuel droplet behavior does not effect the air flow.

Under these conditions the air flow can be calculated first and independently of the fuel droplet behavior. An existing UTRC computer code (ADD code) currently in use by NASA, will be used to calculate the axisymmetric or two-dimensional air flow in the premixing passages. This code was developed to solve the internal flow strong interaction problem using a forward marching numerical procedure that does not require iteration between the core flow and the wall boundary layers. This code can treat arbitrary inlet flow conditions. The pressures, temperatures, and velocities are then stored on a data file to be used in calculating the fuel droplet performance.

The fuel droplets will be treated as individual particle classes, each satisfying Newton's law, a heat transfer, and a mass transfer equation to account for nonequilibrium heat up and evaporation of liquid droplets in a moving gas stream. The particle classes will be defined by initial droplet size, three initial velocity components, and initial location. Each particle class will have associated with it a number density such that summation over all classes will yield the fuel flow rate. To permit the treatment of multicomponent fuels the computer code will keep track of the fraction of fuel vaporized as well as the pressure and temperature so that the distillation process can be described as the droplet vaporization proceeds. In addition the code will be constructed to model droplet dynamics when they may shatter or coalesce. To accomplish this, at the end of each calculation time step, the physical characteristics of the particle classes in each element of volume will be examined and droplets redistributed among existing classes according to a simple model of droplet coalescence or shattering. As the droplet calculation procedes the mass of fuel evaporated in each unit of volume will be stores on a data file.

The final calculation to be performed will be the gas phase turbulent diffussion processes in which the source term is determined from the mass of fuel evaporated. The turbulent properties of the flow will be determined by analogy of turbulent mass transfer to momentum transfer through a

turbulent Schmidt number using the calculated turbulent eddy viscosity from the ADD code air flow calculation.

Program Status

This technical program consists of three phases; computer model development, computer model calibration, and computer model verification. The program is presently in the early stages of phase one. Theoretical/empirical models for the problem have been selected and the computer code is in the process of bring written.

EFFECT OF FUEL SPRAYS ON EMISSIONS*

J.A. Nicholls†
Gas Dynamics Laboratories, Department of Aerospace Engineering
The University of Michigan, Ann Arbor, Michigan 48109

This program is aimed at operating a research gas turbine combustor under realistic conditions such that the influence of individual variables (in particular, fuel spray characteristics) on emissions can be determined. The special combustor allows independent control over drop size, fuel-air ratio, air inlet temperature, pressure, reference velocity, and residence time. Also, it lends itself to theoretical modeling and turbulent intensity measurements through use of laser velocimetry.

The combustor utilizes 37 needles for liquid fuel injection wherein each is surrounded coaxially with the primary airflow. Control of the air velocity largely determines the Sauter mean diameter (SMD) of the resultant spray. Other major components of the facility are the high pressure air supply, the air preheater, an enclosure for elevated pressure operation, and the exhaust system. A water cooled sampling probe, with steam heat to ensure sample integrity, is used for collecting the sample for the emissions instrumentation. Validity of the emissions results is tested by using the results in a comprehensive data analysis program to calculate the input fuel-air ratio. Comparison of this value with measured input values, along with the calculated summation of mole fractions, offers a good check on the measurements.

---

*To be presented at the Premixed-Prevaporized Combustor Technology Forum, NASA Lewis Research Center, January 9, 10, 1979. This research is supported under NASA NSG 3148, Dr. Larry Cooper, Project Monitor.

†Major contributions were made by the following personnel: Research Scientists D.R. Glass and C.W. Kauffman; Students D. Pelaccio, J. Draxler, R. Wood, S. Correa, and O. Kitapliglu; and Professor J.F. Driscoll.

An approximate one dimensional analysis of the combustor behavior, along with some kinetic implications, is briefly mentioned. This work has been published elsewhere [1,2] and hence no details are given here. Also, a few laser doppler velocimetry determinations of turbulence level and flow velocity have been presented elsewhere [3] and are only briefly mentioned. Some calculations on the influence of residence time, drop size distribution, and gas properties on the emissions index are presented and discussed.

The main results of this paper are in the form of emissions results for a range of operating conditions. A number of graphs are presented and discussed which show the variations of emissions levels with one variable at a time, among those variables listed in paragraph one. In every case the fuel is Jet A, the pressure is atmospheric, and combustion is restricted to a primary zone.

A short movie of the combustor in operation is shown.

References

1. Patil, P.B., Sichel, M., and Nicholls, J.A., "Analysis of Spray Combustion in a Research Gas Turbine Combustor," Combustion Science and Technology, Vol. 18, 1978, pp. 21-31.

2. Patil, P.B., Sichel, M., and Nicholls, J.A., "Calculation of CO Concentration for Liquid Fueled Gas Turbine Combustor," presented at Central States Section, The Combustion Institute, Purdue University, April 3-5, 1978.

3. Driscoll, J.F. and Pelaccio, D.G., "Laser Velocimetry Measurements in a Gas Turbine Research Combustor," presented at the Third International Workshop on Laser Velocimetry, Purdue University, July 1978.

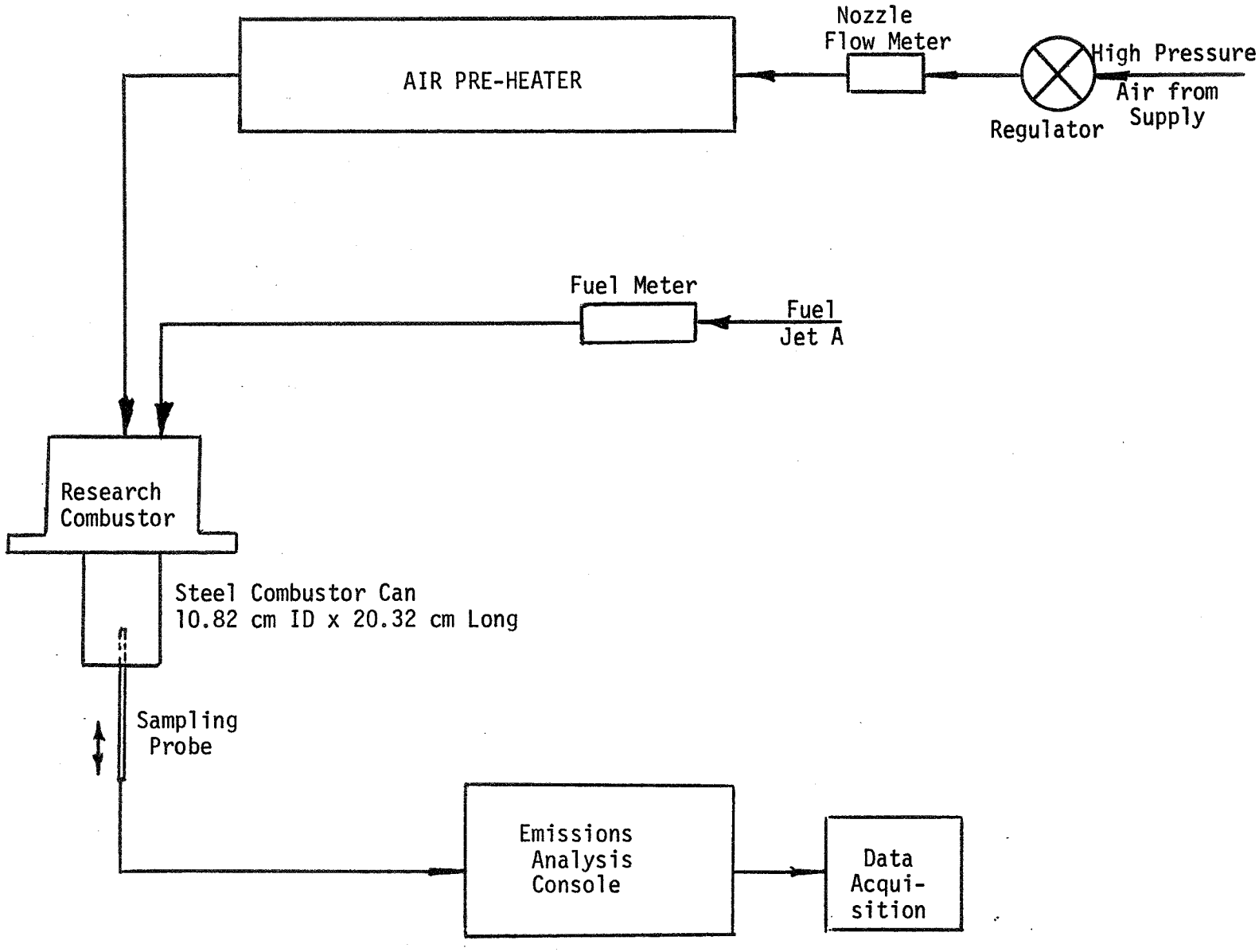

Figure 1. Schematic of Flow System

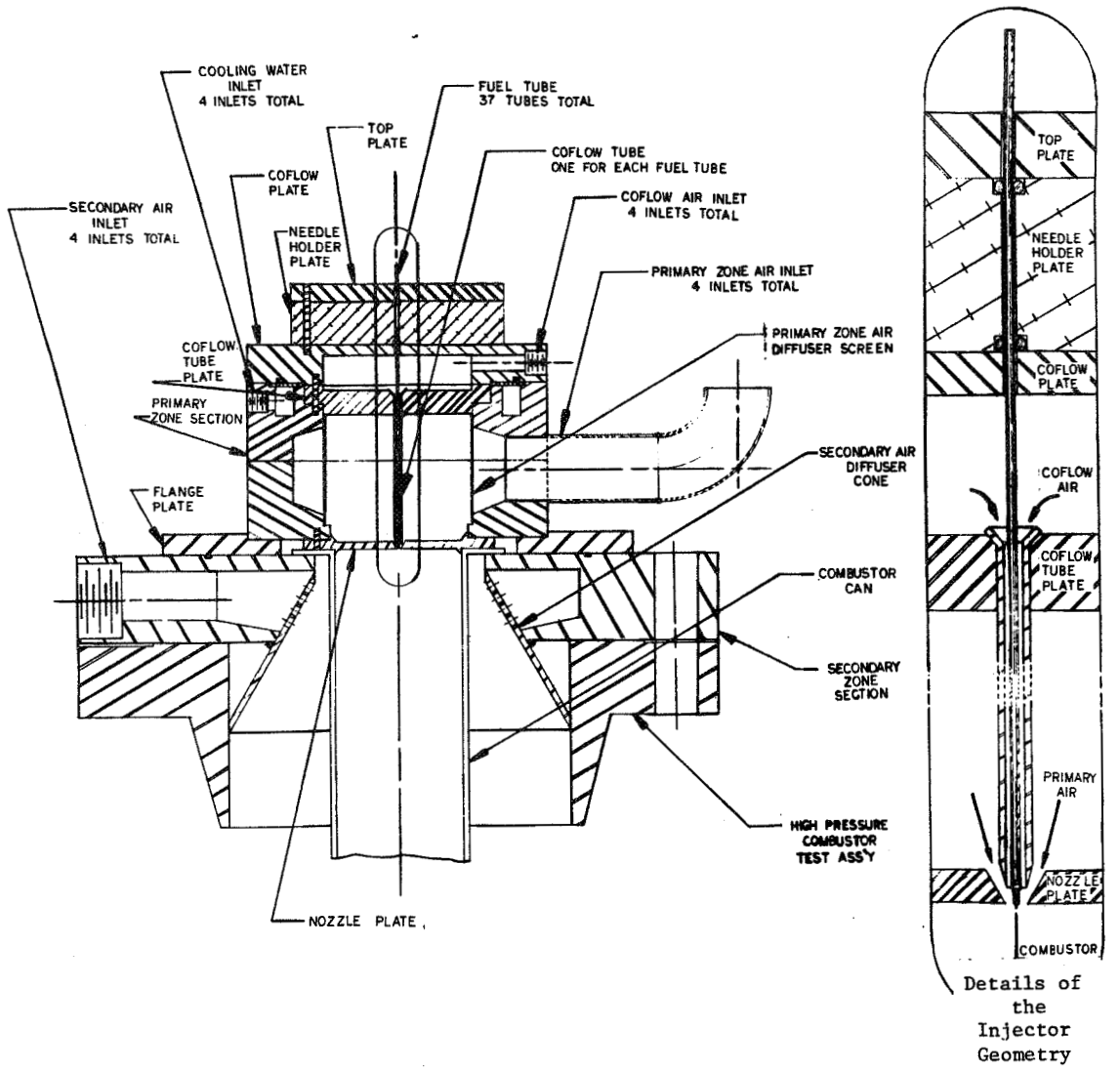

Figure 2. Fuel Droplet and Air Preparation System and Combustor.

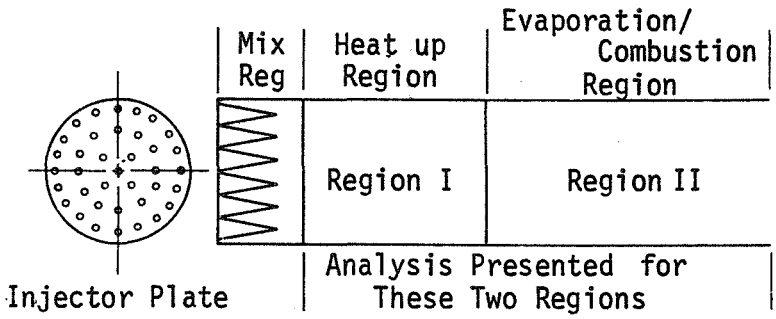

$\lambda_1 = k_1\lambda$ $\qquad\qquad$ $\lambda_2 = k_2\lambda$

λ = laminar coefficient of heat conduction

k_1, k_2 related to scale and intensity of the turbulence

u_1 = burning velocity

$u_1 \propto 1/r$ $\qquad$ Effect of drop size

$u_1 \propto (k_1 k_2)^{-1/2}$ $\qquad$ Effect of turbulence

Figure 3. One Dimensional Analysis

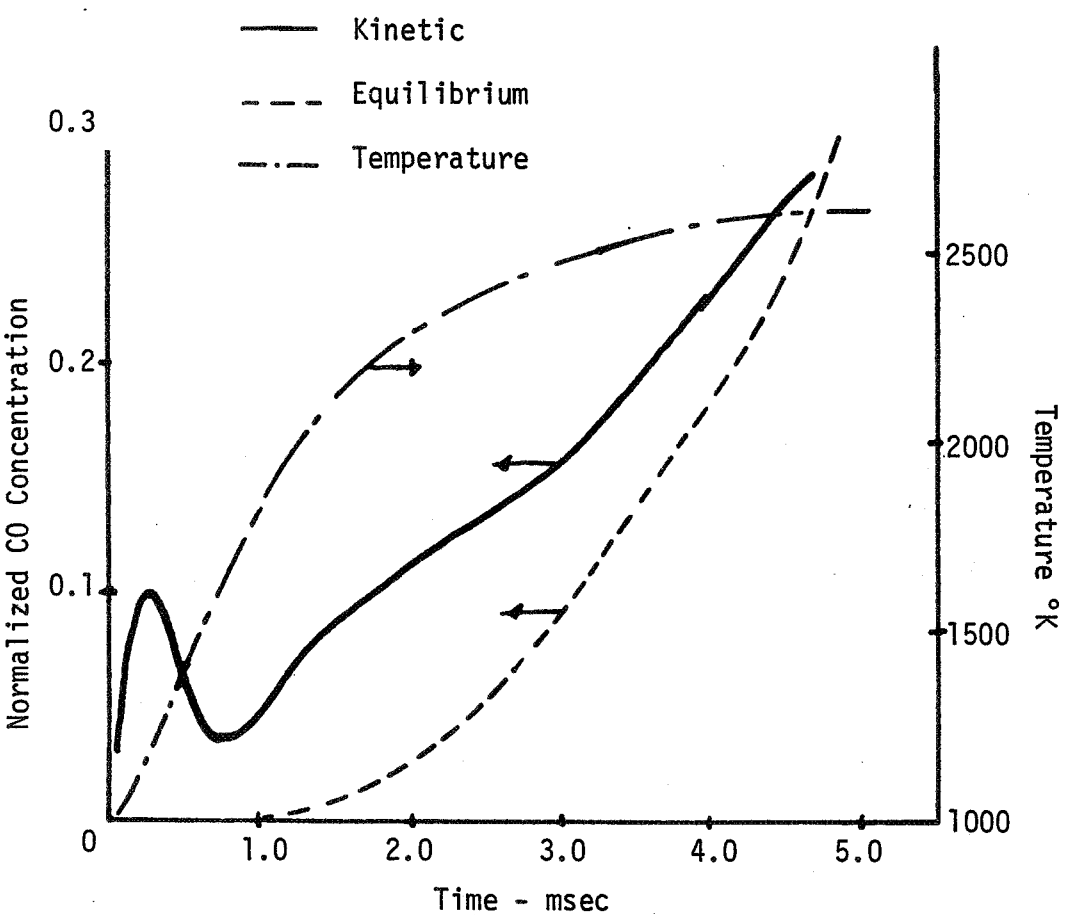

Figure 4. Inaccuracy of the Local Equilibrium Assumption for CO Concentration

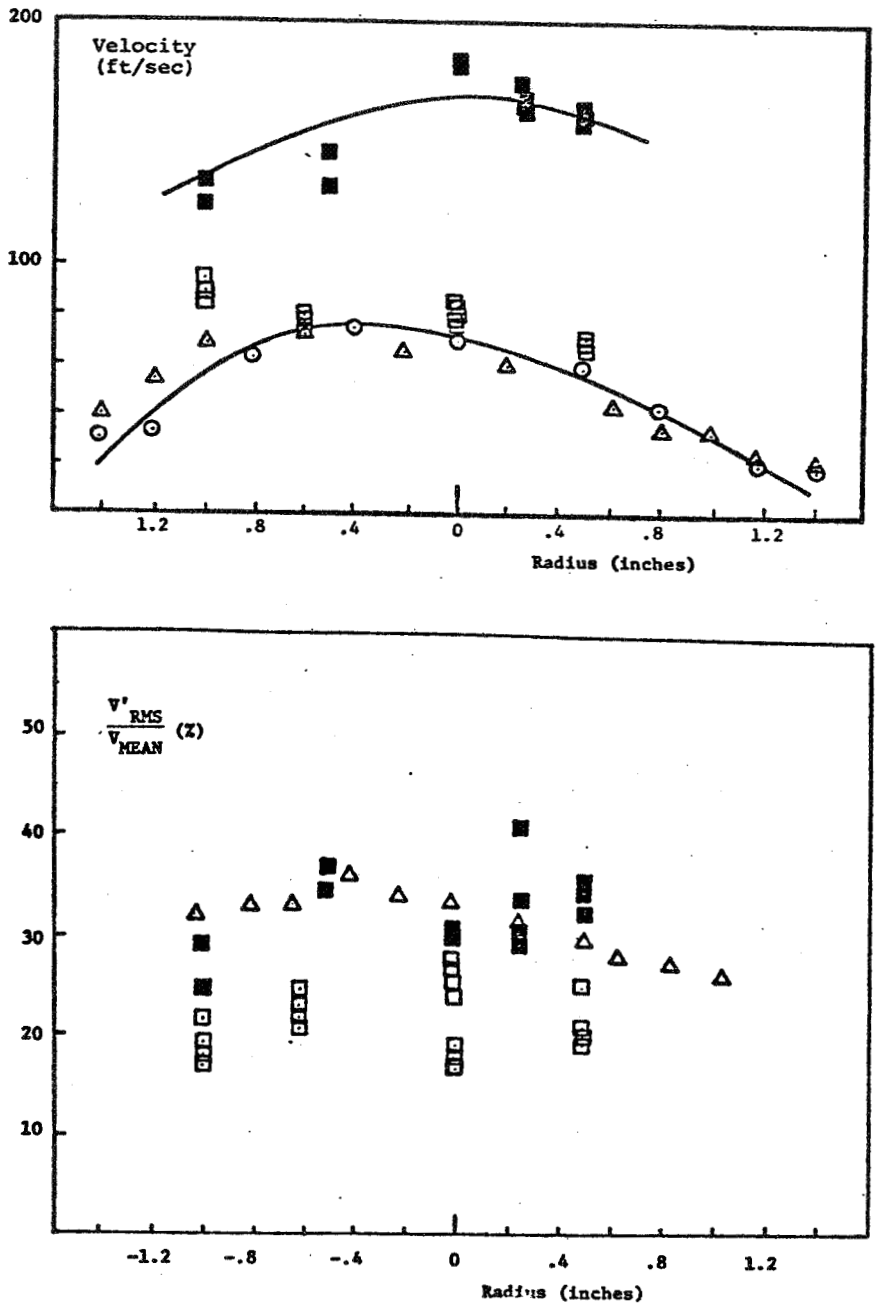

ϕ = 0.9

P = 1 atm

$\dot{m}$ = .158 lbm/sec

■ LDV Hot Flow

□ LDV Cold Flow

o Pitot Cold Flow

△ Hot Wire Cold Flow

Figure 5. Laser Velocimetry Measurements

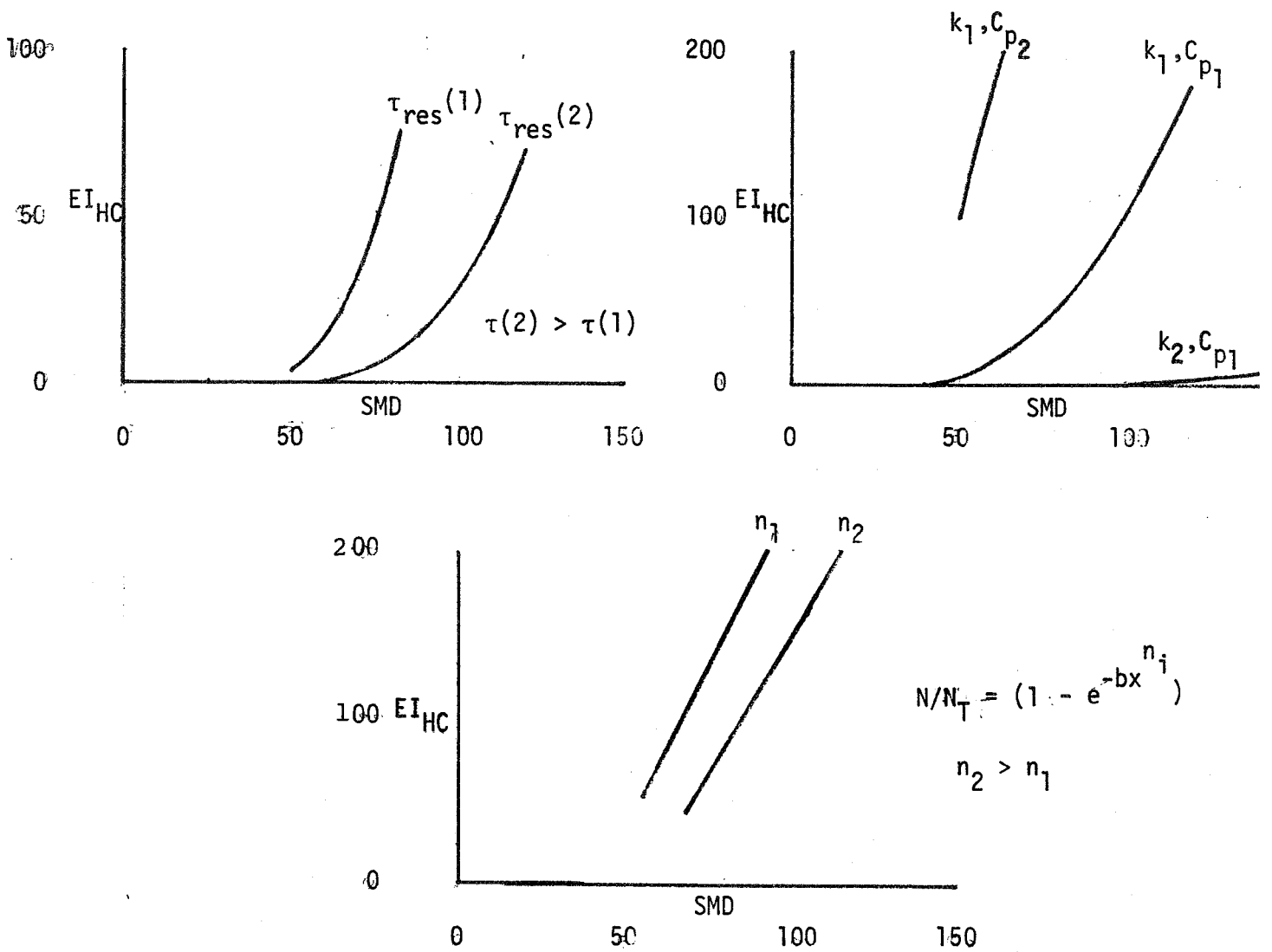

Figure 6. Influence of Residence Time, Gas Properties, and Drop Distribution Function on Emissions Index.

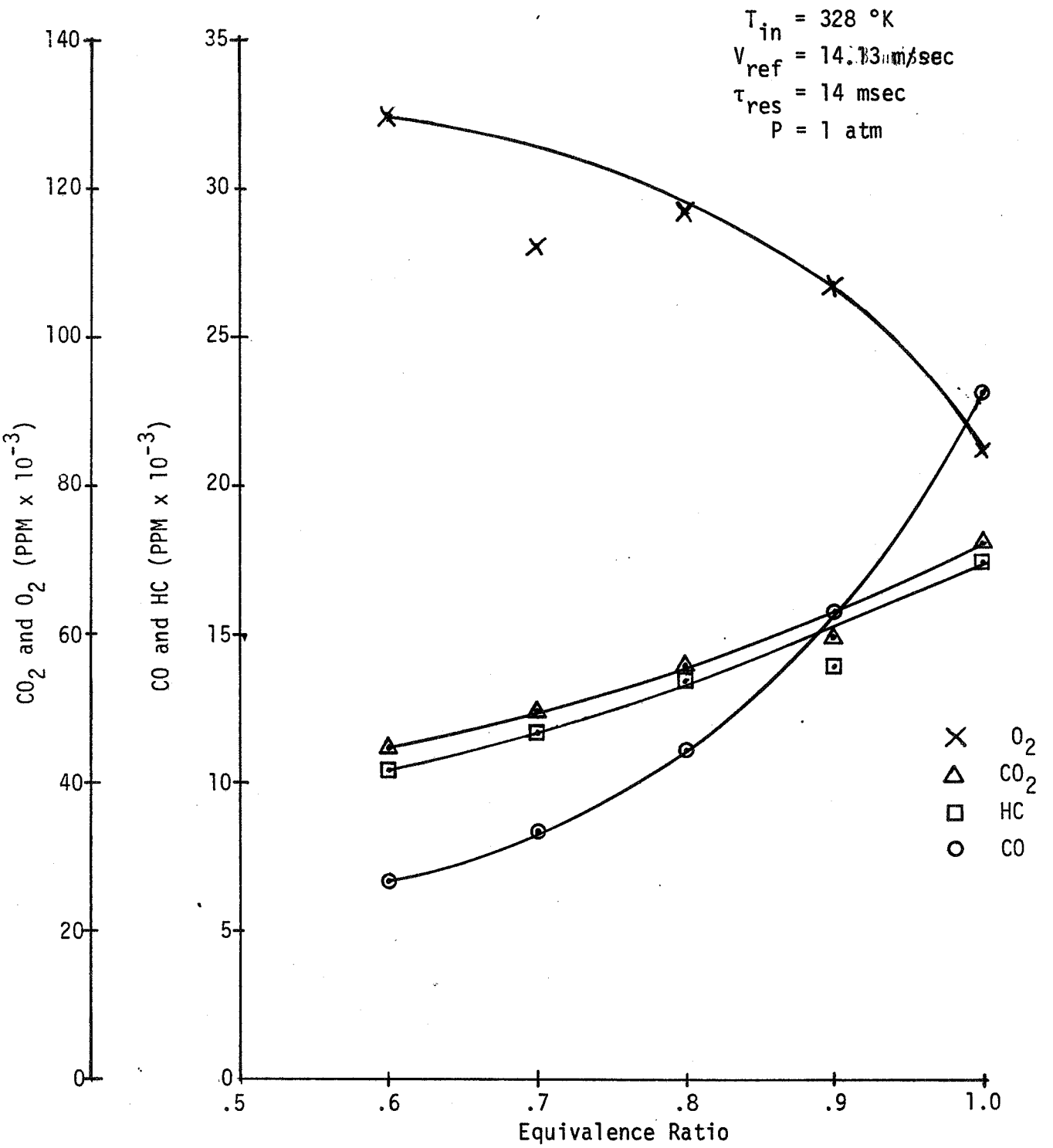

Figure 7. Emissions Variation with the Equivalence Ratio

PERFORMANCE OF A MULTIPLE VENTURI FUEL-AIR PREPARATION SYSTEM

by

Robert R. Tacina

A premixed-prevaporized fuel preparation system was designed and tested for use in catalytic reactors for gas turbine applications. A Multiple Conical Tube fuel injector was previously tested that satisfied the goals for a premixed-prevaporized system (spatial fuel-air distribution was within 10 percent of the mean and nearly 100 percent vaporization was achieved at an inlet air temperature of 700K). The purpose of the conical tubes was to provide high velocity air for atomization and also straighten the inlet air velocity profile. A refinement of this injector was tried that used Venturi tubes instead of conical tubes to improve the atomization and shorten the residence time. Within this Multiple Venturi Tube fuel injector the throat velocity was increased for better atomization with the total pressure loss designed to be the same as the Multiple Conical Tube fuel injector.

Spatial fuel-air distributions, degree of vaporization, and pressure drop were measured 16.5 cm downstream of the fuel injection plane of the Multiple Venturi Tube fuel injector. Tests were performed in a 12 cm tubular duct. Test conditions were: a pressure of 0.3 MPa, inlet air temperature from 400 to 800K, air velocities of 10 and 20 m/s, and fuel-air ratios of 0.010 and 0.020. The fuel was Diesel #2. Spatial fuel-air distributions were within $\pm$ 20 percent of the mean at inlet air temperatures above 450K. At an inlet air temperature of 400K, the fuel-air distribution was within $\pm$ 30 percent of the mean. No distortion in the fuel-air distribution was measured when a 50 percent blockage plate was placed 9.2 cm upstream of the fuel injection plane to distort the inlet air velocity profile. Vaporization of the fuel was 50 percent complete at an inlet air temperature of 400K and the percentage increased linearly with temperature to complete vaporization at 600K. The pressure drop was 3 percent at the design point which was three times greater than the designed value and the single tube experiment value. No autoignition or flashback was observed at the conditions tested. These conditions, except for fuel-air ratio, are in the range where others have obtained autoignition. Thus the autoignition problem is not as severe for a catalytic combustor which operates at fuel-air ratios leaner than the normal flammability limit. Calculation of mean drop size from differing correlations are presented which shows a wide range of calculated mean drop size (13-160 μm).

MULTIPLE CONICAL TUBE FUEL INJECTOR

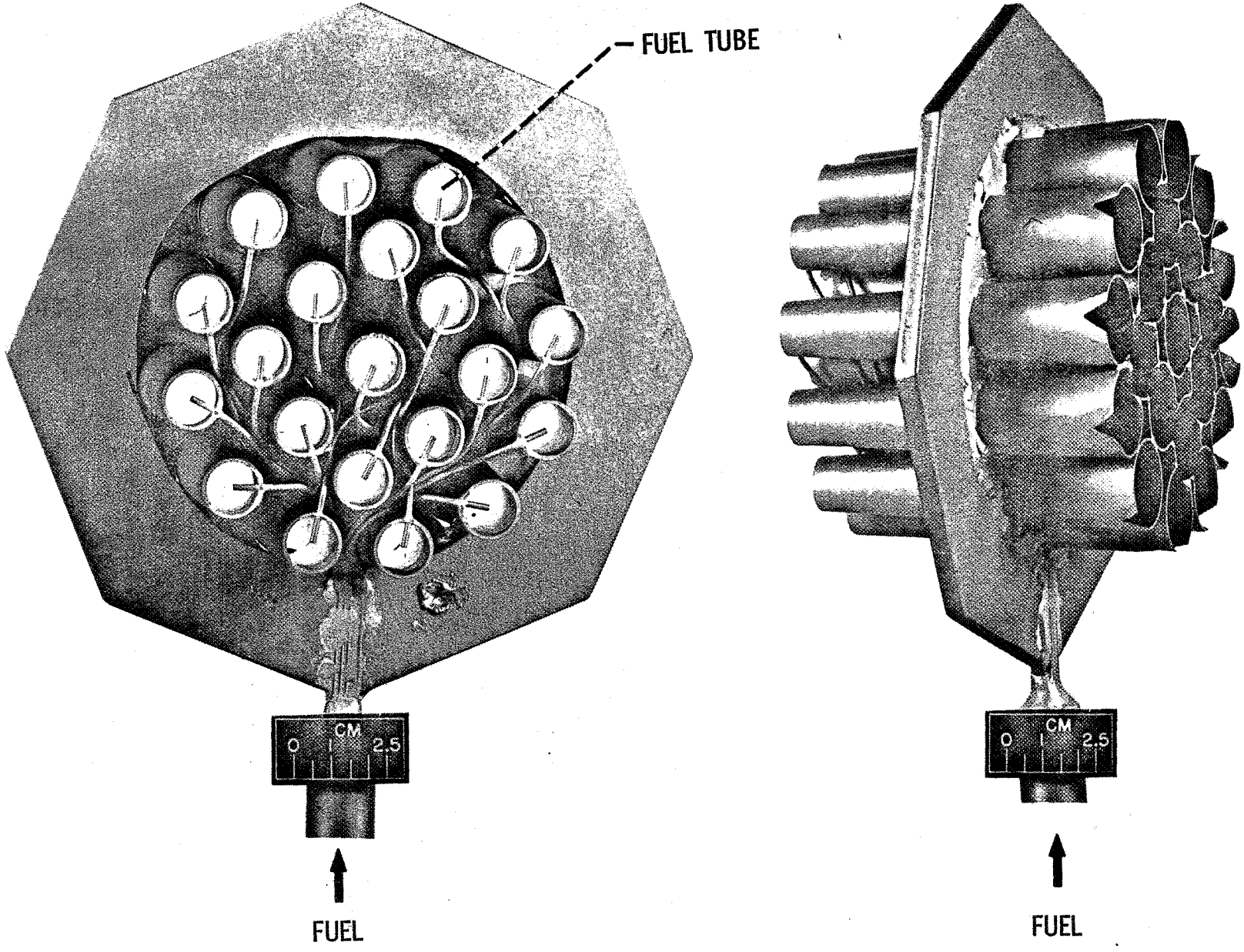

Comparison of Pressure Drop Through Various Single Element Tubes

T_{in} = 300 K, P_{in} = 414 kPa

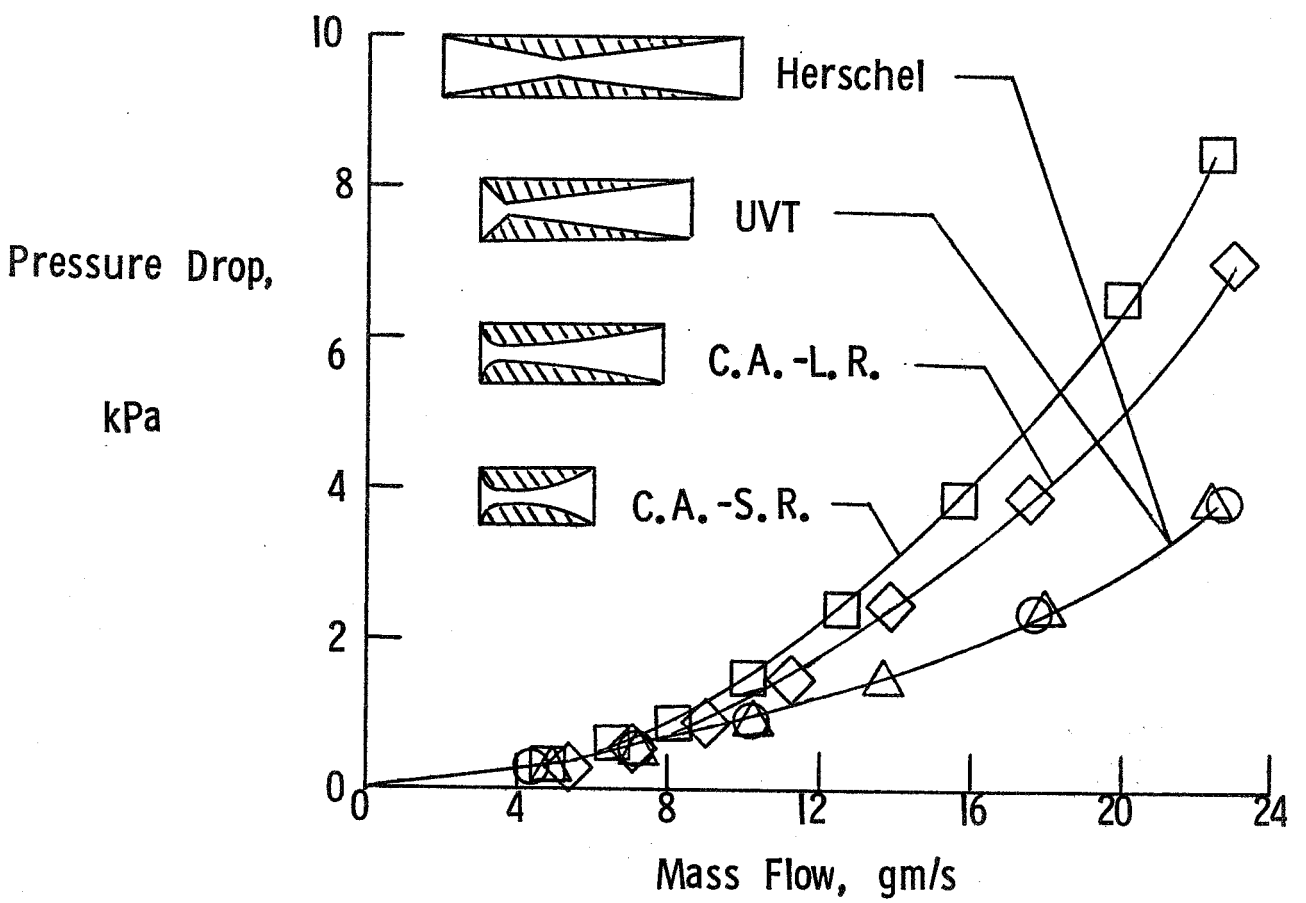

fig. 3

MULTIPLE VENTURI TUBE FUEL INJECTOR

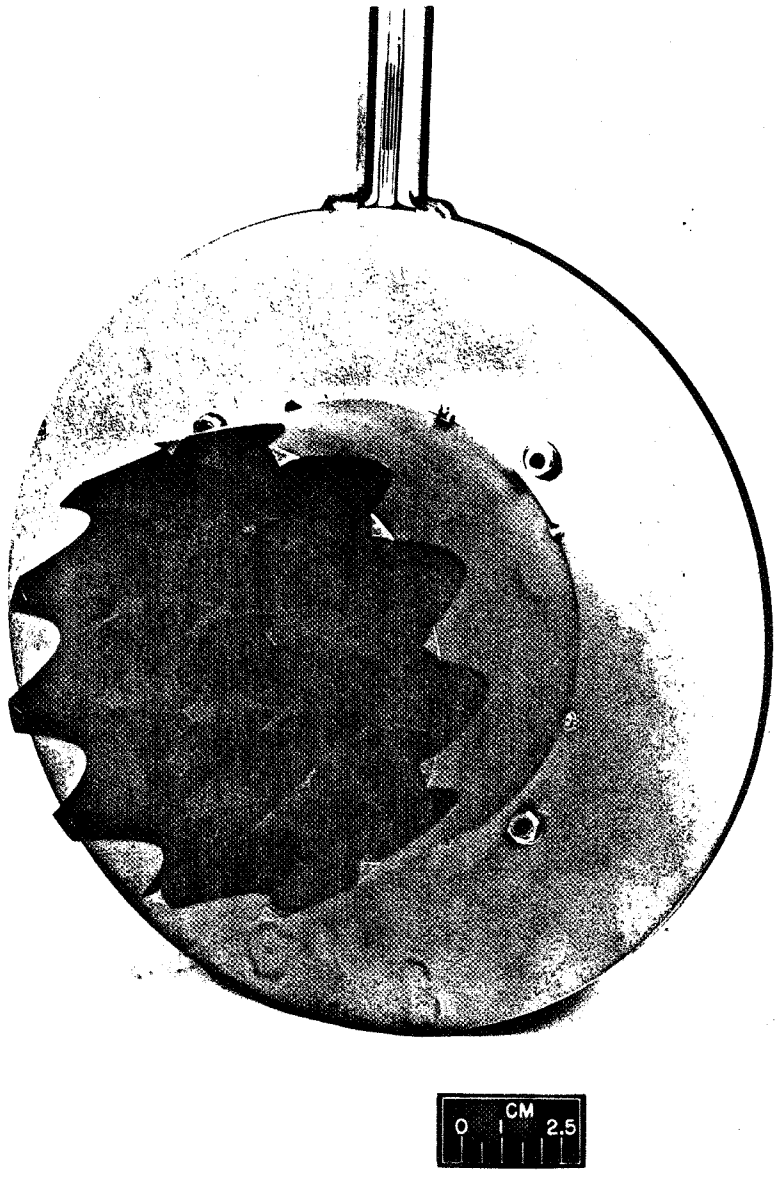

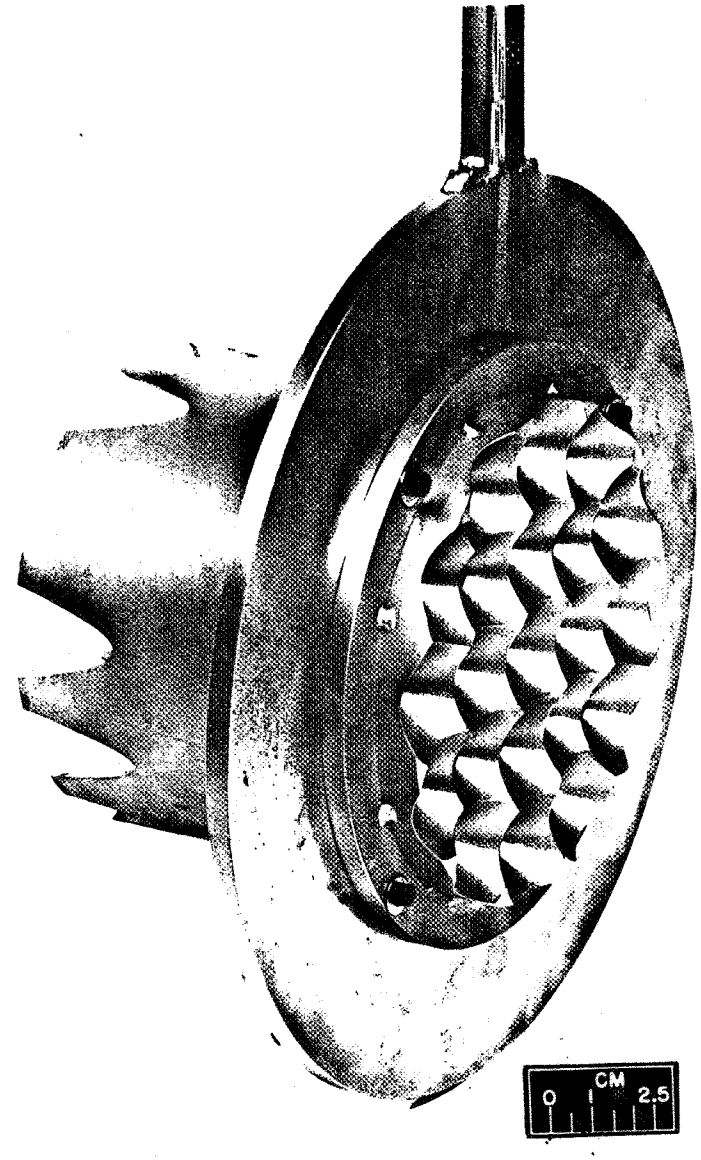

MULTIPLE VENTURI TUBE FUEL INJECTOR

FUEL TUBES

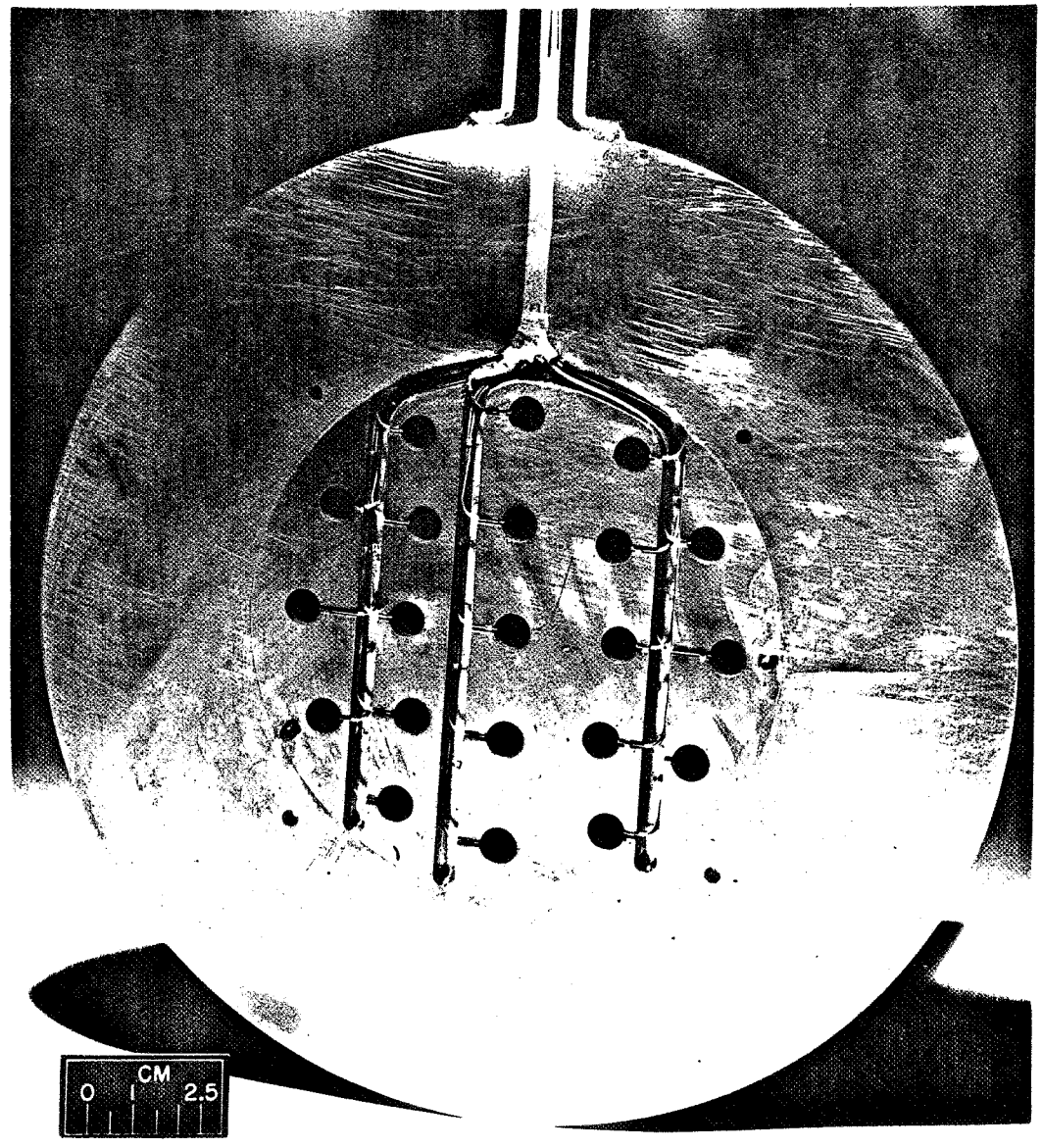

Comparison of Pressure Drop of Single Element UVT Tube and Multiple Element UVT Tube Array

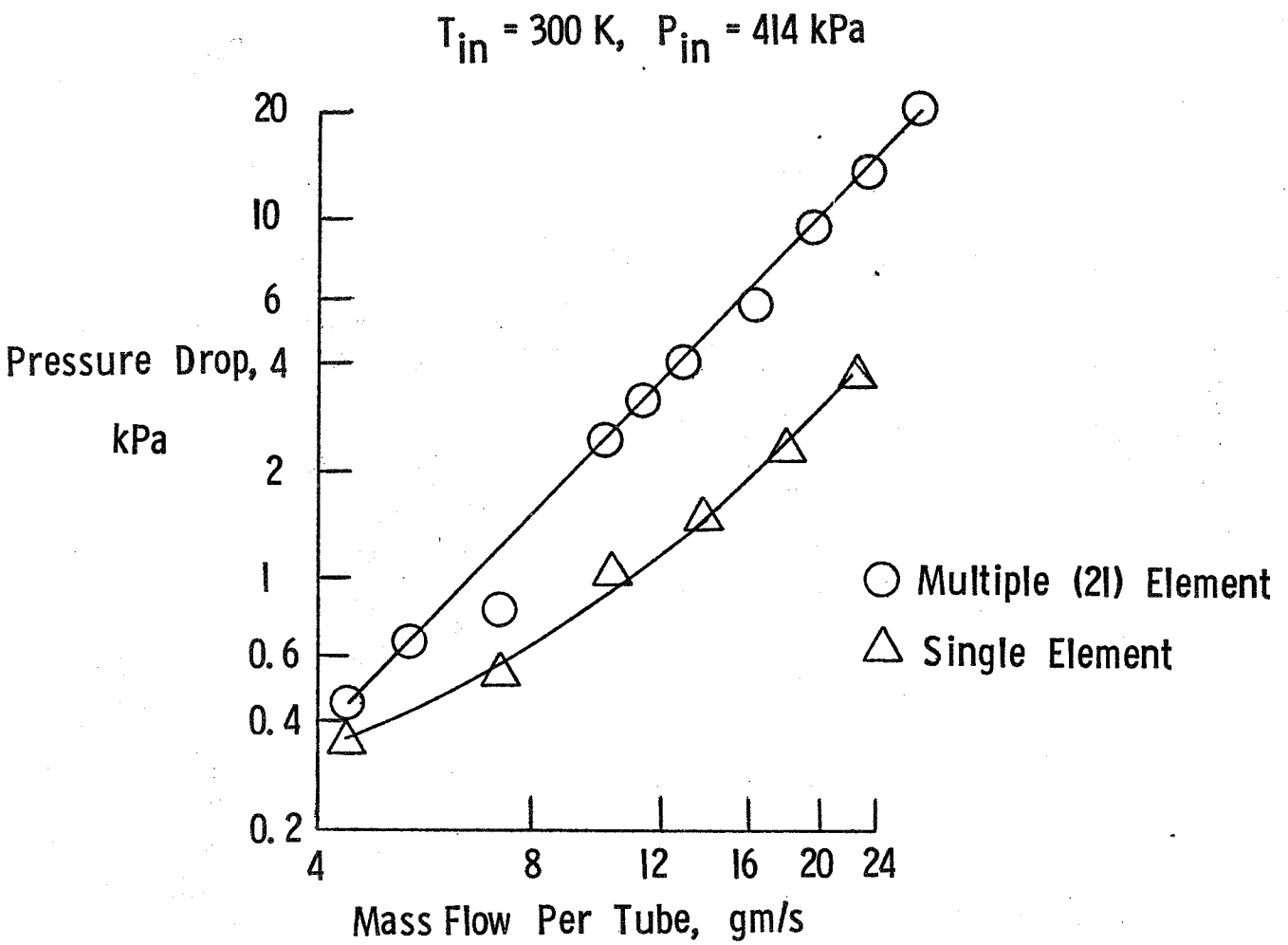

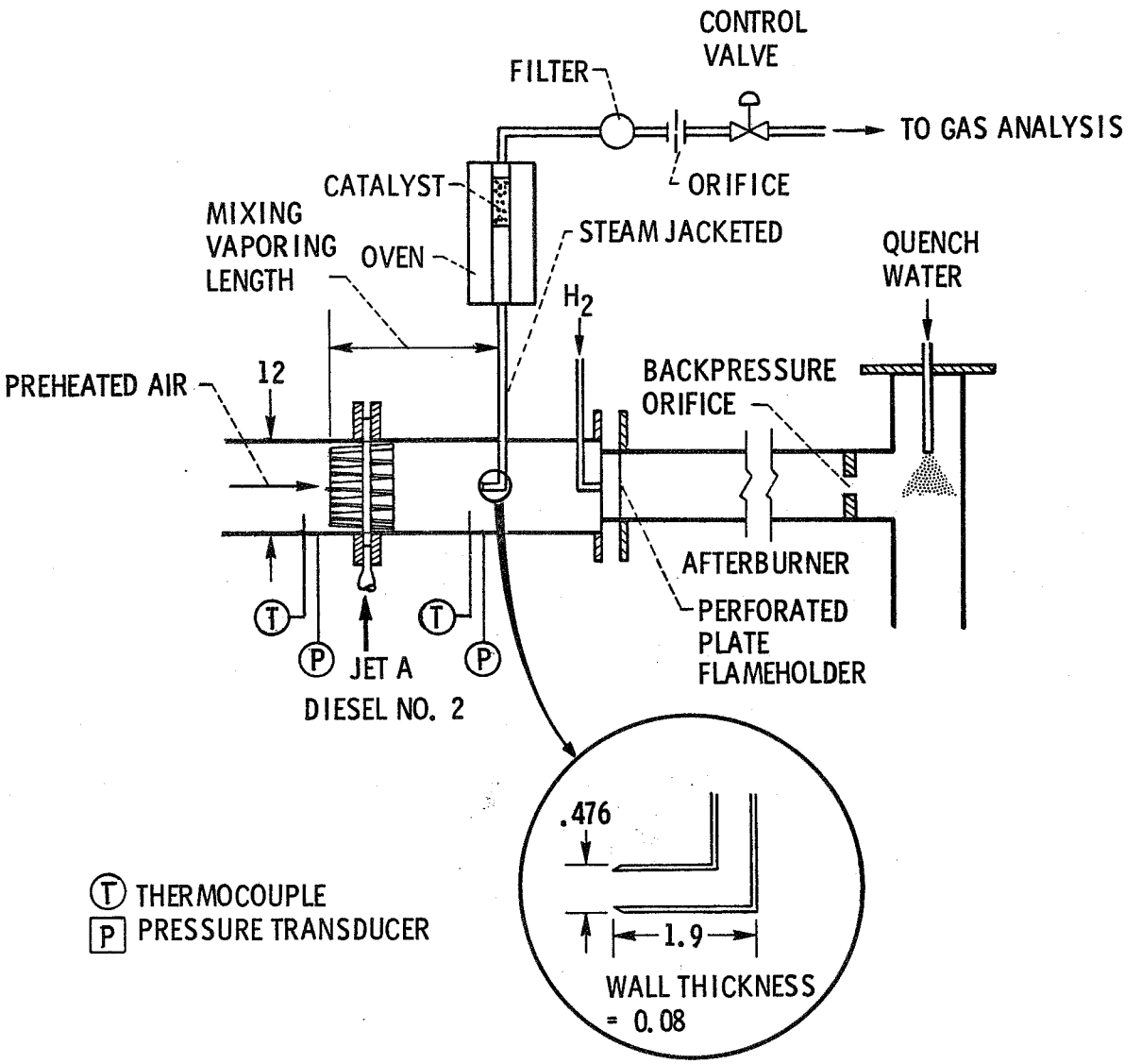

Rig schematic. (Dimensions in cm.)

E-9546

Spatial Fuel-Air Distribution

Multiple Venturi Tube Fuel Injector

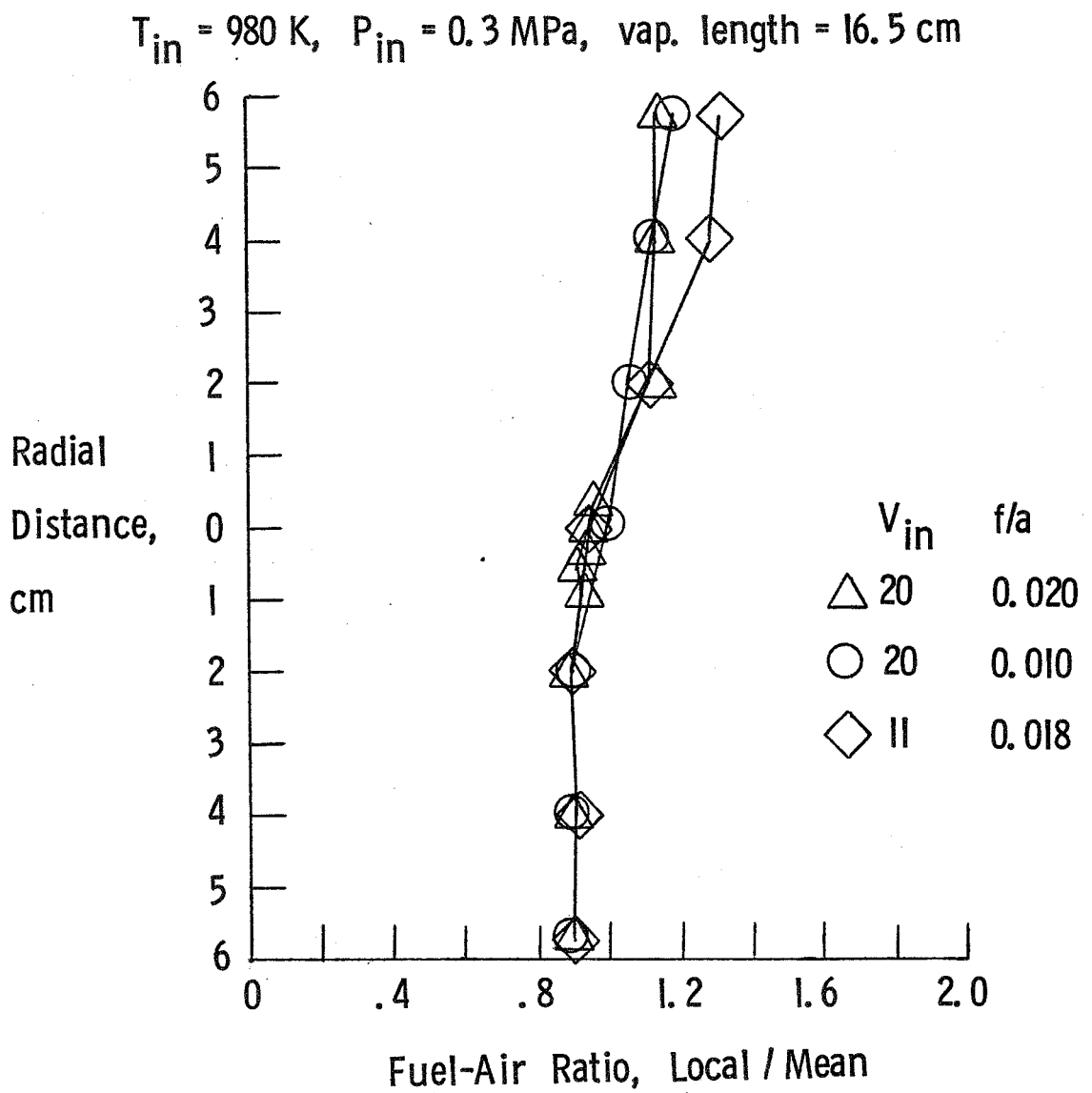

Effect of Inlet Air Temperature on Spatial Fuel-Air Distribution

Multiple Venturi Tube Fuel Injector

P_{in} = 0.3 MPa, V_{in} = 10 m/s, f/a = 0.010, vap. length = 16.5 cm

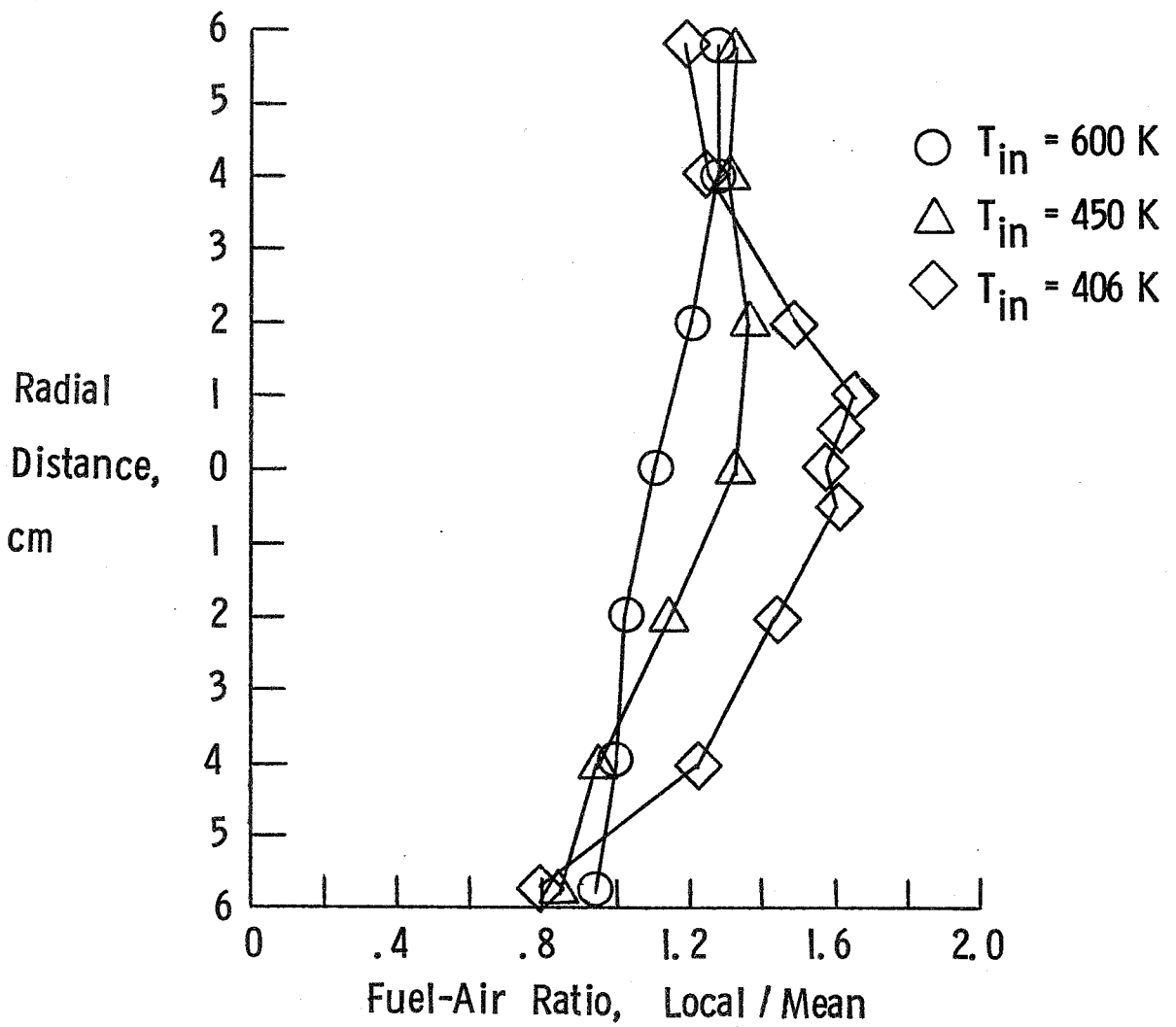

Effect of a Distorted Inlet Air Velocity Profile on Spatial Fuel-Air Distribution

Multiple Venturi Tube Fuel Injector

T_{in} = 600 K, P_{in} = 0.3 MPa, V_{in} = 10 m/s, f/a = 0.020, vap. length = 16.5 cm

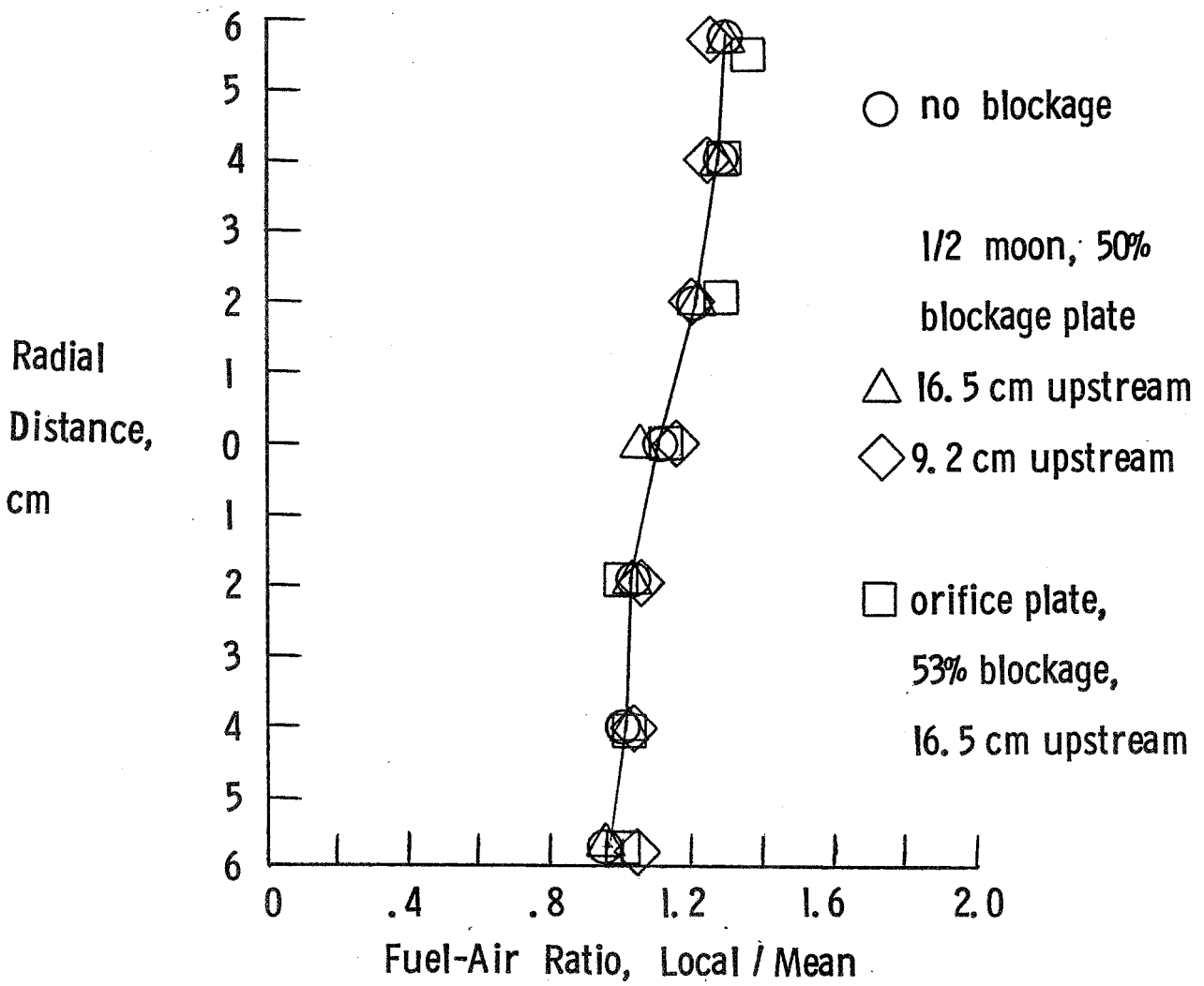

Effect of Inlet Air Temperature on Vaporization

P_{in} = 0.3 MPa, V_{in} = 10 m/s, f/a = 0.020

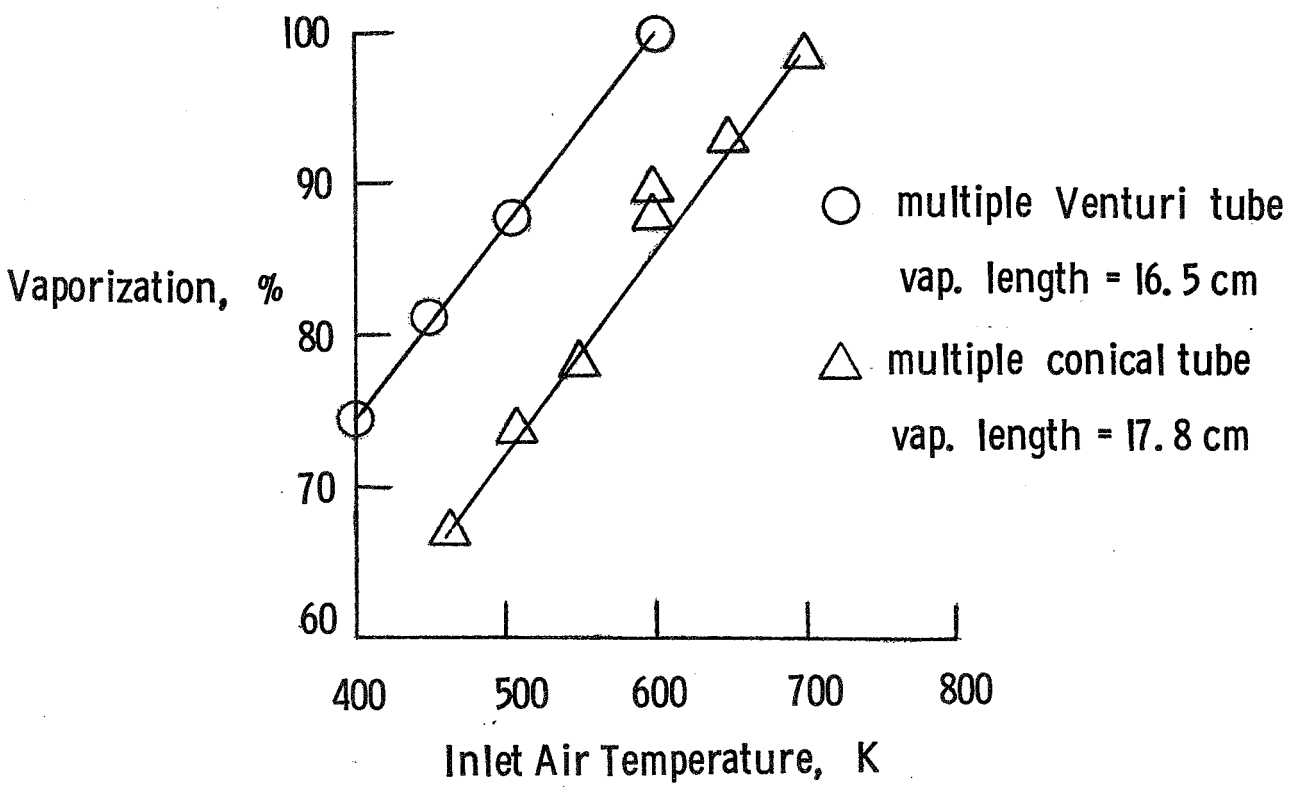

Comparison of Test Conditions with Sturgess* Autoignition Correlation

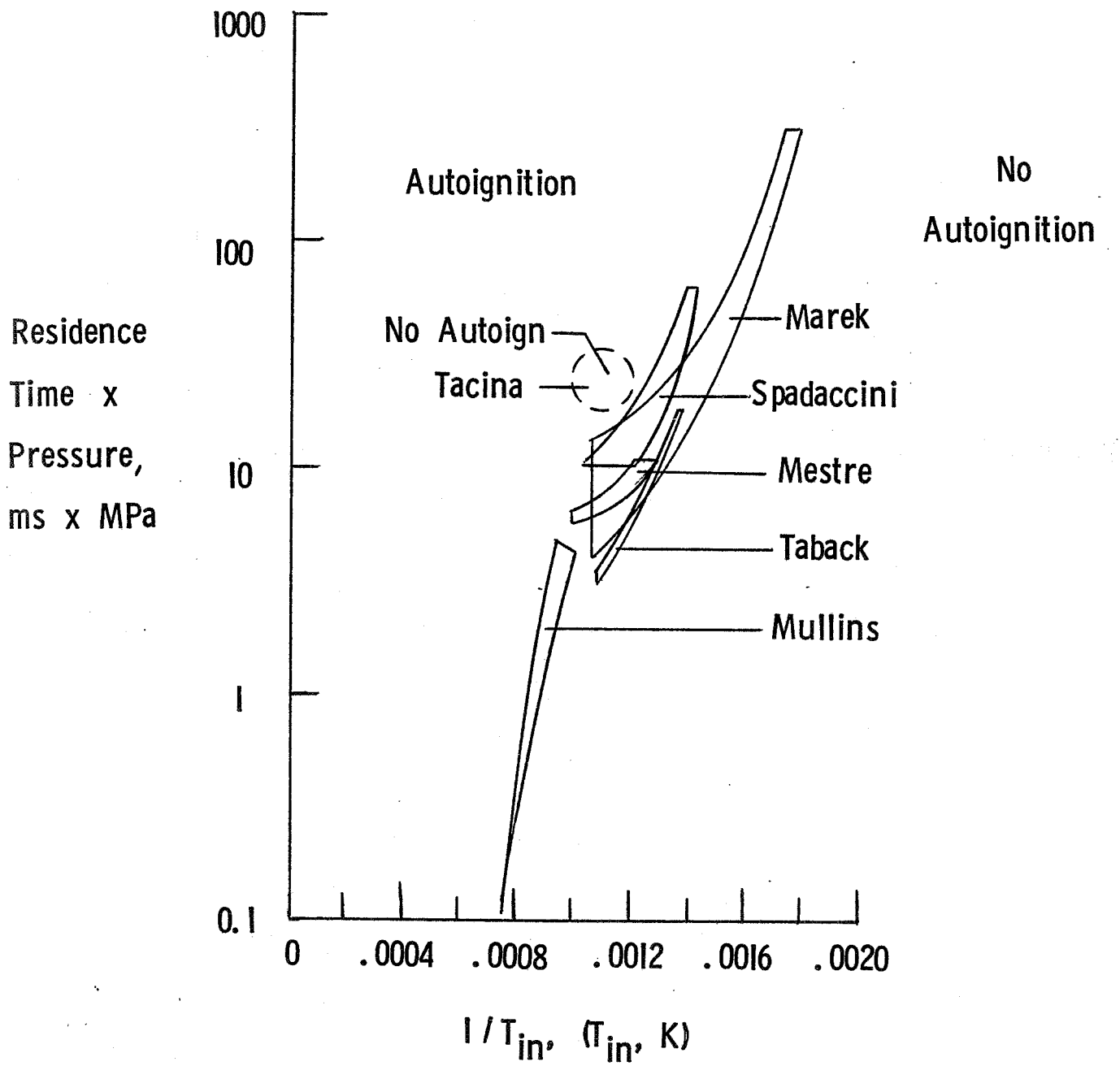

* Pratt-Whitney Aircraft

Mean Dropsize Correlations

Author	Correlation	Dropsize microns
Nukiyama-Tanasawa	$SMD = \frac{585}{u_r}\sqrt{\frac{\sigma}{\rho_L}} + 597\left(\frac{\mu_L}{\sigma \rho_L}\right)^{0.45}\left(1000\,\frac{Vol_L}{Vol_a}\right)^{1.5}$	84
Lorenzetto-Lefebvre	$SMD = 0.95\,\frac{(\sigma w_L)}{u_r \rho_i \rho_a}^{0.33}(1+f/a)^{1.7} + 0.13\left(\frac{D_{orf}}{\sigma_i \rho_i}\right)^{0.5}(1+f/a)^{1.7}$	31
Jasuga	$SMD = 650\,(\sigma\rho_L)^{0.5}(u_r\rho_a)^{-1}(1+f/a) + 120\left(\frac{\mu_L}{\sigma\rho_a}\right)^{0.425}(1+f/a)^{2}$	71
Deysson-Karian	$MMD = \frac{d_a}{Re^*\,V_i^*} f(f/a), \quad Re^* = \frac{\rho_L u_r d_a}{\mu_L}, \quad V_i^* = \frac{\mu_L}{\sqrt{\rho_L \sigma d_a}}$	161
Kim-Marshall	$MMD = \frac{249\,\sigma^{0.41}\mu_L^{0.32}}{(\rho_a u_r^2)^{0.57} A^{0.36} \rho_L^{0.16}} + 1260\left(\frac{\mu_L^2}{\sigma\rho_L}\right)^{0.17}(f/a)^{0.5}$	13
Weiss-Worsham	$MMD = 0.61\left(\frac{\sigma}{\rho_a u_r^2}\right)\left(\frac{u_r\mu_L}{\sigma_L}\right)^{2/3}\left(1+\frac{10^3\rho_a}{\rho_L}\right)\left(\frac{w_L\rho_L\,\sigma\,\mu_a}{\mu_L}\right)^{1/12}$	73

$SMD_{avg} = 72$

AUTOIGNITION OF FUELS

Louis J. Spadaccini
United Technologies Research Center

The primary objectives of this research program are to (1) develop a critical experiment capable of determining the autoignition characteristics of aircraft-type fuels in air at elevated temperatures and pressures, and (2) apply the equipment and techniques developed to mapping the ignition delay times of several hydrocarbon fuel-air mixtures. Autoignition data are required for establishing design criteria pertinent to advanced gas turbine engines which employ fuel prevaporization and premixing. The program is directed toward design of the experiment, fabrication of the test equipment, empirical verification that the variables which affect autoignition can be controlled in a manner such that useful quantitative results can be obtained, and parametric evaluation of the autoignition characteristics of several liquid hydrocarbon fuels.

The spontaneous ignition characteristics of hydrocarbon fuels in air have been a subject of investigation for many years; however, none of the previous investigators has been completely successful in isolating and evaluating each of the experimental variables in a controlled manner and over ranges representative of those encountered in advanced gas turbine engines. Consequently, a thorough examination of past efforts in this area was undertaken in order to properly define a critical experiment that determines the effects of all the known or suspected variables on autoignition. It was concluded that parametric autoignition data pertinent to gas turbine engines can be best acquired by conducting a continuous flow experiment using dry, unvitiated air, and providing independent control of pressure, temperature, and fuel-air mixture residence time. In addition, the experiment should minimize flow disturbances and wall effects, and provide for a determination of the fuel-air mixture distribution and the degree of droplet vaporization. These criteria served as a basis for formulating the technical approach from which the experiment design evolved.

The autoignition test apparatus which was developed in the present program consists of an electrical resistance-type air heater, an inlet plenum and flow straightener, a specially-designed premixing-type fuel injector for generating a relatively uniform fuel-air distribution, a cylindrical mixer/vaporizer section comprising several flanged spool pieces to permit length variation over the range 2.5 cm to 150 cm in increments of 2.5 cm, an expander section which provides a sudden expansion at the autoignition station and a water quench, a scavenger afterburner, and a remotely-operated throttle valve located in the exhaust ducting. Details of the test hardware are described in Ref. 1 and shown schematically in the attached illustrations. The inner surface of the mixer/vaporizer sections is relatively smooth and free of wake-producing imperfections as a result of internal machining and the use of alignment

dowels. Theoretical analyses of the need for wall cooling to preclude the possibility of ignition in the boundary layer were not able to conclusively demonstrate that cooling would not be required, therefore, the design provides the capability for internal wall cooling; however, this feature is optional (the inner wall has sufficient strength to permit uncooled operation). Uniform inlet velocity profiles are assured by flow baffles and straight sections, and the inlet temperature and pressure are measured using fixed probes.

Normal operating procedure consists of establishing a prescribed condition within the test duct and gradually increasing the air temperature or pressure until autoignition occurs at the exit of the mixer/vaporizer section. This continuous test procedure ensures an accurate determination of the conditions at autoignition. The ignition delay time is equal to the residence time of the fuel-air mixture between the point of injection and the axial position of the flame, and it is computed based upon the average flow velocity. The occurrence of autoignition is determined indirectly using a thermocouple, a differential pressure transducer and photodetectors to make simultaneous measurements of the temperature-rise, pressure-rise and illumination delay times. Upon ignition, the test is terminated abruptly by shutting off the fuel flow and thereby purging the rig with inlet air flow. This test arrangement permits independent variation of each of the important experimental variables (i.e., pressure, temperature, velocity, residence time, and fuel-air ratio) within a fixed range of test conditions.

The generation of a uniform mixture is a prerequisite for the evaluation of the importance of fuel-air ratio; therefore, techniques for obtaining rapid vaporization and mixing with a minimum flow disturbance were studied and several candidate fuel injectors were fabricated and tested. Two fuel injector designs have demonstrated high potential for achieving a uniform spatial distribution of fuel in air. The first, a multiple-strut injector, is one in which fuel is injected normal to the airflow from a large number of injection sites and into segments of approximately equal area. The number and size of the injection orifices were determined from consideration of liquid jet penetration, orifice plugging, and injector sensitivity to combustor pressure oscillations. Efficient atomization results as a consequence of the high shear forces created by the interaction of the high-velocity airstream and the low-velocity fuel jets. Flow disturbance and, therefore, pressure loss are minimized by a streamline shaped design. The second injector is a multiple conical tube type which consists of a concentric array of venturi-shaped air passages into each of which an individual and regulatable flow of fuel is injected near the entrance. Fuel is supplied by means of a small diameter tubing that is sufficiently long to provide ample pressure loss to minimize the effect of rig pressure fluctuations on the fuel flow rate. Airflow nonuniformities are reduced as a result of the pressure loss incurred and atomization is improved by the shear forces created by the increased air velocity.

Parametric tests to map the ignition delay characteristics of Jet-A fuel were conducted at pressures of 10, 15, 20, 25, and 30 atm, inlet air temperatures up to 900K and fuel-air equivalence ratios of 0.3, 0.5, 0.7, and 1.0. Residence times in the range of 1 to 50 msec were obtained by interchanging spool pieces to create six different mixer/vaporizer lengths (6, 23, 53, 84, 99, and 130 cm) and by testing at two different

airflow rates (0.5 and 1.0 kg/sec). The resulting free-stream velocities were in the range 20 to 100 m/sec. As expected, the results indicate that the ignition delay times decrease with increasing air temperature and pressure. Also, the data show that, for lean mixtures, ignition delay times decrease with increasing equivalence ratios.

Future work will concentrate on obtaining detailed autoignition data for a variety of fuels, including JP-4, No. 2 diesel oil, ERBS and cetane, and investigating the effects of chemical and physical properties of fuels on autoignition.

References

Spadaccini, L. J.: Development of an Experiment for Determining the Autoignition Characteristics of Aircraft-Type Fuels. NASA CR-135329, September, 1977.

LIST OF FIGURES

Introduction

- Premixed-prevaporized combustion can provide low NOx emissions
- Autoignition is a serious problem
- Existing autoignition data are inadequate

Ignition Delay

- Physical delay
  - Droplet formation, heating and vaporization
  - Diffusion
  - Mixing
- Chemical delay
  - Preflame reactions
  - Cool-flame ignition, $\Delta T \sim 400K$
  - Hot-flame ignition, $\Delta T \sim 1500K$

Ignition Indicators

- Temperature rise
- Pressure rise
- Light emission
- Formation of critical species

Candidate Test Apparatus for Ignition Delay Measurements

	Disadvantages
• Constant volume bomb	Difficult to premix low-vapor-pressure fuels without significant chemical reaction
• Motored and fired reciprocating engines	Varying pressure, temperature, velocity, turbulence and fuel spray characteristics
• Shock tube	Difficult to adapt for use with low vapor pressure fuels
• Continuous flow rig Continuous combustion Intermittent combustion	Susceptible to flashback

Correlation of Ignition Delay Data

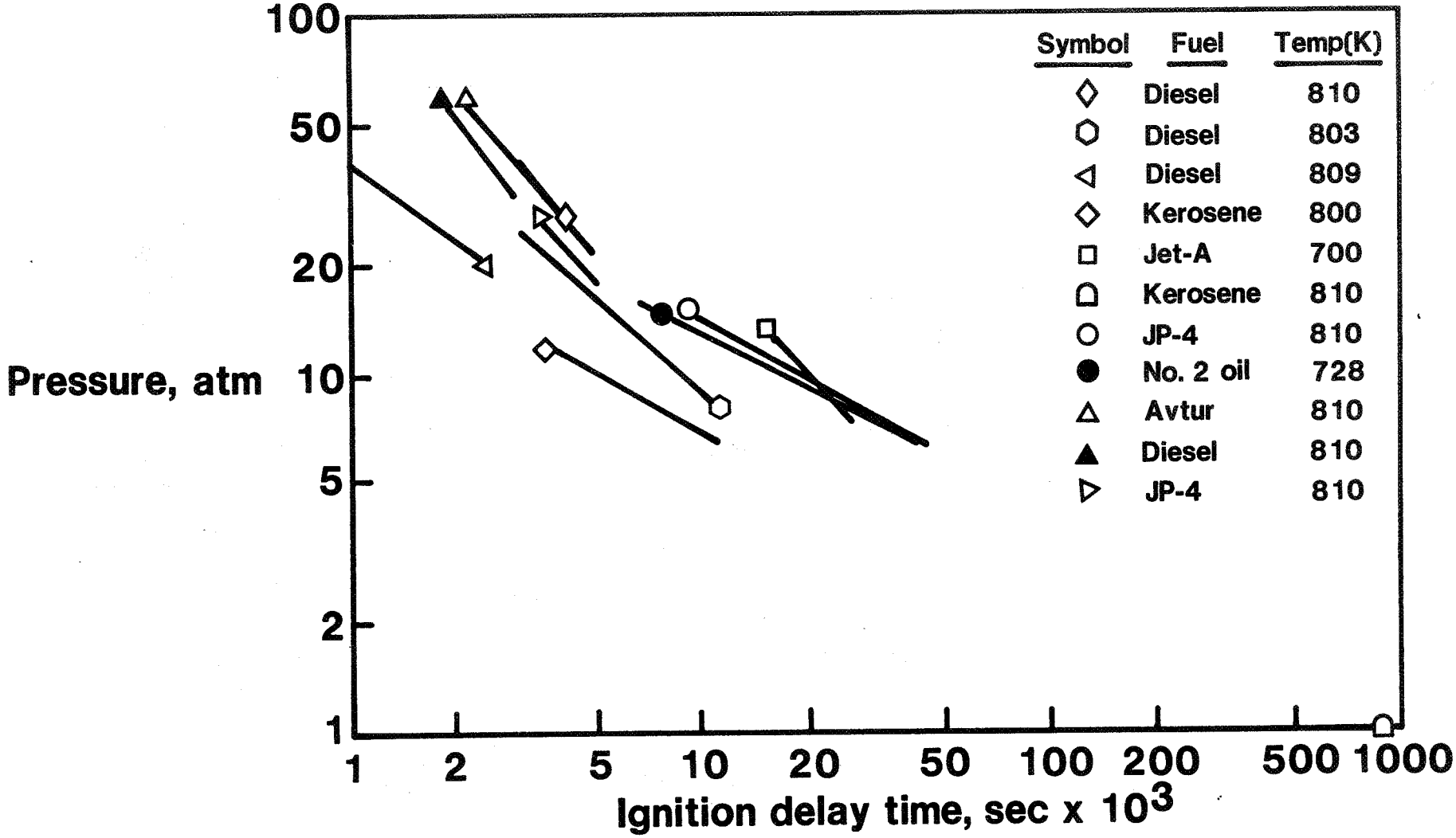

Autoignition Test Assembly

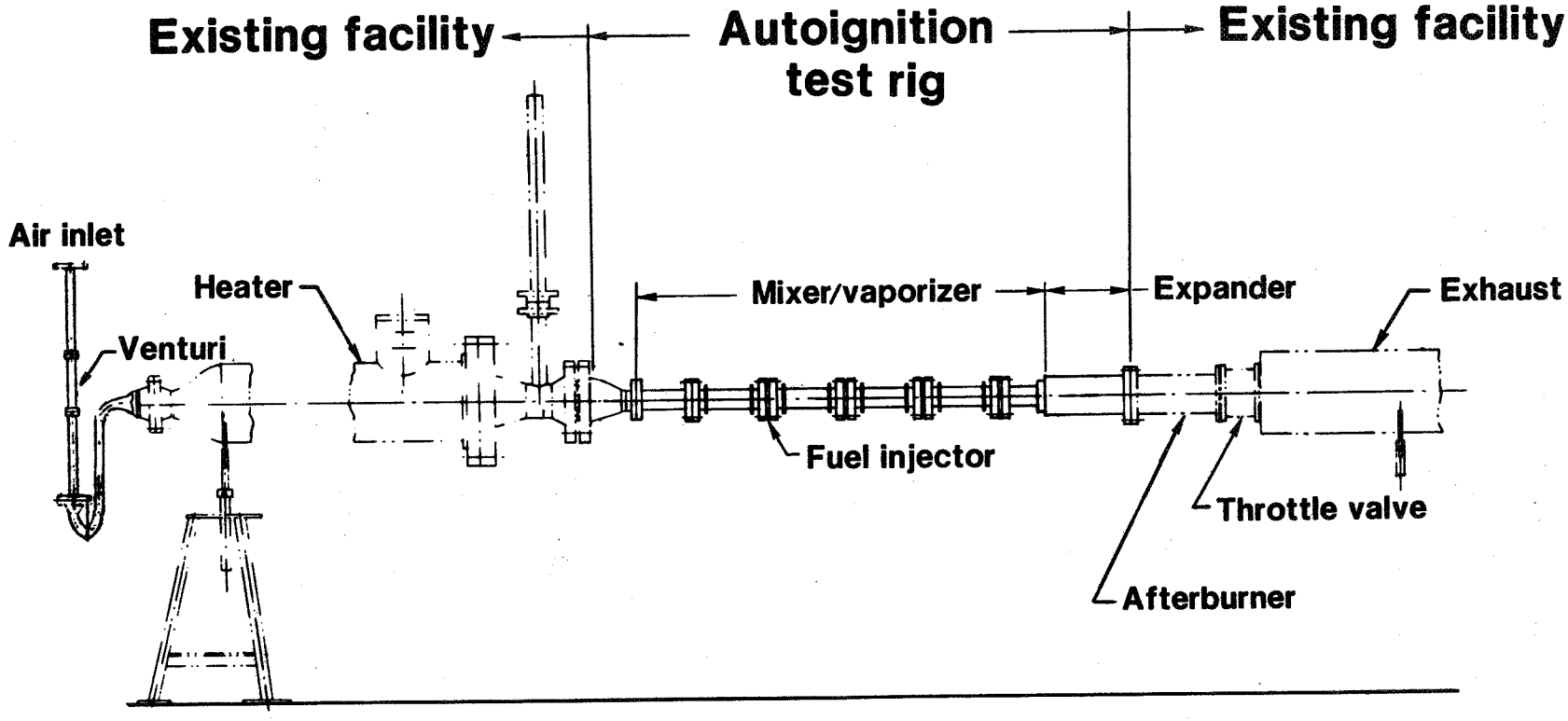

Autoignition Test Section

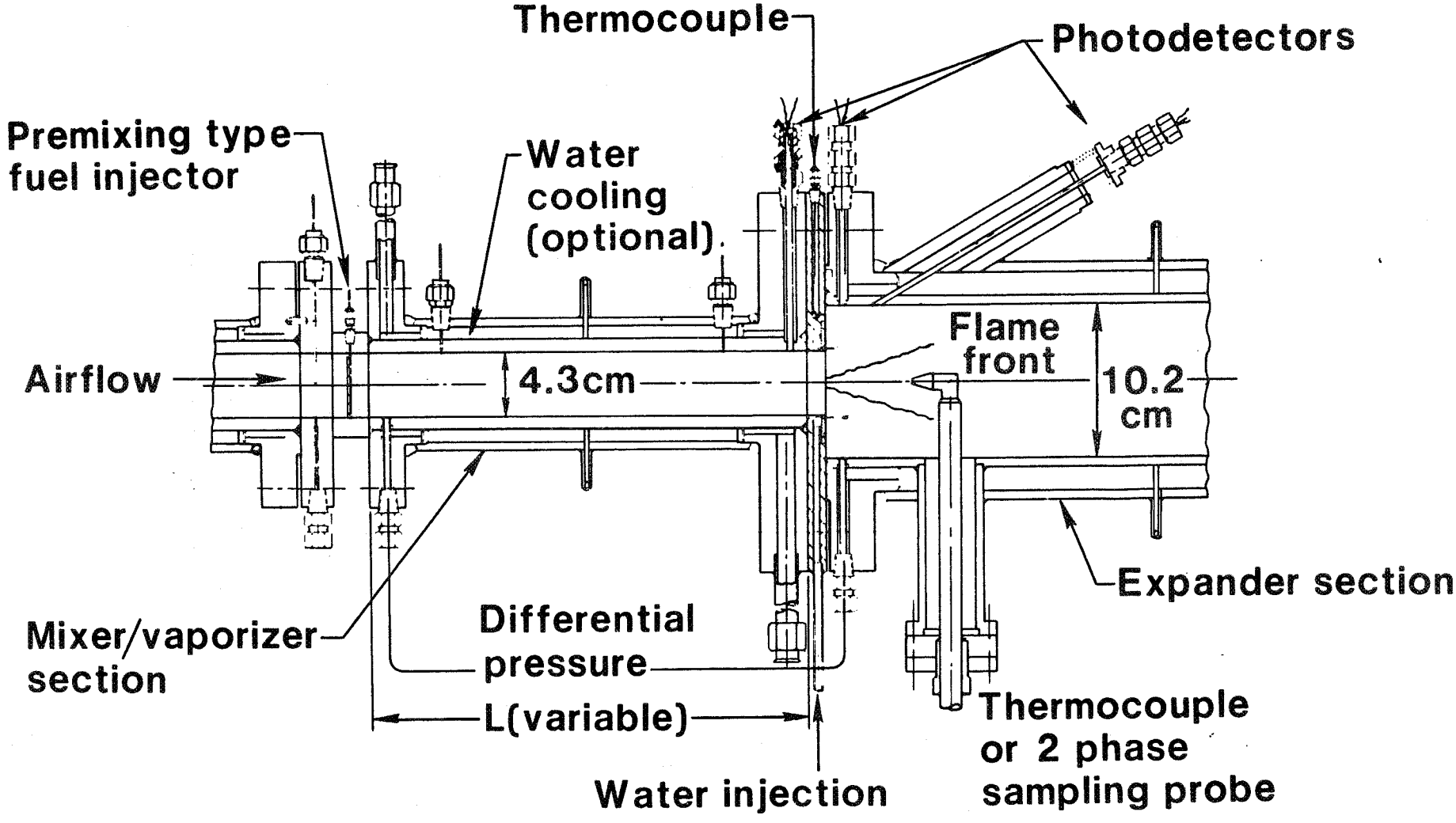

Fuel Injector Design Criteria

- Rapid vaporization and mixing
- Minimum flow disturbance
- Insensitive to combustor pressure oscillations
- Low pressure loss

Distributed Source Injector

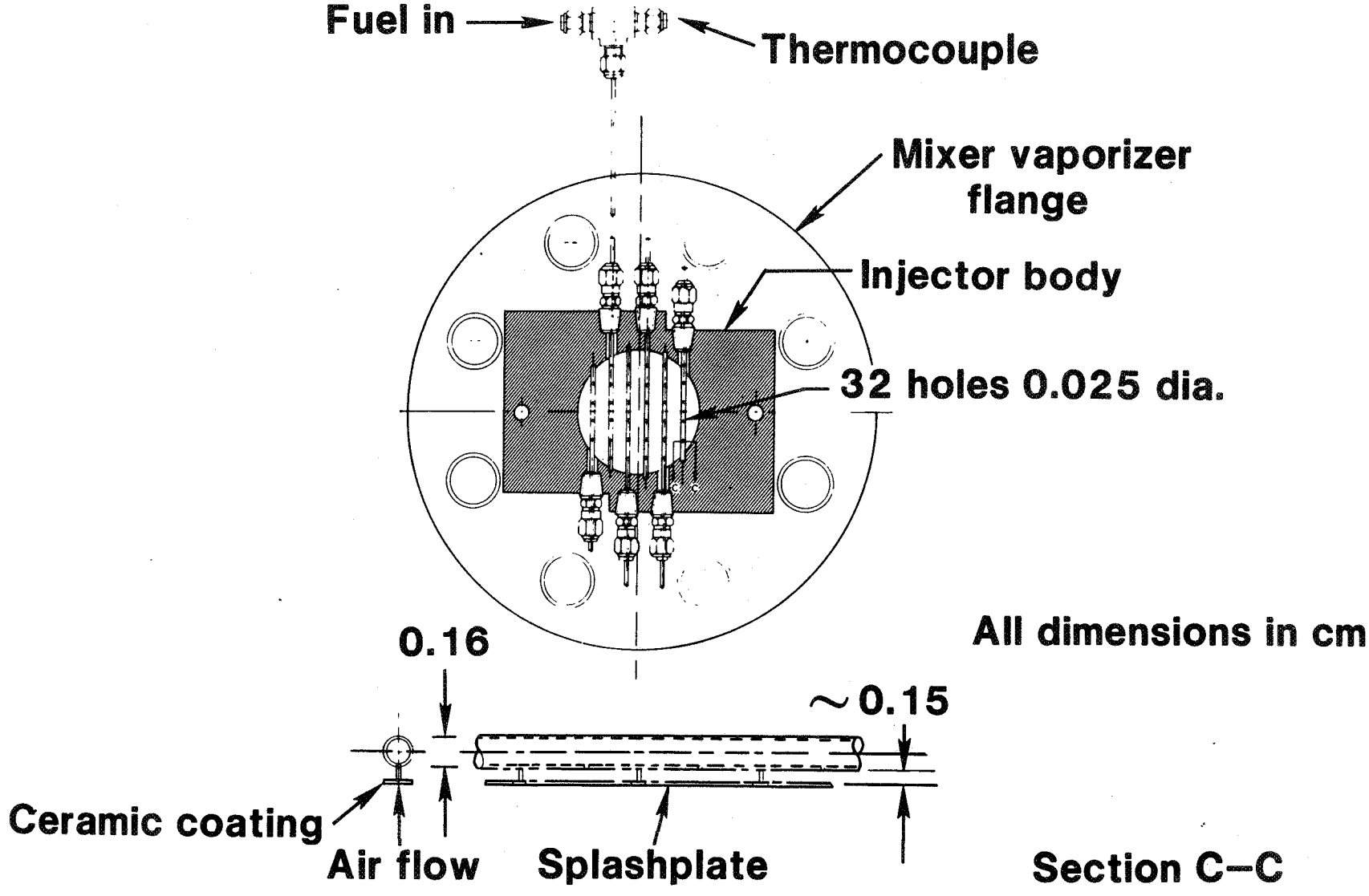

Distributed Source Cross-Stream Injector

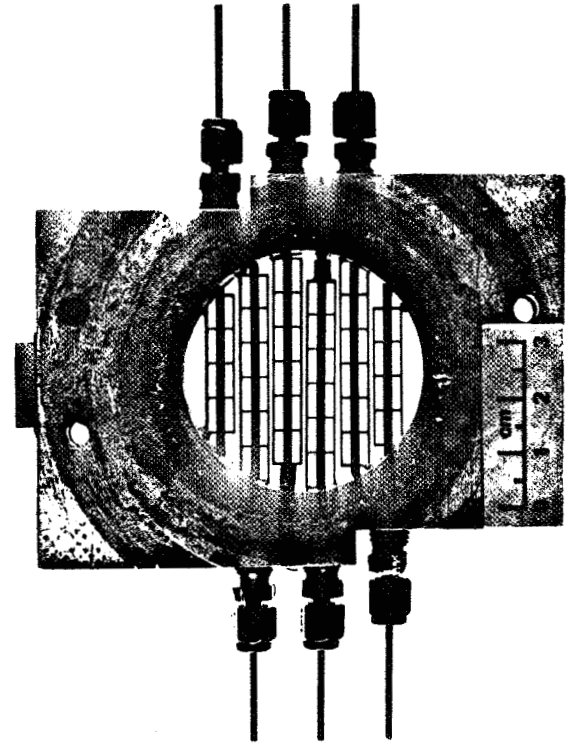

Spray Distribution from Distributed Source Cross-Stream Injector

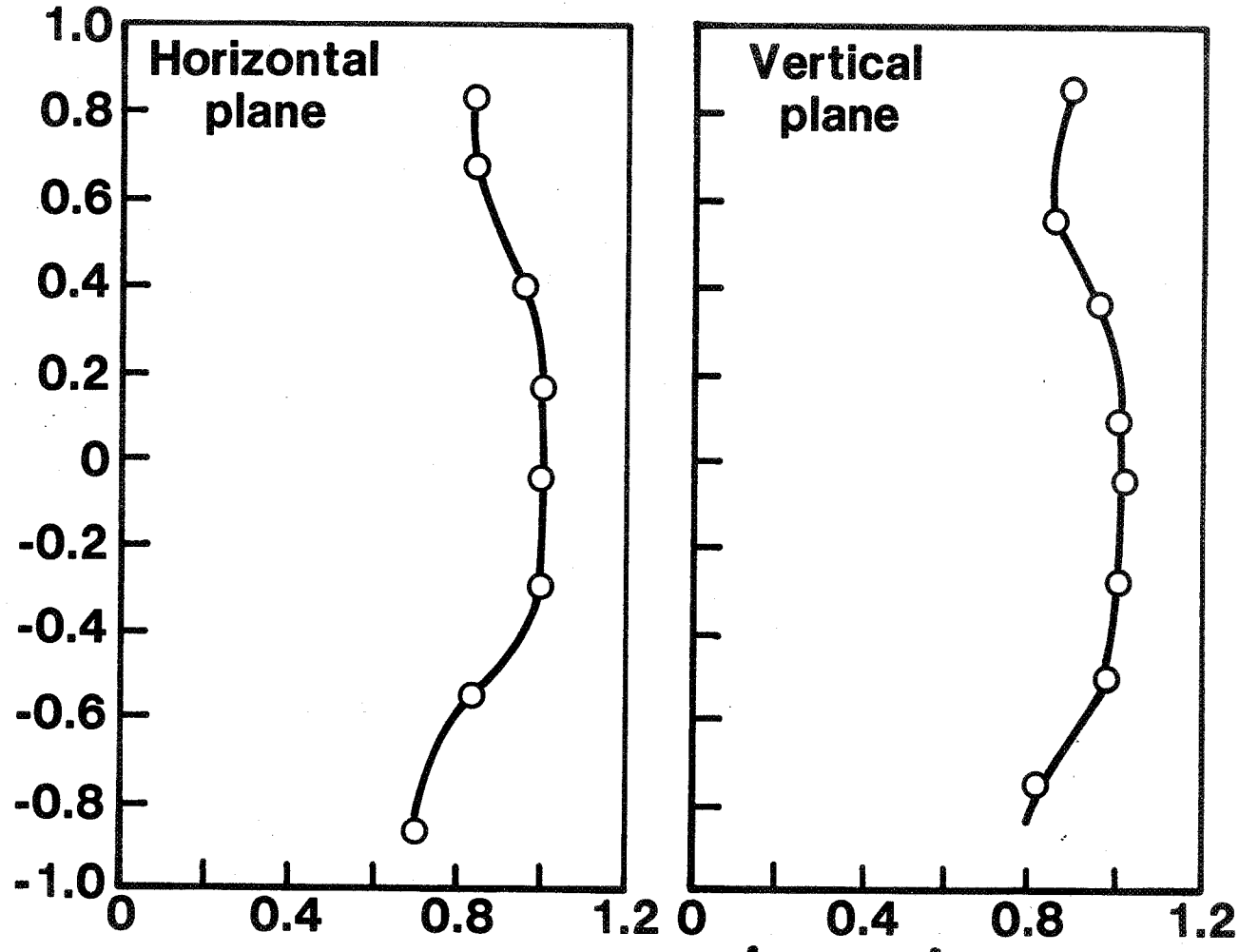

Radial position
R / R_o

Liquid distribution~$\dot{W}_{local} / \dot{W}_{mean}$

Streamline-Shaped Distributed Source Cross-Stream Injector

Blockage = 55 percent

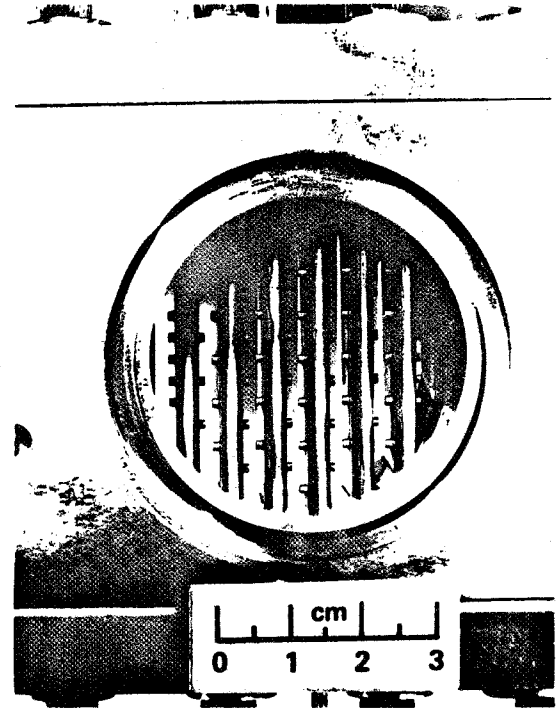

Streamline -Shaped Injector Element

All dimensions in cm

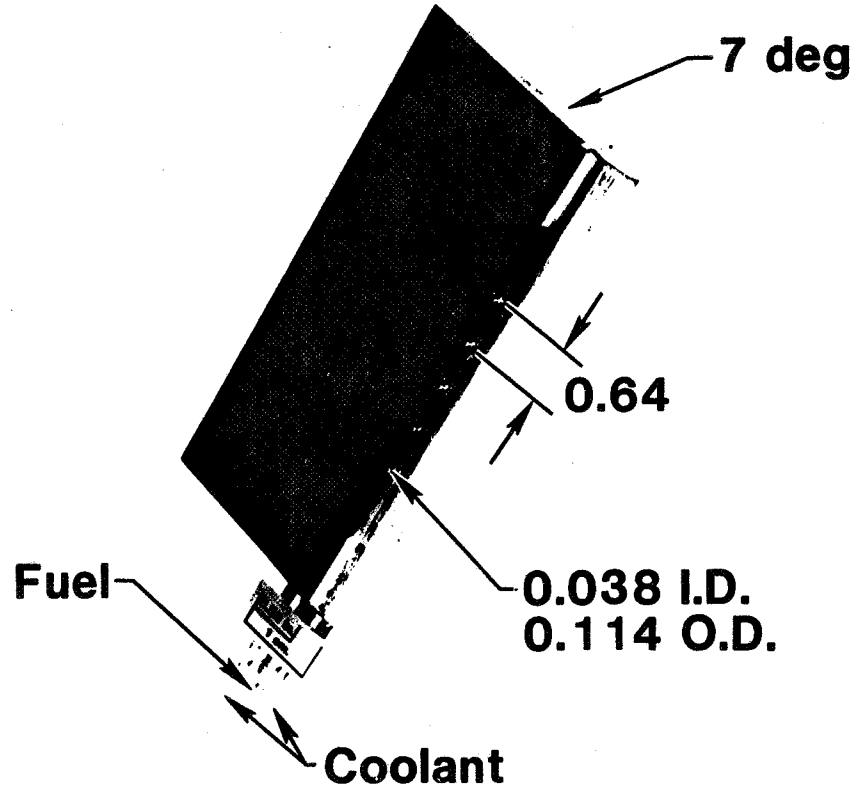

Spray Distribution from Streamline-Shaped Distributed Source Injector

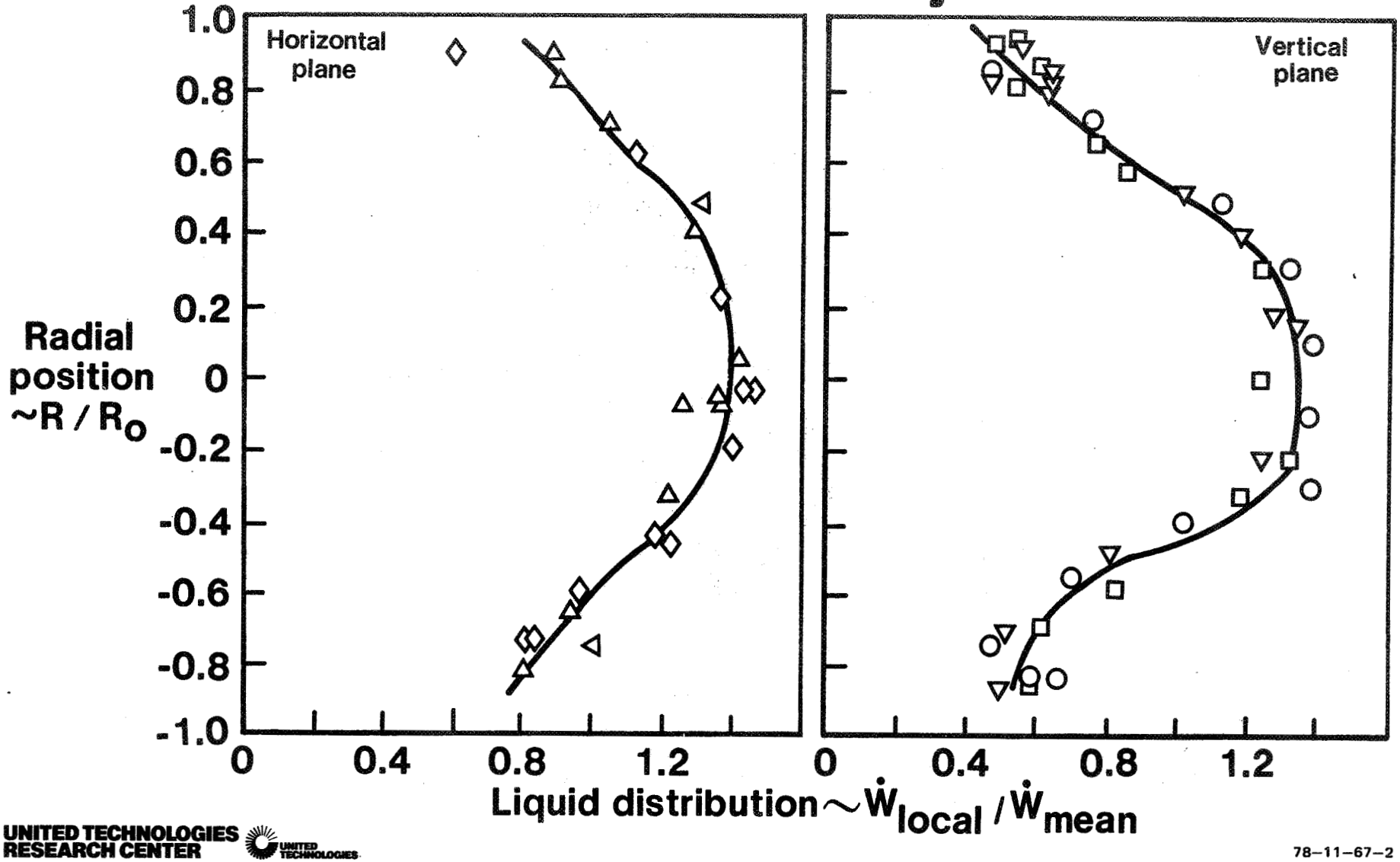

UNITED TECHNOLOGIES RESEARCH CENTER

78-11-67-2

Carbon Dioxide Distribution from Streamline-Shaped Distributed Source Injector

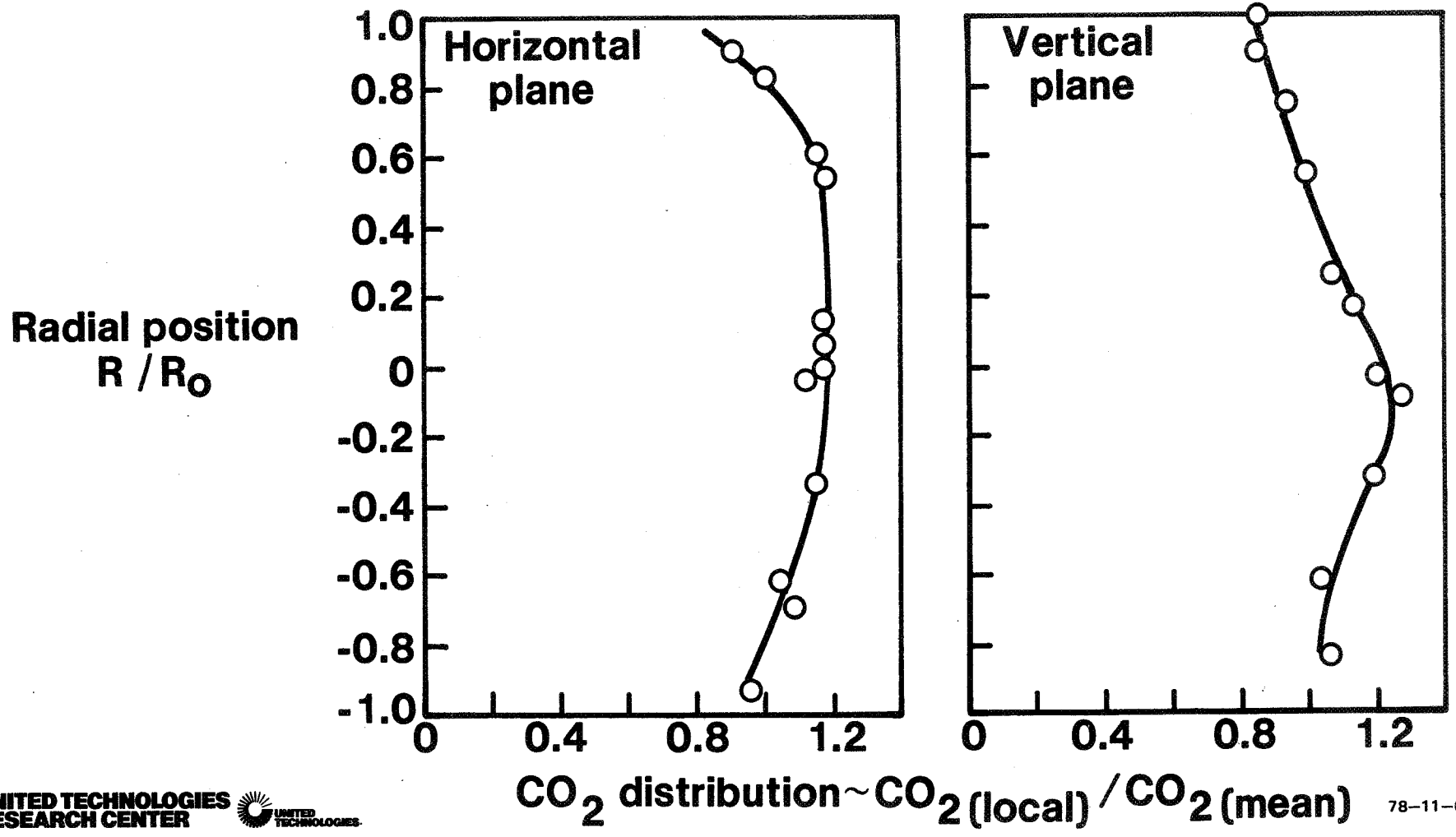

Ignition Delay of Jet-A Fuel in Air

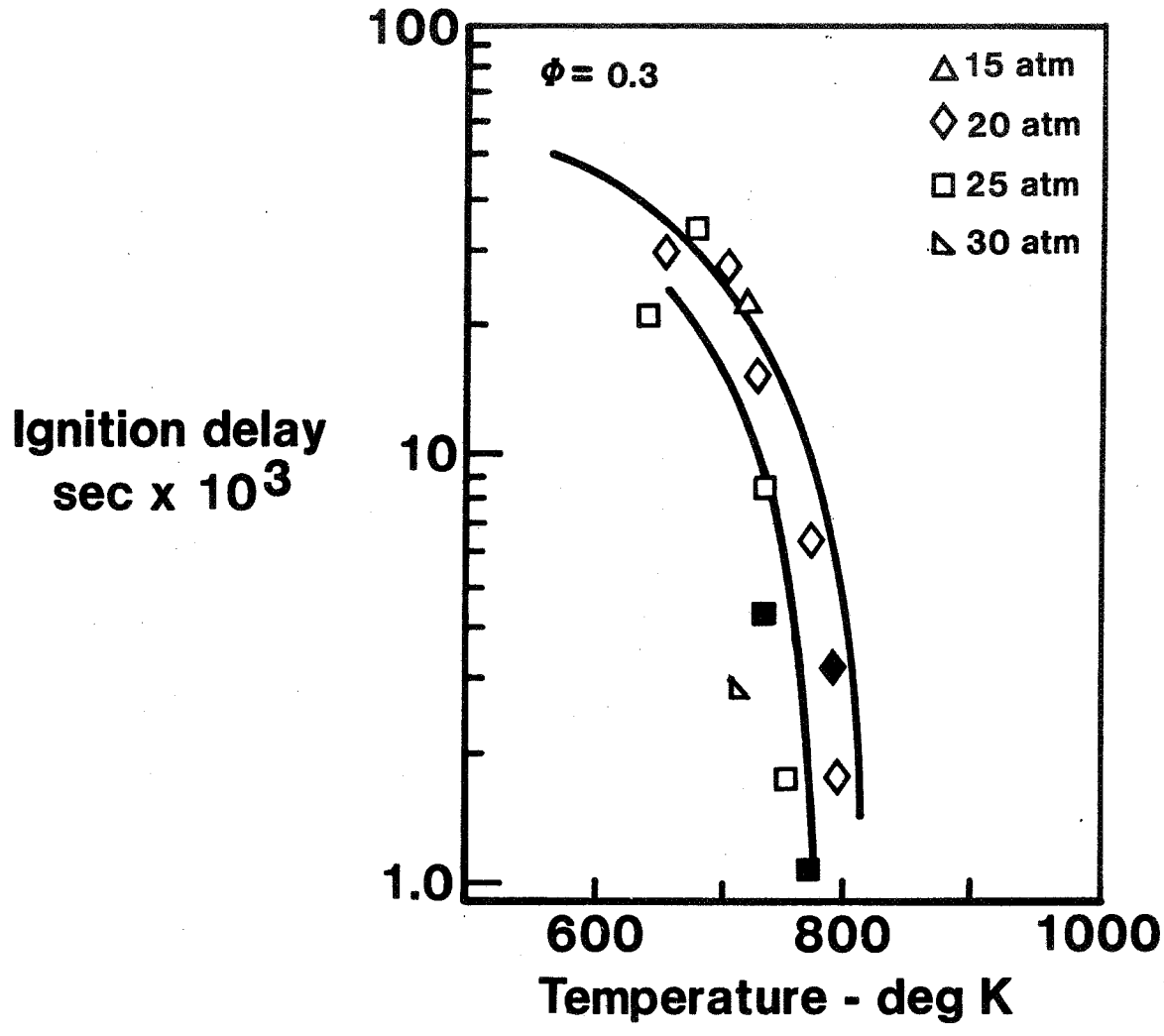

Ignition Delay of Jet-A Fuel in Air

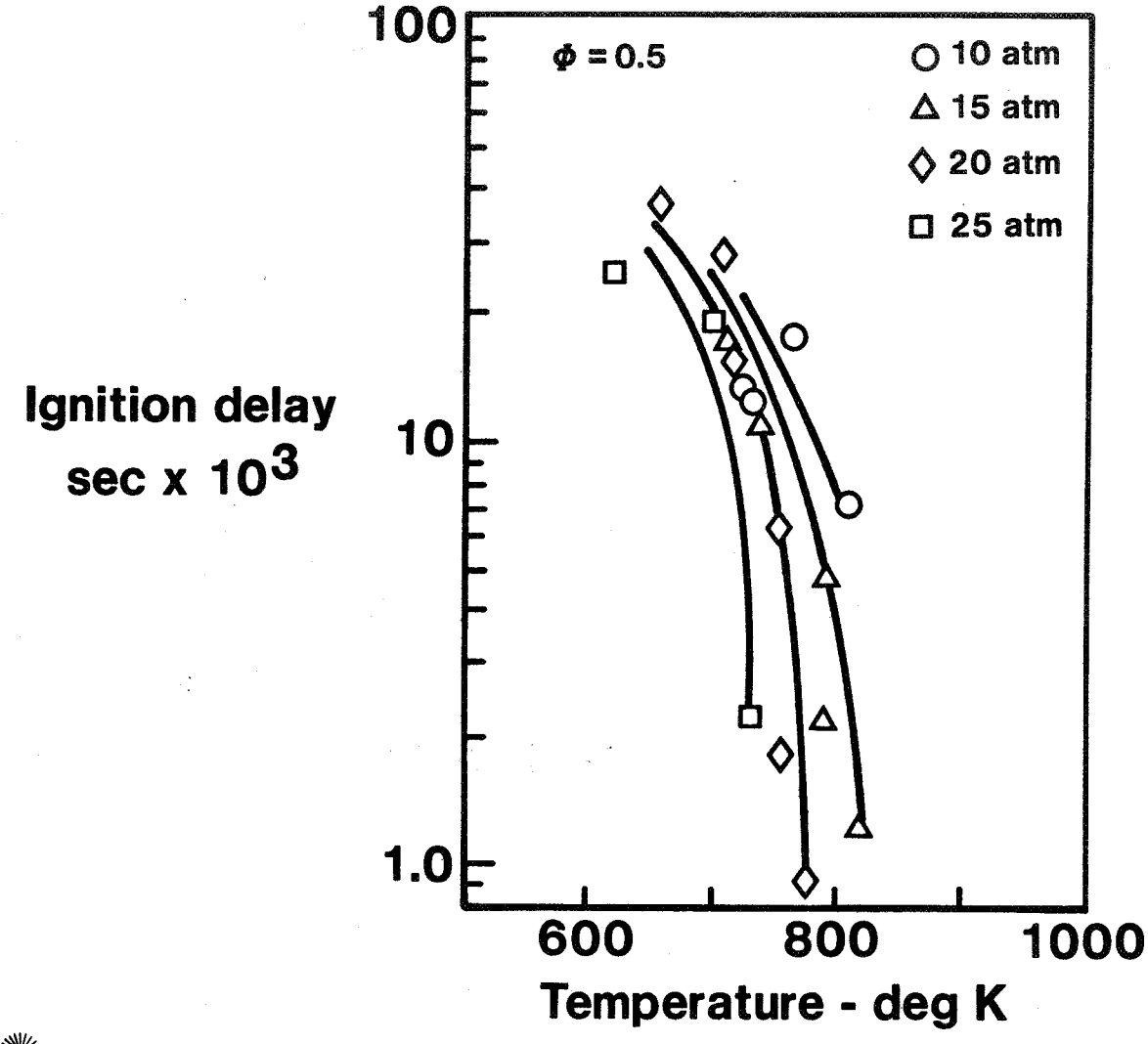

Multiple Conical Tube Injector

Blockage = 70 percent

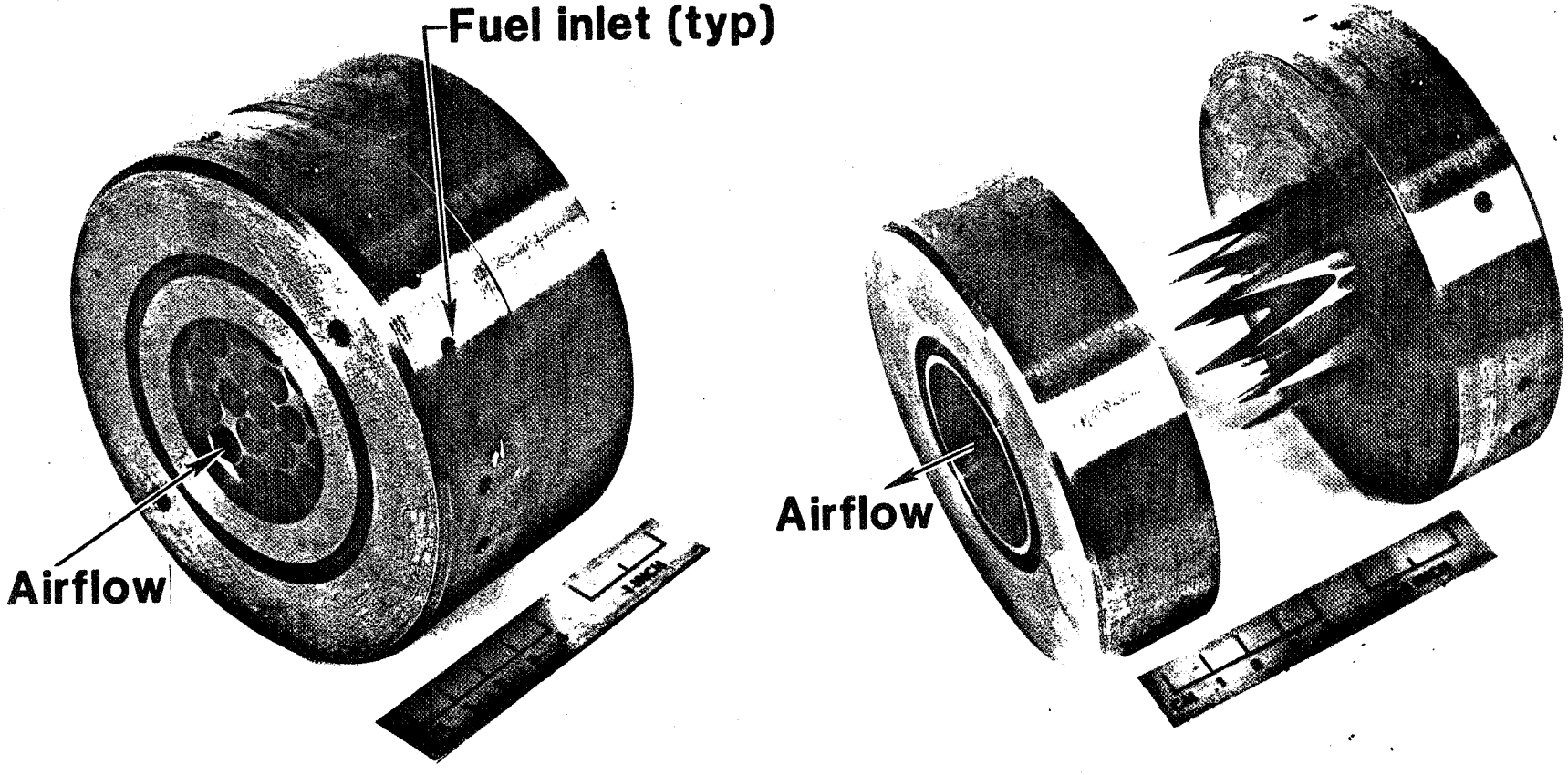

Program Summary
Autoignition of Fuels

- **Phase I**
  - Develop critical autoignition experiment
- **Phase II**
  - Develop premixing-type fuel injector and determine the autoignition characteristics of Jet-A fuel
- **Phase III**
  - Determine the autoignition characteristics of a variety of fuels and investigate the effects of chemical composition and structure

Emissions Measurements for a Lean Premixed Propane/Air System at Pressures Up to 30 Atmospheres

A series of experiments was conducted in which the emissions of a lean premixed system of propane and air were measured at pressures of 5, 10, 20 and 30 atm in a flametube apparatus. Measurements were made for inlet temperatures between 600K and 1000K and combustor residence times from 1.0 to 3.0 msec.

Figure 1 is a schematic of the test rig. Propane, heated to a temperature of 380K, was injected as a gas through a 52 point matrix into a dry heated stream of air. The mixture was ignited downstream of a water-cooled perforated plate flameholder and emissions measured at downstream locations by a water-cooled sampling probe. Residence time was calculated from probe position assuming an instantaneous temperature rise to the adiabatic flame temperature.

Figures 2, 3 and 4 present emissions measurements for NO_x, CO and UHC as functions of combustor residence time for various equivalence ratios, entrance temperatures and pressures. NO_x emission index appears to vary directly with residence time. Hydrocarbon species disappear within the first two milliseconds. CO levels peak around one millisecond and then fall rapidly until equilibrium is reached sometime between 2.0 and 2.5 milliseconds residence time.

Figure 5 illustrates typical behavior of emissions as a function of equivalence ratio for a fixed residence time. NO_x levels rise exponentially from the lean stability limit but tend to flatten out at high equivalence ratio. CO drops rapidly as equivalence ratio increases from the lean stability limit eventually reaching chemical equilibrium within the fixed combustor residence time and follows the equilibrium curve from that point on. Unburned hydrocarbon levels decrease with increasing equivalence ratio.

Figures 6 through 10 present correlations of NO_x emission index with adiabatic flame temperature for a fixed residence time of 2 msec and pressures from 5 to 30 atm. Adiabatic flame temperature is seen to be an excellent correlating parameter, combining the individual effects of entrance temperature and equivalence ratio. Furthermore, there appears to be a universal curve which fits

all NO_x emission data, independent of pressure. At operating conditions combining low inlet temperature and low pressure, some NO_x data falls below this universal curve. It is likely that this is simply a reflection of the inadequacy of the assumption of instantaneous temperature rise in the residence time calculation at these conditions.

Figure 11 illustrates the pressure reduction sampling probe used to obtain the preceding data. The high pressure gas sample was first expanded into a low pressure (2 atm) dump tube to slow reactions. A small portion of this low pressure sample was then withdrawn through a water-cooled tube and analyzed for emissions.

Figure 12 illustrates a rapid thermal quench sampling probe which maintains a constant pressure in the sampling tube.

Figure 13 illustrates a sampling probe which combines the pressure reduction and rapid thermal quench techniques in a single design.

Figure 14 illustrates how sampling probe design affects emission measurements. NO_x and UHC measurements are virtually identical using thermal, pressure and pressure/thermal quenching techniques. CO levels are quite sensitive to quench technique and can drop substantially in the sampling probe if reaction rates are not adequately retarded. Since a straight pressure reduction sampling probe was used to obtain the emissions data presented in Figures (1) through (4), CO levels reported there are probably lower than actual. The breakpoint, or point at which measured CO levels cross the equilibrium curve and reverse their slope, is not affected by this phenomenon.

Figure 15 presents the adiabatic flame temperature corresponding to CO breakpoint conditions for 2 msec residence time as a function of inlet temperature and pressure. An adiabatic flame temperature of 2050K is seen to be a good correlation of the breakpoint phenomenon.

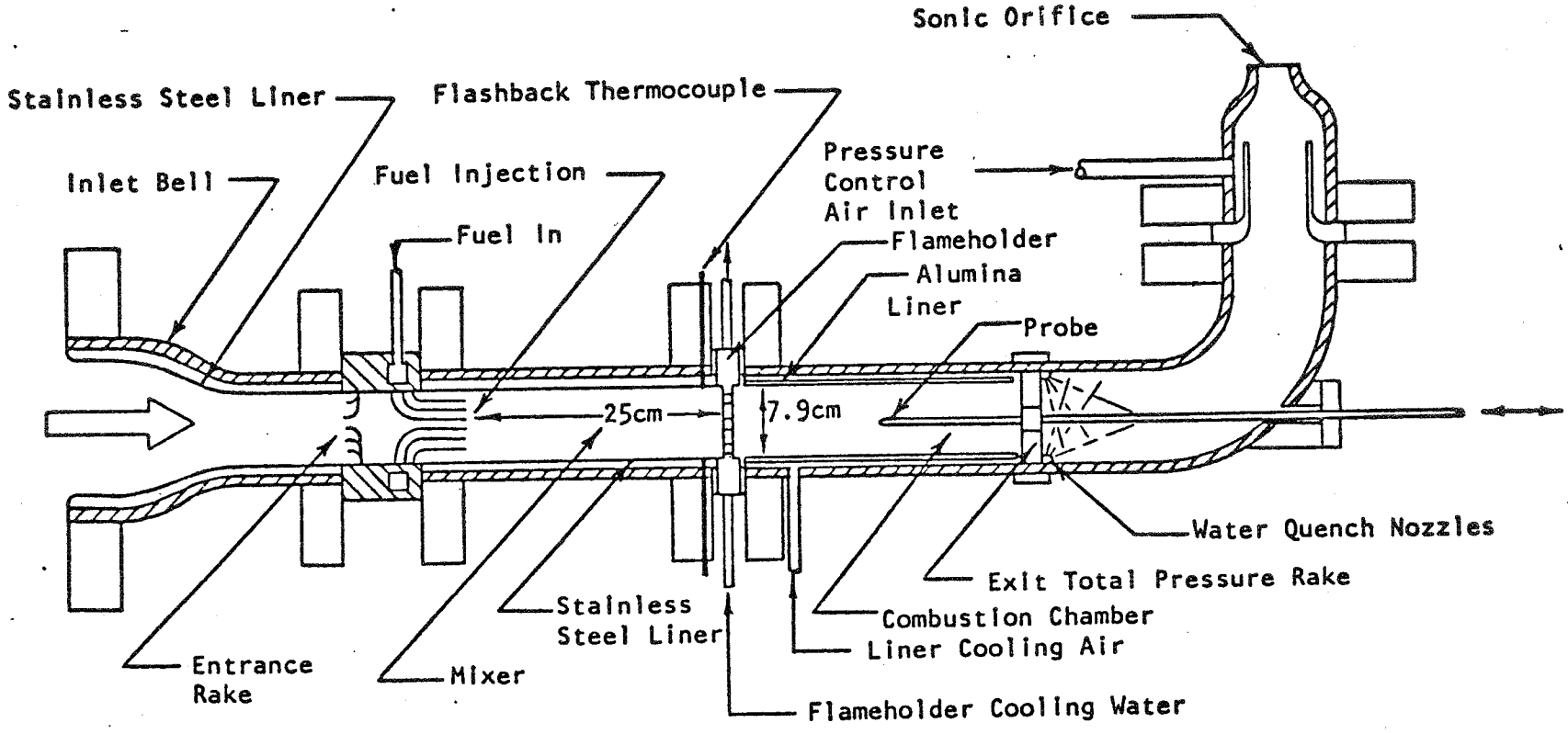

FIGURE 1. COMBUSTION TEST RIG

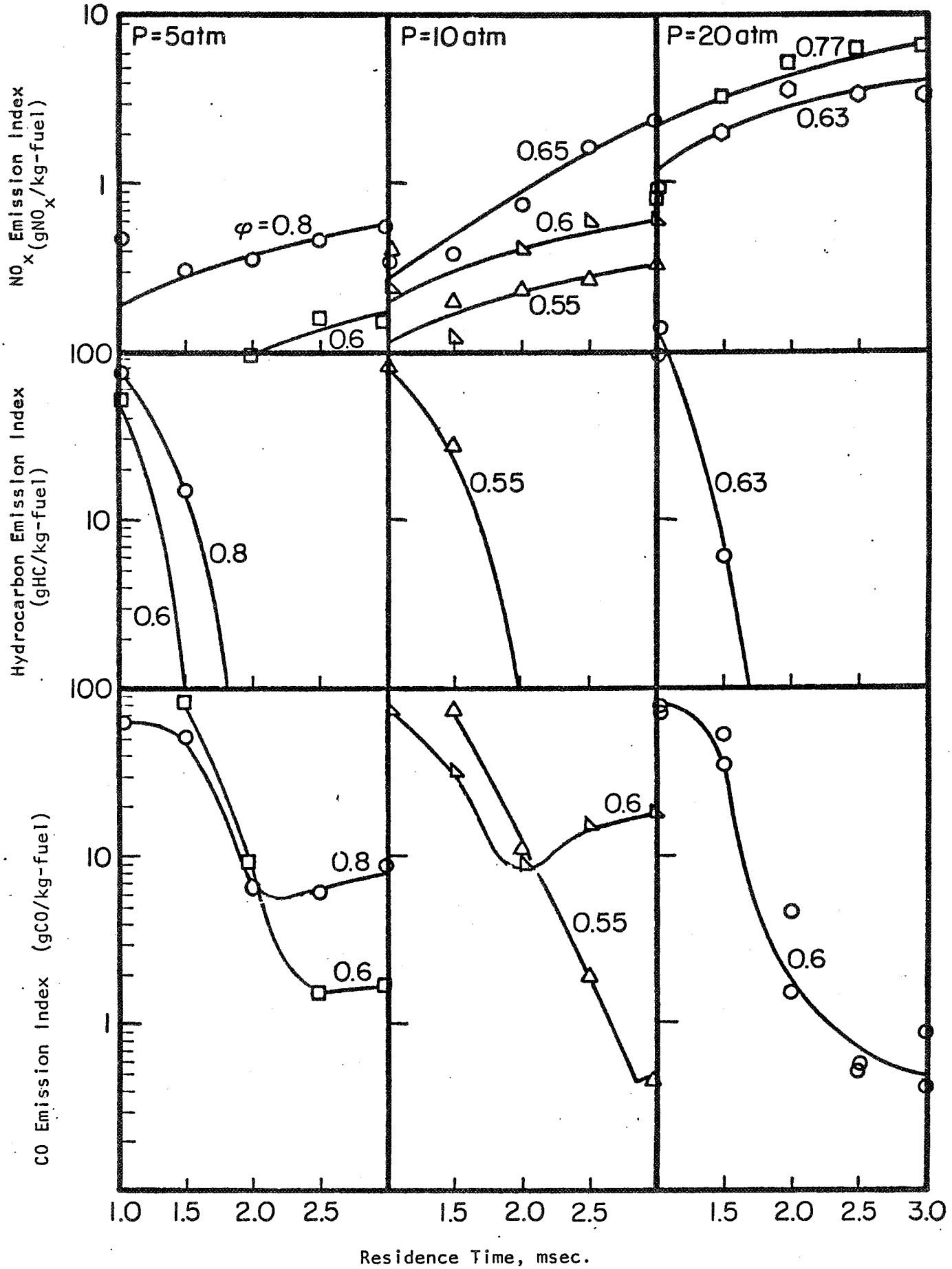

FIGURE 2. EMISSION INDICES AS A FUNCTION OF COMBUSTOR RESIDENCE TIME (T_3=600K)

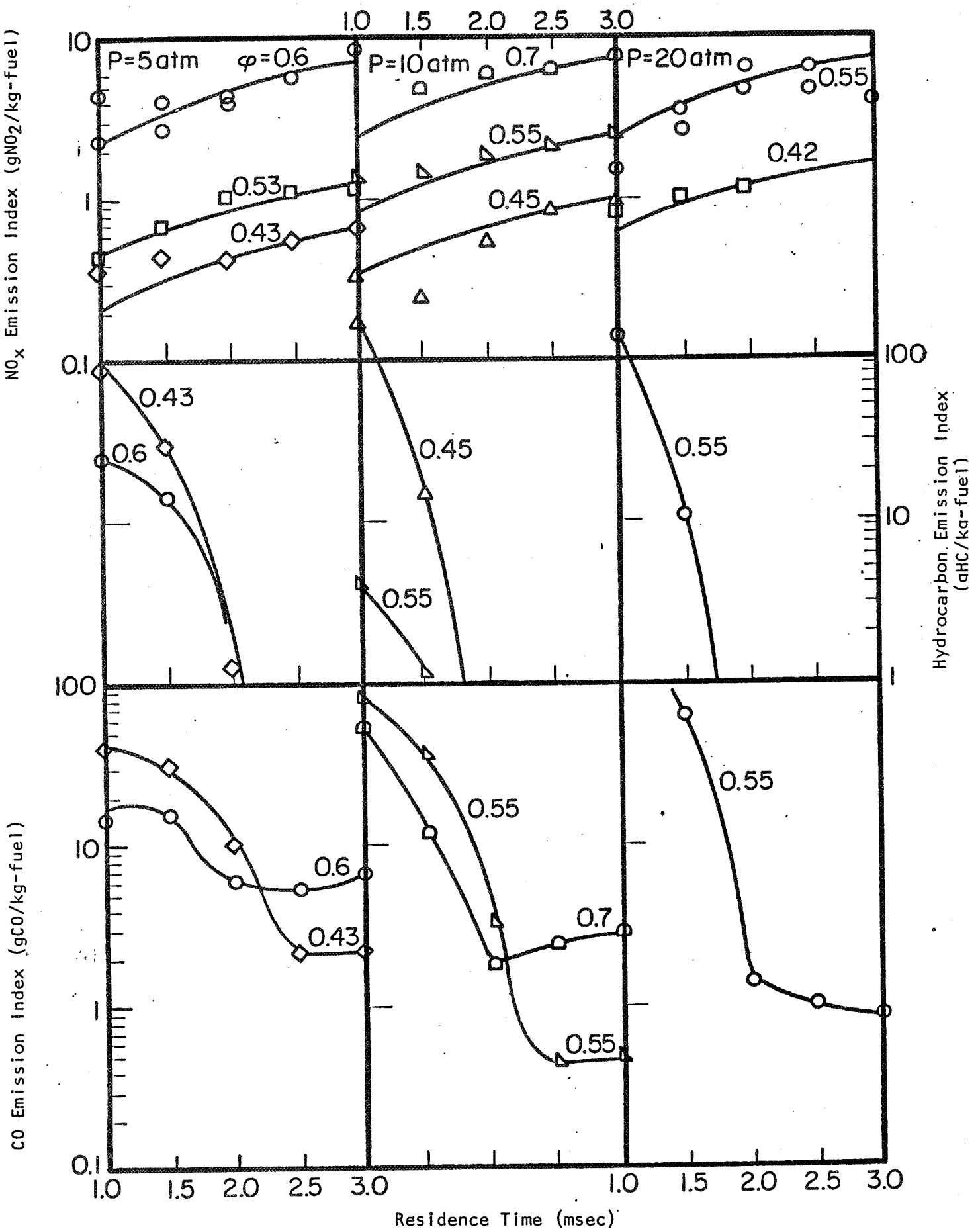

FIGURE 3. EMISSION INDICES AS A FUNCTION OF COMBUSTOR RESIDENCE TIME (T_3=800K)

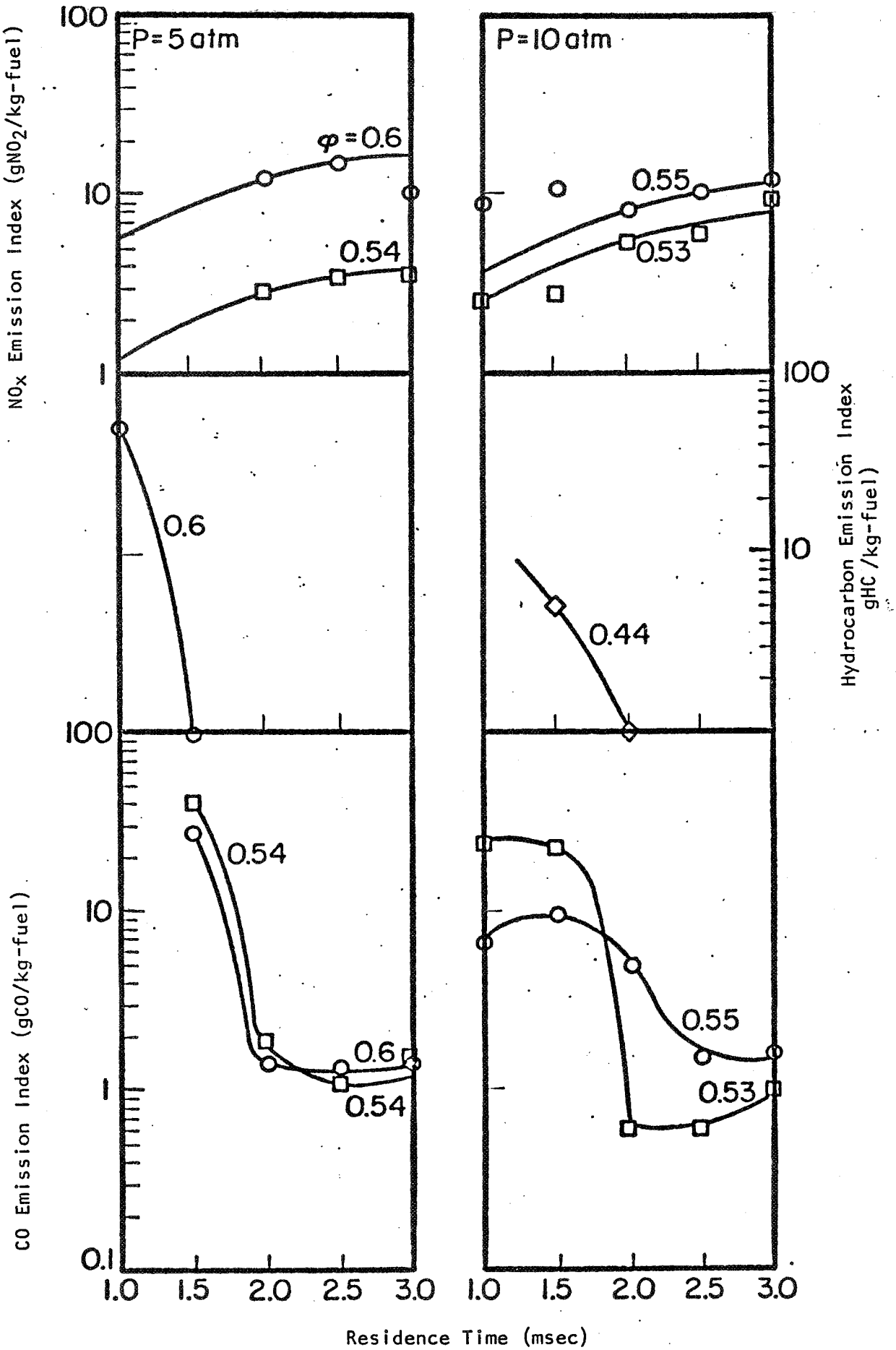

FIGURE 4. EMISSION INDICES AS A FUNCTION OF COMBUSTOR RESIDENCE TIME (T_3=1000K)

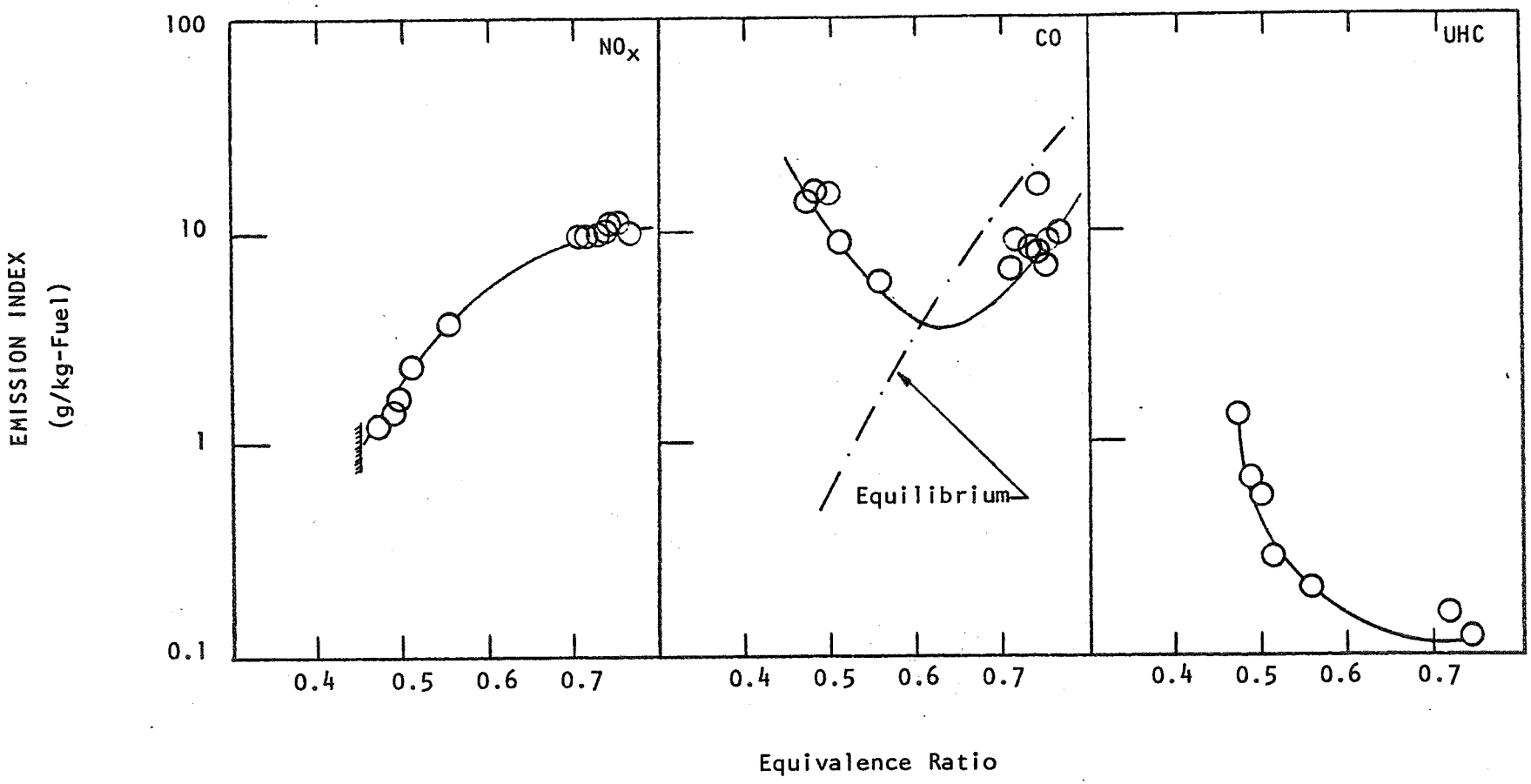

Inlet Temperature = 800K

Inlet Pressure = 30 atm

Residence Time = 2 msec

FIGURE 5. EMISSION MEASUREMENTS

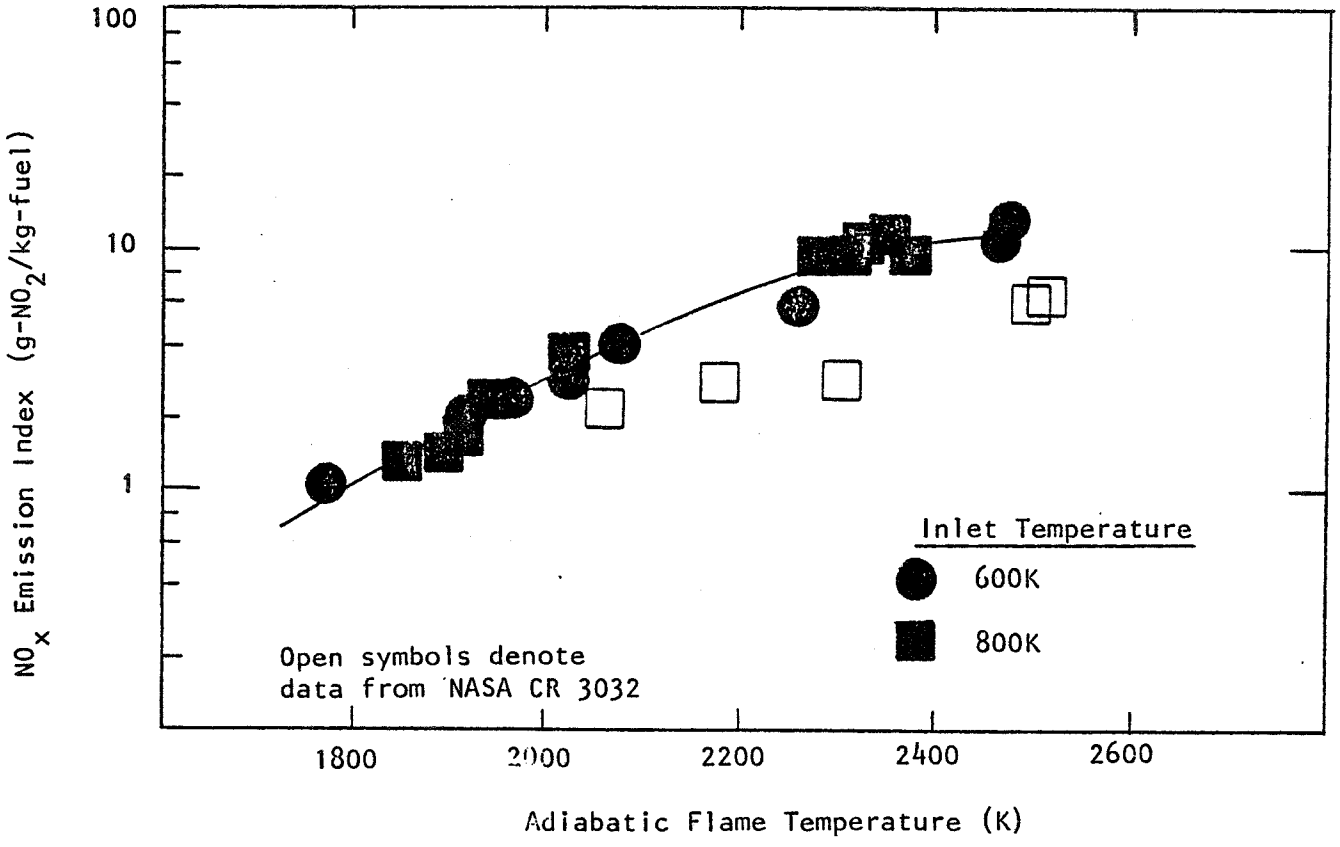

FIGURE 6. CORRELATION OF NO_x EMISSION INDEX FOR 2 MSEC RESIDENCE TIME WITH ADIABATIC FLAME TEMPERATURE (P=30 atm)

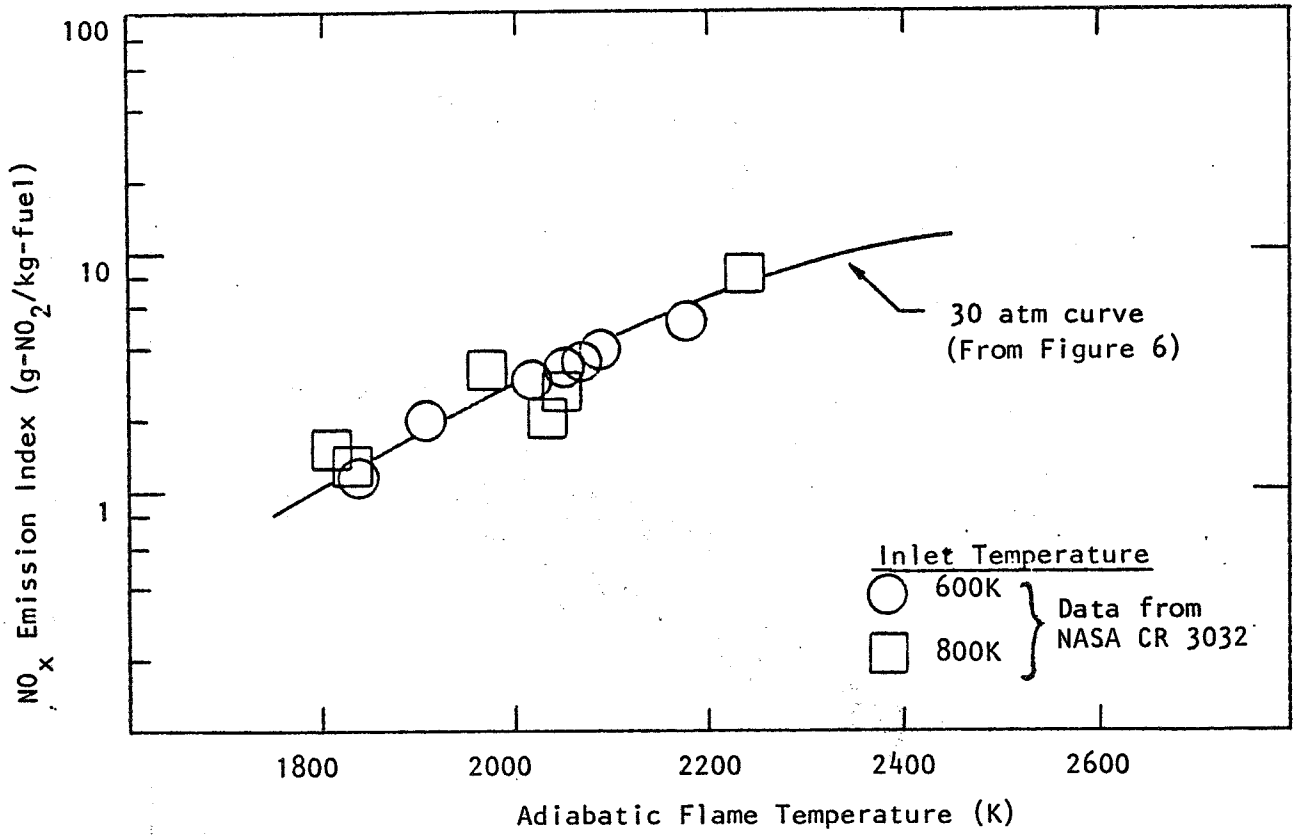

FIGURE 7. CORRELATION OF NO_X EMISSION INDEX FOR 2 MSEC RESIDENCE TIME WITH ADIABATIC FLAME TEMPERATURE (p=20 atm)

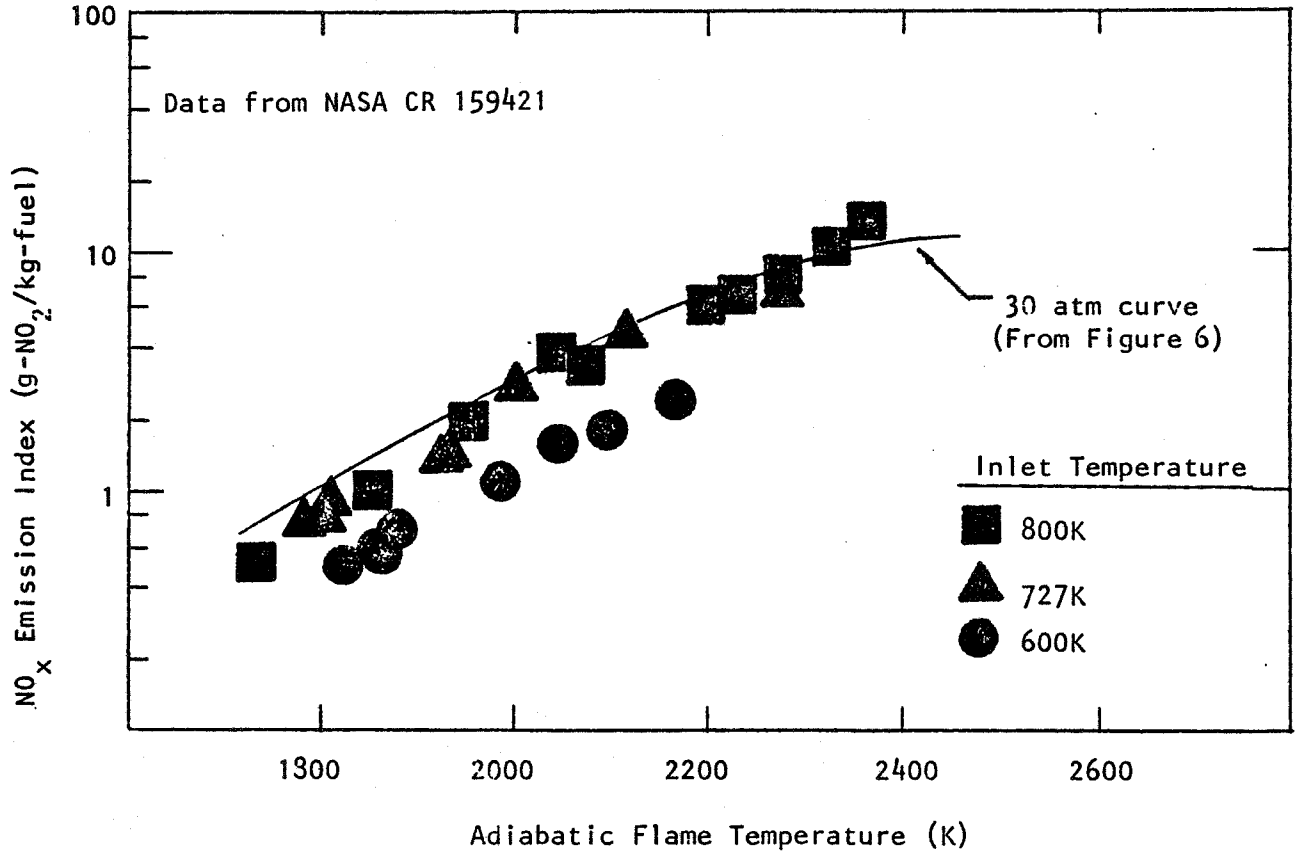

FIGURE 8. CORRELATION OF NO_X EMISSION INDEX FOR 2MSEC RESIDENCE TIME WITH ADIABATIC FLAME TEMPERATURE. (P=10 atm)

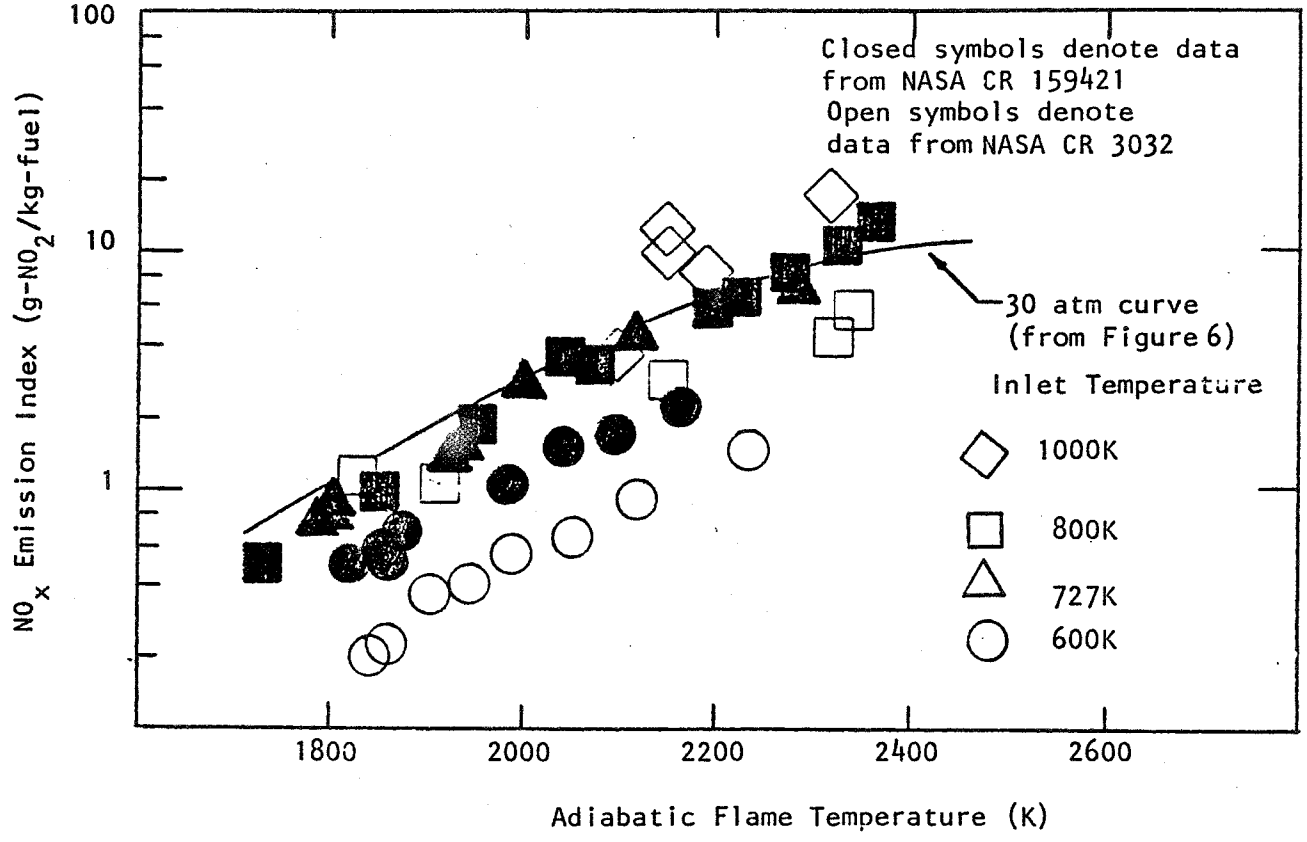

FIGURE 9. CORRELATION OF NO_x EMISSION INDEX FOR 2MSEC RESIDENCE TIME WITH ADIABATIC FLAME TEMPERATURE (P=10 atm)

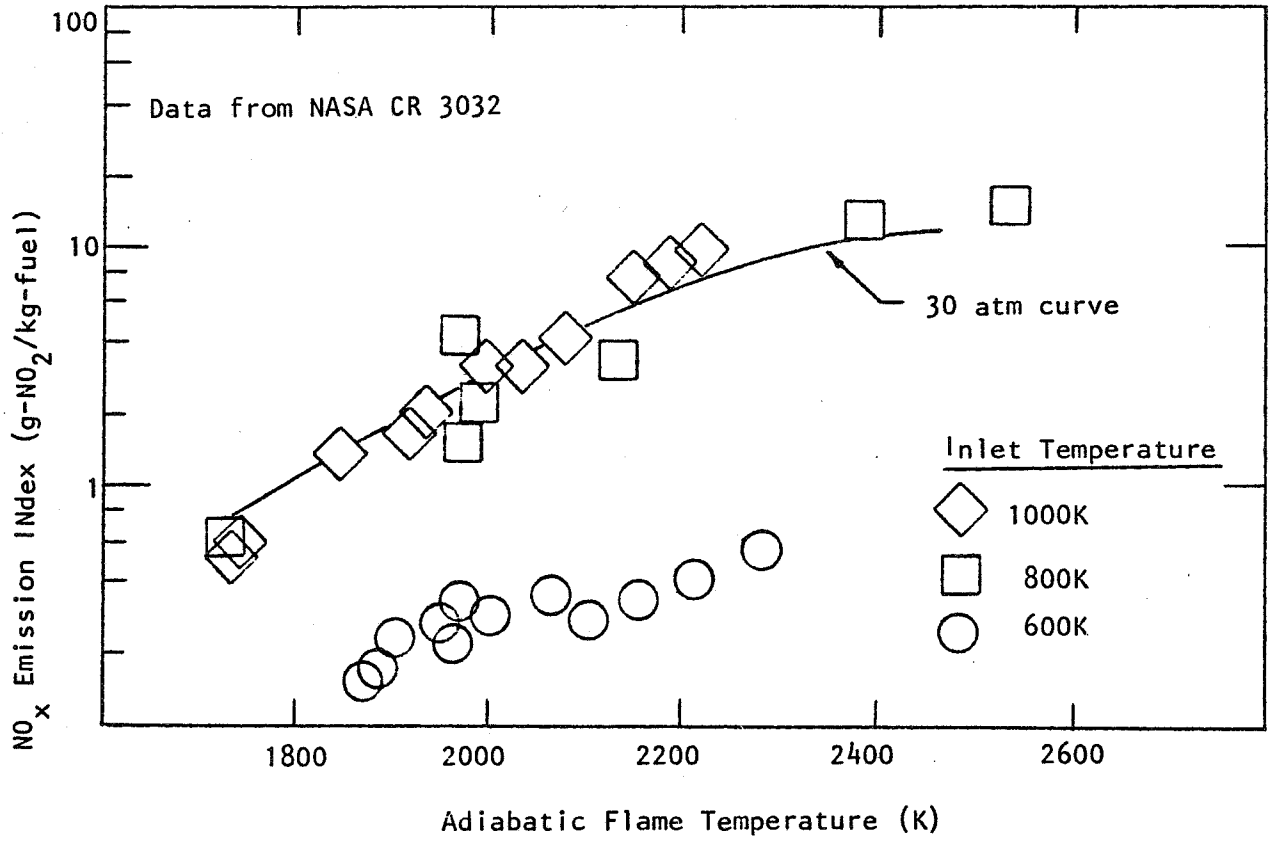

FIGURE 10. CORRELATION OF NO_x EMISSION INDEX FOR 2 MSEC RESIDENCE TIME WITH ADIABATIC FLAME TEMPERATURE (p=5 atm)

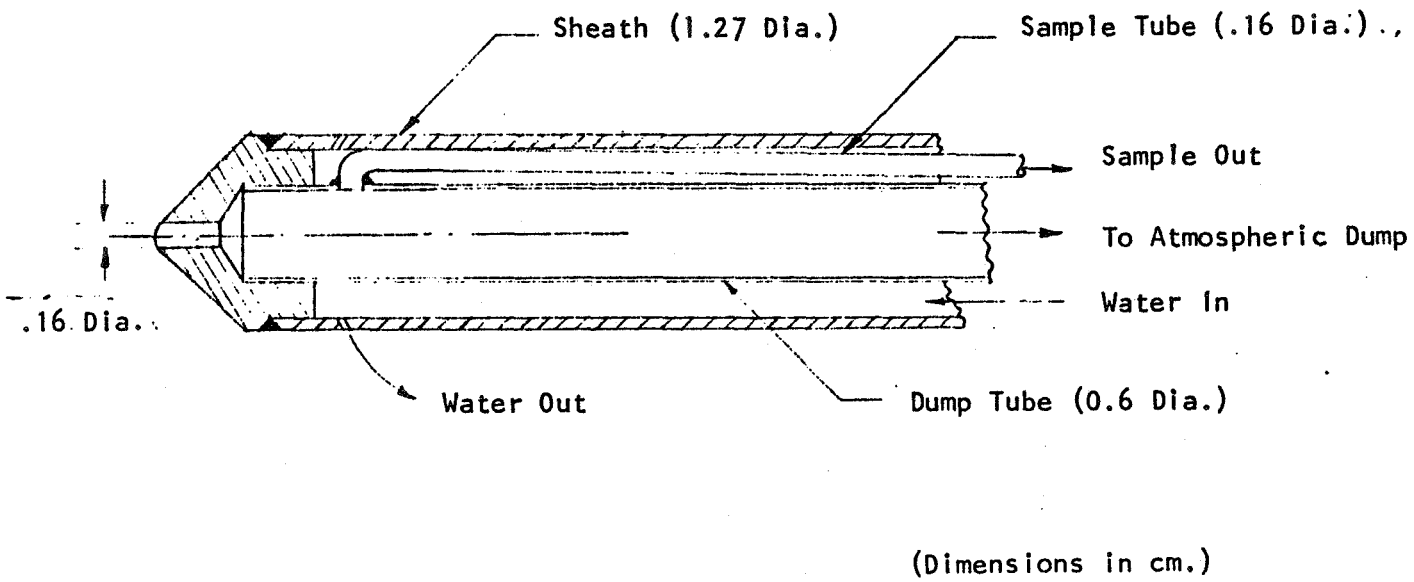

FIGURE 11. PRESSURE REDUCTION SAMPLING PROBE WITH MODERATE THERMAL QUENCH

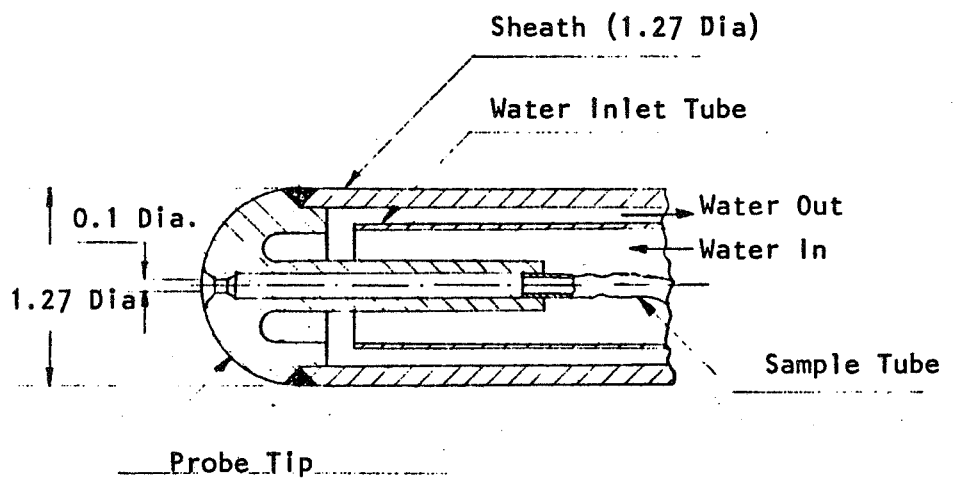

(Dimensions in cm.)

FIGURE 12. THERMAL QUENCH PROBE

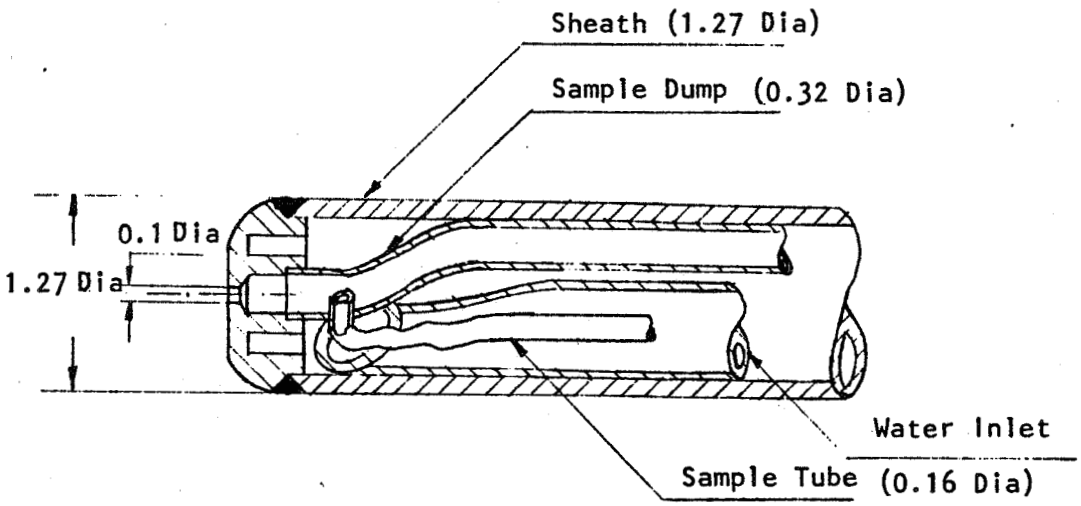

FIGURE 13. PRESSURE/THERMAL-QUENCH PROBE

(Dimensions in cm.)

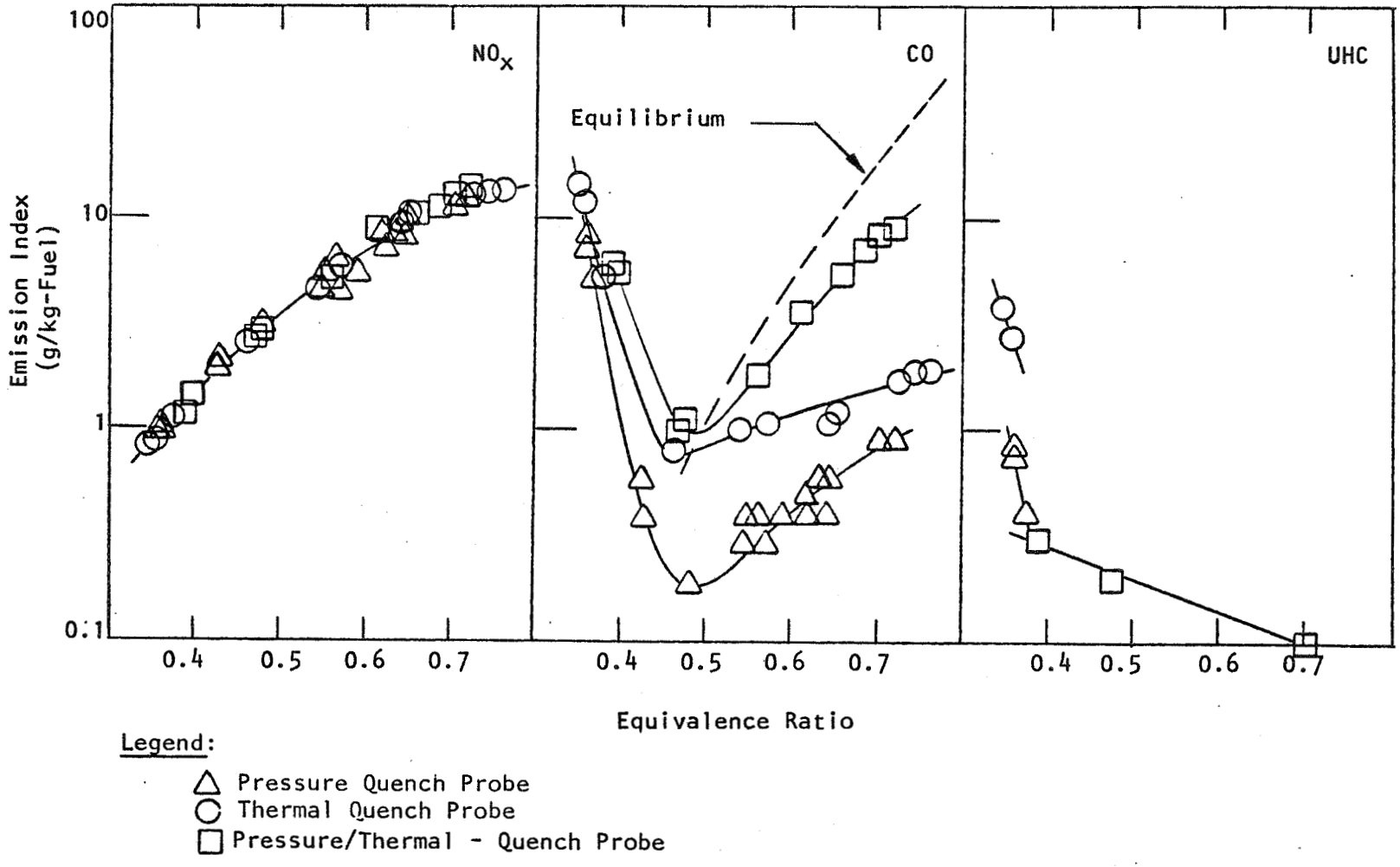

FIGURE 14. COMPARISON OF EMISSIONS MEASUREMENTS USING THERMAL, PRESSURE AND PRESSURE/THERMAL QUENCH PROBE DESIGNS. (T = 800K, p = 10 atm.)

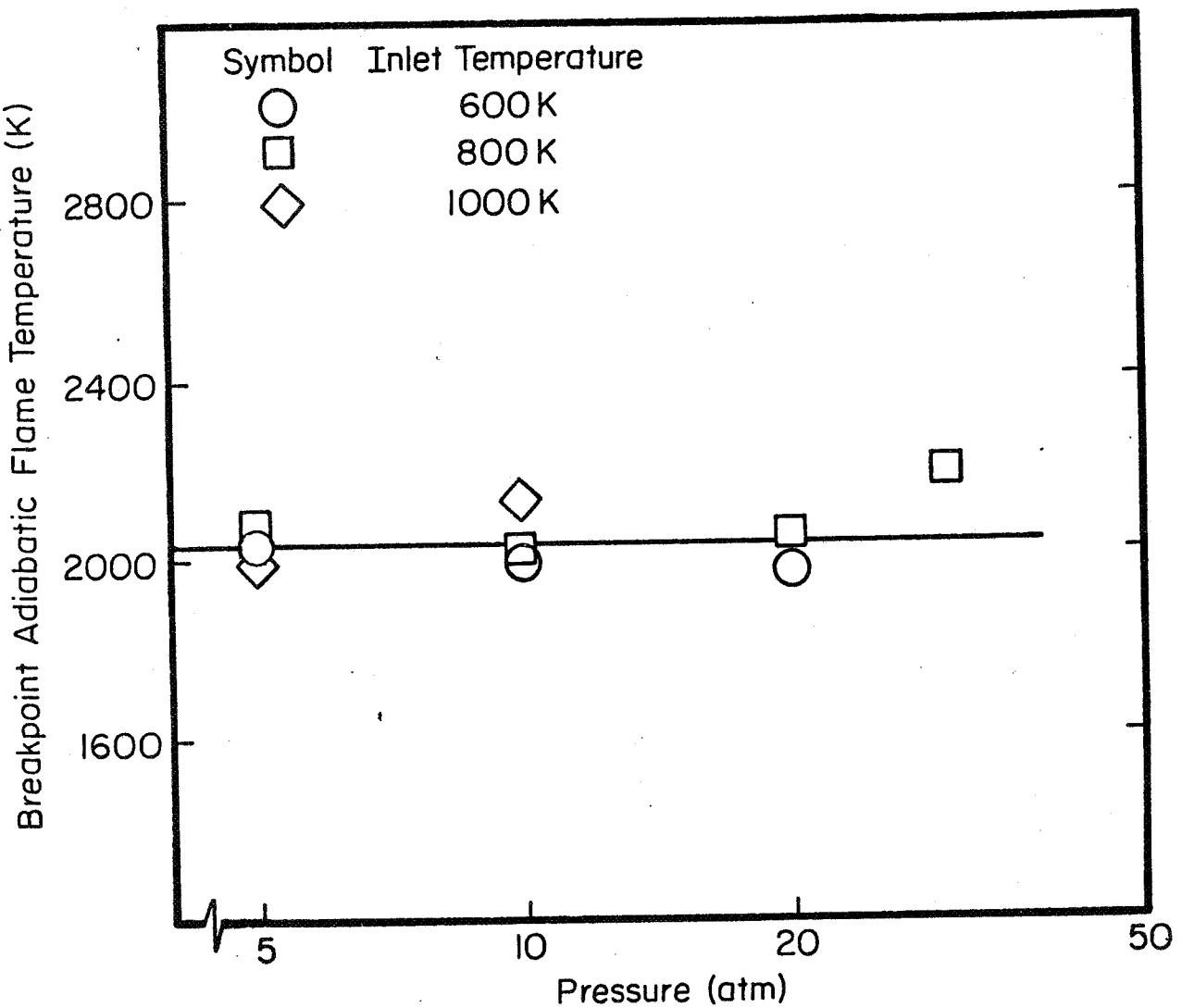

FIGURE 15. ADIABATIC FLAME TEMPERATURE CORRESPONDING TO CO BREAKPOINT AT 2 MSEC RESIDENCE TIME.

THE EFFECT OF DEGREE OF FUEL VAPORIZATION UPON EMISSIONS FOR A PREMIXED - PREVAPORIZED COMBUSTION SYSTEM

L. P. COOPER

The report presents test results from a study which was conducted to assess the impact of the degree of fuel vaporization upon emissions from a flametube combustor burning premixed, "partially" vaporized fuel-air mixtures. Tests were conducted at an inlet air pressure of 3×10^5 pascals, inlet air temperatures of 600K and 700K, a reference velocity of 35 meters per second and equivalence ratios of .6 and .72 using Jet A fuel.

The tests reported herein were conducted in a closed duct test facility as shown in figure 1. Incoming air to the test section was preheated to temperatures from 600K to 700K by a non-vitiating preheater. Jet A fuel was injected into this airstream through two different fuel injectors (figure 2-3) manifolded together and mounted in series upstream of a watercooled perforated plate flameholder (figure 4). The fuel-air mixture burned in a watercooled combustor section. Samples of the fuel-air mixture upstream of the flameholder were obtained for analysis to determine the local degree of fuel vaporization and the fuel-air ratio. Samples of the combustion products were analyzed to determine gaseous emissions.

Results of effects of vaporization on NO_x emissions are presented in figure 5. The data displays an effect of vaporization on NO_x which differs with equivalence ratio. For an equivalence ratio of .6, decreasing the fuel vaporization leads to a nearly linear increase in NO_x. However, for equivalence ratios of .72, changes in vaporization had very little impact on NO_x emissions. Both slight increases and decreases were found.

Results on the effect of vaporization on CO emissions are shown in figure 6a and 6b for two different sample measurement distances from the flameholder. In figure 6a (48 cm. probe location) the data displays uniform decreases in the CO level with increasing vaporization. Data for 79 cm. probe position is shown in figure 6b and shows the combustion of CO to be essentially complete and the degree of vaporization having little effect upon the CO emissions.

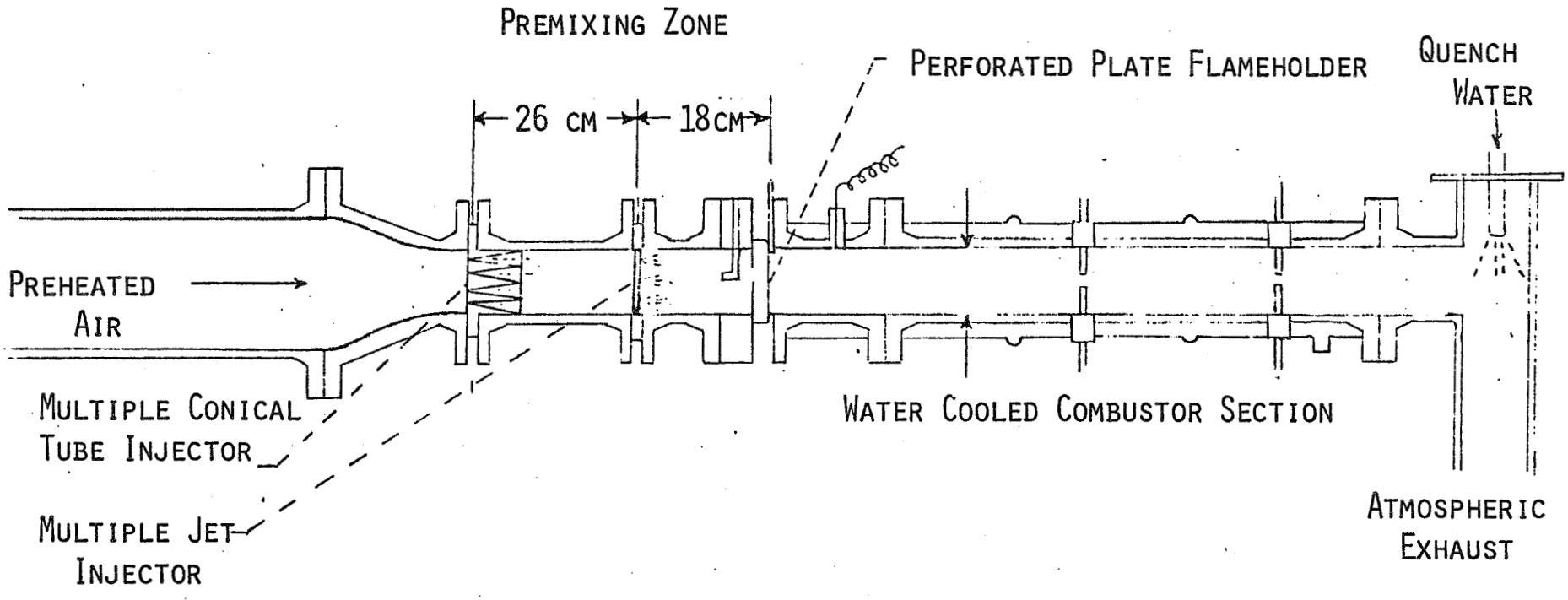

FIGURE 1. RIG SCHEMATIC (DIMENSIONS IN CM.)

MULTIPLE JET INJECTOR

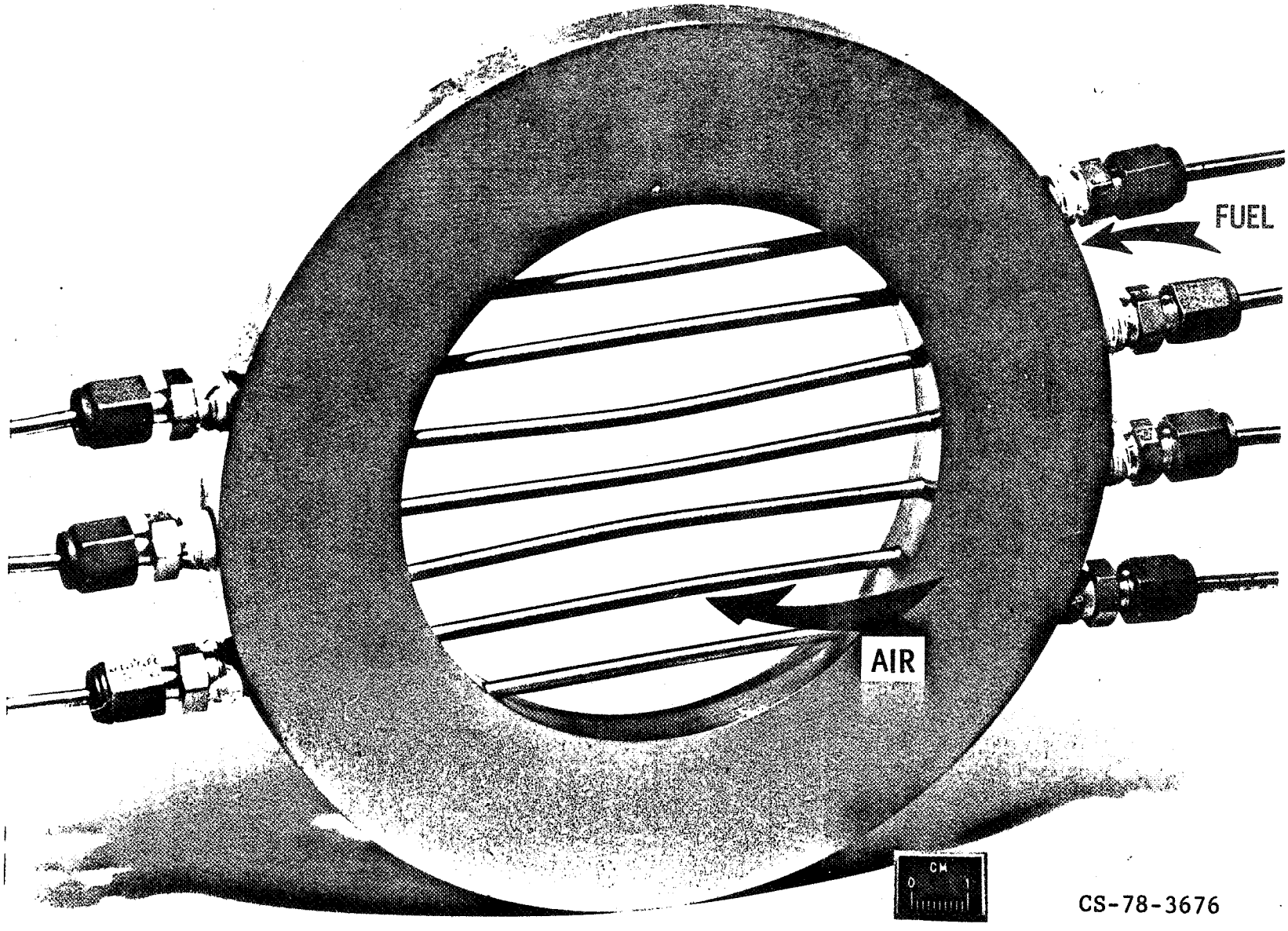

FIGURE 2 - MULTIPLE JET INJECTOR

MULTIPLE CONICAL TUBE INJECTOR

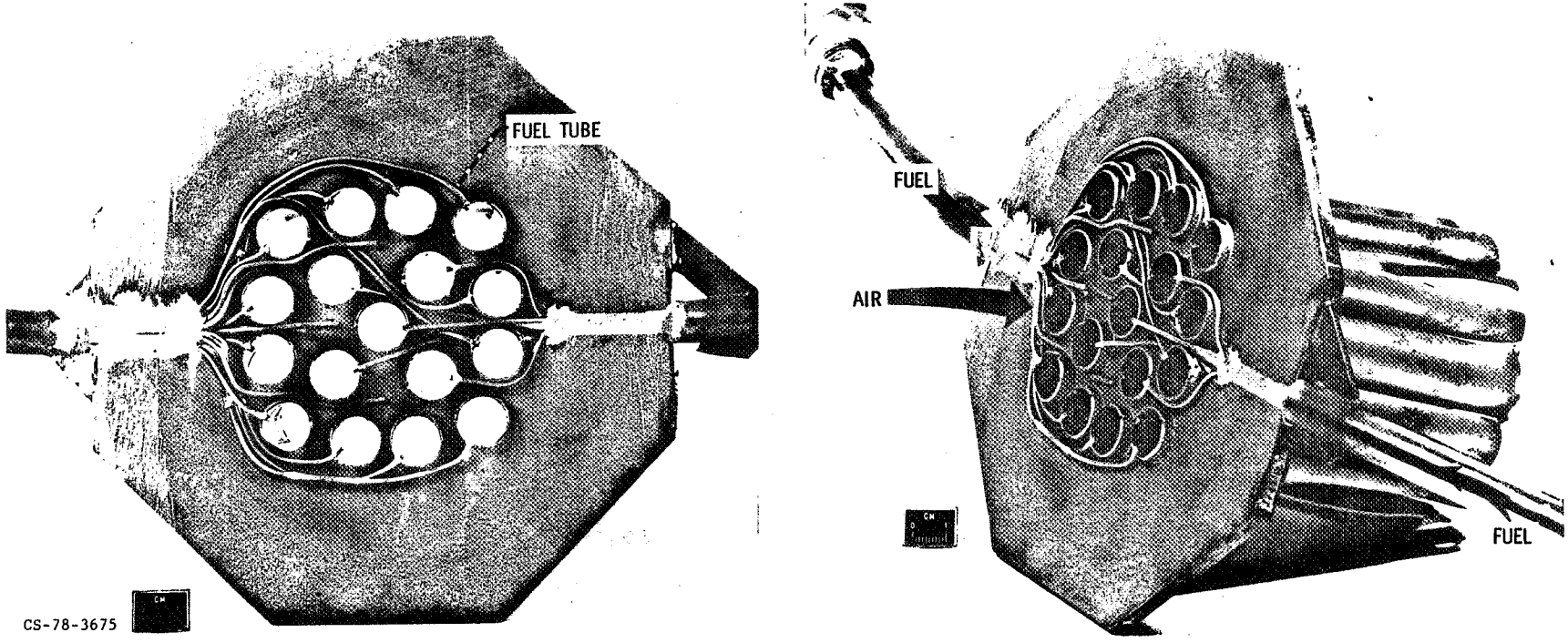

FIGURE 3 - MULTIPLE CONICAL TUBE INJECTOR

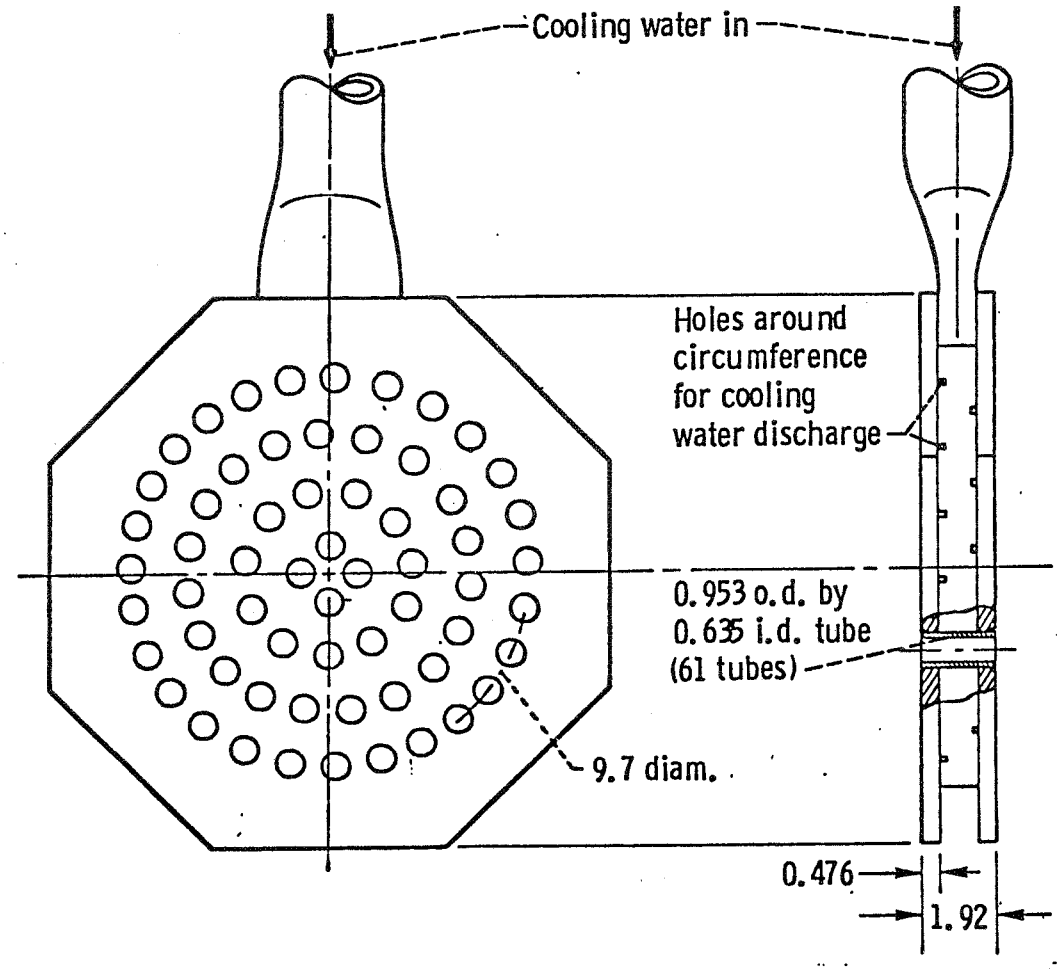

FIGURE 4. PERFORATED PLATE FLAMEHOLDER, BLOCKAGE OF 75 PERCENT.

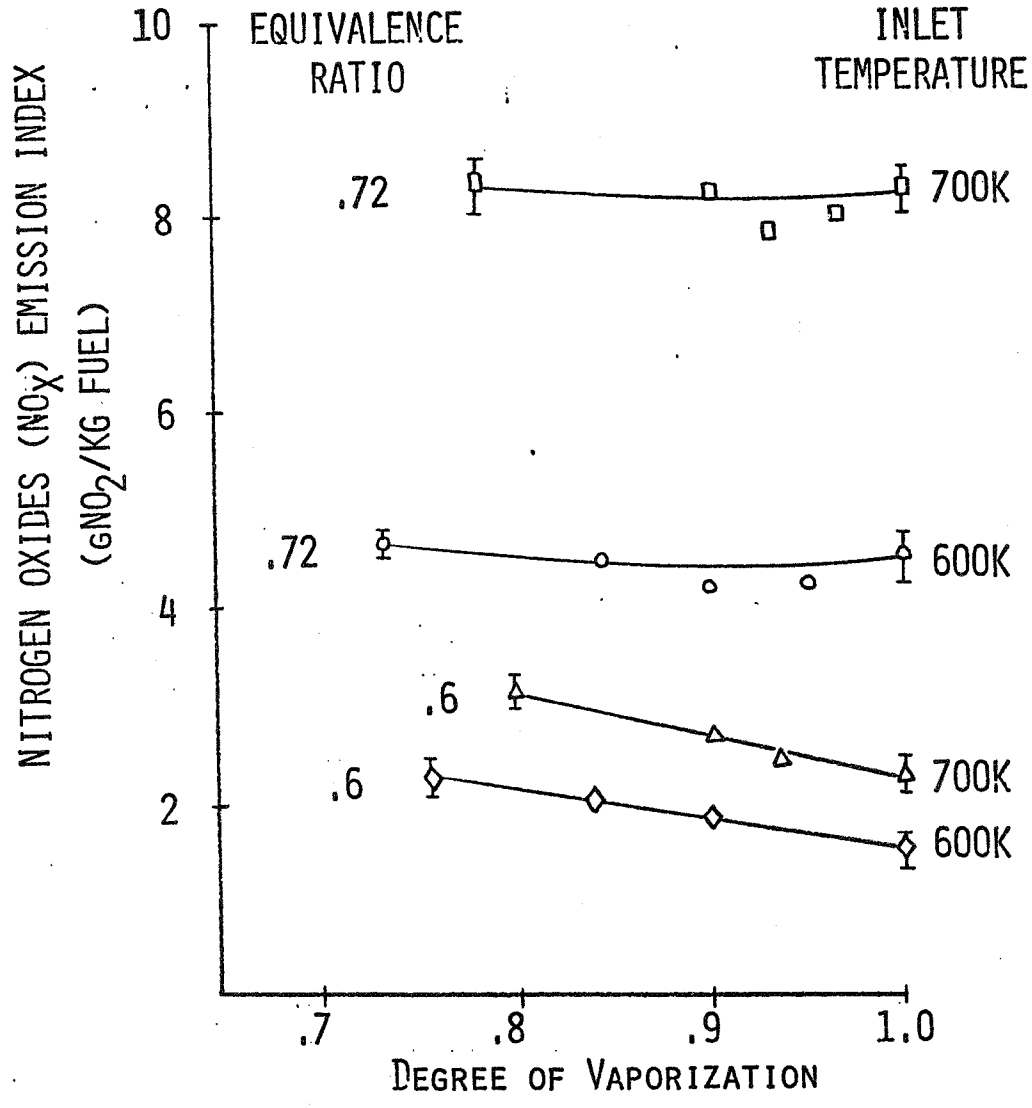

FIGURE 5. EFFECT OF DEGREE OF VAPORIZATION ON NITROGEN OXIDES EMISSION INDEX OVER A RANGE OF INLET TEMPERATURES AND EQUIVALENCE RATIOS.

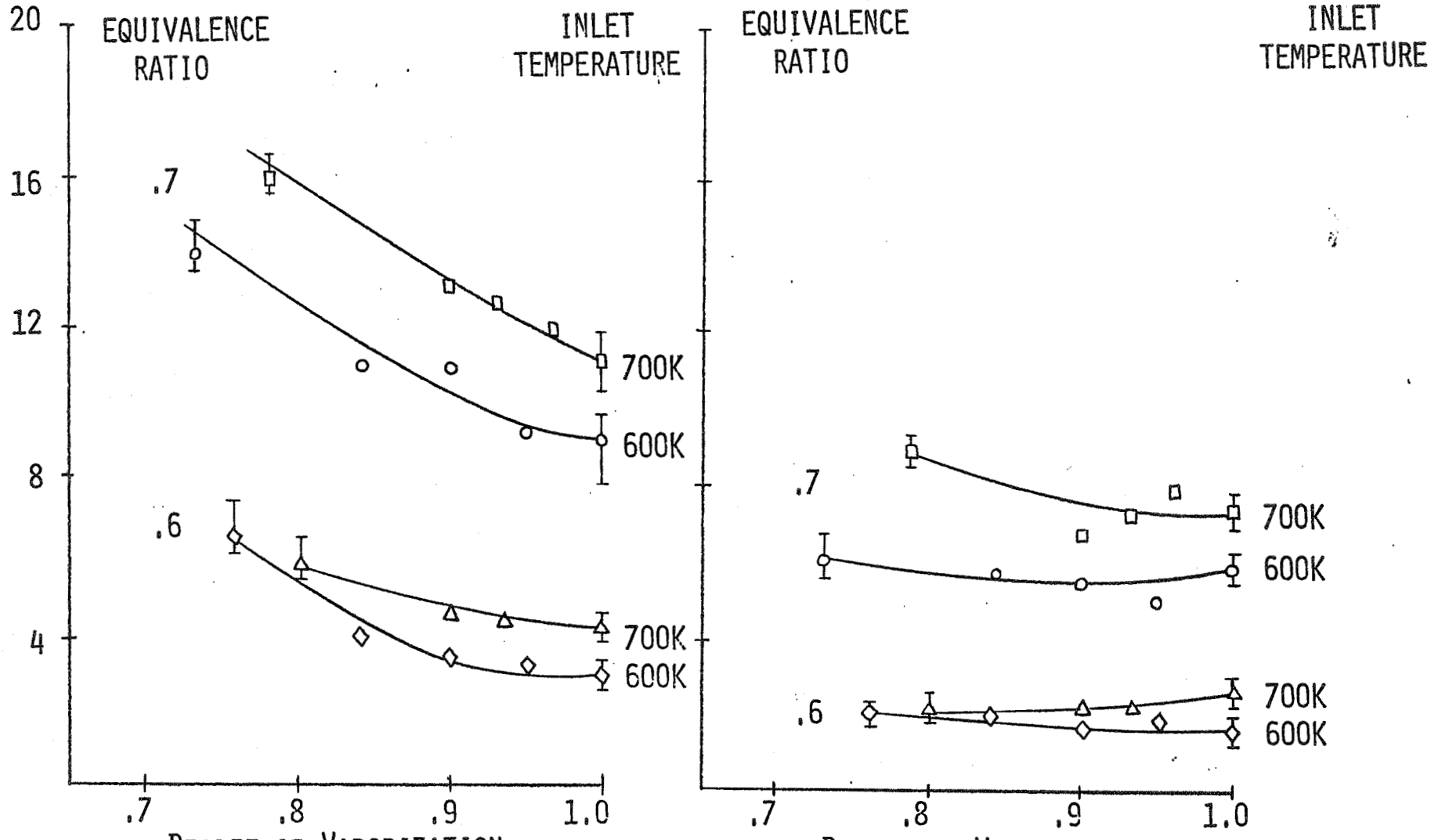

FIGURE 6. EFFECT OF DEGREE OF VAPORIZATION ON CARBON MONOXIDE EMISSIONS INDEX OVER A RANGE OF INLET TEMPERATURES AND EQUIVALENCE RATIOS AT TWO SAMPLE PROBE LOCATIONS.

A Study of the Effect of Fuel/Air Nonuniformity on Nitric Oxide Emissions

by

Valerie Lyons

Airbreathing Engines Division
NASA Lewis Research Center
Cleveland, Ohio

A study of the effect of fuel/air nonuniformity on exhaust emissions was performed in a flame tube combustor using Jet A fuel. The experiments were performed at a pressure of .3 Mpa and a reference velocity of 25 meters/second for three inlet air temperatures of 600, 700, and 800 K. The gas sample measurements were taken at locations 18 cm. and 48 cm. downstream of the perforated plate flameholder as shown in the rig schematic in figure 1. Nonuniform fuel/air profiles were produced using the fuel injector shown in figure 2 by separately fueling the inner five fuel tubes and the outer ring of twelve fuel tubes. Six fuel/air profiles were produced for nominal overall equivalence ratios of .5 and .6. An example of three of these profiles and their resultant NO_x emissions are shown in figure 3 and 4.

Figures 5 and 6 show NO_x emission indices which have been mass-weighted before determining a mean value of the particular fuel/air profile. These mean E. I. values are plotted versus a fuel/air nonuniformity parameter, s, which is the standard deviation from the mean of the local equivalence ratio profile for the particular fuel/air profile studied.

The uniform fuel/air profile cases produced uniform and relatively low NO_x profile levels. When the profiles were either center-peaked or edge-peaked, the overall mass-weighted NO_x levels increased. The maximum increase in NO_x was sixteen-fold deviation from the uniform profile values for the 600K inlet air temperature, ϕ nominal = .5 case as seen in figure 5. For the ϕ nominal = .6 case, 800 K inlet air, the NO_x showed a five-fold maximum increase from the uniform case (see figure 6). Figure 6 also shows that changing the inlet air temperature produced no change in the overall trends in the effect of nonuniformity on NO_x.

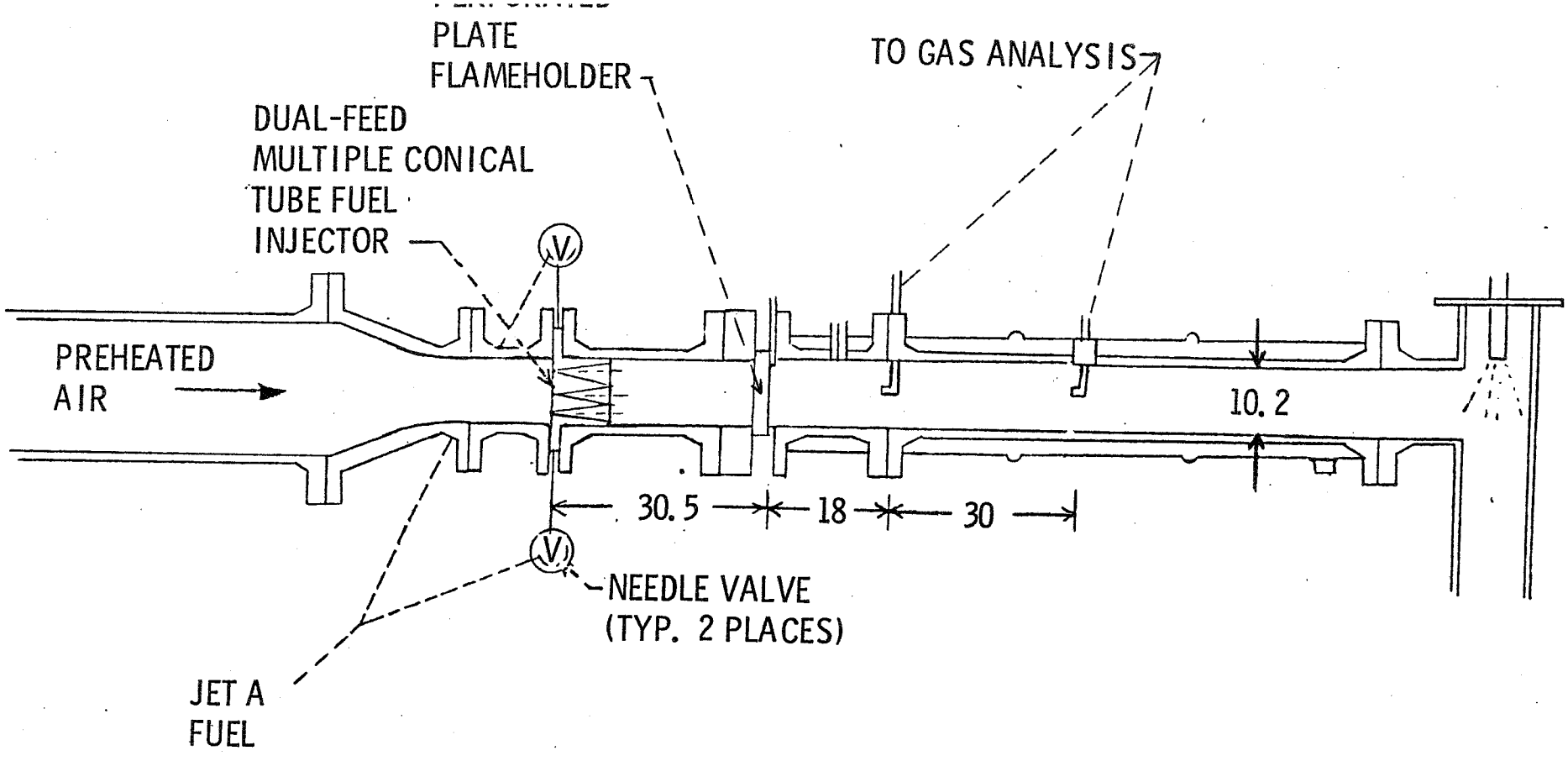

FIGURE 1 - Rig schematic (all dimensions in cm).

MULTIPLE CONICAL TUBE INJECTOR

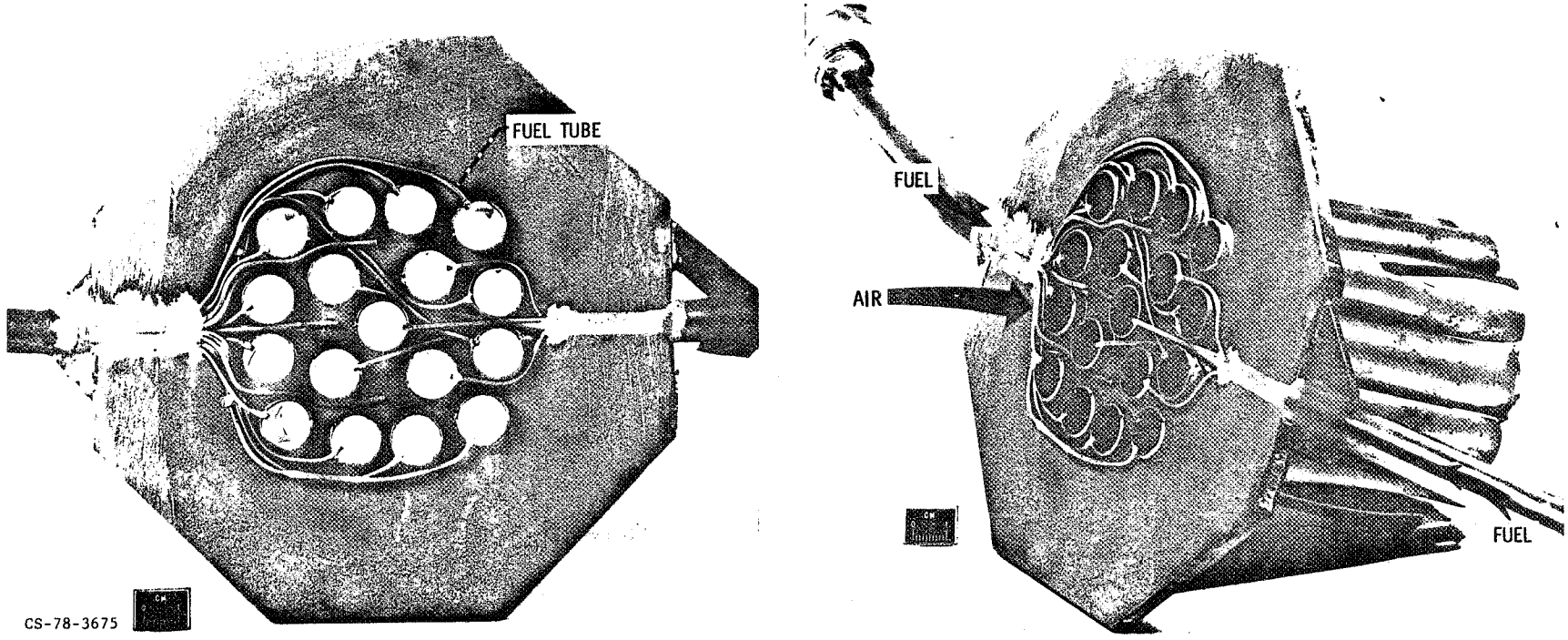

FIGURE 2

THREE FUEL/AIR PROFILES FOR A NOMINAL EQUIVALENCE RATIO OF 0.6 AND INLET AIR TEMPERATURE OF 600°K.

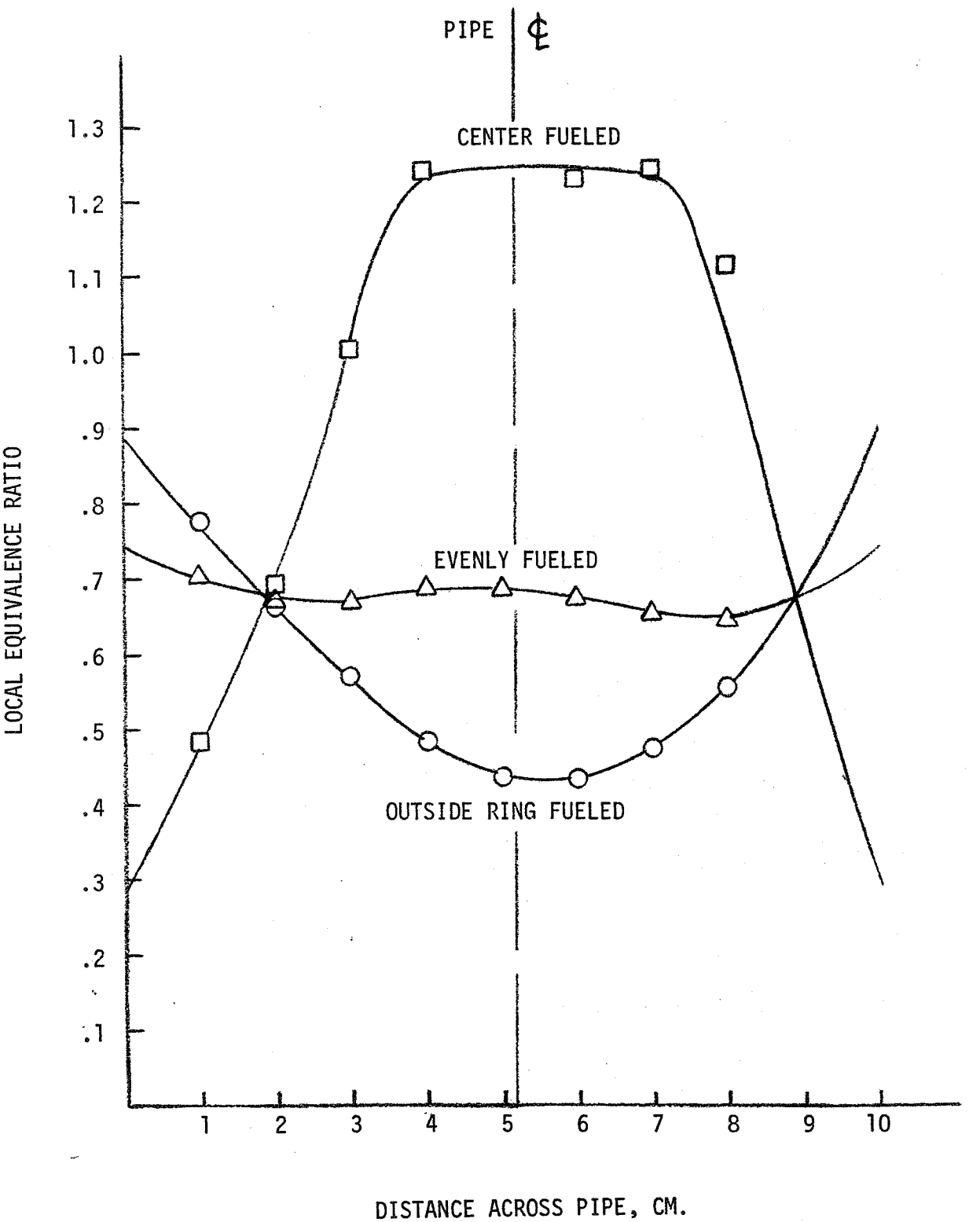

FIGURE 3

THREE NO_X EMISSIONS-PROFILES PRODUCED BY THREE DIFFERENT FUEL/AIR PROFILES AT AN INLET AIR TEMPERATURE OF 600°K FOR A NOMINAL EQUIVALENCE RATIO OF 0.6.

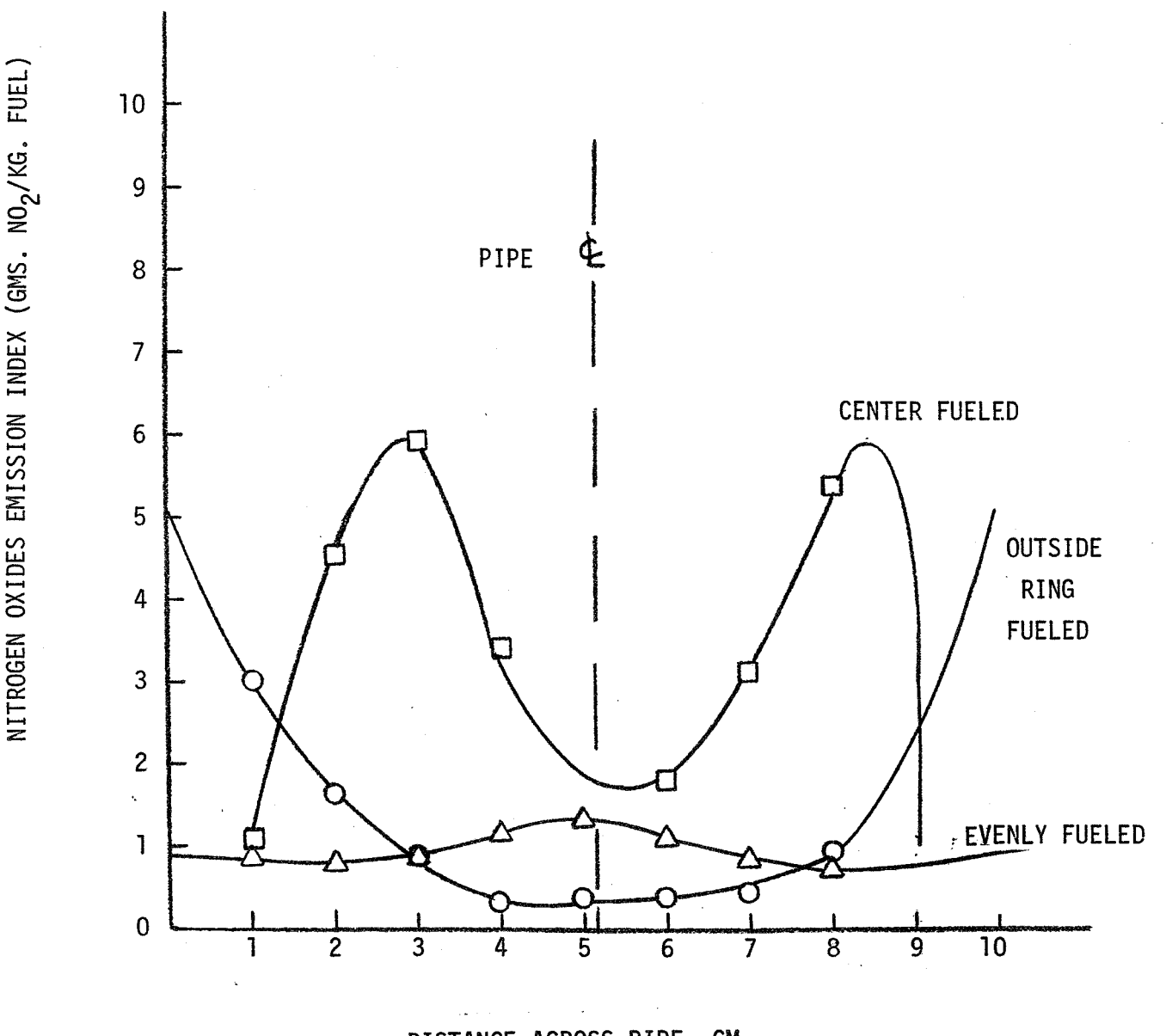

FIGURE 4

THE EFFECT OF FUEL/AIR NONUNIFORMITY ON NO_X EMISSIONS FOR TWO NOMINAL EQUIVALENCE RATIOS AT AN INLET AIR TEMPERATURE OF $600^{\circ}K$.

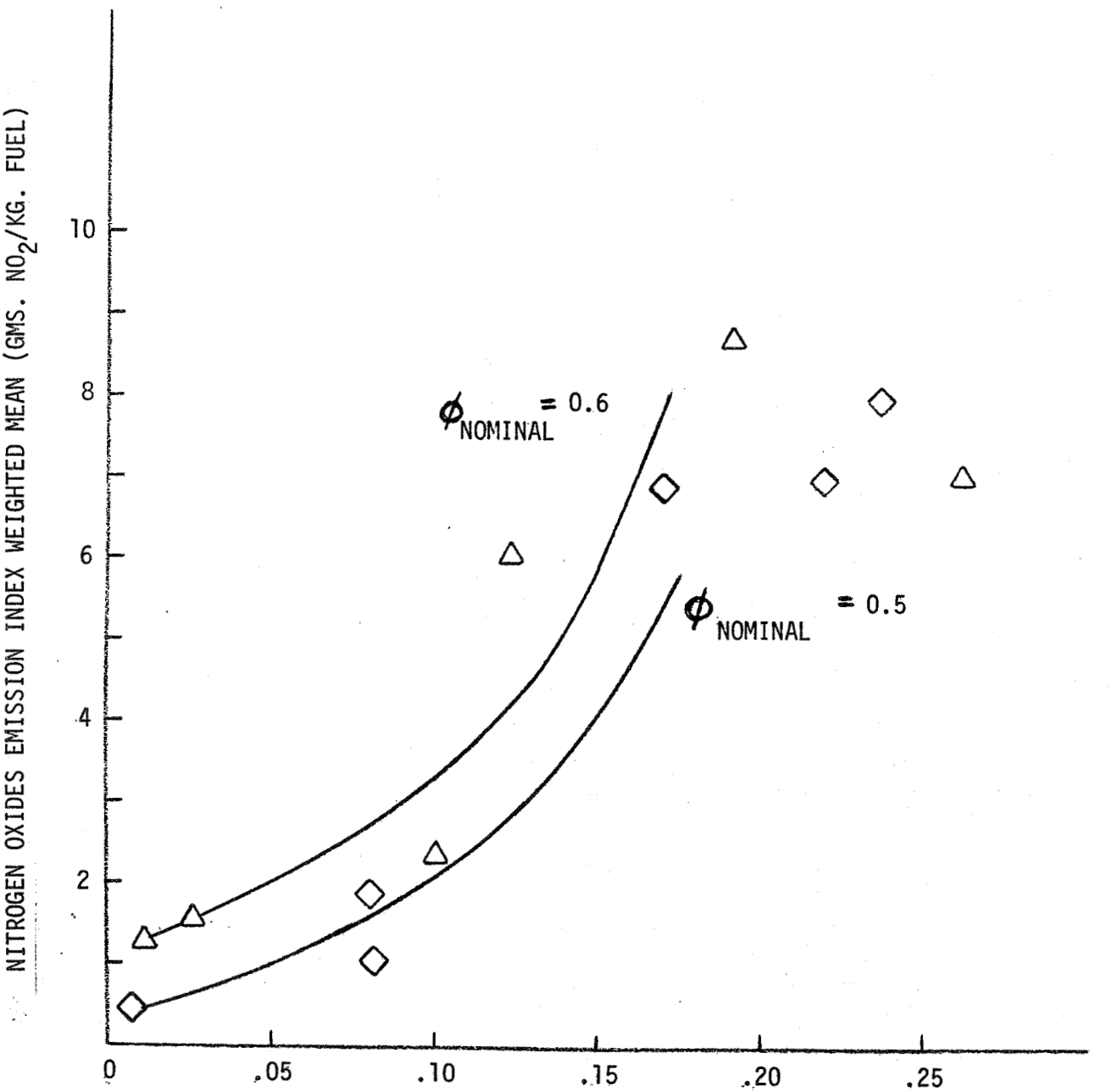

FIGURE 5

EFFECT OF AIR INLET TEMPERATURE ON NO_X EMISSIONS PRODUCED BY NONUNIFORM FUEL/AIR DISTRIBUTIONS AT A NOMINAL EQUIVALENCE RATIO OF 0.6.

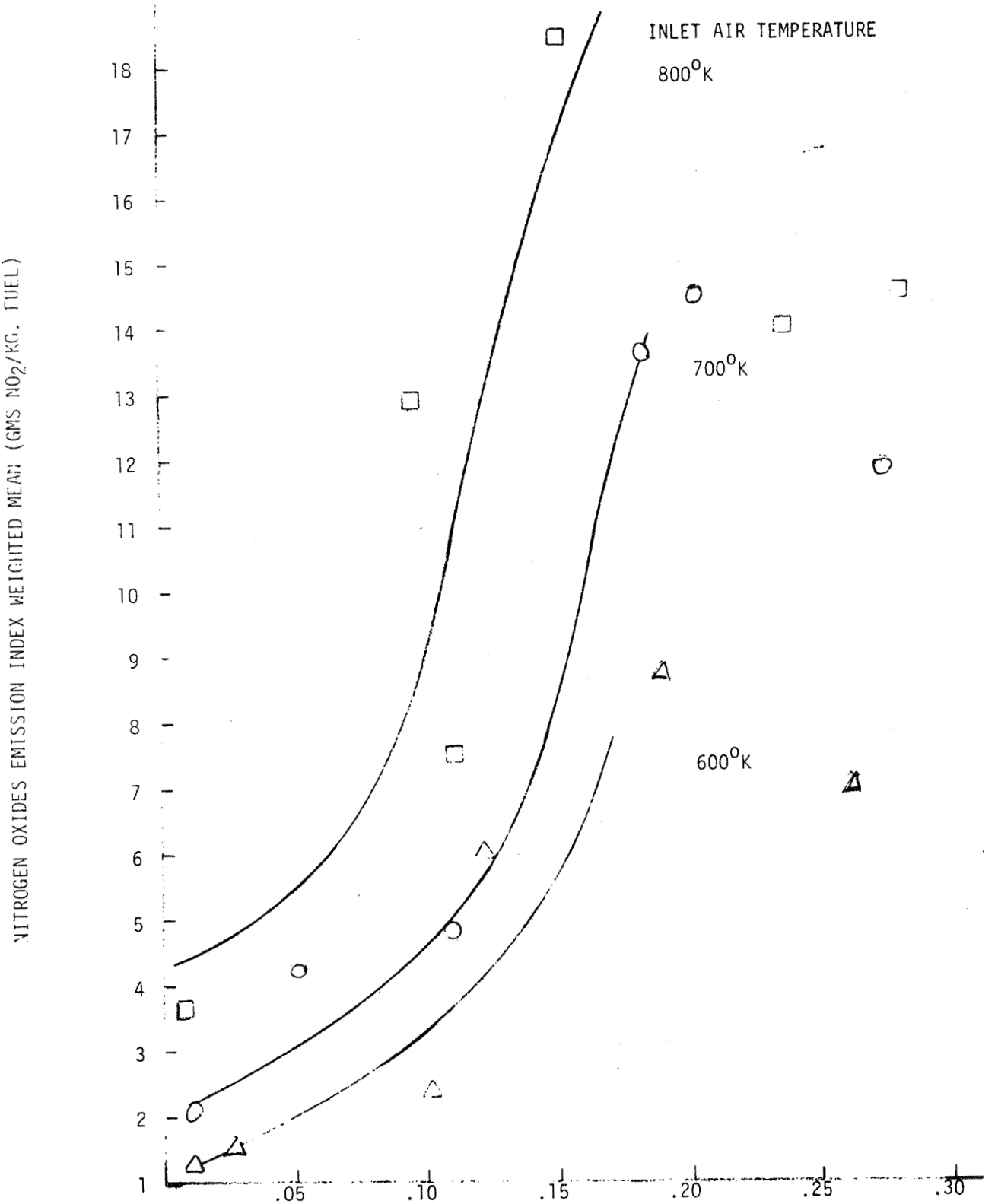

FIGURE 6 FUEL/AIR NONUNIFORMITY PARAMETER, S

Experimental Study of the Effects of Flameholder Geometry on Emissions and Performance of Lean Premixed Combustors

Emission levels and performance of twelve flameholder designs were investigated in a lean, premixed propane-air system at inlet conditions of 800K and 10 atm. The flameholders tested represent six design concepts with two values of blockage for each concept. The design concepts consisted of the following geometries: perforated plate, wire grid, single cone, multiple cone, vee gutter and swirl cone. Measurements were made at reference velocities of 35 m/s, 25 m/s and 20 m/s at combustor stations 10 cm and 30 cm downstream of the flameholder.

Emissions measurements at a combustor station 30 cm downstream of the flameholder show flameholder pressure drop to be a principal determinant of emissions performance. Increasing pressure drop decreases emissions of NO_x, CO and unburned hydrocarbons. For a given flameholder configuration, increasing blockage increases the pressure drop. It appears that the higher intensity of turbulence in the reaction zone associated with the larger pressure drop designs is responsible for the reduction in the emission levels of all species (NO_x, CO and UHC). The details of flameholder geometry appear to be of second order importance except for their effect on total pressure loss.

Sampling measurements at a station 10 cm downstream of the flameholder display greater sensitivity to the details of design geometry. The vee gutter design, which produces one of the lowest CO and UHC characteristics at the 30 cm station, has a large region of incomplete combustion at the 10 cm combustor station.

The lean stability limit was found to correspond to an equivalence ratio of 0.4 for the 800K/10 atm inlet conditions of this experiment. This limit represents an adiabatic flame temperature of 1700K. Flameholder geometry has no appreciable effect on the lean stability limit.

The single and multiple cone flameholder designs which were provided with hollow base cavities suffered burn damage to their downstream surface as reference velocity was reduced. This "burnback" damage occurred without encountering flashback. At an equivalence ratio of 0.7, all incidents of flashback occurred at reference velocities producing maximum components of axial velocity at the flameholder exit station between 30 m/s and 40 m/s. The 70% and 80% blockage perforated plates and the 73% blockage wire grid flameholder did not produce flashback at the lowest velocities (7-9 m/s) at which tests could be conducted.

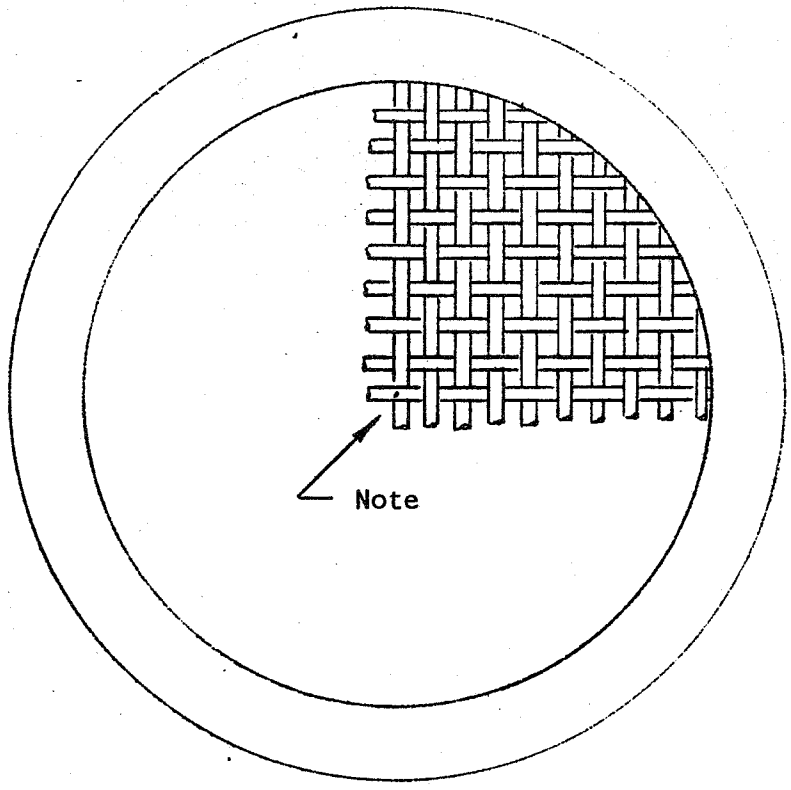

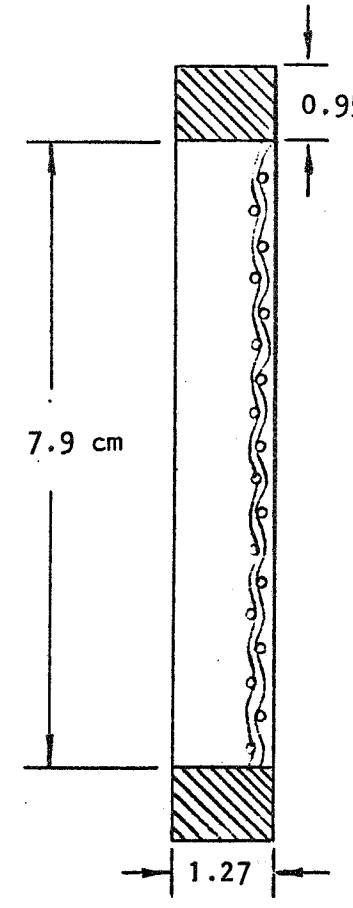

Note: One ply of 0.16 cm (0.20 cm) wire for 60% (73%) blockage. Square grid, 0.42 cm center-to-center spacing

FIGURE 1. WIRE GRID FLAMEHOLDER DETAILS

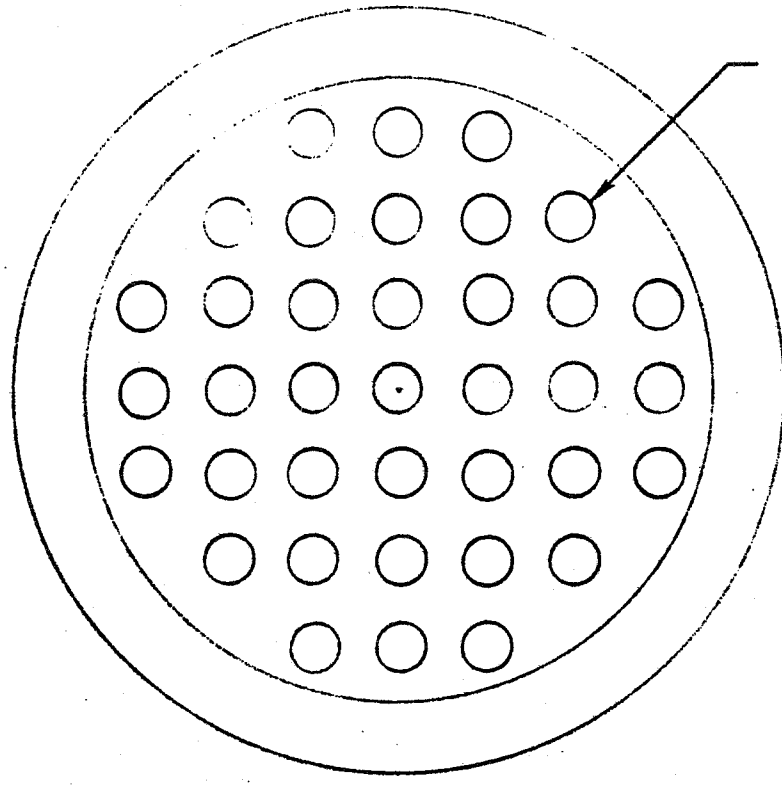

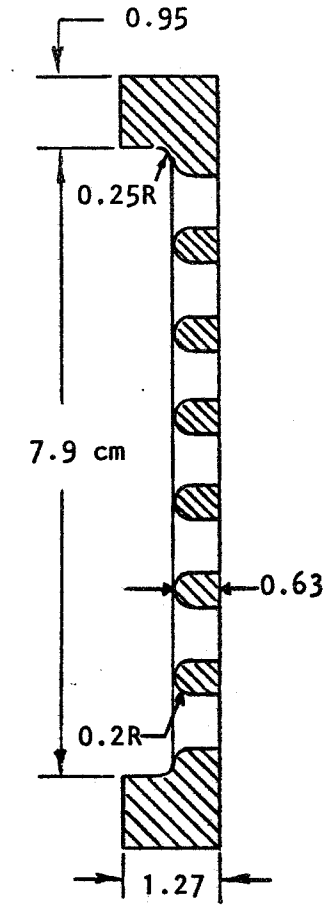

Note: 37 holes on 1.09 x 1.09 grid
Hole dia. 0.71 cm for 70% blockage. Hole dia 0.56 cm for 80% blockage

FIGURE 2. PERFORATED PLATE FLAMEHOLDER DETAILS

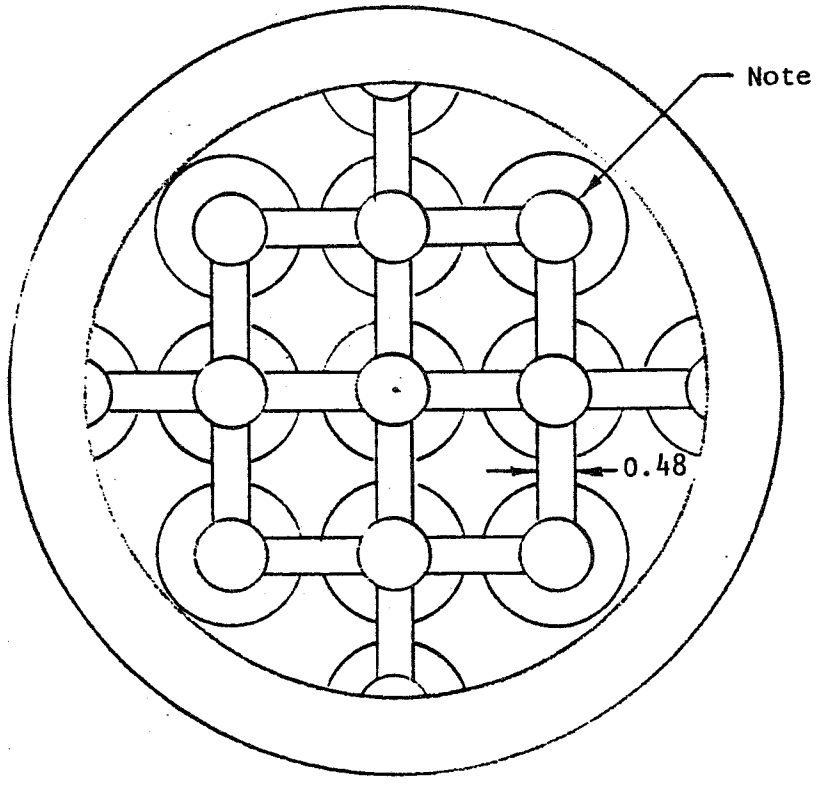

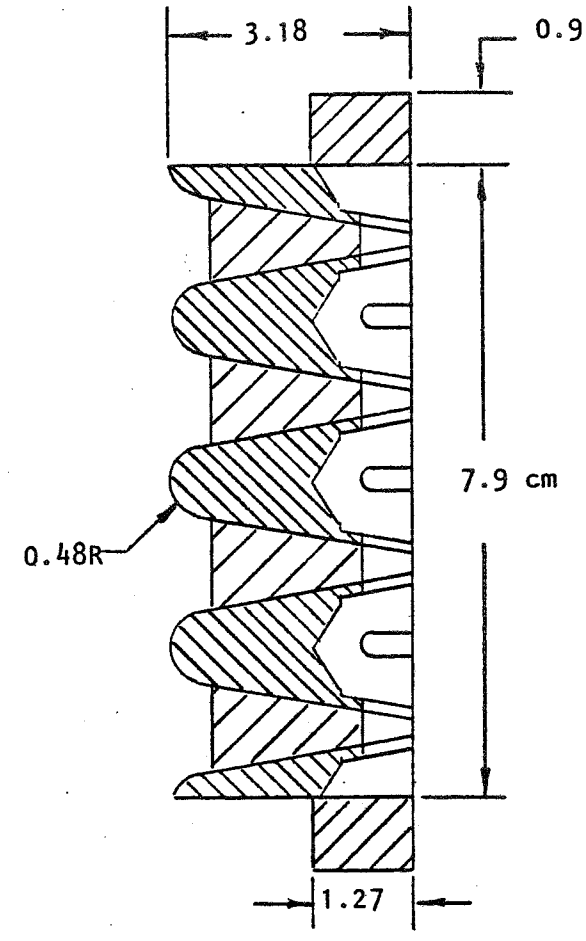

Note: 1.9 cm base diameter,
10^{o} half-angle cones
on 2.1 x 2.1 cm grid

FIGURE 3. Multiple Cone Flameholder Details (70% Blockage)

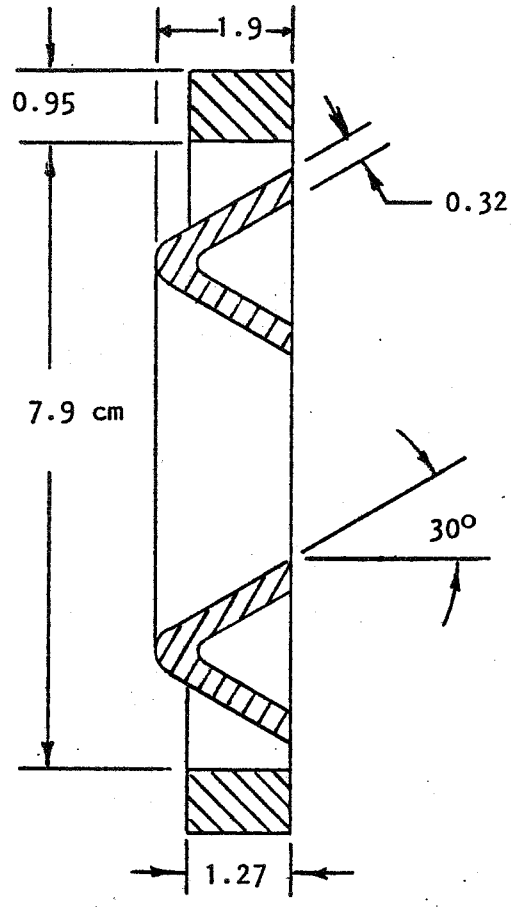

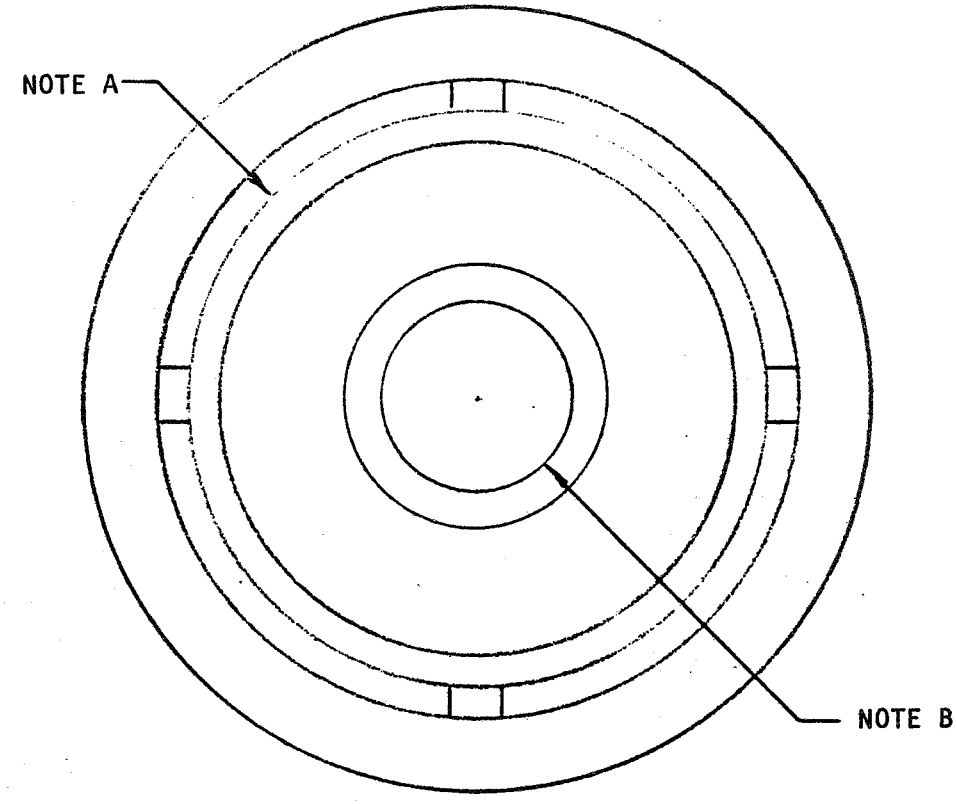

NOTES

A. For 70% blockage, 7.32 cm dia.
   For 80% blockage, 7.52 cm dia.

B. For 70% blockage, 3.05 cm dia.
   For 80% blockage, 2.54 cm dia.

FIGURE 4. VEE GUTTER FLAMEHOLDER DETAILS

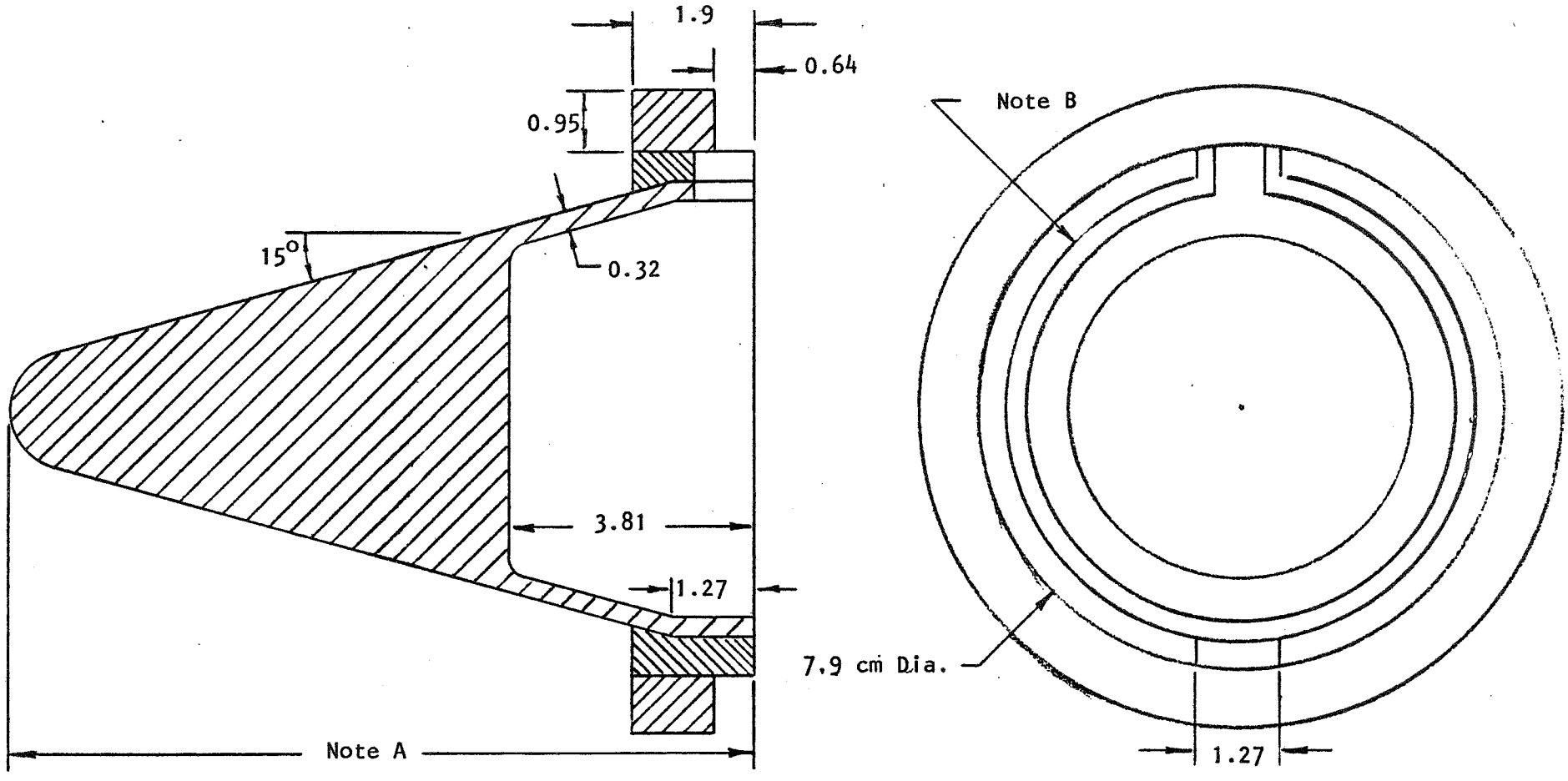

NOTES

A. 11.6 cm for 70% Blockage
   10.5 cm for 80% Blockage

B. 6.35 cm Dia. for 70% Blockage
   7.00 cm Dia. for 80% Blockage

FIGURE 5. SINGLE CONE FLAMEHOLDER DETAILS

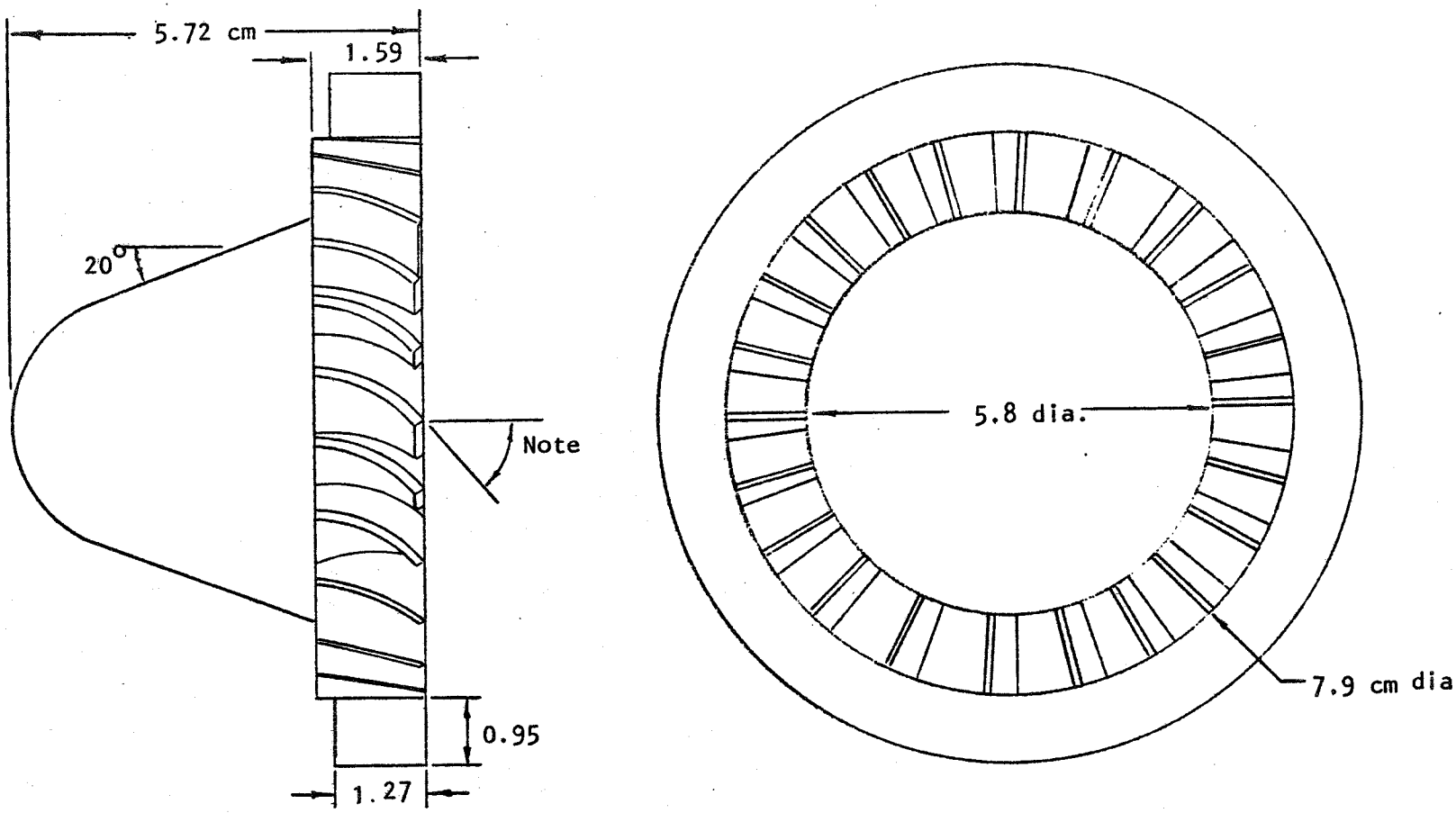

Note: 40° for 73% Blockage
50° for 83% Blockage

FIGURE 6. SWIRL FLAMEHOLDER DETAILS

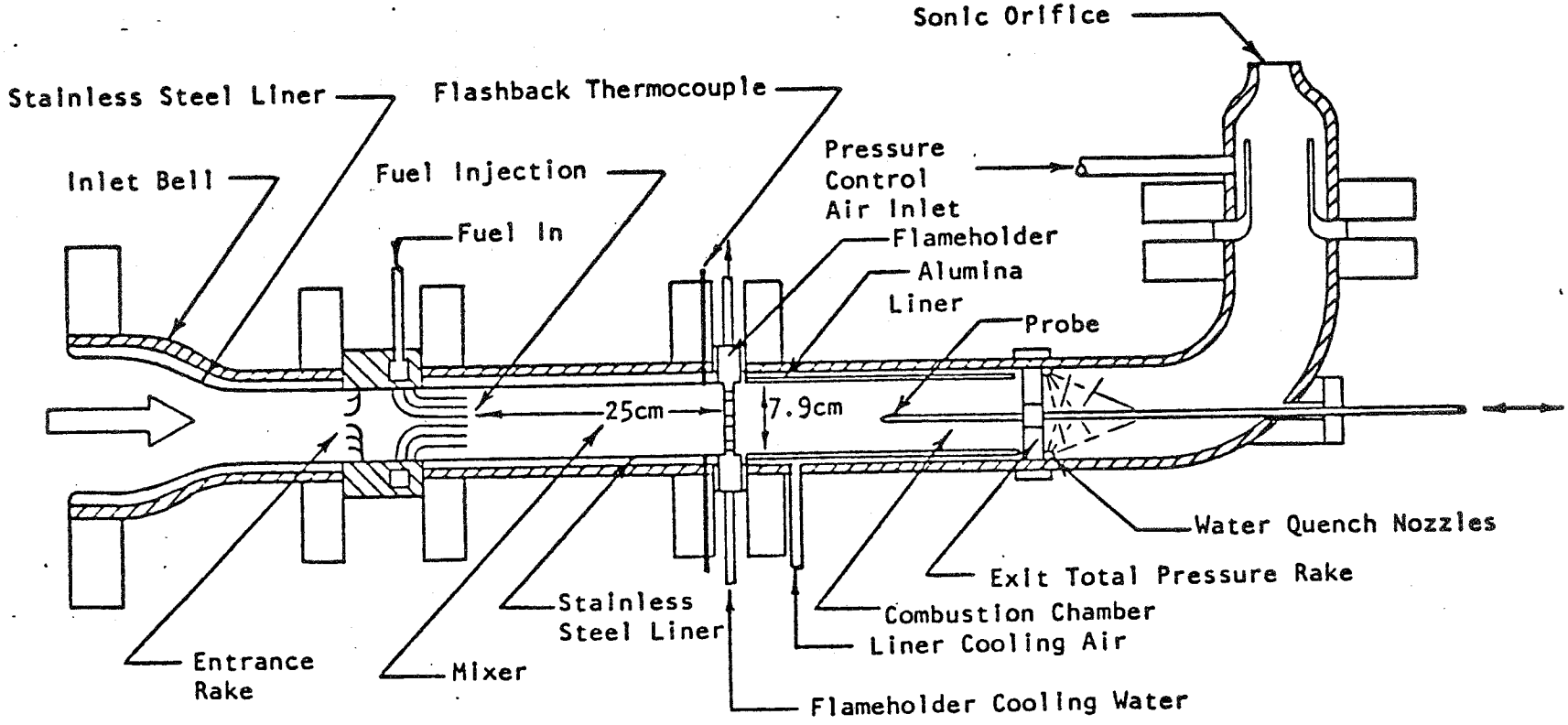

FIGURE 7. COMBUSTION TEST RIG

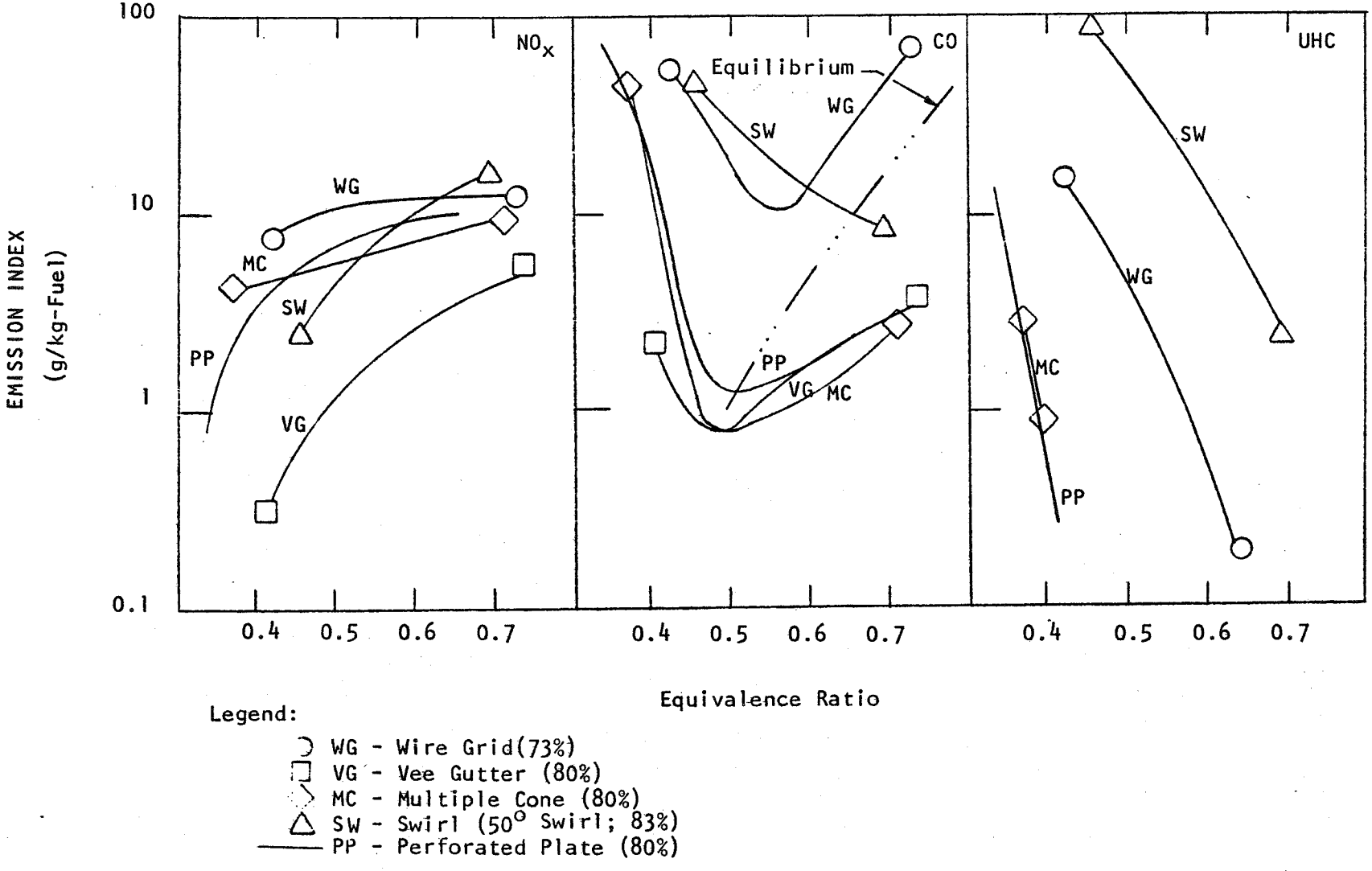

FIGURE 8. COMPARISON OF EMISSION LEVELS FOR HIGH BLOCKAGE FLAMEHOLDERS (V_{ref} = 35 m/s; x = 30 cm)

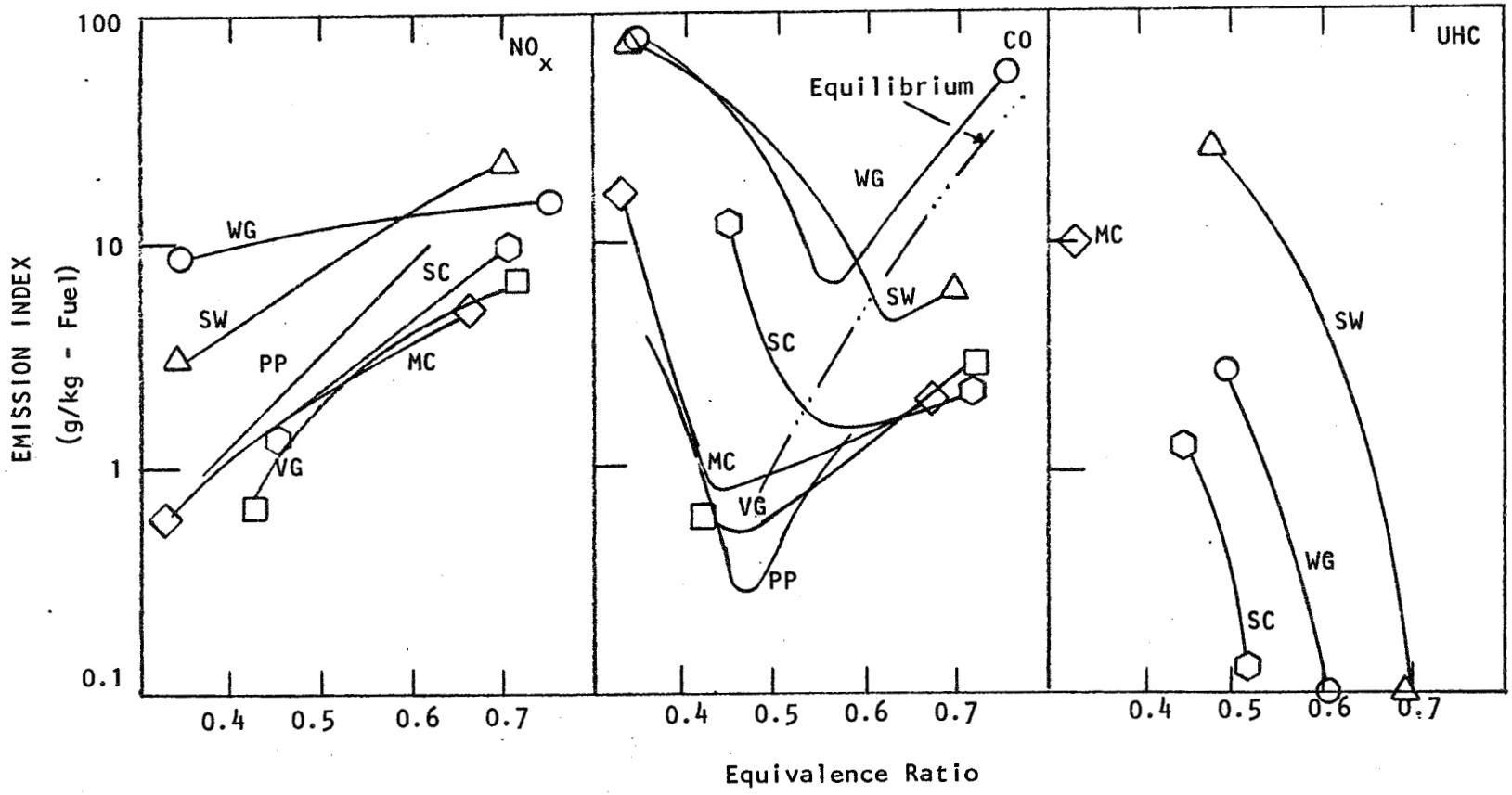

Legend:

- WG - Wire Grid (73%)
- VG - Vee Gutter (80%)
- MC - Multiple Cone (80%)
- SW - Swirl (50° Swirl, 83%)
- SC - Single Cone (80%)
- PP - Perforated Plate (80%)

FIGURE 9. COMPARISON OF EMISSION LEVELS FOR HIGH BLOCKAGE FLAMEHOLDERS (V_{ref} = 25 m/s; x = 30 cm)

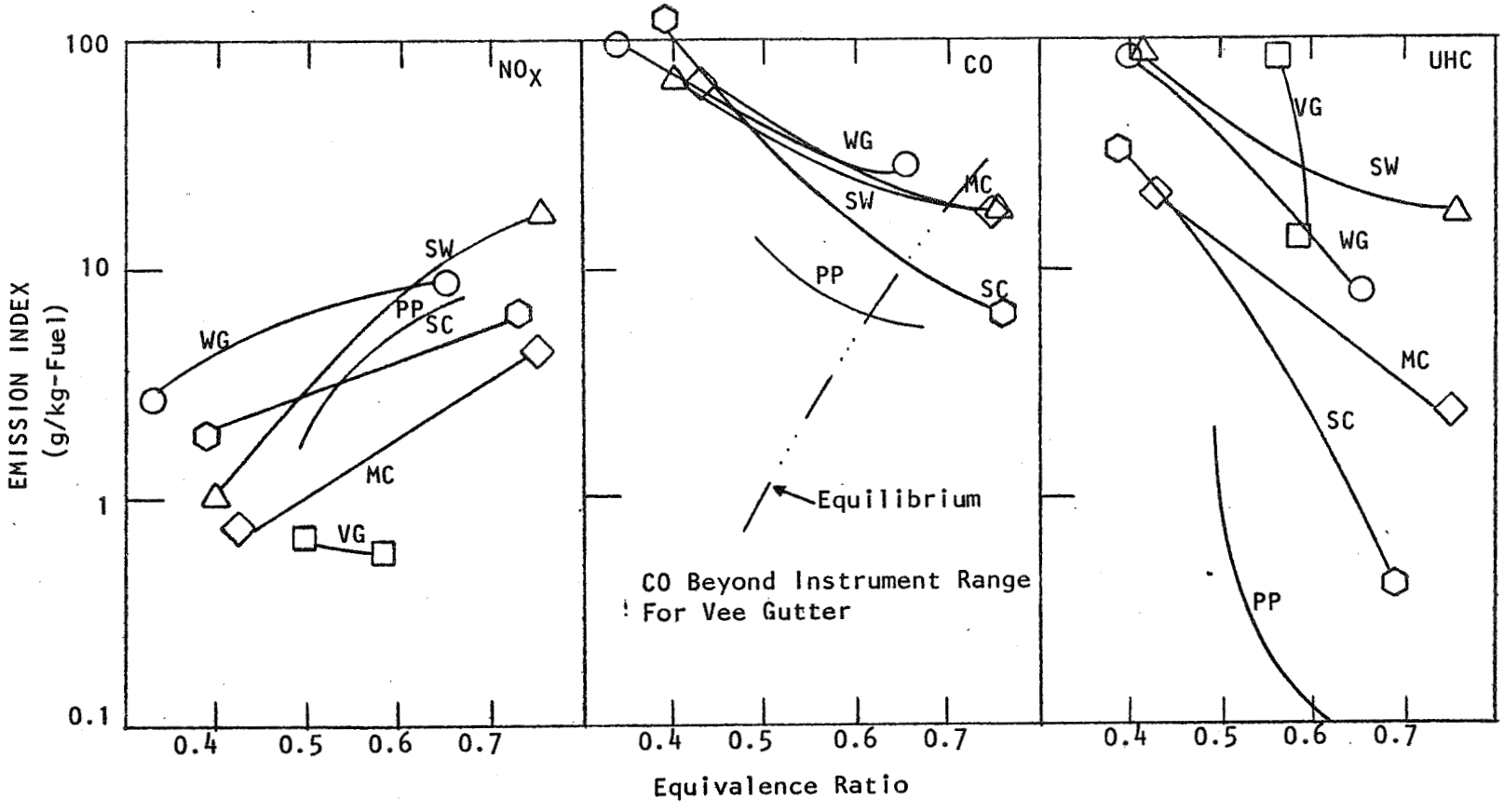

Legend:

- WG - Wire Grid (73%)
- VG - Vee Gutter (80%)
- MC - Multiple Cone (80%)
- SW - Swirl (50° Swirl; 83%)
- SC - Single Cone (80%)
- PP - Perforated Plate (80%)

FIGURE 10. COMPARISON OF EMISSION LEVELS FOR HIGH BLOCKAGE FLAMEHOLDER (V_{ref}=25 m/s; x = 10 cm)

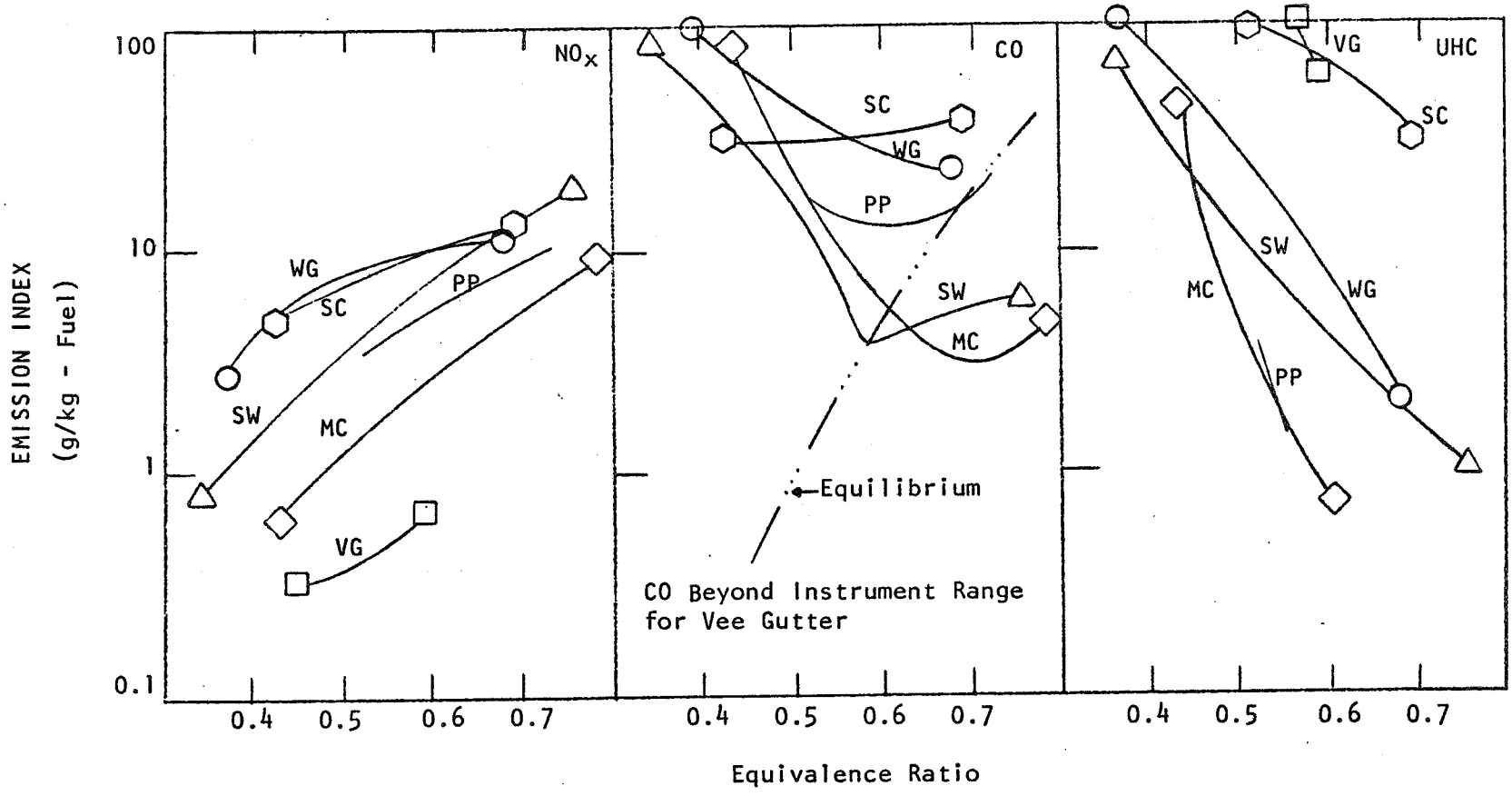

Legend:

- WG - Wire Grid (73%)
- VG - Vee Gutter (80%)
- MC - Multiple Cone (80%)
- SW - Swirl (50° Swirl; 83%)
- SC - Single Cone (80%)
- PP - Perforated Plate (80%)

FIGURE 11. COMPARISON OF EMISSION LEVELS FOR HIGH BLOCKAGE FLAMEHOLDERS (V_{ref} = 20 m/s; x = 10 cm)

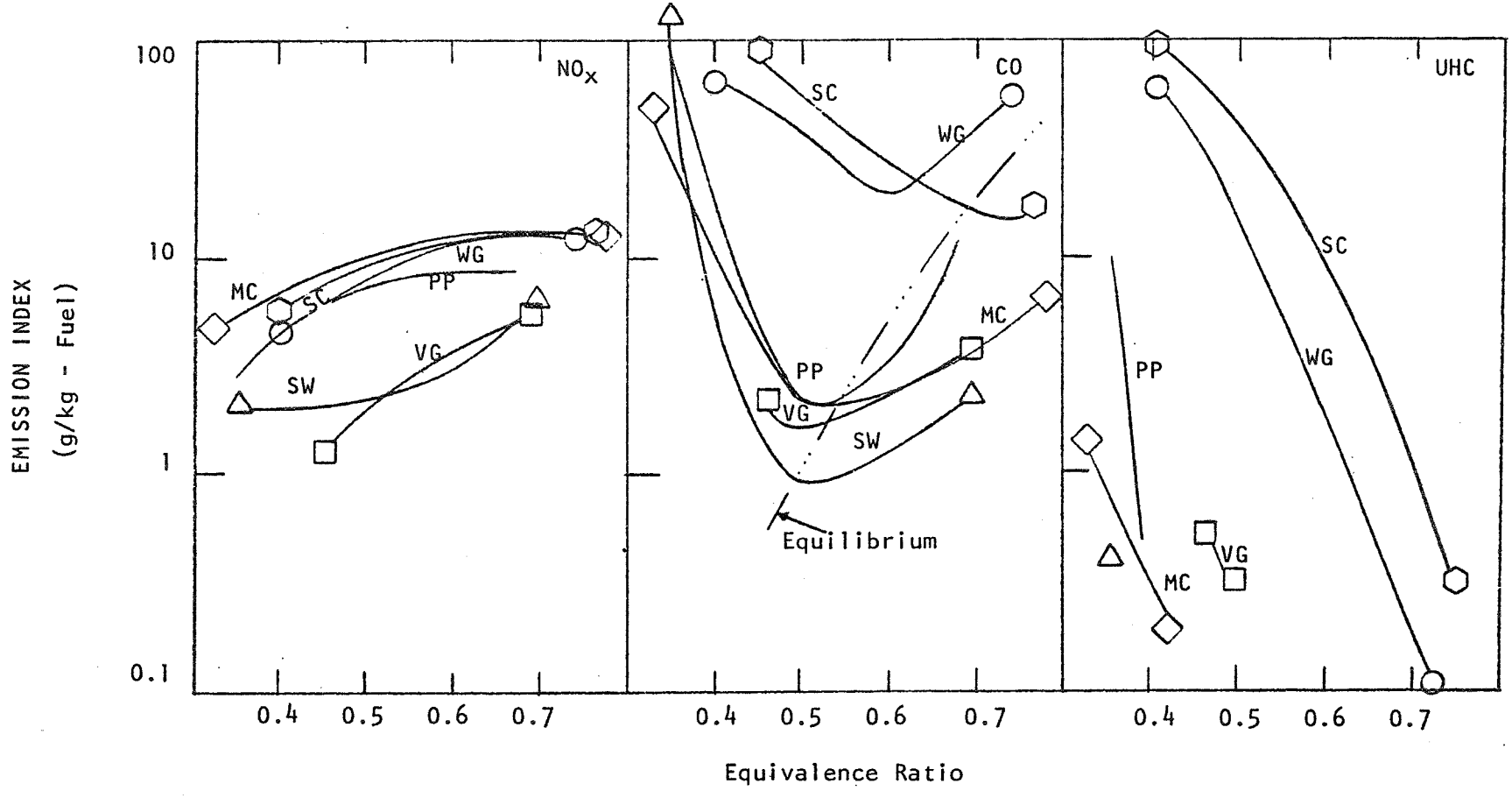

Legend:

- WG - Wire Grid (60%)
- VG - Vee Gutter (70%)
- MC - Multiple Cone (70%)
- SW - Swirl (40° Swirl; 73%)
- SC - Single Cone (70%)
- PP - Perforated Plate (70%)

FIGURE 12. COMPARISON OF EMISSION LEVELS FOR LOW BLOCKAGE FLAMEHOLDER (V_{ref} = 35 m/s; x = 30 cm)

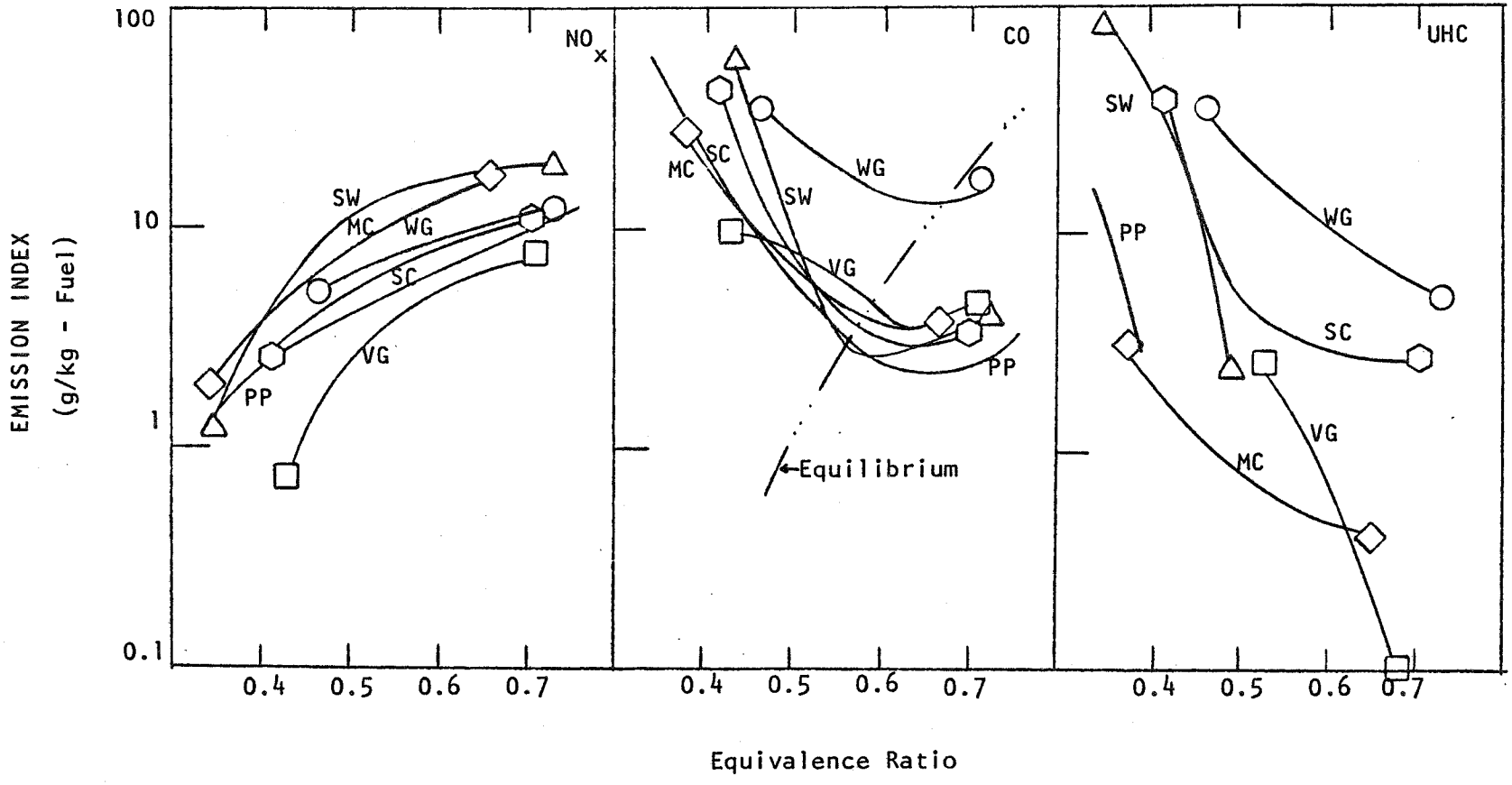

Legend:

- WG - Wire Grid (60%)
- VG - Vee Gutter (70%)
- MC - Multiple Cone (70%)
- SW - Swirl (40° Swirl; 73%)
- SC - Single Cone (70%)
- PP - Perforated Plate (70%)

FIGURE 13. COMPARISON OF EMISSION LEVELS FOR LOW BLOCKAGE FLAMEHOLDERS (V_{ref} = 25 m/s; x = 30 cm)

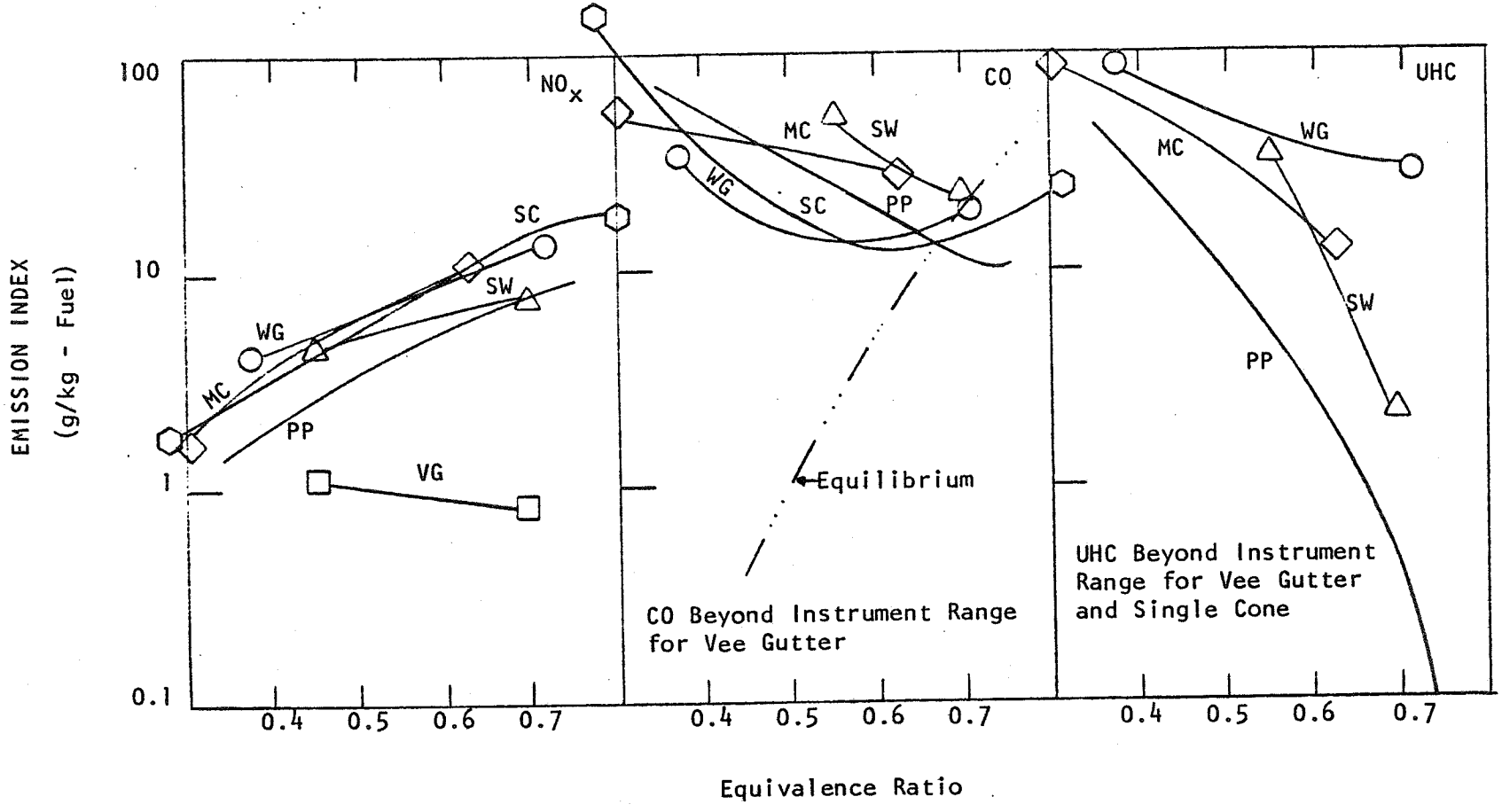

Legend:

- WG - Wire Grid (60%)
- VG - Vee Gutter (70%)
- MC - Multiple Cone (70%)
- SW - Swirl (40° Swirl; 73%)
- SC - Single Cone (70%)
- PP - Perforated Plate (70%)

FIGURE 14. COMPARISON OF EMISSION LEVELS FOR LOW BLOCKAGE FLAMEHOLDERS (V_{ref} = 25 m/s; x = 10 cm)

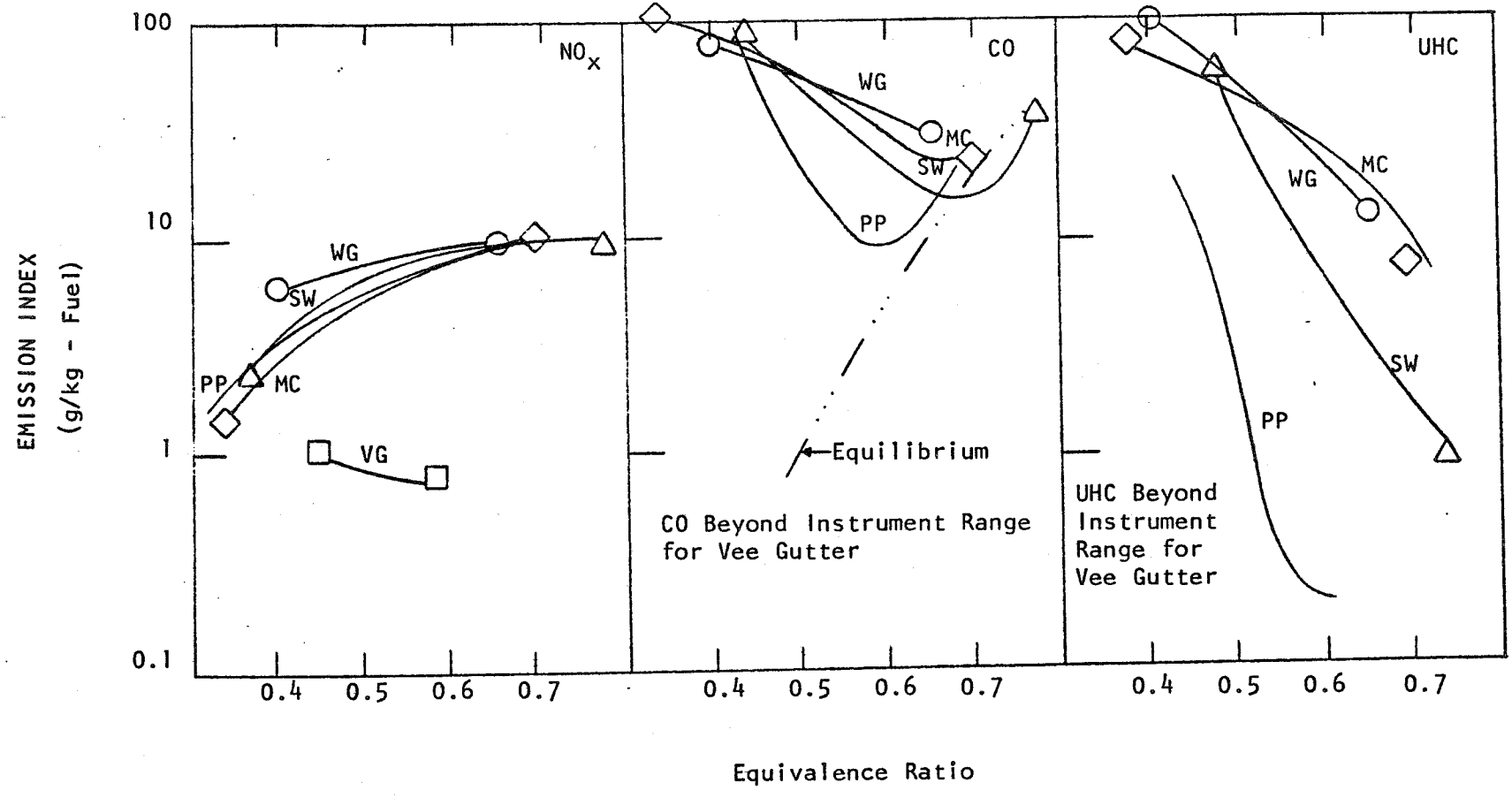

Legend:

- WG - Wire Grid (60%)
- VG - Vee Gutter (70%)
- MC - Multiple Cone (70%)
- SW - Swirl (40° Swirl; 73%)
- PP - Perforated Plate (70%)

FIGURE 15. COMPARISON OF EMISSION LEVELS FOR LOW BLOCKAGE FLAMEHOLDERS (V_{ref} = 20 m/s; x = 10 cm)

TABLE I

SUMMARY OF FLAMEHOLDER CHARACTERISTICS

TYPE	BLOCKAGE	BLOCKAGE DEPTH	IGNITION PERIMETER	IGNITION WIDTH	CHAR. WAKE DIMENSION	DESCRIPTION
Wire Grid	60%	0.16cm	300cm	0.27cm	0.16cm	0.16cm dia. wire - 0.42cm wire spacing
	73%	0.20cm	230cm	0.22cm	0.20cm	0.20cm dia. wire - 0.42cm wire spacing
Perforated Plate	70%	0.64cm	83cm	0.71cm	0.84cm	37 holes - 0.71cm dia.
	80%	0.64cm	65cm	0.56cm	0.99cm	37 holes - 0.56cm dia.
Multiple Cone	70%	3.2cm*	71cm	1.03cm	1.9cm	1.9cm base dia. cones - 2.1cm spacing
	80%	3.2cm*	102cm	0.79cm	1.9cm	1.9cm base dia. cones - 1.9cm spacing
Vee Gutter	70%	1.9cm*	33cm	3.05cm	2.1cm	30° half angle - 2.88cm OD annulus
	80%	1.9cm*	32cm	2.54cm	2.5cm	30° half angle - 2.96cm OD annulus
Single Cone	70%	10.5cm*	20cm	0.79cm	6.4cm	15° half angle - 6.35cm dia. hollow base
	80%	11.6cm*	22cm	0.48cm	7.0cm	15° half angle - 7.00cm dia. hollow base
Swirl	73%	1.8cm	18cm	1.07cm	12.0cm	40° turning vanes - hub/tip ratio 0.73
	83%	1.8cm	18cm	1.07cm	20.0cm	50° turning vanes - hub/tip ratio 0.73

*Blockage varies across this distance attaining full value only at exit plane.

TABLE II

FLAMEHOLDER PRESSURE DROP SUMMARY

GEOMETRY	BLOCKAGE (%)	RESISTANCE COEFFICIENT k	$\frac{\Delta p}{P_T}$ (% at V_{ref} = 25 m/s)
Wire Grid	60	1.0	0.8
Wire Grid	73		2.1
Perforated Plate	70	1.6	2.5
Perforated Plate	80		5.8
Multiple Cone	70	1.5	2.3
Multiple Cone	80		5.4
Vee Gutter	70	2.2	3.3
Vee Gutter	80		7.1
Single Cone	70	1.5	2.3
Single Cone	80		5.4
40^{o} Swirl	73	1.8	3.4
50^{o} Swirl	83	0.9	4.8

TABLE III

LEAN STABILITY LIMIT

GEOMETRY	BLOCKAGE (%)	V_r=20m/s LSL	V_r=25m/s LSL	V_r=35m/s LSL
Wire Grid	60	<.40	.35	<.42
Wire Grid	73	<.37	.32	.38
Perforated Plate	70	.30	.35	<.30
Perforated Plate	80	<.48	.35*	.32
Multiple Cone	70	.32	.29	.24
Multiple Cone	80	.38	.32**	.30
Vee Gutter	70	.44	.42	.44
Vee Gutter	80	.44	.35	.41
Single Cone	70	--	.28	.32
Single Cone	80	<.42	.38	--
40° Swirl	73	.32	.32	.33
50° Swirl	83	.30	.30	.34

*On one test, 0.45

**On one test, 0.42

TABLE IV

FLAMEHOLDER FLASHBACK/BURNBACK SUMMARY

GEOMETRY	BLOCKAGE (%)	MODE	$\dot{V}_{ref}$ (m/s)	$V_{max\text{-}axial}$ (m/s)
Wire Grid	60	Flashback	14	35
	73	No Failure	<9	<33
Perforated Plate	70	No Failure	<7	<23
	80	No Failure	<8	<40
Vee Gutter	70	Flashback	9	30
	80	Not Tested		
40^{o} Swirl	73	Flashback	11	31
50^{o} Swirl	83	Flashback	10	38
Single Cone	70	Burnback	20	67
	80	Burnback	20	100
Multiple Cone	70	Burnback	18	60
	80	Burnback	7	35

PARAMETRIC STUDY OF THE EFFECTS OF FLAMEHOLDER BLOCKAGE ON THE EMISSIONS AND PERFORMANCE OF LEAN PREMIXED-PREVAPORIZED COMBUSTORS

by

Robert A. Duerr

The report presents test results from a parametric study of the effects of flameholder blockage on the emissions and performance of lean premixed-prevaporized combustors. Tests were conducted at inlet air pressures of 3×10^5 and 5×10^5 pascals, inlet air temperatures of 600K, 700K and 800K, reference velocities from 20 to 35 meters per second, and equivalence ratios from the lean stability limit to 0.7 using Jet A Fuel.

The tests reported herein were conducted in a closed duct test facility as shown in figure 1. Inlet air to the test section was preheated to temperatures from 600K to 800K using a nonvitiating preheater. A contraction section lowered the flow area by a factor of four. To insure good atomization, fuel was injected in the upstream direction through the fuel injector shown in figure 2. The fuel-air mixture passed through a mixer-vaporizer tube which ended in a diffuser section to return to the original flow area. The conical flameholder used in these tests was mounted in the diffuser cone at one of two axial positions to give a flameholder blockage area ration of either 56% or 80%. Figure 3 shows the 5.0 cm diameter cone mounted at the 80% blockage position. The fuel-air mixture burned in a water-cooled combustion section. Gas sampling of the combustion products was accomplished by two sets of four

multipoints probes, one of which is shown in figure 4.

Results form the tests support the theory that flameholder blockage is one of the major determinants of the size and shape of the recirculation zone as shown schematically in figure 5. The test data in figure 6 show that higher blockage with its larger recirculation zone provides more residence time which leads to more NO_x formation. These data were taken with the gas sampling probes that were 30 cm. downstream of the flameholder station; thus, the plug flow residence time is the same for both sets of blockage data.

The total residence time of combustion gases is the sum of the recirculation zone residence time and a plug flow residence time. A comparison of test data in which the plug flow residence time of the 56% flameholder blockage data is approximately twice that of the 80% blockage data is shown in figure 7. Since the NO_x levels are relatively close, especially at high flame temperatures, this implies that the total residence times are approximately equal. Thus, the recirculation zone size for the 80% blockage flameholder is approximately twice that of the 56% blockage flameholder. A well stirred reactor computed model prediction is also shown in figure 7 to indicate the approximate true residence time of the gases in the combustor.

FLAMEHOLDER TEST RIG

DIMENSIONS IN cm

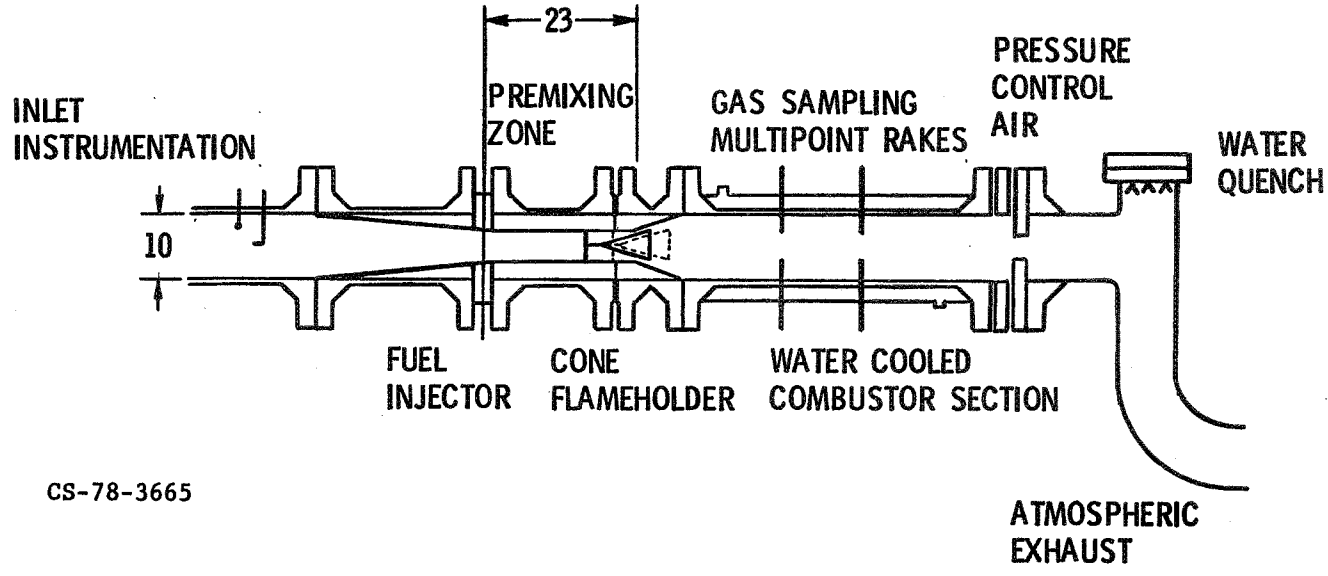

FIGURE 1.

FUEL INJECTOR

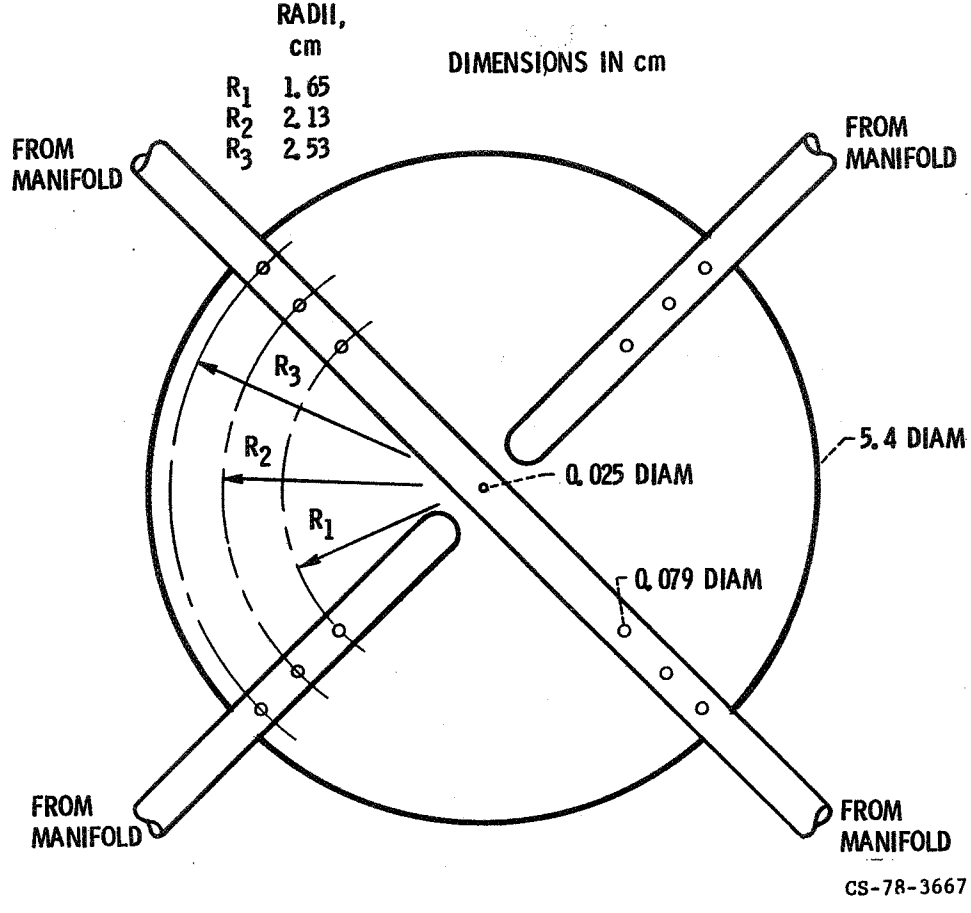

FIGURE 2.

NASA
C-78-386

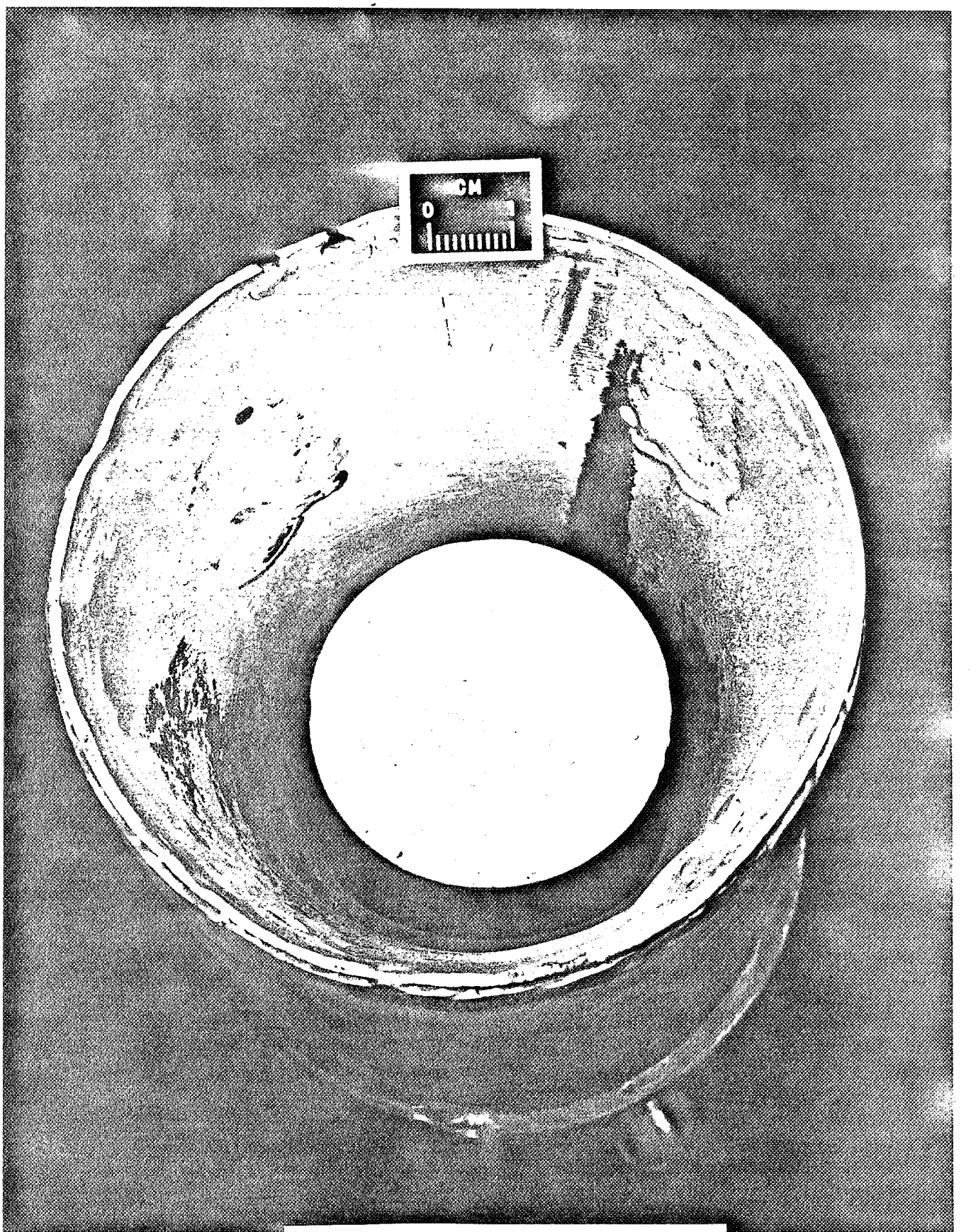

FIGURE 3. MOUNTED FLAMEHOLDER

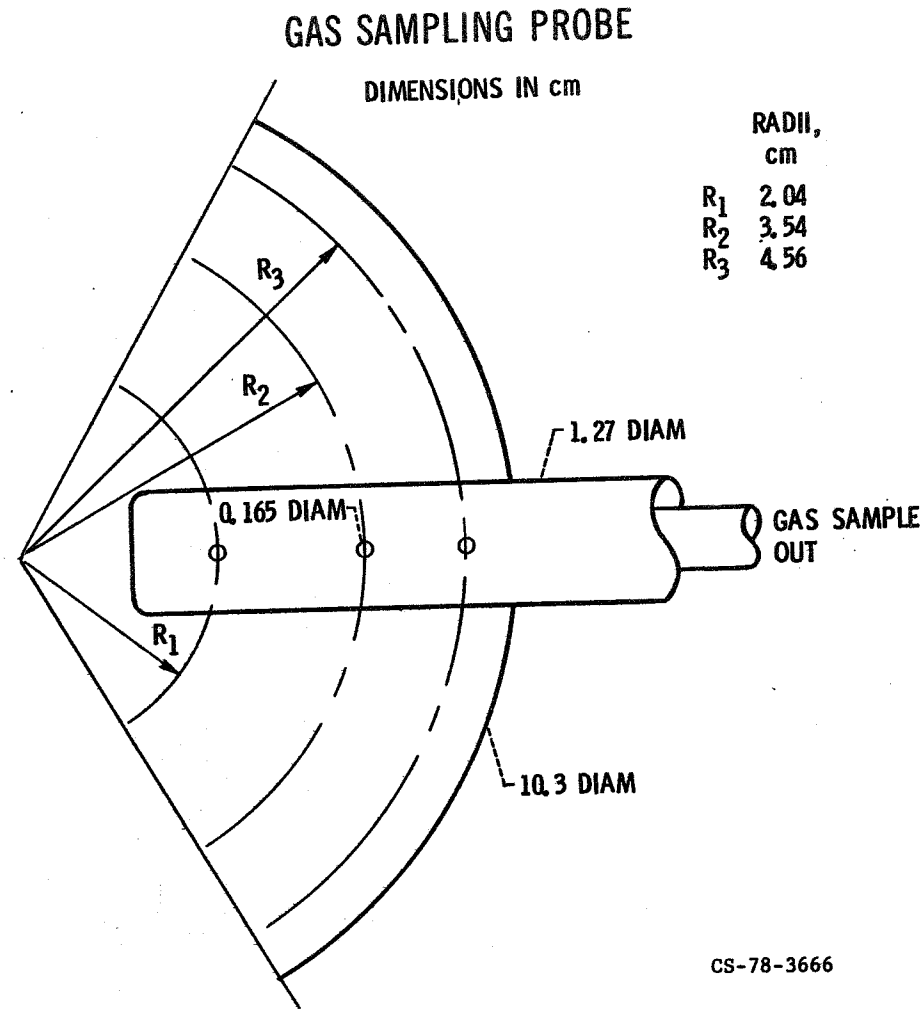
GAS SAMPLING PROBE
DIMENSIONS IN cm
RADII, cm
R_1 2.04
R_2 3.54
R_3 4.56
R_3
R_2
R_1
1.27 DIAM
0.165 DIAM
GAS SAMPLE OUT
10.3 DIAM
CS-78-3666

FIGURE 4.

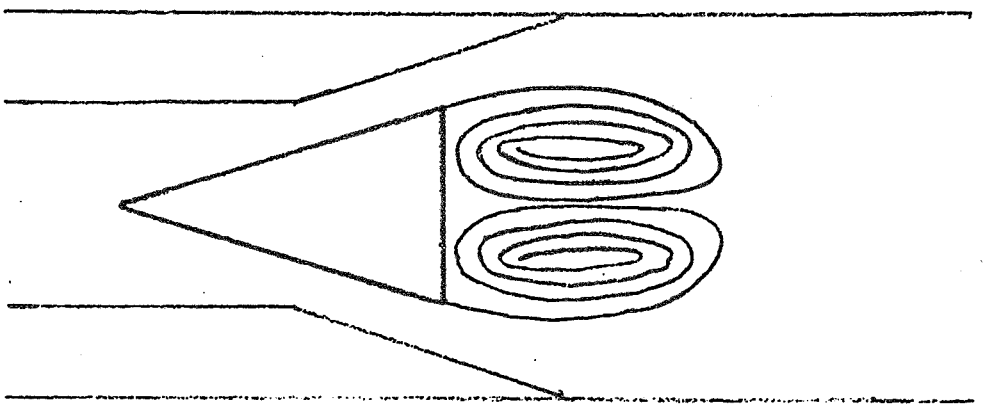

56% FLAMEHOLDER BLOCKAGE

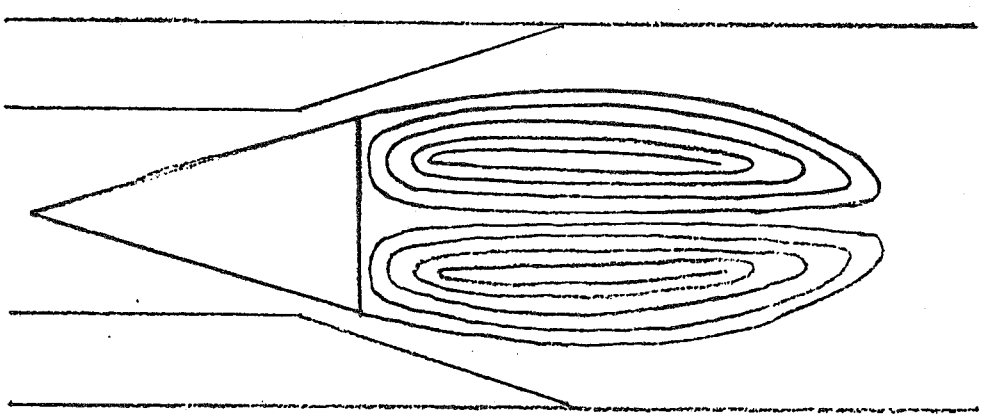

80% FLAMEHOLDER BLOCKAGE

FIGURE 5 RECIRCULATION ZONE SIZES.

FIGURE 6 EFFECT OF BLOCKAGE ON NO_X

INLET PRESSURE 3 ATM
REFERENCE VELOCITY 35 M/S
INLET AIR TEMPERATURE 600-800K
SAMPLING LOCATION 30 CM

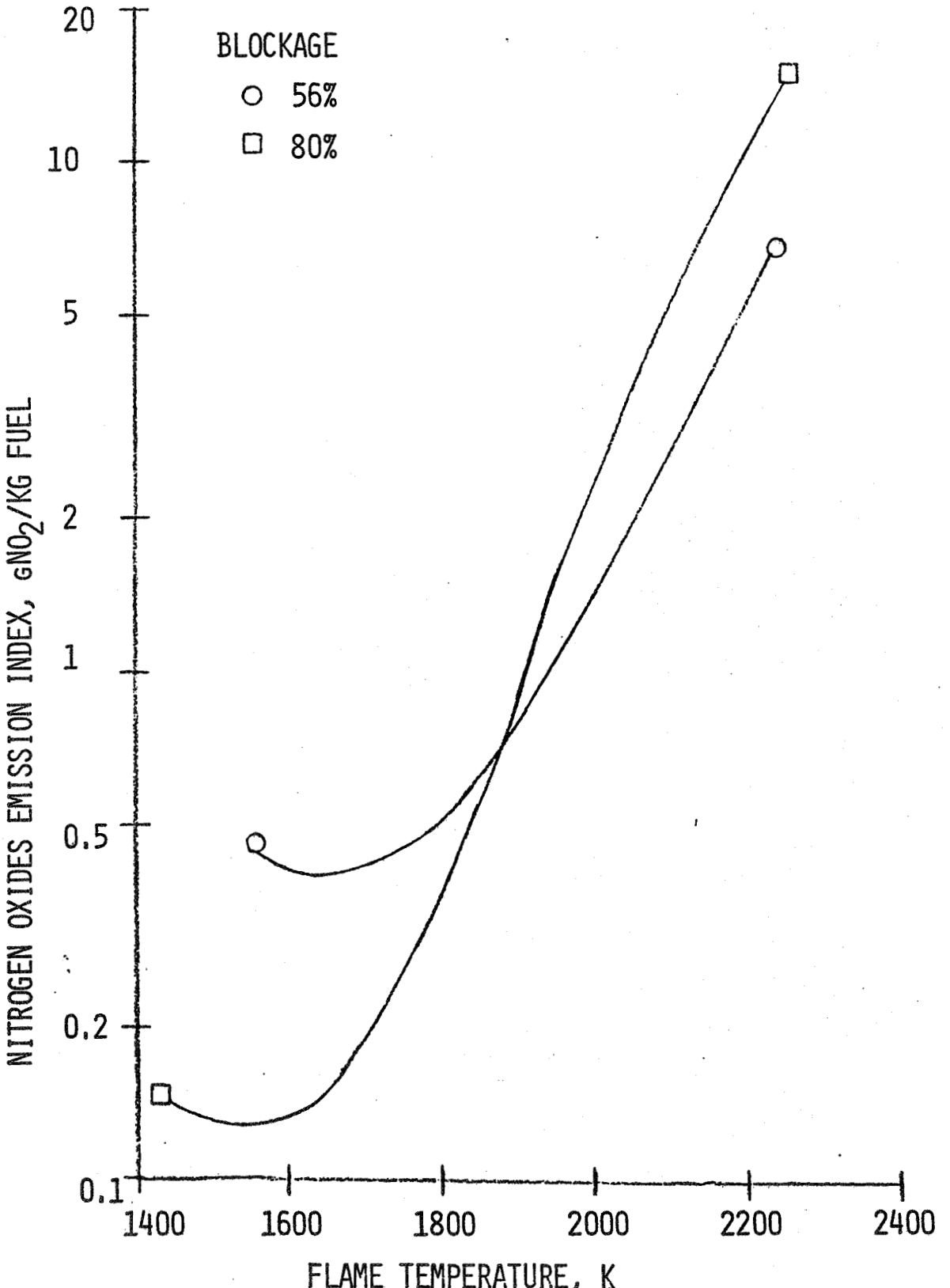

FIGURE 7. COMPARISON OF RECIRCULATION ZONE SIZE:
INLET PRESSURE 3 ATM
REFERENCE VELOCITY 35 M/S
INLET AIR TEMPERATURE 600-800K

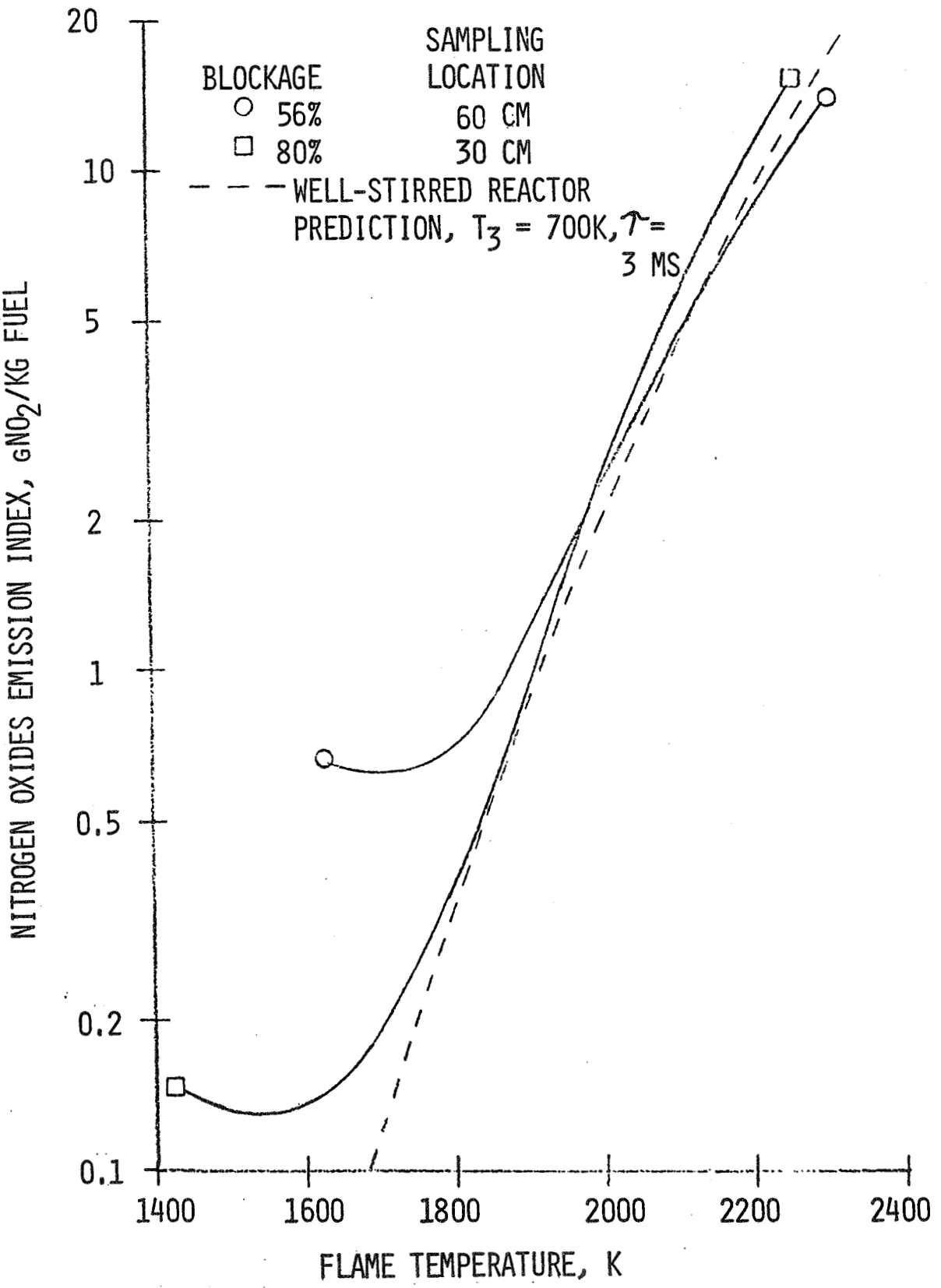

LEAN STABILITY AUGMENTATION STUDY

John B. McVey and Jan B. Kennedy
United Technologies Research Center
East Hartford, Connecticut

An analytical and experimental program was conducted to investigate techniques and develop technology for improving the lean combustion limits of premixing, prevaporizing combustors applicable to gas turbine engine main burners. In the analytical conceptual design study, three concepts for improving lean stability limits were selected for experimental evaluation among twelve approaches considered. Concepts were selected on the basis of the potential for improving stability limits and achieving emission goals, the technological risks associated with development of practical burners employing the concepts, and the penalties to airline direct operating costs resulting from decreased combustor performance, increased engine cost, increased maintenance cost and increased engine weight associated with implementation of the concepts. Tests of flameholders embodying the selected concepts were conducted in an axi-symmetric flametube test rig having a nominal diameter of 10.2 cm at a pressure of 10 atm and at a range of entrance temperatures simulating conditions to be encountered during stratospheric cruise. A total of sixteen test configurations were examined in which lean blowout limits, pollutant emission characteristics, and combustor performance were documented.

The use of hot gas pilots, catalyzed flameholder elements, and heat recirculation to augment lean stability limits was considered in the conceptual design study. On the basis of the results of the study, three classes of augmented flameholders were designed and tested. The first class involved the use of cavities or recesses located in the downstream face of a perforated plate flameholder--these configurations are referred to as Self-Piloting Recessed Perforated Plates. The second class involved the use of tube bundles wherein the inner diameter of the tubes and/or the rearface of the tube array was treated with a platinum/rhodium catalyst. These configurations were referred to as Catalyzed Tube Flameholders. The third class of flameholders involved the direct injection of gaseous or liquid fuel into the recirculation regions formed behind V-gutter or perforated plate flameholders. This class of flameholders is referred to as Piloted Flameholders. The primary goal of the program was to achieve stable operation of the combustors at equivalence ratios as low as 0.25. It was desired that the NO_x emission index be less than 1.0 g/kg at the design conditions (T_o = 600 K, ϕ = 0.6). It was also desired that the combustor operate efficiently over a range of entrance temperatures from 600 to 800 K, a range of equivalence ratios from 0.3 to 0.6, and that the maximum emission of nitric oxides be less than that corresponding to an emission index of 3.0 g/kg.

The most promising configuration identified in this program involved the injection of pilot fuel into the base or recirculation region of a bluff-body flameholder. It was determined that with a pilot fuel flow equal to 5 percent of the total fuel flow at the design conditions, combustor blowout did not occur as fuel flow was decreased to levels corresponding to an overall equivalence ratio of 0.25. For this configuration, the NO_x emission index at the design point was less than half of the design goal and, at off-design conditions, the maximum NO_x emission index goal was exceeded only for the T_o = 800 K, ϕ = 0.6 case. At the lower entrance temperature conditions tested (T_o = 700 and 600 K), the measured combustion efficiencies were unacceptably low and further effort is required to obtain the desired performance. No substantial improvement in blowout limits was achieved for the self-piloting recessed perforated plate configurations or the catalyzed tube configurations.

LIST OF FIGURES

NASA Lean Stability Augmentation Study

- **Objective :** Attainment of improved lean blowout limits
- **Tasks :**
  - I Conceptual design study
  - II Experimental design
  - III Fabrication and installation
  - IV Combustor tests
  - V Final design and test
  - VI Reports and records

Program Goals

Conditions:

$P = 10$ atm

$\underline{600} \leq T_i \leq 800$ K

$0.25 \leq \phi_p \leq \underline{0.6}$

$V_{ref} = 25$ m/sec

Emissions:

$EI_{NO_X} < 1.0$ at design; < 3.0 overall

$EI_{CO} < 10.0$ at design

$EI_{UHC} < 1.0$ at design

Performance:

$\eta_{comb.} \geq 0.99$ for $0.3 \leq \phi \leq 0.6$

$\Delta P/P < 0.05$

Bluff Body Flame Stabilization Process

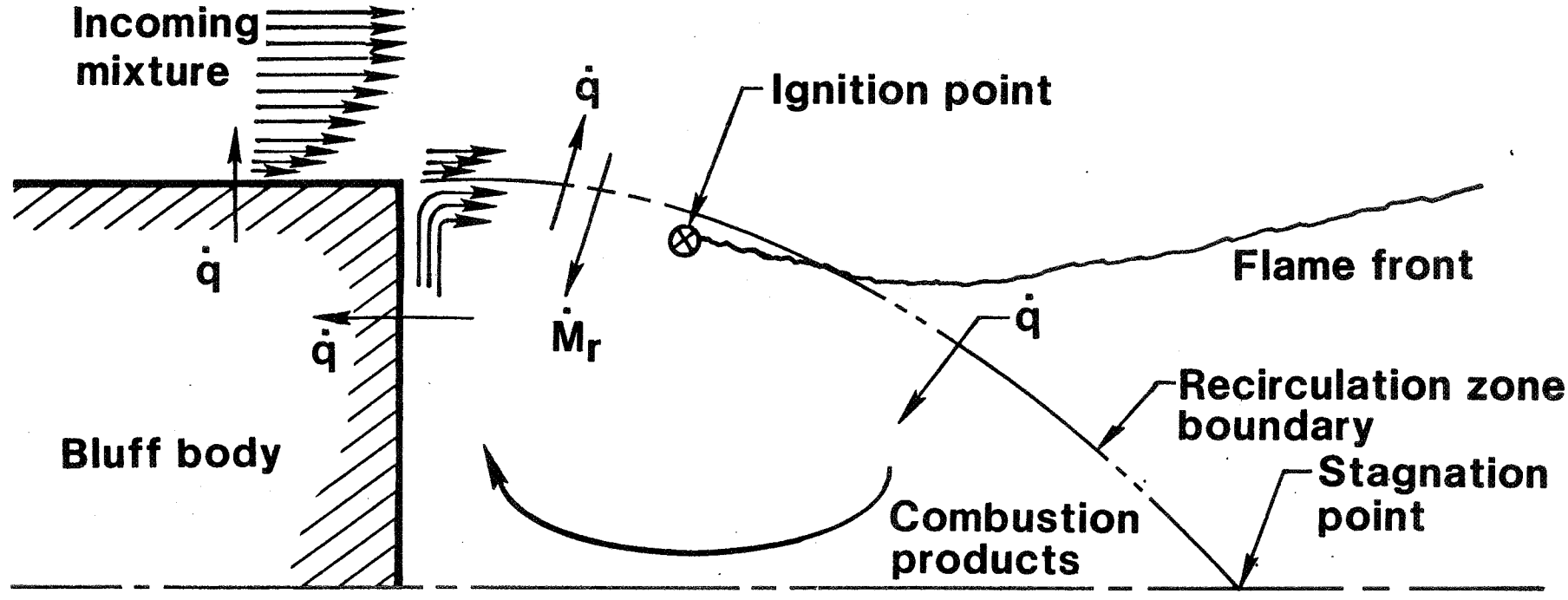

UNITED TECHNOLOGIES RESEARCH CENTER

77-12-172-3

Lean Stability Augmentation Study Test Facility

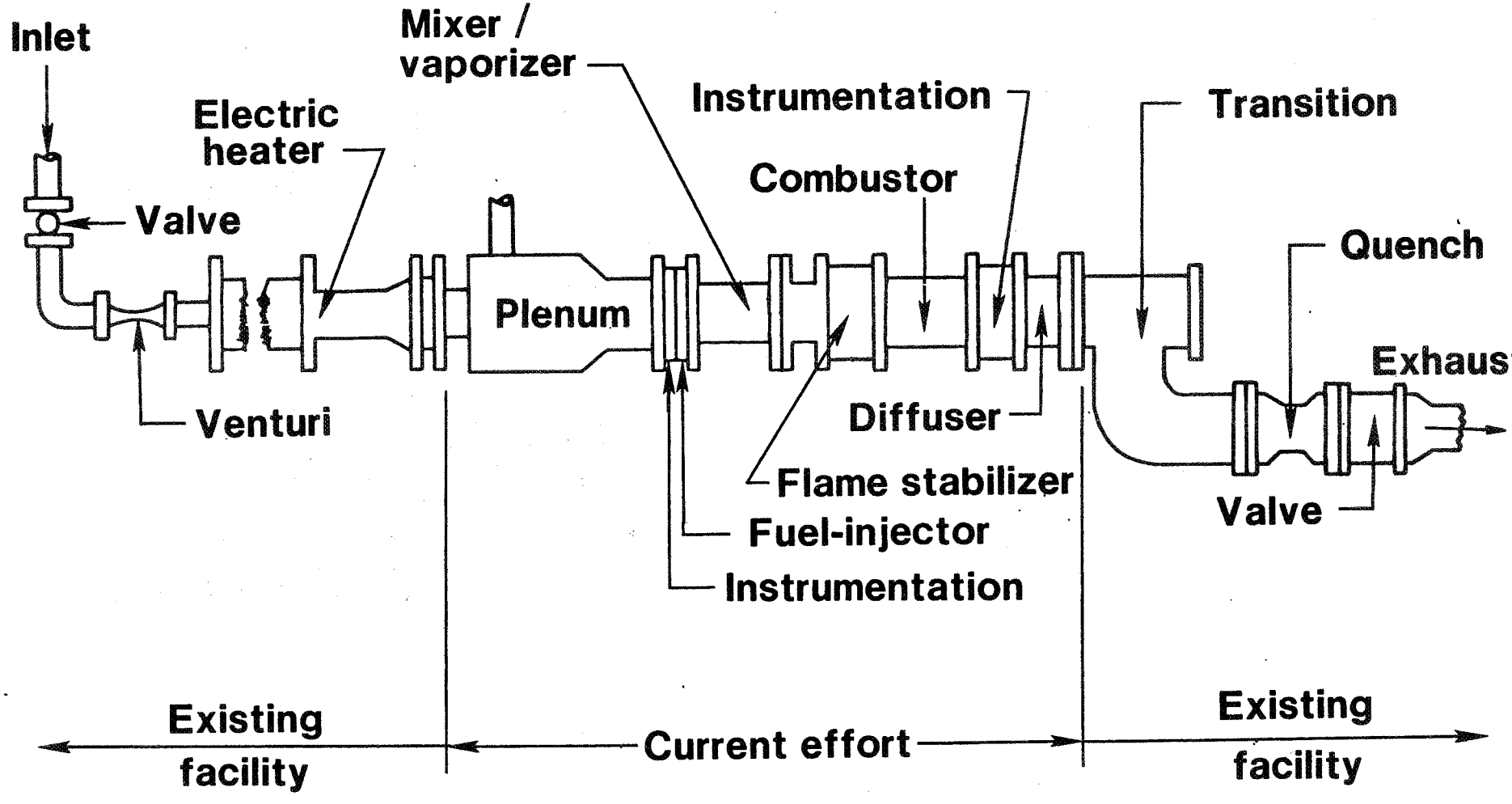

Fuel Injector – Airflow Nozzle

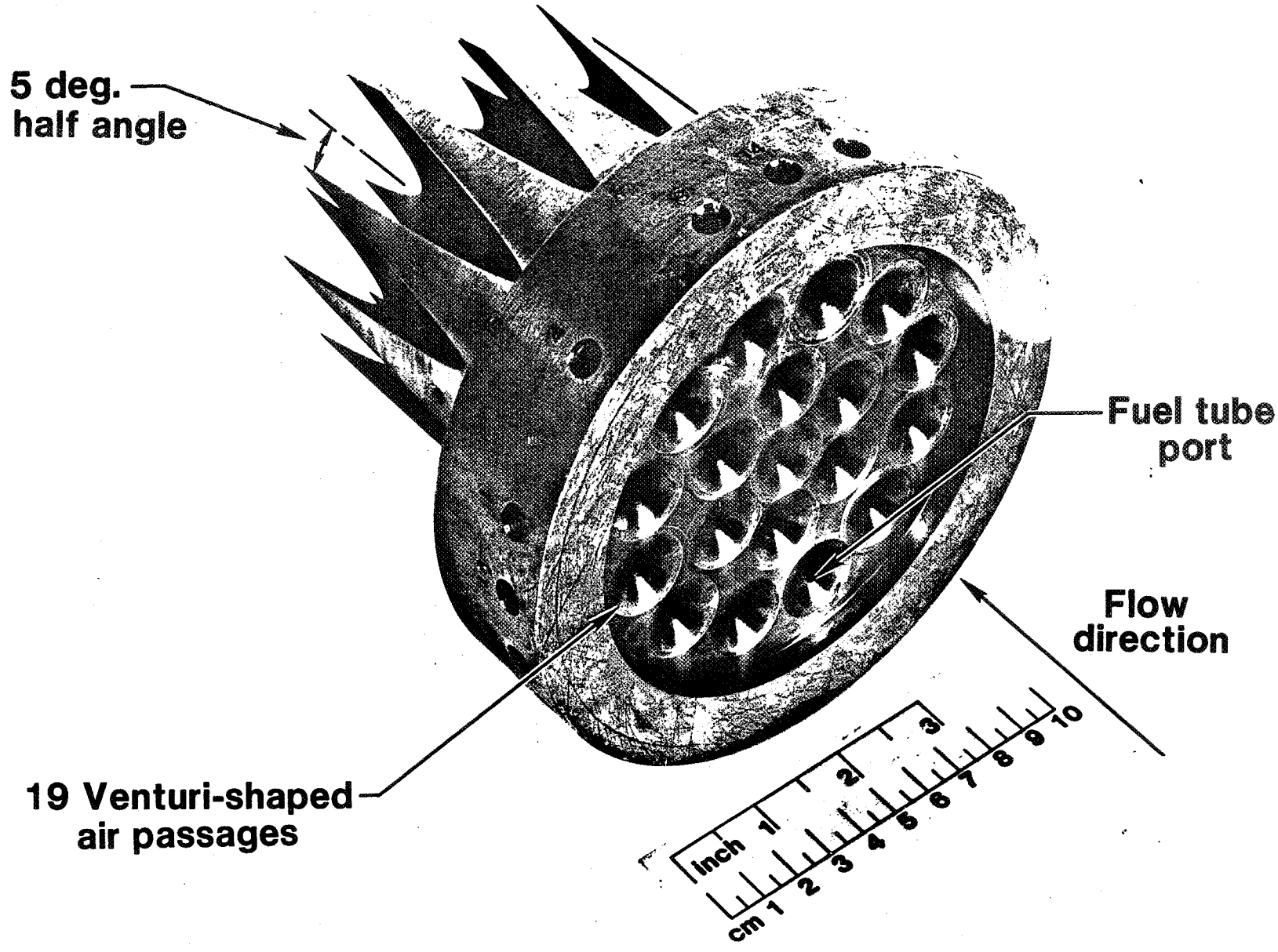

Emission - Probe Tip Construction

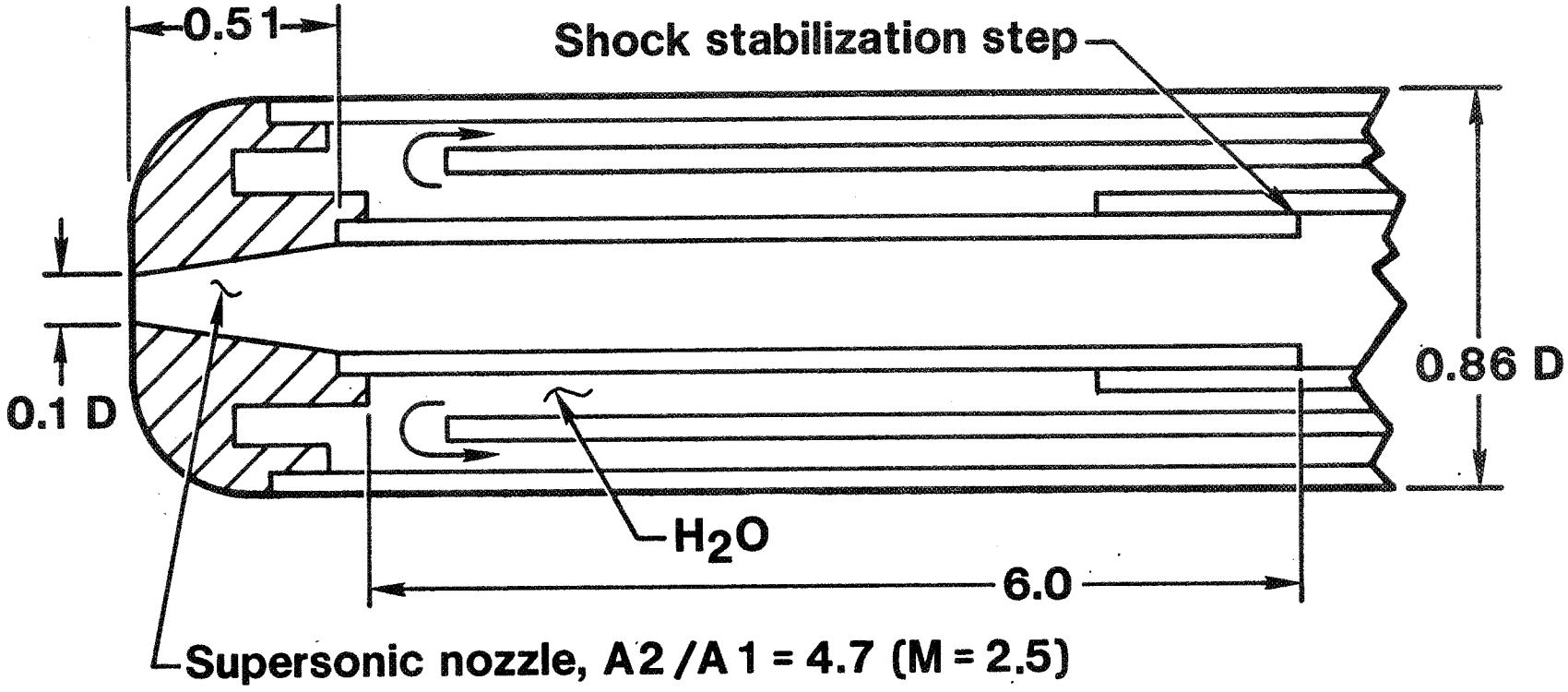

Note: All dimensions in cm

Baseline Flameholder Blowout Limits

75% blockage perforated plate

$(\Delta P/P_T)_{cold}$ =2.3%

P=10 atm

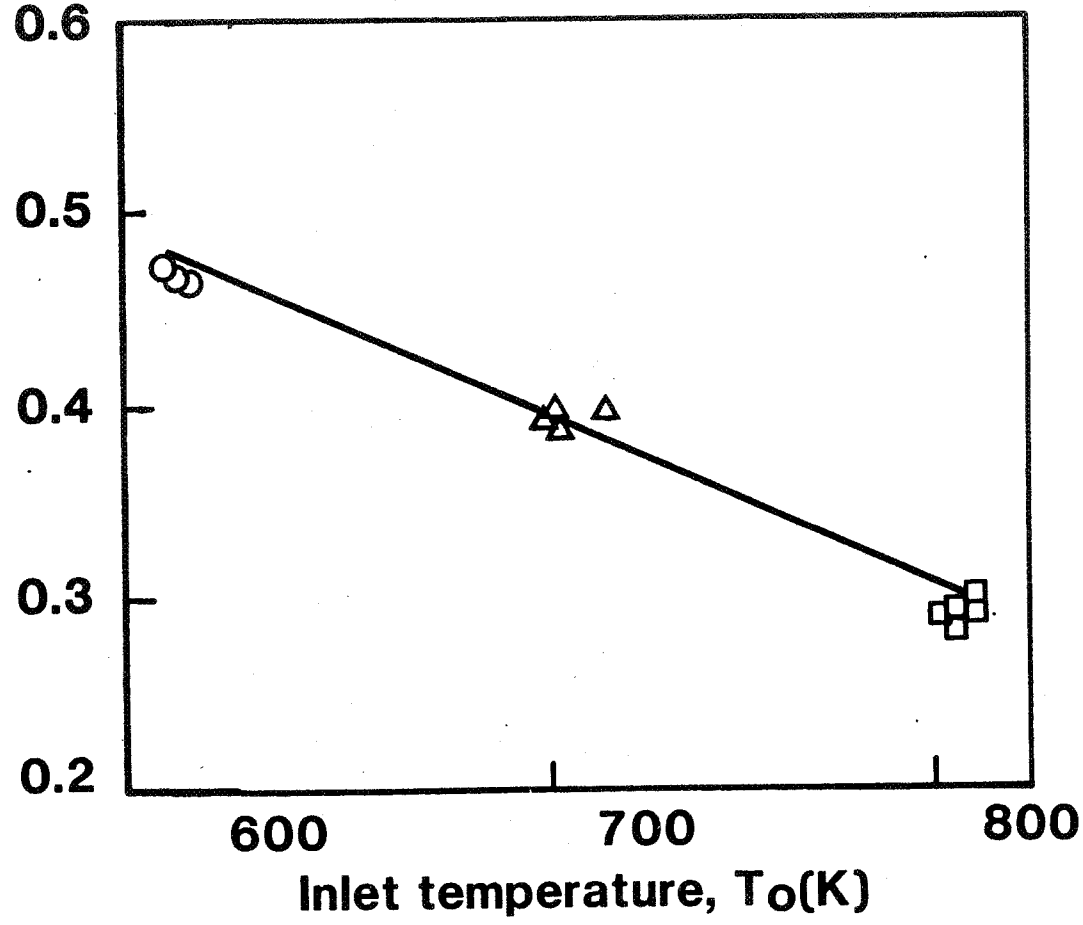

Variation of Blowout Flame Temperature with Inlet Temperature

Baseline configration

P=10 atm

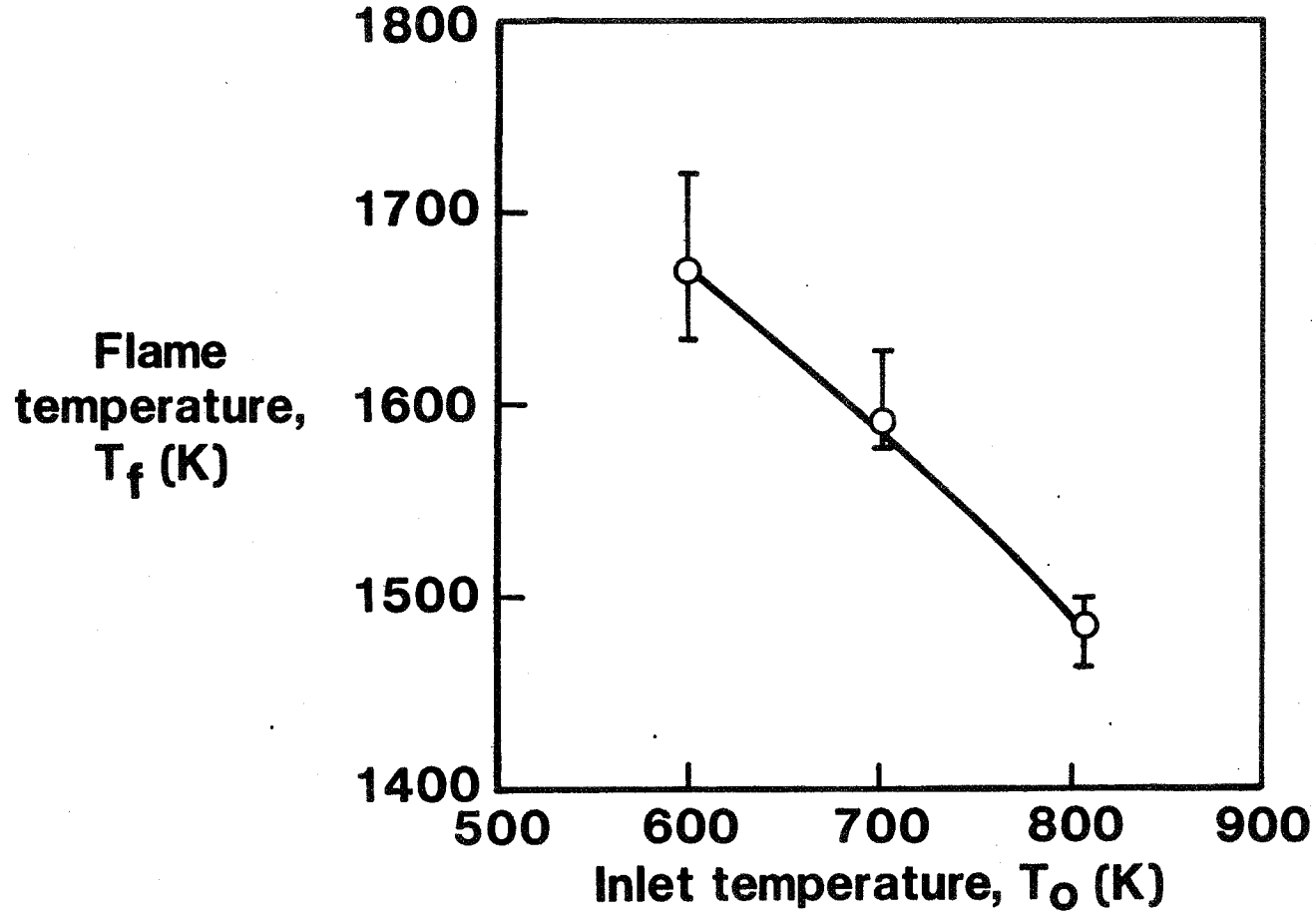

Self-piloting Recessed Perforated Plate Flameholders

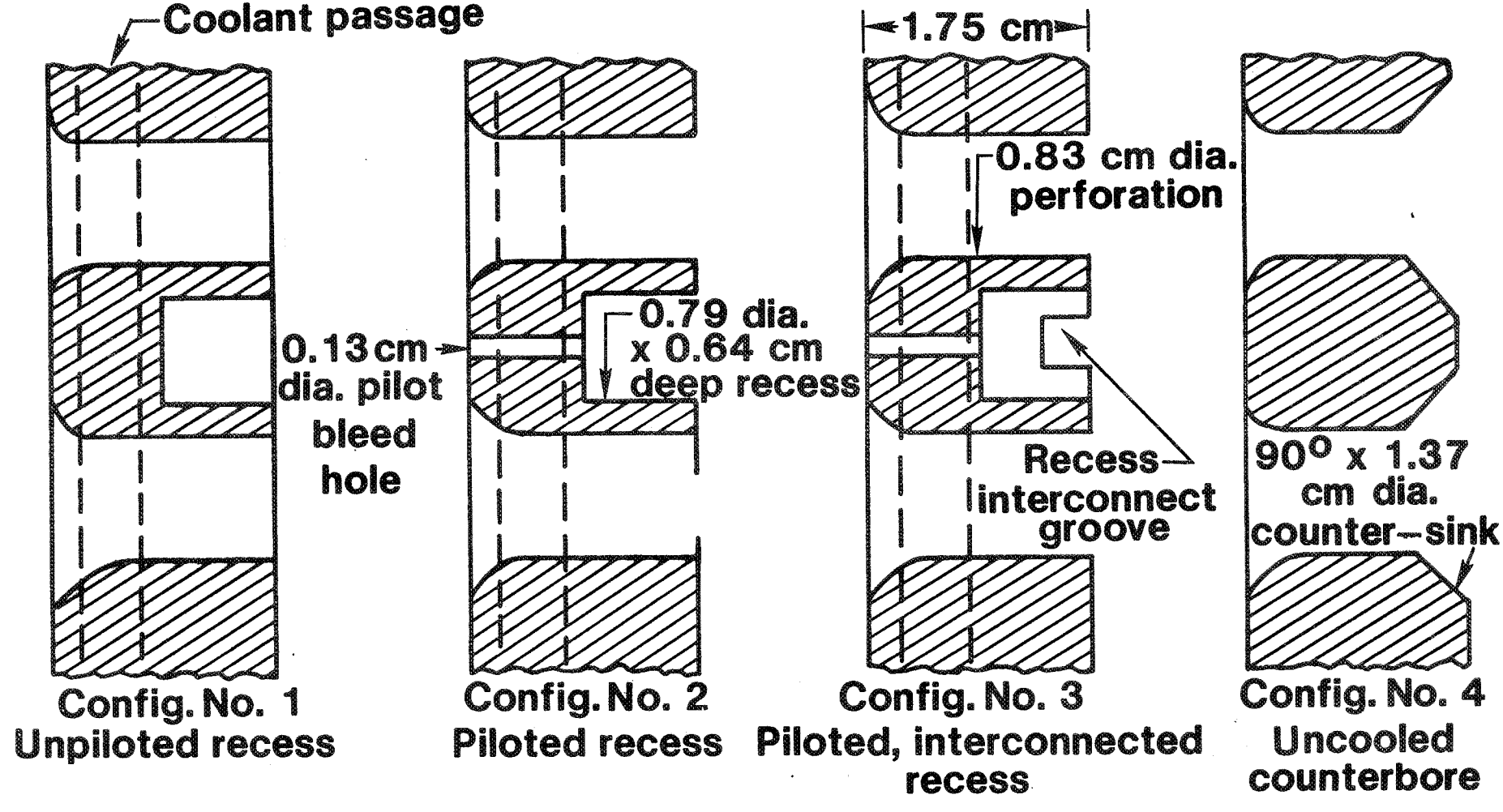

Recessed Self-piloting Perforated Plate Flameholder

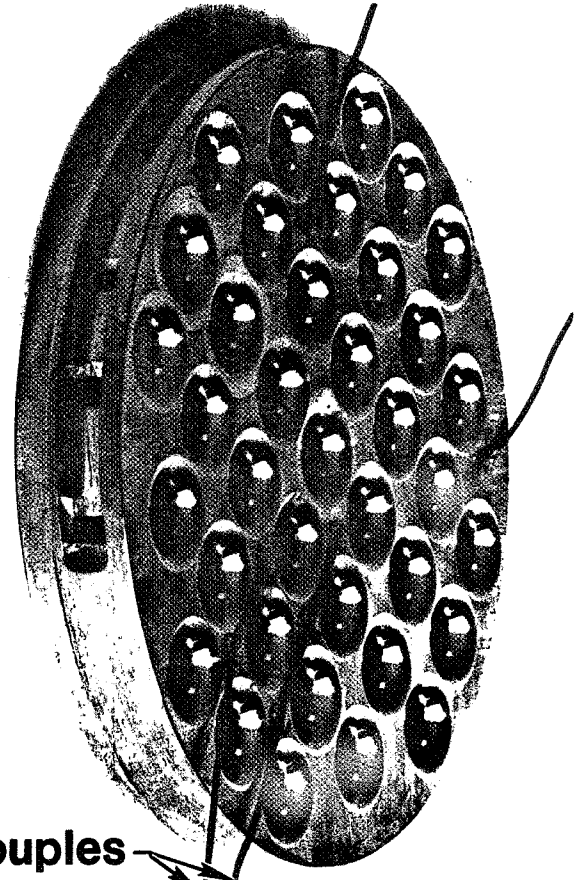

Front view

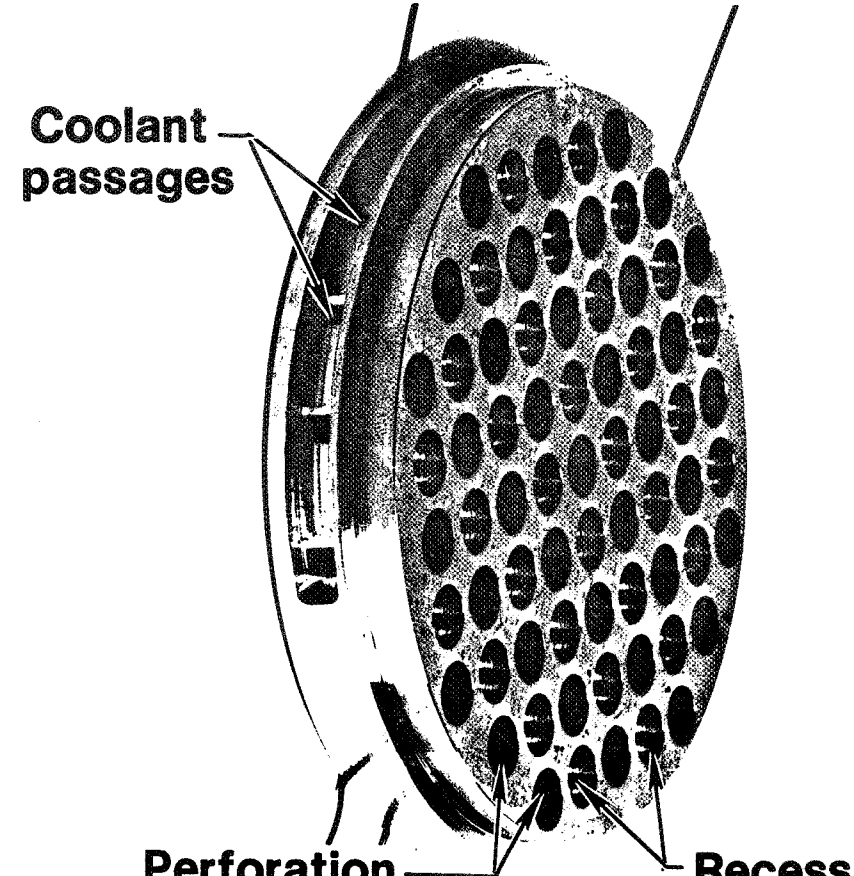

Rear view

UNITED TECHNOLOGIES RESEARCH CENTER

78–241–C
78–241–D

78–11–58–1

Lean Stability Limits

Self-Piloting Recessed Perforated Plate Series

Configuration

- ○ Recess only
- □ Recess + pilot
- △ Interconnected recesses + pilot
- ▽ Countersink
- ● Final 80% blkg; deep counter bore

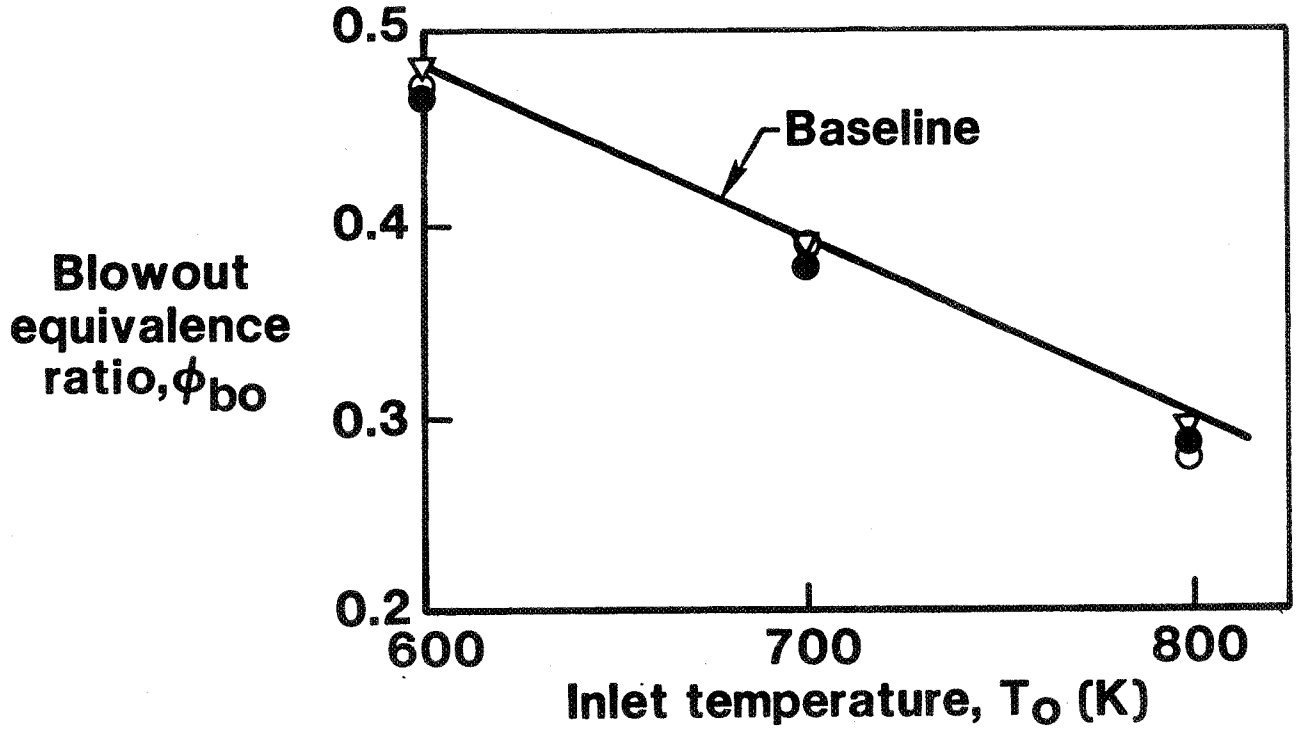

Self-Piloting Recessed Perforated Plate Final Design

Note: All dimensions in cm
80% blockage

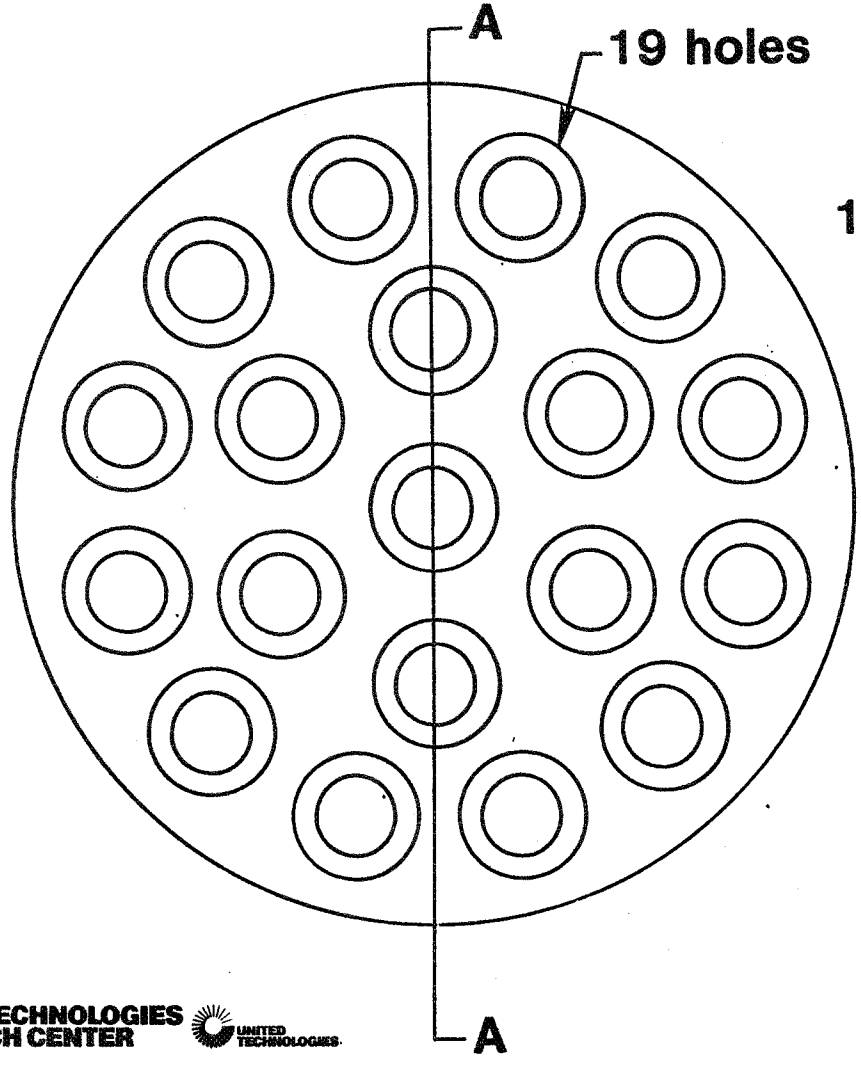

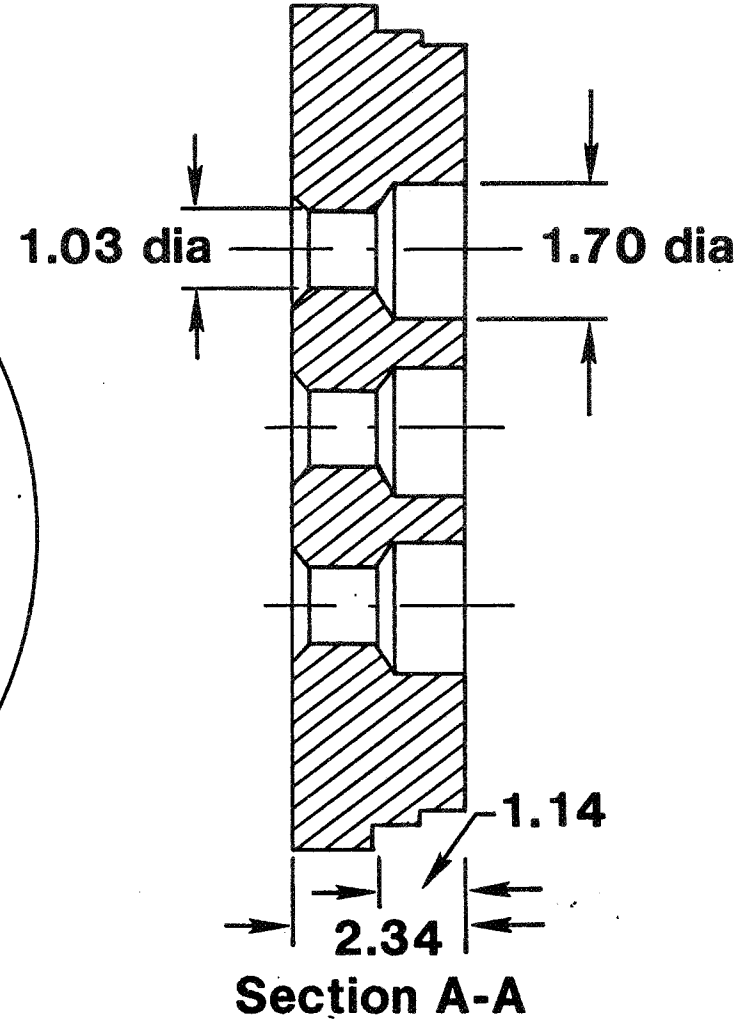

Section A-A

Effect of Flameholder Characteristics on Combustor Performance

	Config.	Blkg.	ΔP/P	NH	C'bore depth (cm)
– – –	SPRPP-4	75	0.024	37	0.27
———	SPRPP-F	80	0.037	19	1.14

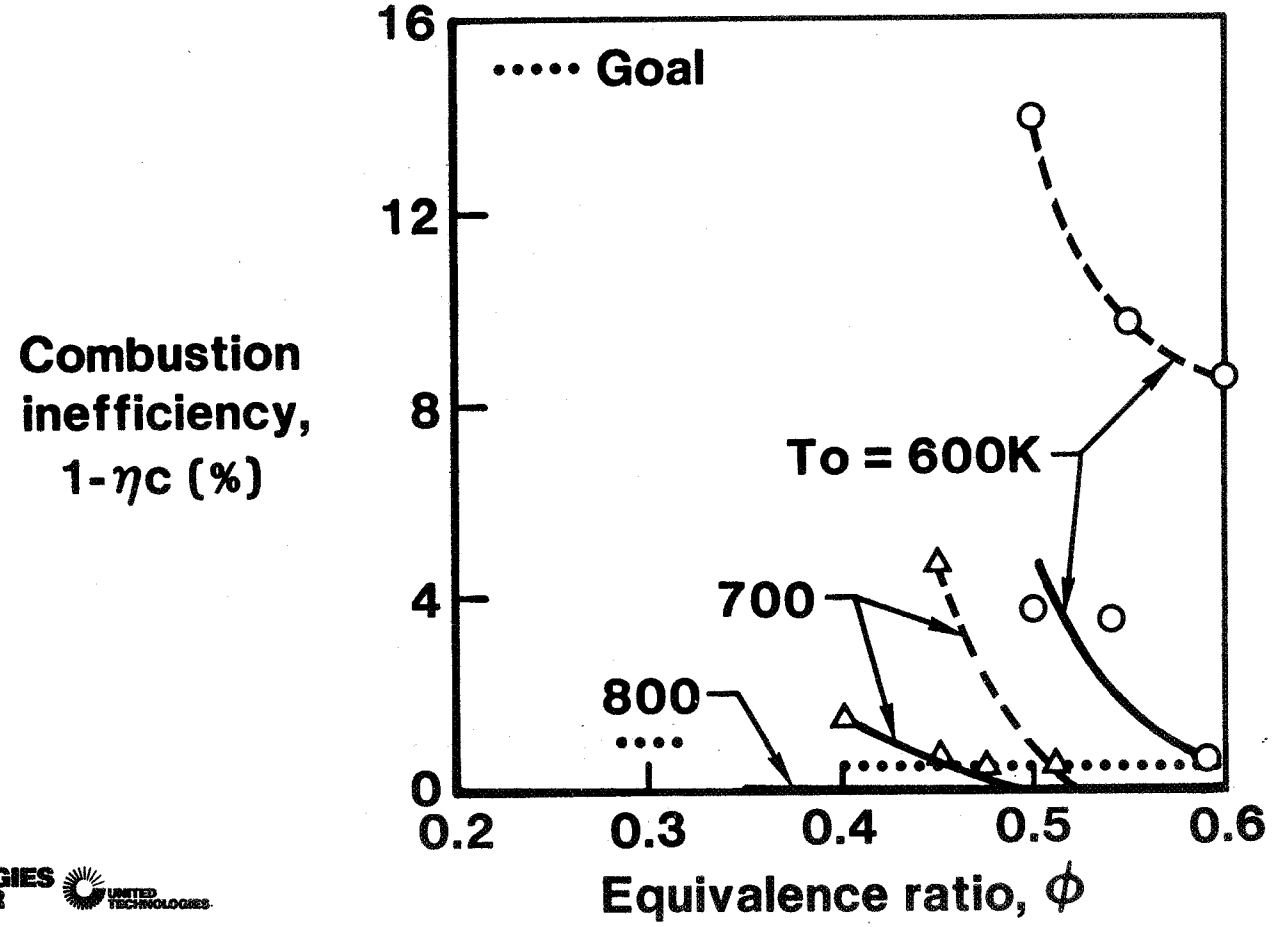

Variation of NO Emissions with Flame Temperature

SPRPP final design

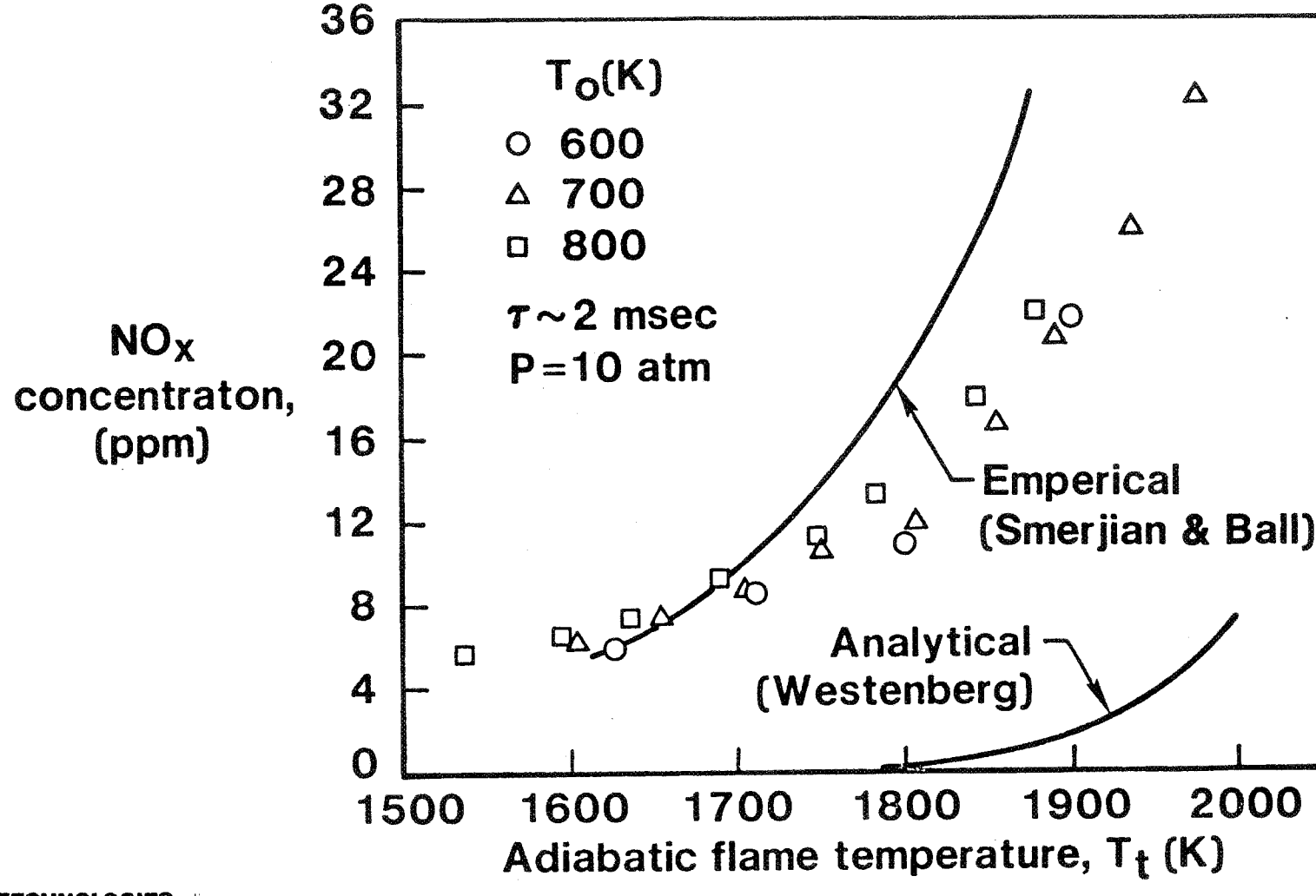

Variation of CO Emissons with Flame Temperature

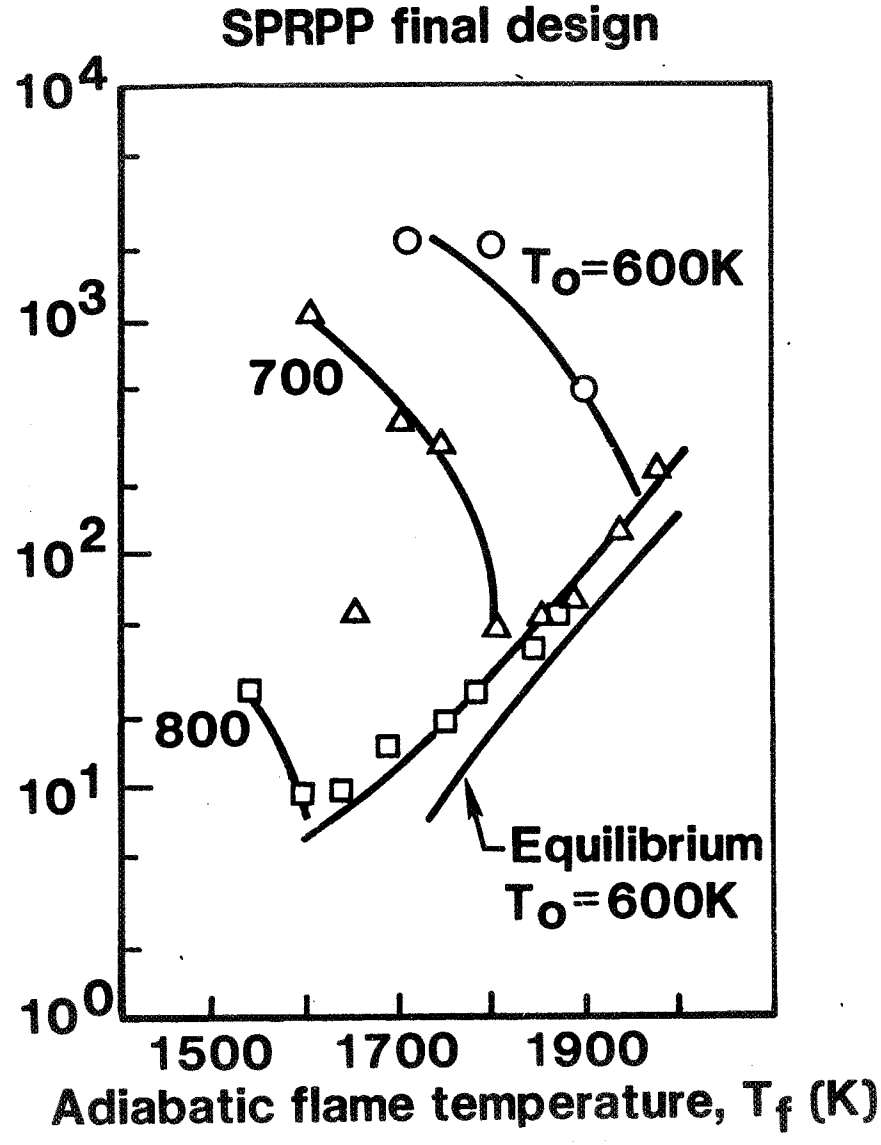

$\tau \sim$ 2 msec
P = 10 atm

UNITED TECHNOLOGIES RESEARCH CENTER

78–11–88–13

Catalyzed Tube Flameholder Configurations

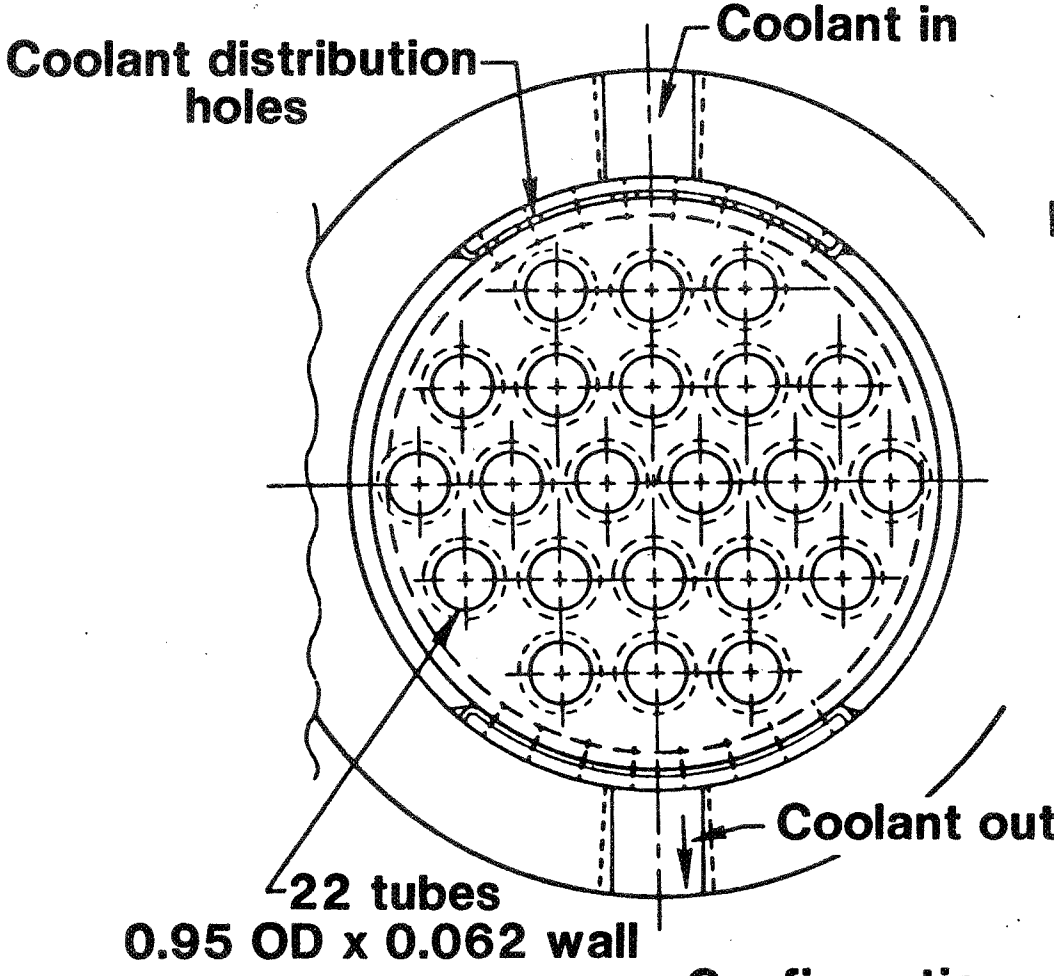

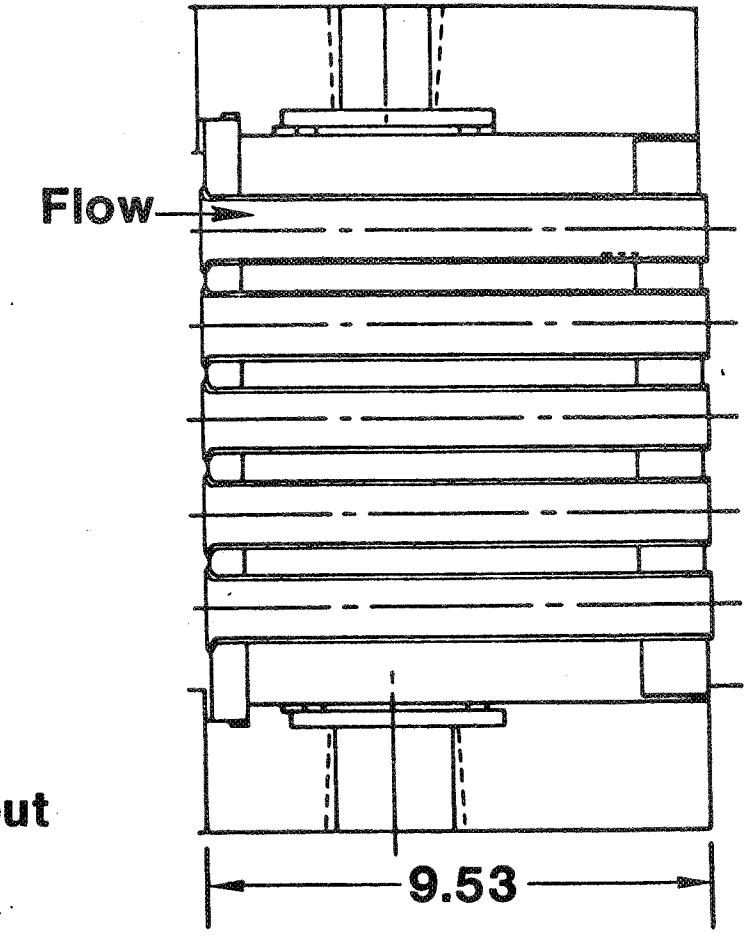

Configuration	Catalyzed surfaces
No. 1	Tube ID, 8.9 cm, rear plate
No. 2	Tube ID, 8.9 cm
No. 3	Tube ID, 4.45 cm

Catalyzed Tube Flameholder Final Design

Note: All dimensions in cm

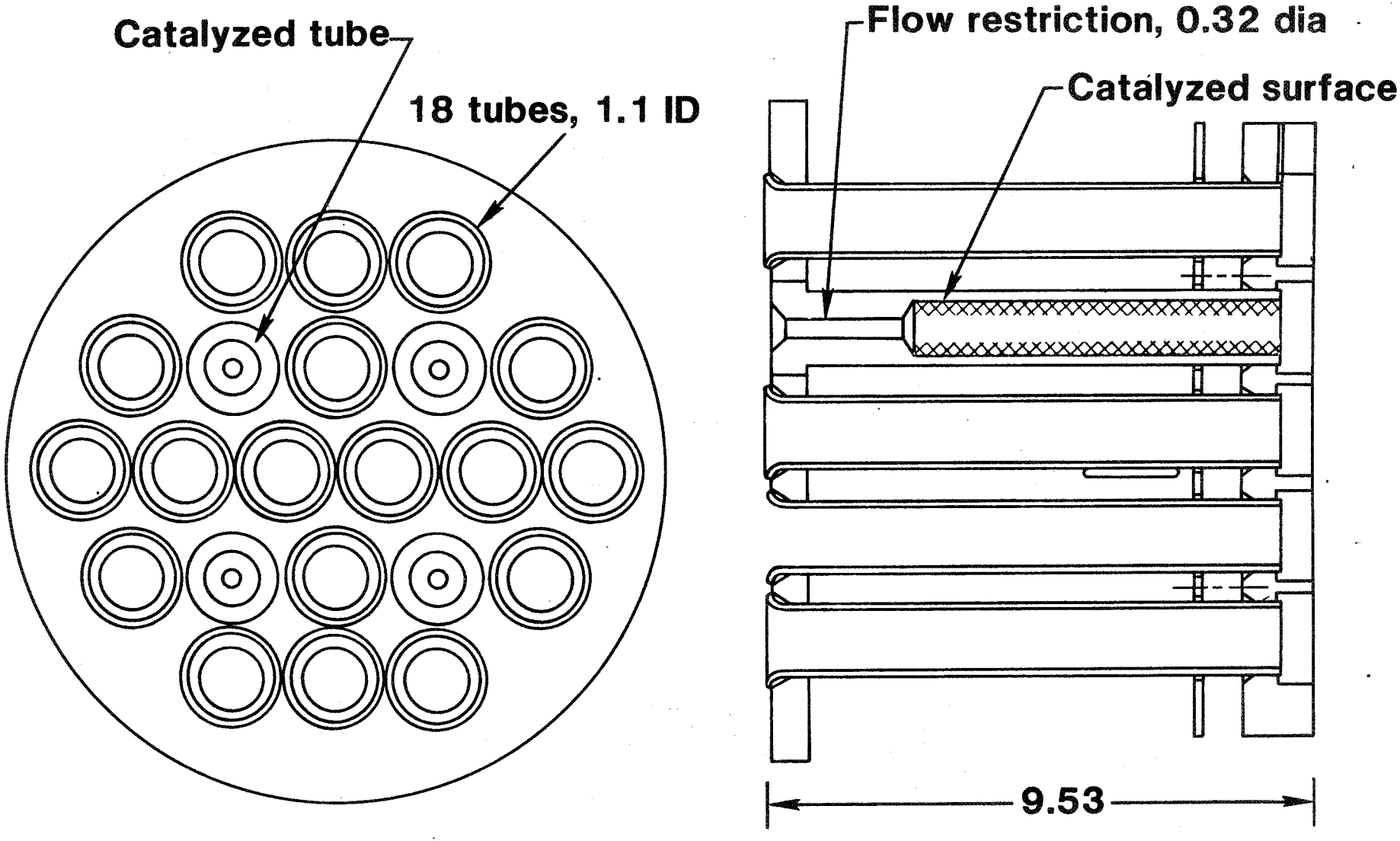

Catalyzed Tube Flameholder

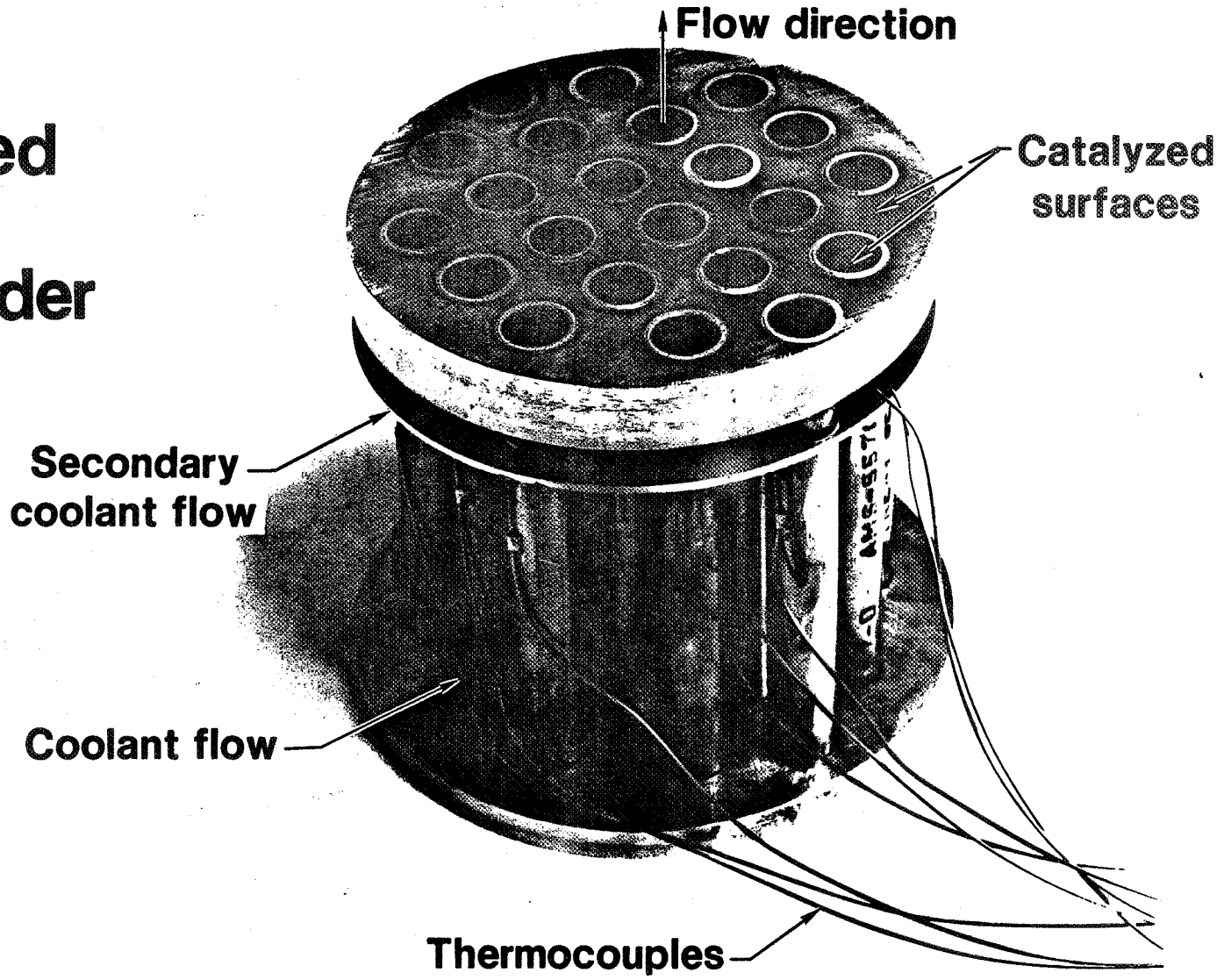

UNITED TECHNOLOGIES RESEARCH CENTER

78–241–F 78–09–169–1

Lean Stability Limits

Catalyzed tube flameholder series

Configuration

- ○ 3.75 in. tube + rear face
- □ 3.75 in. tube
- △ 2.0 in. tube
- ▽ 2.0 in. tube-heated

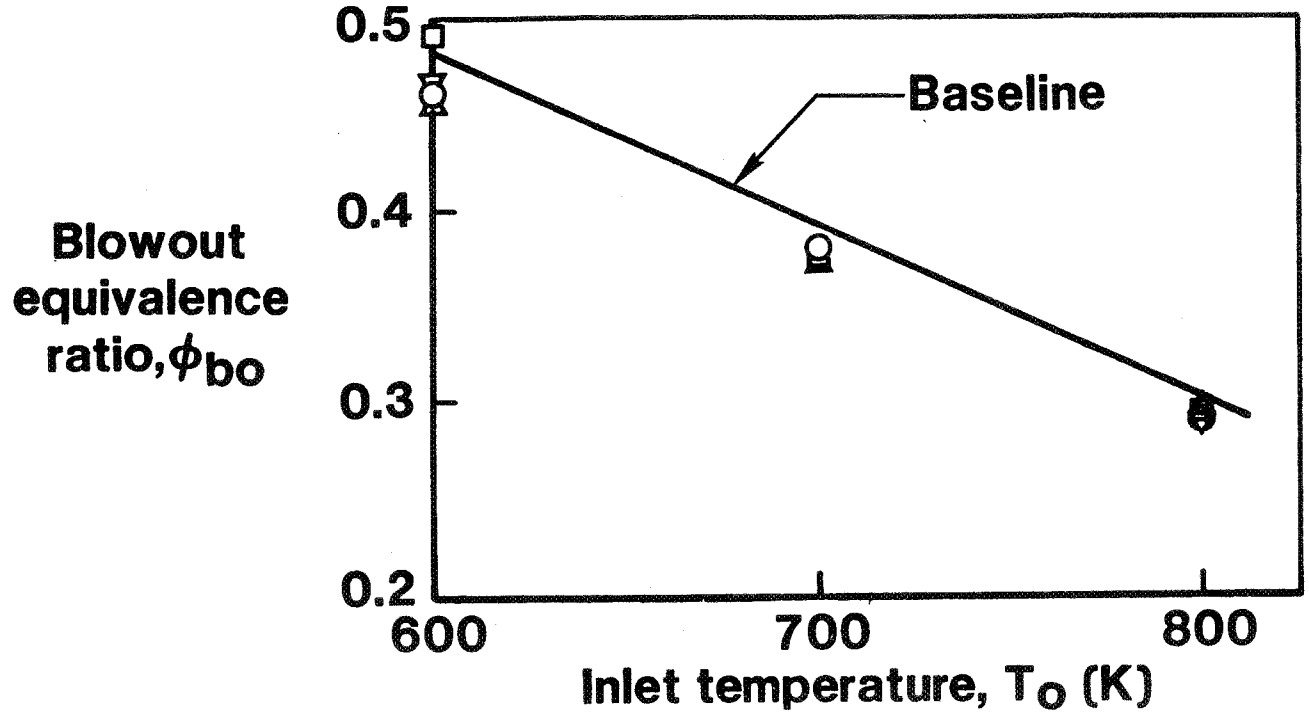

Piloted V-Gutter Flameholder Configuratons

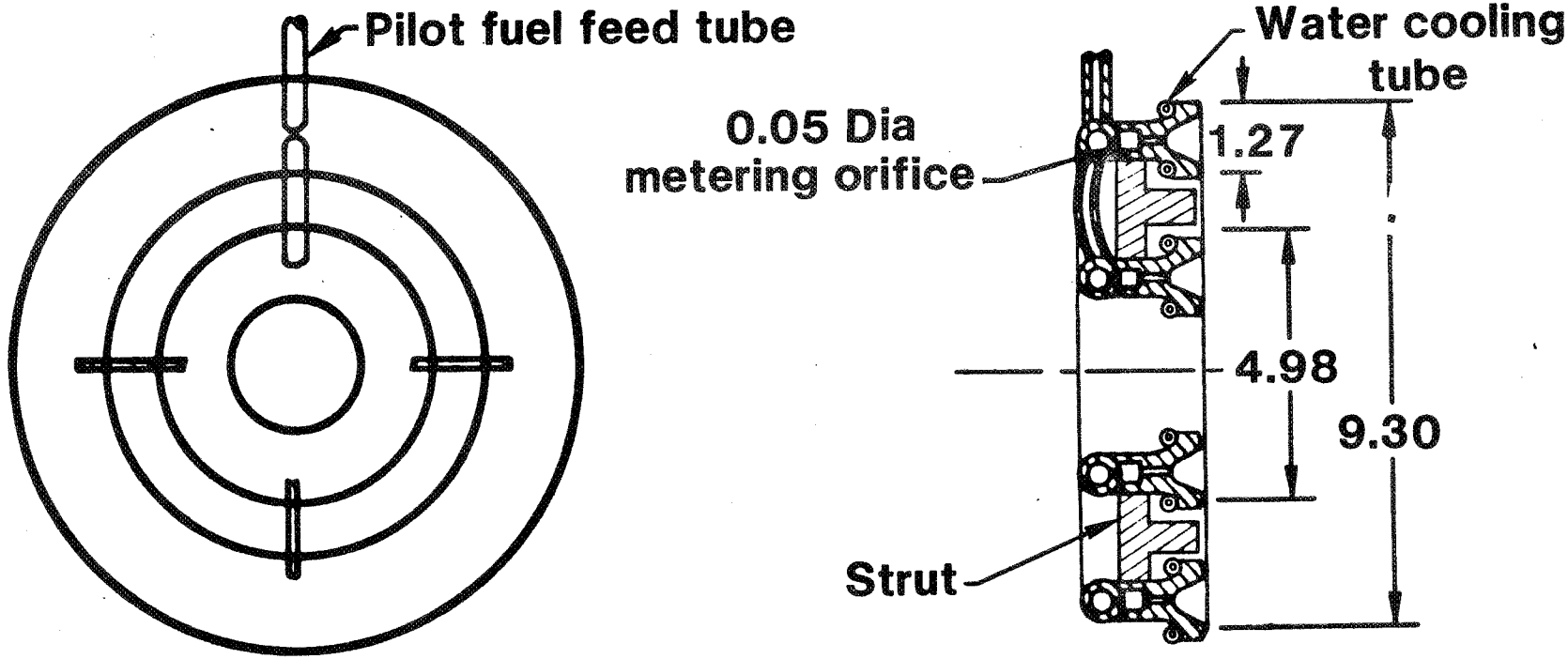

Note: All dimensons in cm

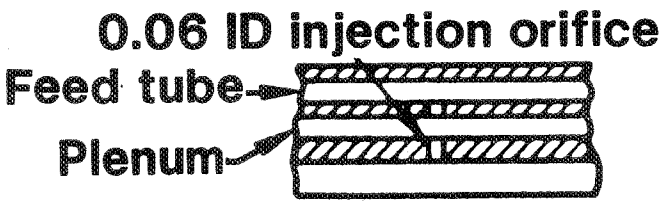

Config No. 1
Axial pilot injection

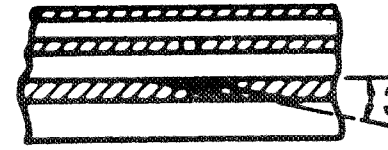

Config No. 2
Tangential pilot injection

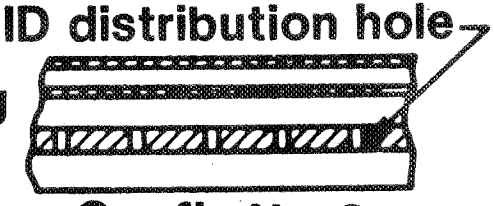

Config No. 3
Distributed pilot injecton

Piloted V-Gutter Flameholder

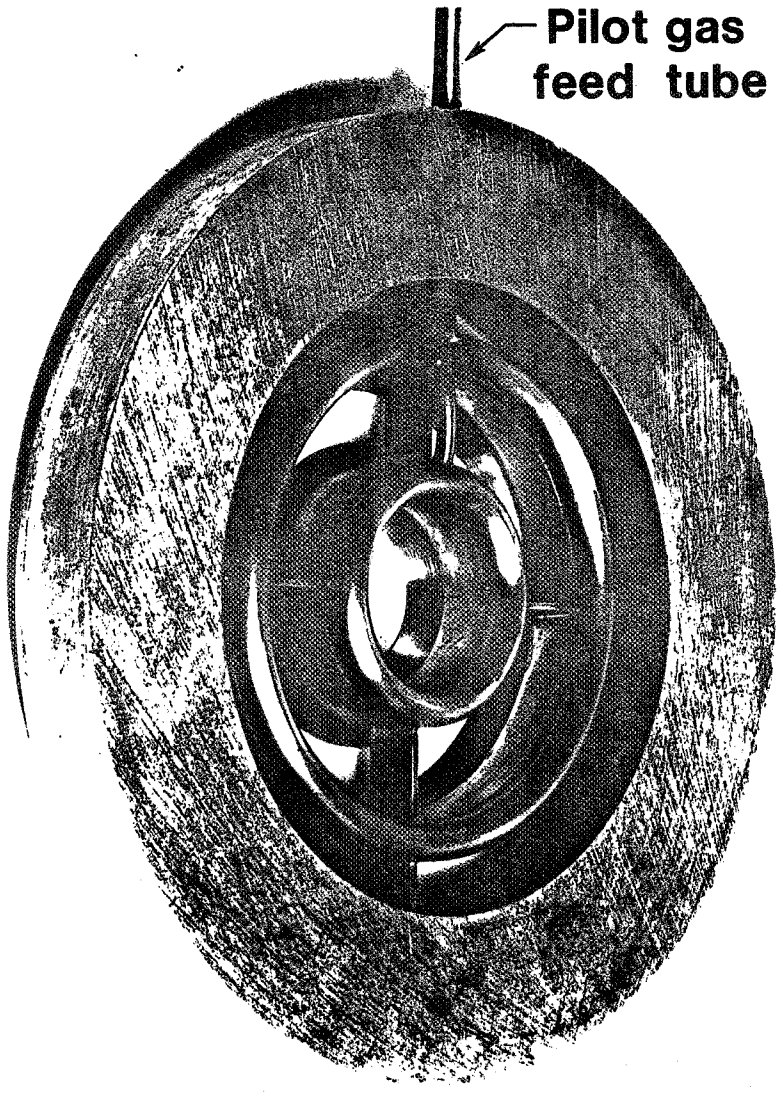

Front view

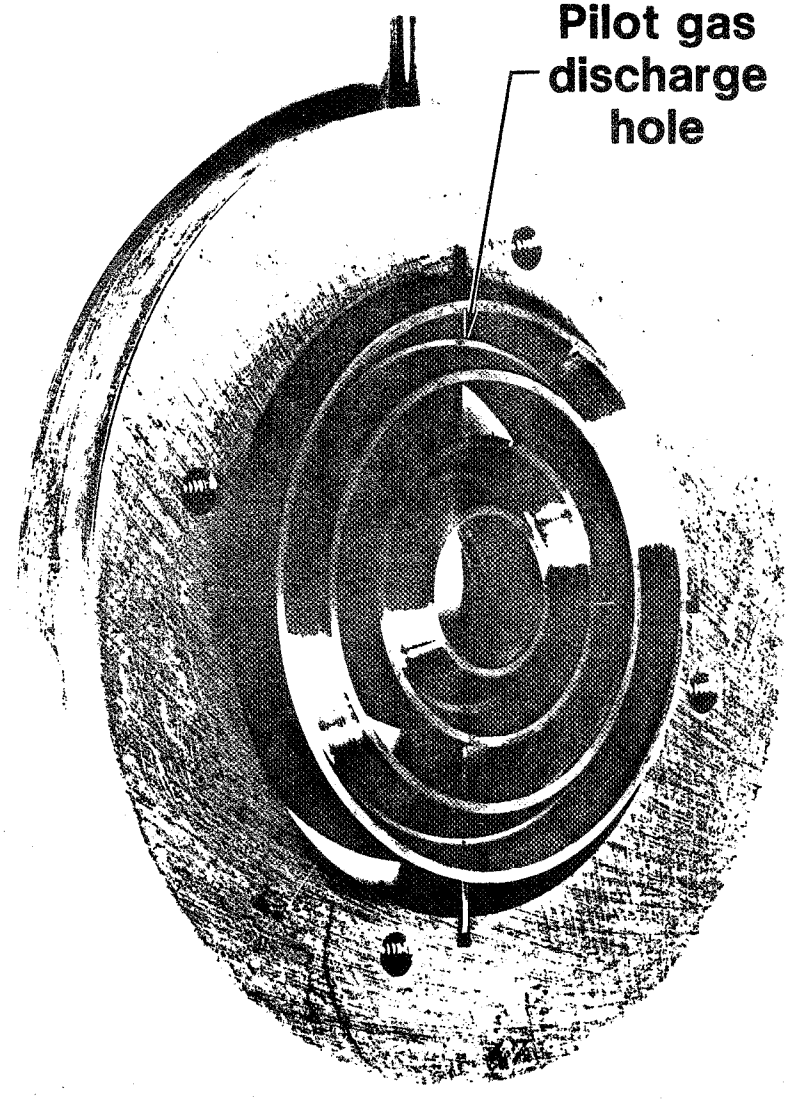

Rear view

UNITED TECHNOLOGIES
RESEARCH CENTER

78–241–B
78–241–E

78–11–58–5

NOX Emissions - V-Gutter Flameholder

Configuration 1

Note: $\dot{W}_{f,p}$=const=0.05x$\dot{W}_{f,\,tot}$, ϕ=0.6

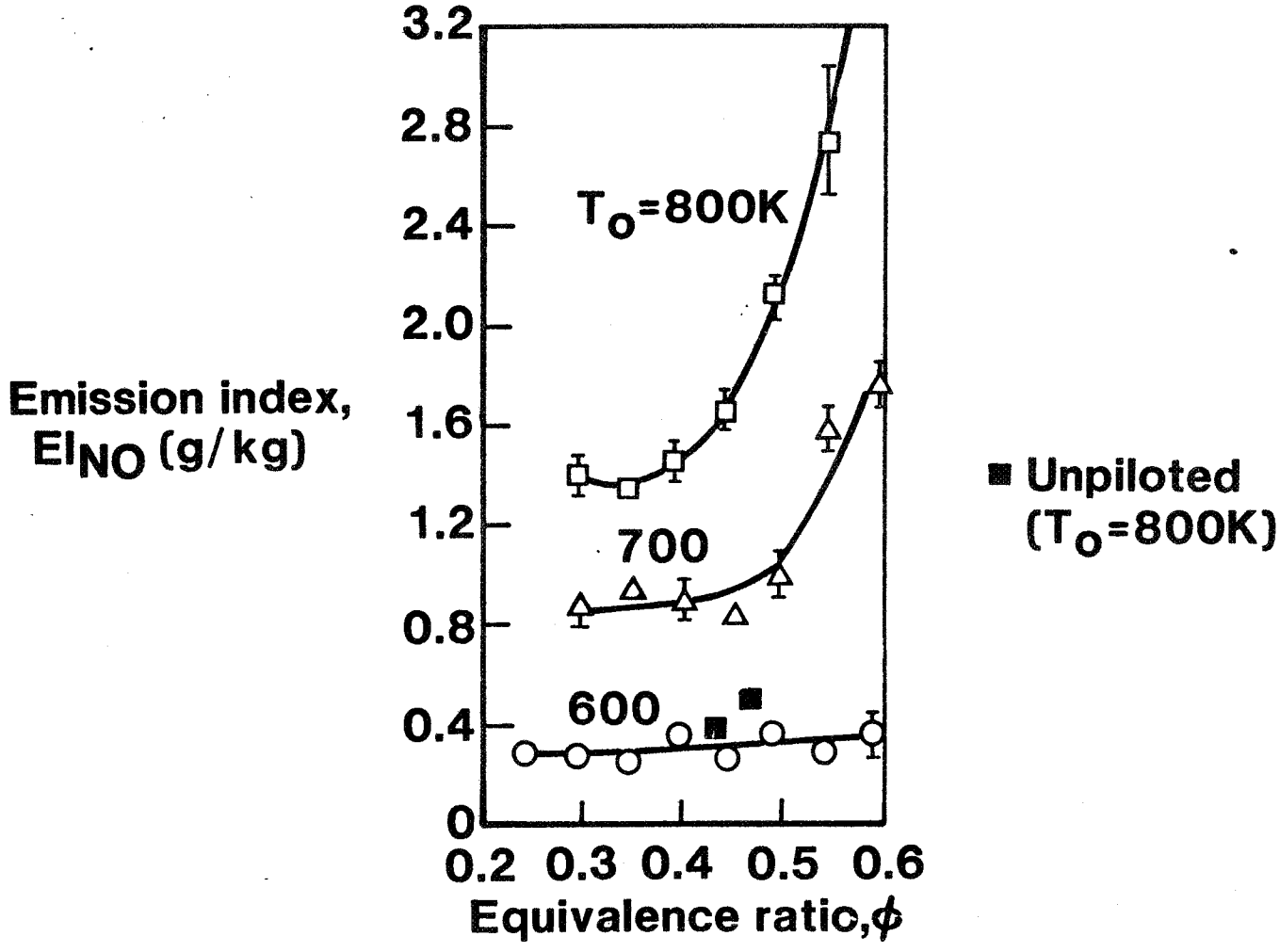

MODELLING TURBULENT FLAME IGNITION AND BLOWOUT

by

Krishnan Radhakrishnan and John B. Heywood

Department of Mechanical Engineering
Massachusetts Institute of Technology

A statistical mixing model incorporating an overall rate equation to describe the fuel oxidation process has been developed for studies of ignition and blowout in a combustor primary zone. This zone is treated as a partially stirred reactor whose composition is described by a statistical ensemble of equal mass fluid elements. This ensemble experiences mixing interactions, which represent the turbulent mixing process, at time intervals governed by an empirically determined mixing frequency. Each mixing interaction is computed by randomly selecting two different elements which are then allowed to mix completely so that they reach a mean composition depending on their thermodynamic states prior to mixing. The two elements then separate, and the chemical kinetics proceed depending on their new composition and temperature.

Material flows into and out of the primary zone are simulated by element additions and removals at a rate governed by the residence time of the reactor. The randomness of the flow in the primary zone is simulated by randomly choosing elements to be taken out of the reactor and replacing them with unburnt elements at the inlet conditions.

Imperfect premixing (i.e. the presence of small-scale composition nonuniformities) of the fuel-air mixture flow into the primary zone is accounted for by assuming a Gaussian distribution in the fuel fraction about the mean fuel fraction. The nonuniformity of the inlet mixture is then quantified by defining an unmixedness parameter, s, equal to the coefficient of variation of the distribution. A value of $s = 0$ corresponds to complete premixing; increasing s corresponds to increasingly imperfectly premixed mixtures.

To simulate the ignition process, the ensemble of fluid elements is initialized by assuming that all the elements are unburnt. The spark is replaced by igniting a few elements at time $t = 0$. The ensemble properties (assumed equal to the mean of the properties of the elements) are calculated as a function of time. Non-ignition is characterized by the ensemble burnt fraction, $\overline{B}$, decreasing with time; successful ignition requires a growth in $\overline{B}$. The lean ignition limit is defined as the leanest mixture which can be ignited. To simulate blowout, most (or all) of the elements are assumed fully burnt at $t = 0$ and the ensemble properties are allowed to evolve with time. Blowout is characterized by $\overline{B}$ continuously decreasing with time to approach zero. The lean blowout limit is defined as the richest mixture that blows out.

The procedures outlined above were used to examine the effects of inlet temperature, pressure and velocity, on the lean limits of uniform mixtures. Comparisons were made with available data. The influence of inlet mixture nonuniformity was explored by varying s. The flameholder and combustor modelled for this study are described by Radhakrishnan (1978). The length of the primary zone was assumed equal to the length of the recirculation zone.

The results of the parametric study are as follows. Increases in mixture inlet temperature T_u lead to higher temperature burnt products and hence increased burning rates. Hence, at constant inlet velocity, U, the limits will decrease with T_u: or for constant fuel-air equivalence ratio, ϕ, U at ignition and blowout will increase with T_u. This behavior is displayed by the model predictions. The predicted blowout limits agree well with the experimental data; however, the predicted limits are richer. This is attributed to the different fuels used in the modelling (CH_4) and experimental work (C_3H_8). We predict that neither the lean ignition nor blowout limit has a strong dependence on the pressure. This is consistent with the findings of Bolt and Harrington (1967) and Roffe and Venkatramani (1978a). Increases in U lead to lower residence times and faster mixing rates and hence richer lean limits. The predicted blowout limits again compare favorably with the experimental findings: for reasons given above, the ignition limits are richer.

With increased mixture nonuniformity, the predicted lean ignition limit is leaner. The value of s in a typical combustor primary zone is about 0.5. For this value of s, the model predicts the lean ignition limit to be about 25 percent less than that for the uniform case. Although quantitative comparisons between the model predictions and the experimental data are not possible, our experimental data shows a substantial decrease in the lean limits when the distance over which the fuel and air are allowed to mix is decreased (thereby making the fuel-air mixture less uniform).

This work was supported by NASA Grant NGR 22-009-378.

References

Anderson, D.N. (1975); NASA Technical Memorandum, TM X-71592, March 1975.

Anderson, D.N. (1975a); NASA Technical Memorandum, TM X-3301, October 1975.

Bolt, J.A. and Harrington, D.L. (1967); SAE Paper 670467.

Marek, C.J. and Papathakos, L.C. (1976); NASA Technical Memorandum TM X-3383.

Radhakrishnan, K. (1978); Ph.D. Thesis, M.I.T.

Roffe, G. and Venkatramani, K.S. (1978); NASA Contractor Report CR-135424, June 1978

Roffe, G. and Venkatramani, K.S. (1978a); NASA Contractor Report 3032, July 1978.

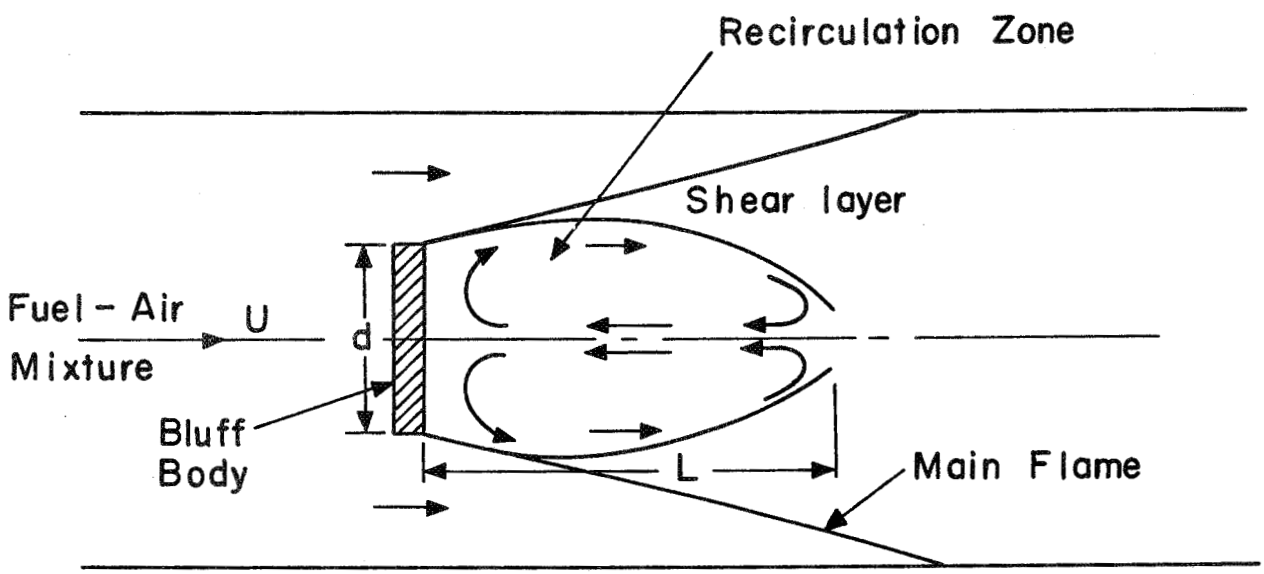

Schematic of Bluff Body Stabilized Flame

Simulation of Recirculation Zone

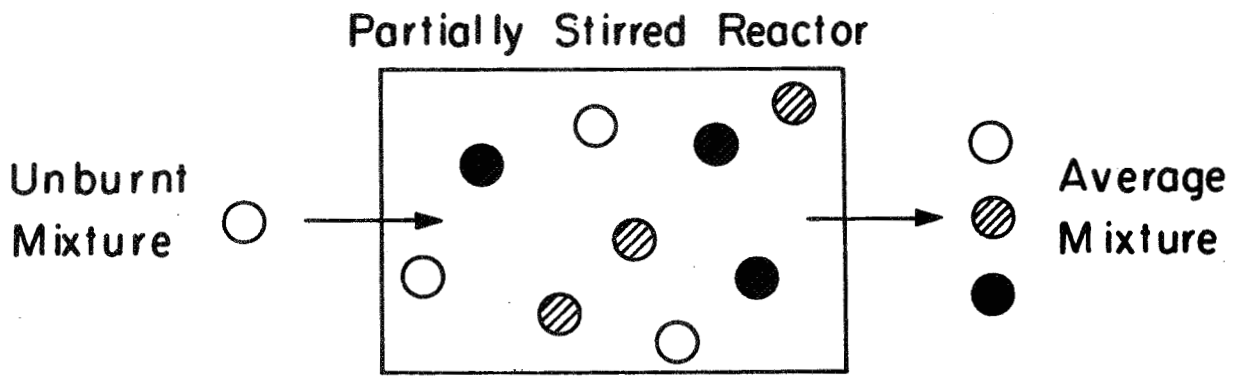

Monte Carlo Mixing Interaction

Element	i	j	i	j
Burnt Fraction	B_i	B_j	$(B_i + B_j)/2$	

Model Parameters And Relations

Mixing Frequency

$$\beta = (P_j/ML^2)^{1/3} = \left(\frac{1}{2}\dot{m}\, U_j^2/ML^2\right)^{1/3}$$

Residence Time

$$\tau_r = (V/\dot{v}) = c\ L/U$$

Chemical Kinetics

$$\frac{d}{dt}[CH_4] = -10^{13.2} \exp(-48400/RT)[CH_4]^{0.7}[O_2]^{0.8} \text{ mole/cm}^3\text{s}$$

Ensemble Property

$$\overline{Z} = \frac{1}{N}\sum_{i=1}^{N} Z_i$$

Example : Ignition

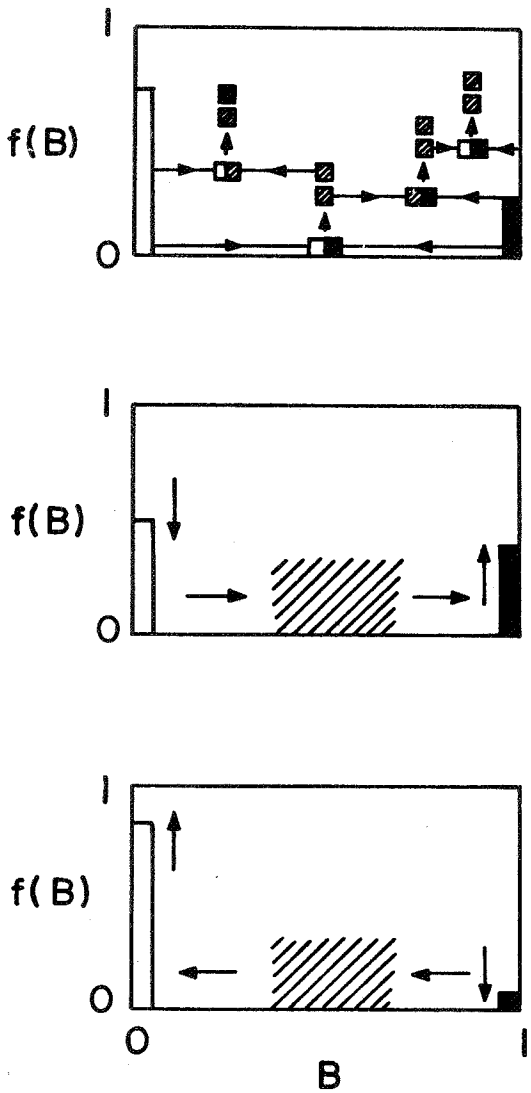

Development of Distribution Function Due to Mixing

Ignition
$\overline{B}$ Increases

No Ignition
$\overline{B}$ Decreases

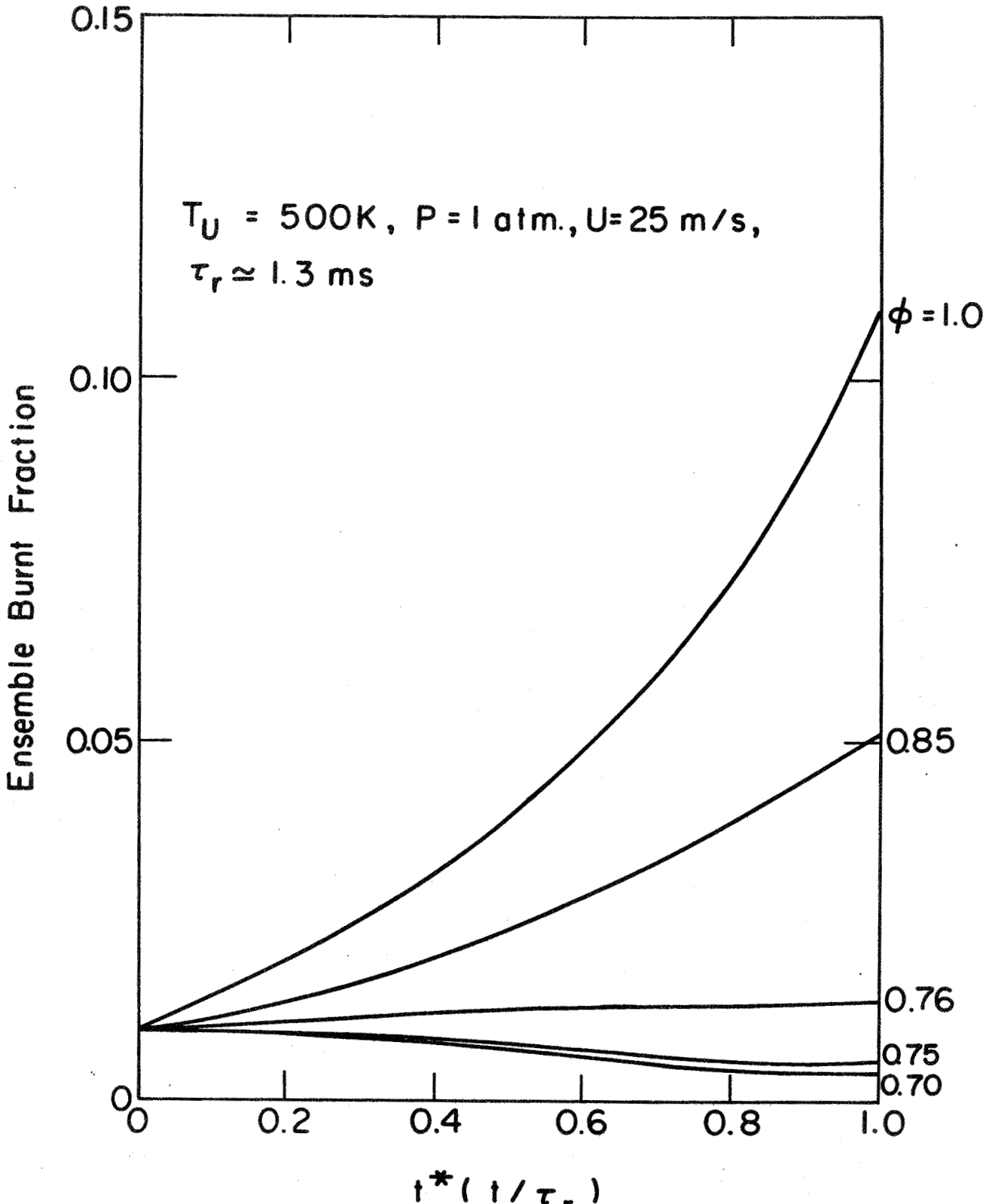

Example: Lean Ignition Limit

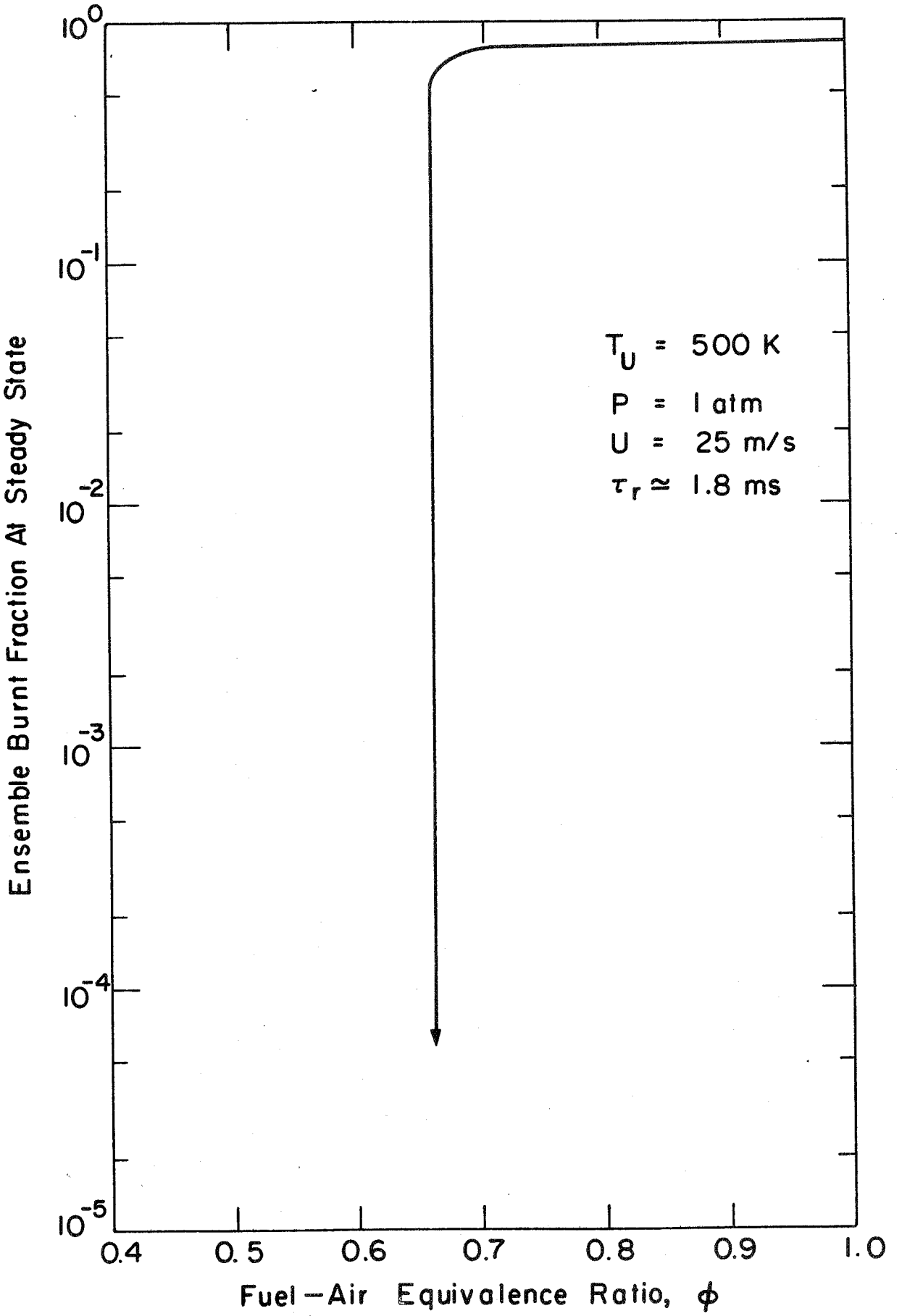

Example: Lean Blowout Limit

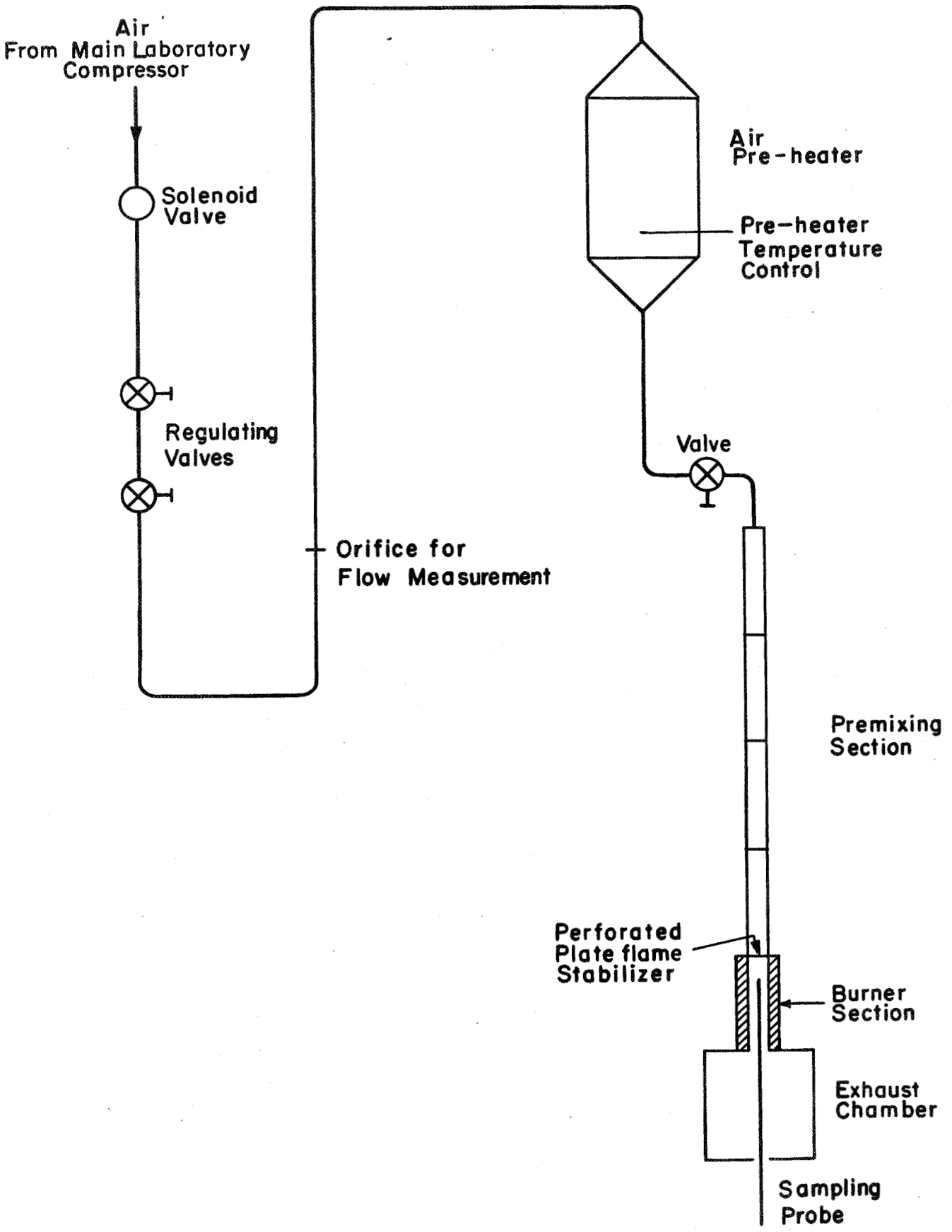

Schematic of Test Facility

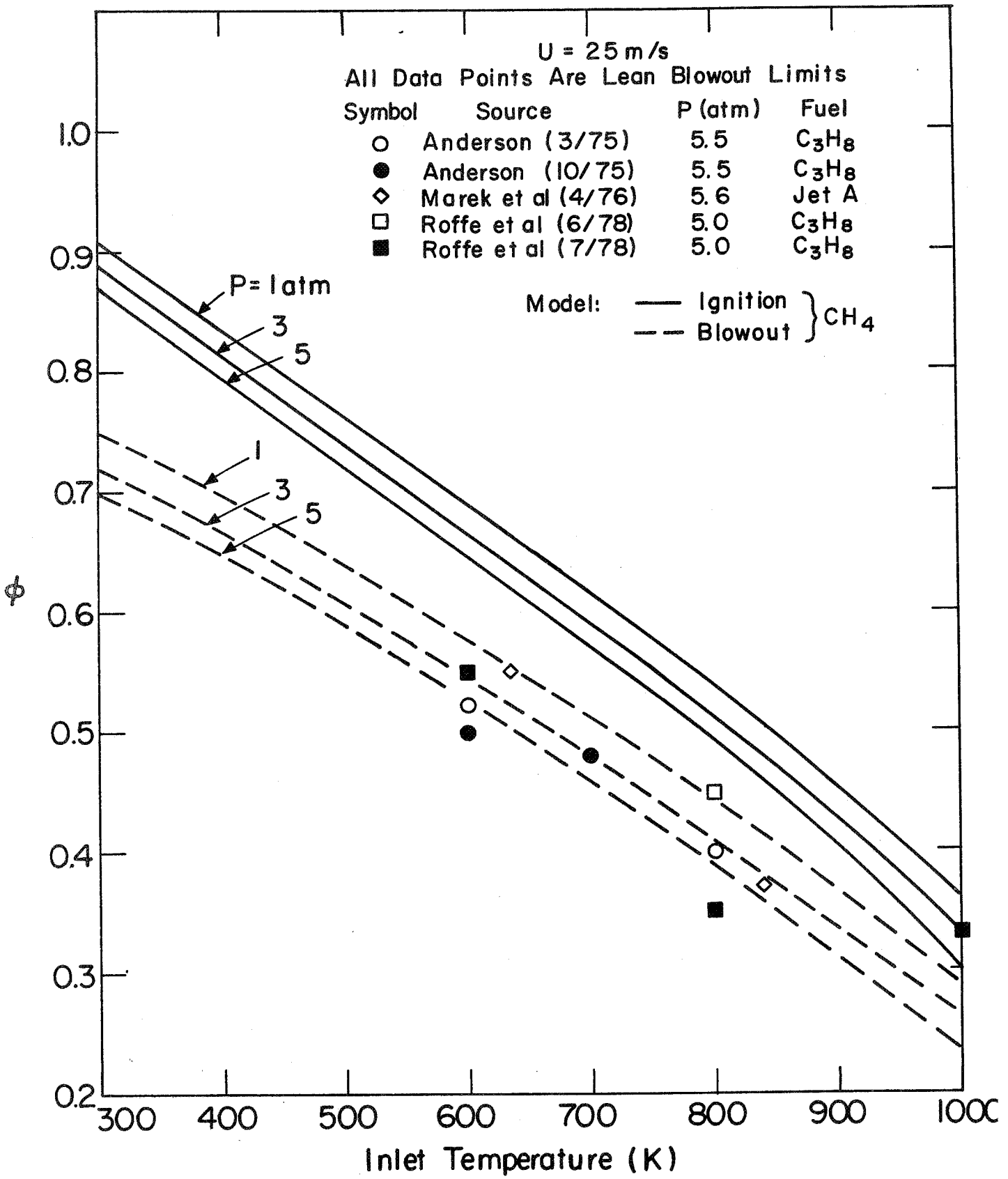

Variations of Predicted Limits with Inlet Temperature for Different Pressures

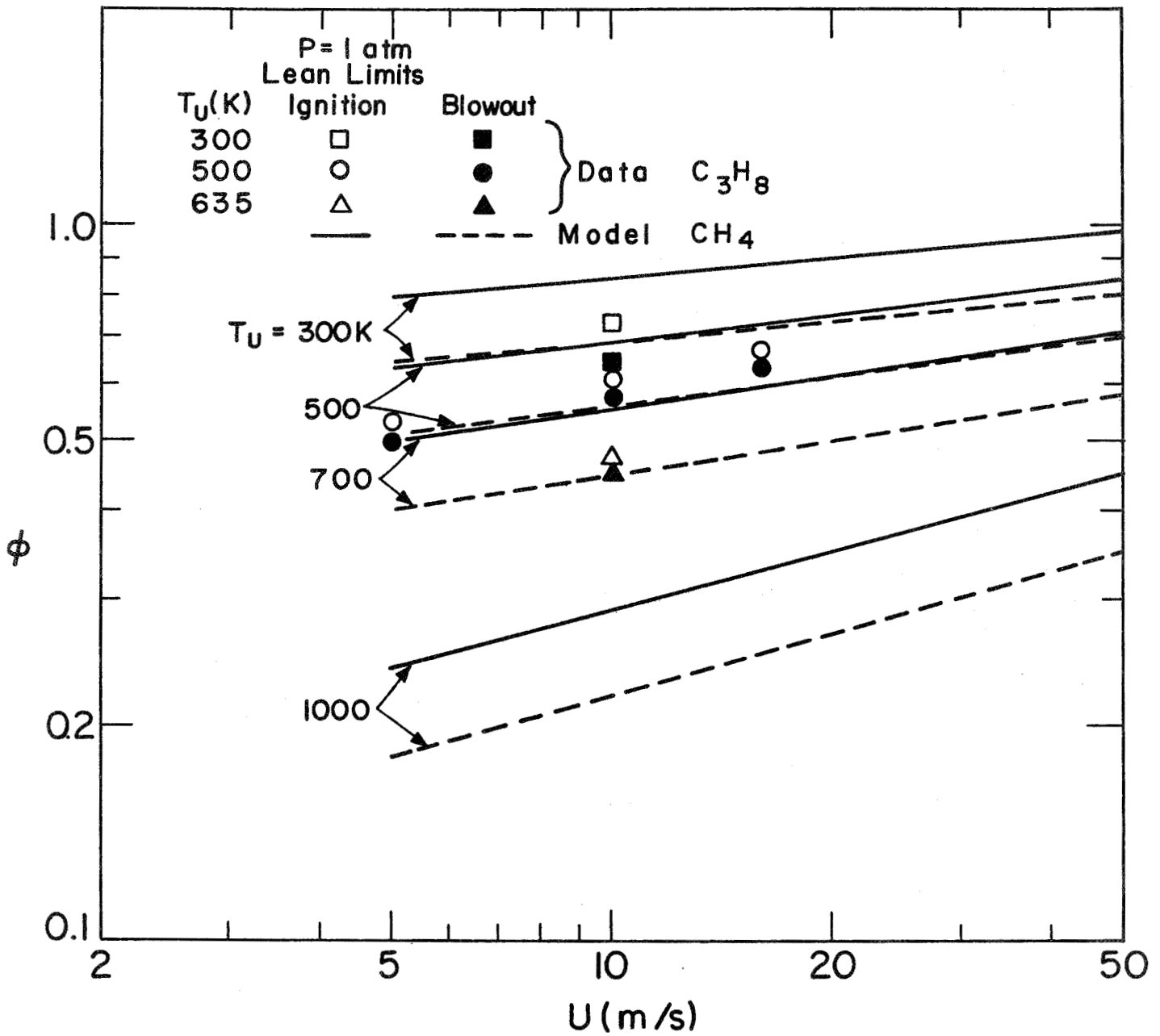

Variations of Measured and Predicted Limits with Velocity

Inlet Mixture Nonuniformity

Gaussian Distribution Function in Fuel Fraction, F

$$f(F) = (2\pi\sigma)^{-1/2} \exp\{-(F-\bar{F})^2/2\sigma^2\}$$

Unmixedness Parameter

$$s = \sigma/\bar{F}$$

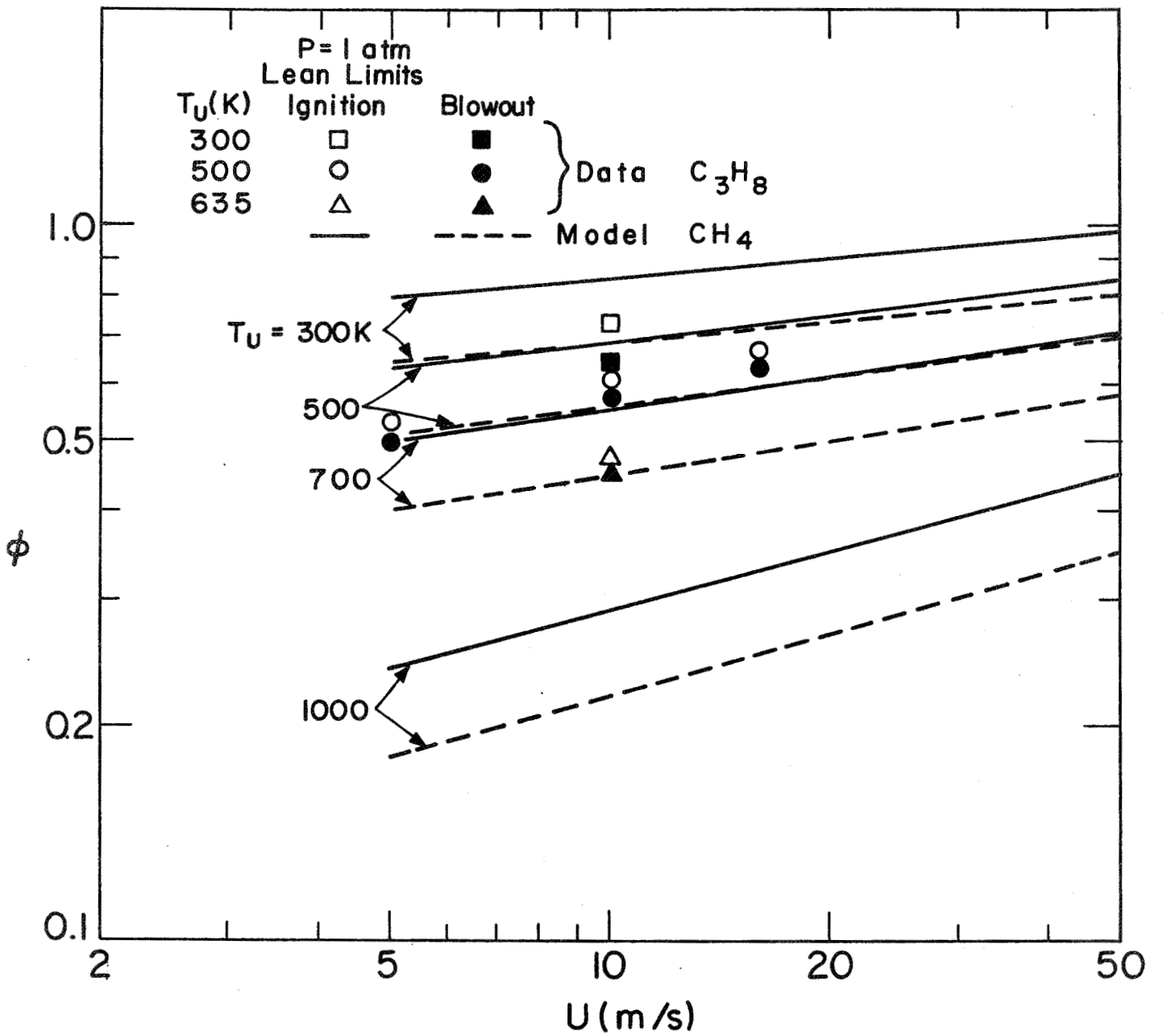

Variations of Measured and Predicted Limits with Velocity

Inlet Mixture Nonuniformity

Gaussian Distribution Function in Fuel Fraction, F

$$f(F) = (2\pi\sigma)^{-1/2} \exp\{-(F-\bar{F})^2/2\sigma^2\}$$

Unmixedness Parameter

$$s = \sigma/\bar{F}$$

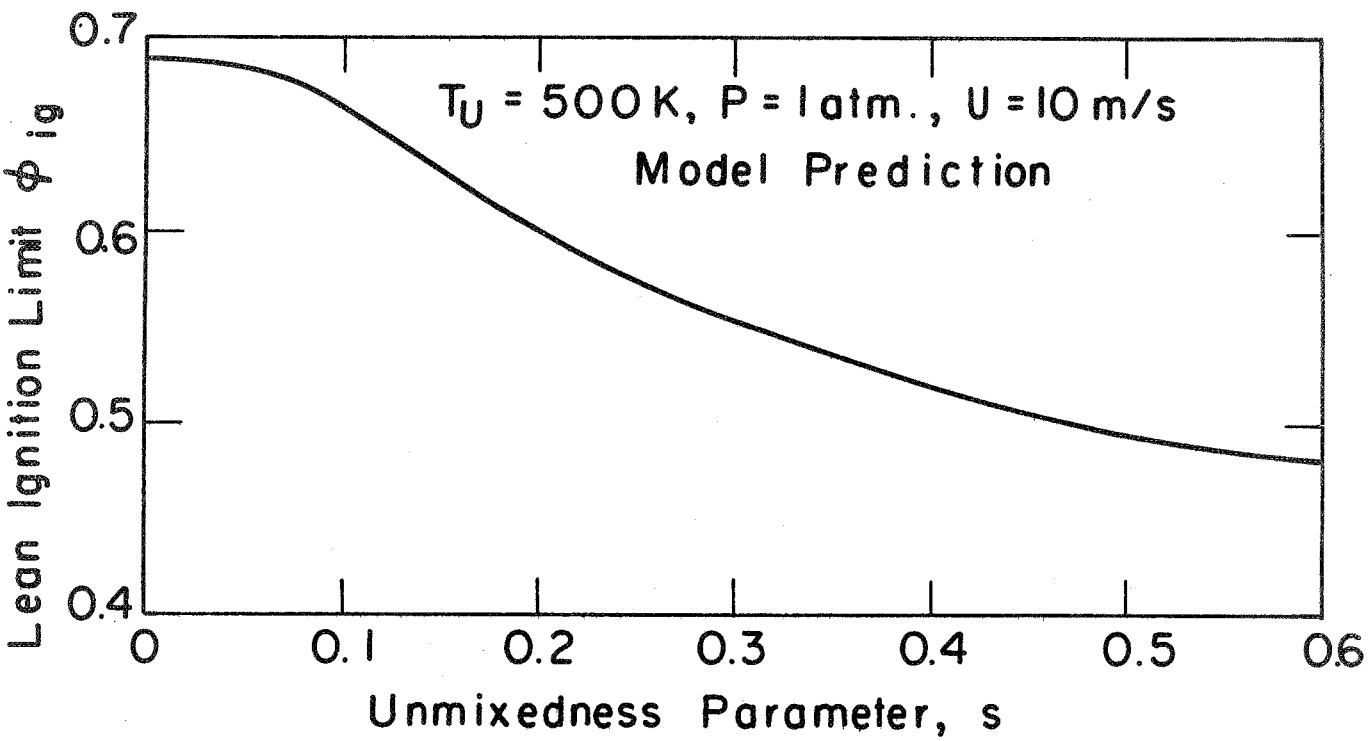

Effect of Inlet Mixture Nonuniformity on the Lean Ignition Limit

Effects of Premixing Length On
The Lean Ignition And Blowout Limits

T_u = 500K U = 10 m/s

P = 1 atm. Fuel: C_3H_8

PML	Experimental Limits (ϕ)	
m	Ignition	Blowout
2.50	0.61	0.57
1.27	0.60	0.56
0.65	0.52	0.48

STABILIZATION OF PREMIXED COMBUSTORS

by
R. F. Sawyer, J. W. Daily, and A. K. Oppenheim
University of California, Berkeley

In order to attain a sufficiently good insight into the fluid mechanical processes taking place in combustors operating on premixed, prevaporized, and preheated gases, an experimental facility has been developed where the flow field is tractable both experimentally and analytically. The test section is for this purpose of rectangular, 7 in. x 2 in. cross-section, fitted with fused quartz windows to provide an unobstructed view of the combustion chamber across its full 2 in. width, over a length of 9 inches.

The configuration adopted for the initial stage of the study is based on the use of a step to stabilize the combustion zone. Its height is 1 in. -- half the width of the combustor. The flow field created in this manner is considered to be representative of the wake generated by a flame holder.

The primary purpose of the experimental apparatus is to provide a facility for studying the effects of the elementary fluid mechanical processes on the stability of a model combustion system in order to further the understanding of the intrinsic mechanism of non-steady phenomena, rather than to provide criteria for unstable operation of combustors, as expressed by overall performance parameters, such as the blowout and flashback limits. The ultimate objective nonetheless -- one should not forget -- is the acquisition of fundamental information that would be instrumental in extending these limits.

Accordingly the program of study embodied the following phases:

1. Determination of the flow field under steady operating conditions

2. Development of diagnostic point measurement techniques

3. Study of non-steady phenomena with particular emphasis on the mechanism of flashback and auto-ignition.

Phase 1 has been essentially completed under the direction of R. F. Sawyer (viz. "An Experimental Study of the Flow Field and Pollutant Formation in a Two-Dimensional Premixed, Turbulent Flame" by A. R. Ganji and R. F. Sawyer, Paper No. 79-0017, A.I.A.A. Seventeenth Aerospace Sciences Meeting, New Orleans, Louisiana, January 15-19, 1979). Phase 2 is nearing completion under the direction of J. W. Daily. Phase 3 is to be conducted under the direction of A. K. Oppenheim. In the enclosed copies of illustrations, the first eight pertain to Phase 1, the following four -- to Phase 2, and the last two -- to Phase 3. The experimental program will be concerned primarily with the observation and measurements of non-steady flow fields associated with transient response of the combustion system to a step change in operating conditions. Of the latter, the particular effect to be studied first will be that of a sudden enrichment of the fuel-air mixture.

FIGURE CAPTIONS

1. Experimental Apparatus

2. Stability Map

3. Schlieren Photographs of Wake Stabilized Combustion Zone at Various Inlet Velocities and Reynolds Numbers (T_0 = 295°K)

4. Two Extracts of Schlieren Movies
   (a) Steady Vortex Sheet
   (b) Vortex Sheet Interacting with Recirculation Zone
   (V_0 = 13.6 m/sec; Re = 8.8 x 10^3/cm; 0 = 0.57: T_0 = 295°K; time interval between frames: 1.22 msec)

5. Extract of Schlieren Movie at High Inlet Temperature
   (V_0 = 13.3 m/sec; Re = 3.9 x 10^3/cm; 0 = 0.53: T_0 = 454°K; time interval between frames: 0.67 msec)

6. Extract of Schlieren Movie Showing Blowout
   (V_0 = 9.2 m/sec; Re = 6 x 10^3/cm; 0 = 0.5: T_0 = 295°K; time interval between frames: 24 msec)

7. Extract of Schlieren Movie Showing Flashback
   (V_0 = 13.2 m/sec: Re = 8.5 x 10^3/cm; 0 = 0.57 switched to 0.68: T_0 = 295°K; time interval between frames 6.6 msec)

8. Pressure Transducer Records Showing the Flashback Mode and Normal Operation

9. Optical System for the Measurement of Density Fluctuations by Rayleigh Scattering

10. Frequency Spectrum of Density Fluctuations along the Center Line Measured by the Rayleigh Scattering Technique

11. Frequency Spectrum of Density Fluctuations Obtained from the Rayleigh Scattering Measurement at two Different Flow Velocities

13. Strategy Adopted for the Development of Numerical Techniques for Modeling Non-Steady Flows in Premixed Combustors

14. Computed Streakline Plots and Vortex Displacement Profiles for Incompressible Flow

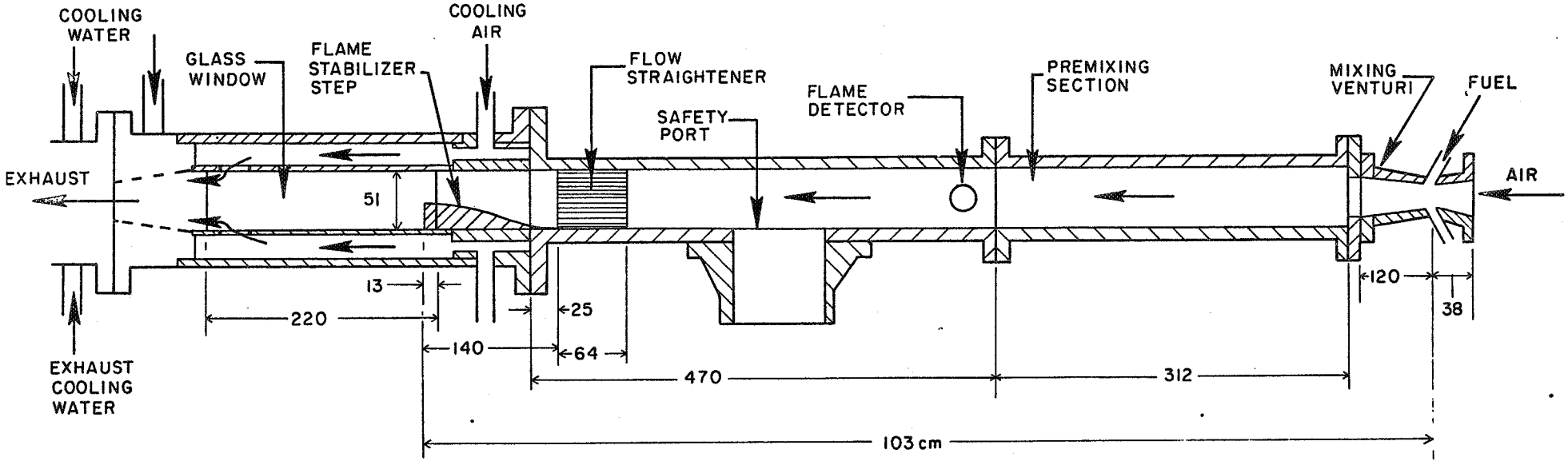

EXPERIMENTAL APPARATUS

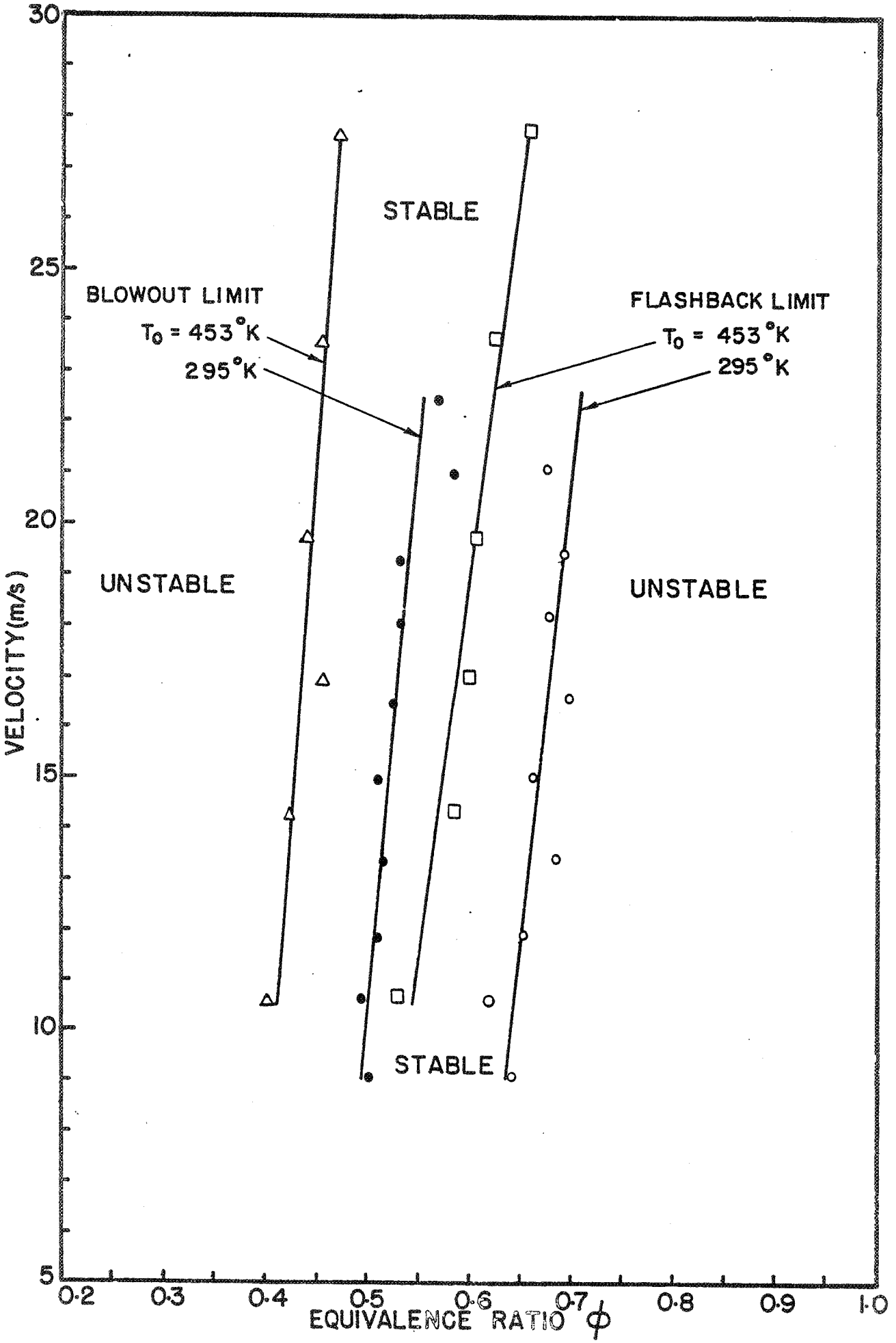
STABLE
BLOWOUT LIMIT
T_0 = 453°K
295°K
FLASHBACK LIMIT
T_0 = 453°K
295°K
UNSTABLE
UNSTABLE
STABLE
VELOCITY (m/s)
EQUIVALENCE RATIO ϕ
30
25
20
15
10
5
0·2
0·3
0·4
0·5
0·6
0·7
0·8
0·9
1·0

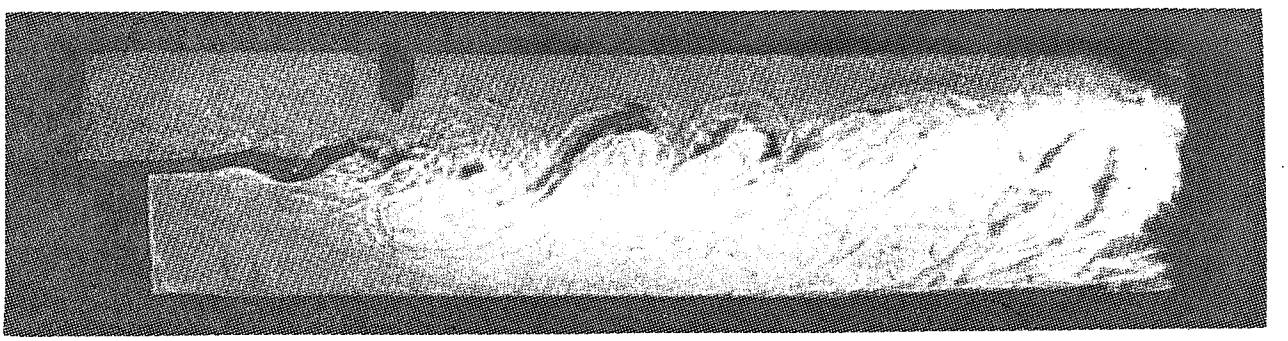

V = 9.1 (m/s) Re = 0.59 × 10⁴/cm ϕ = 0.6 t < 10⁻⁶ (s)

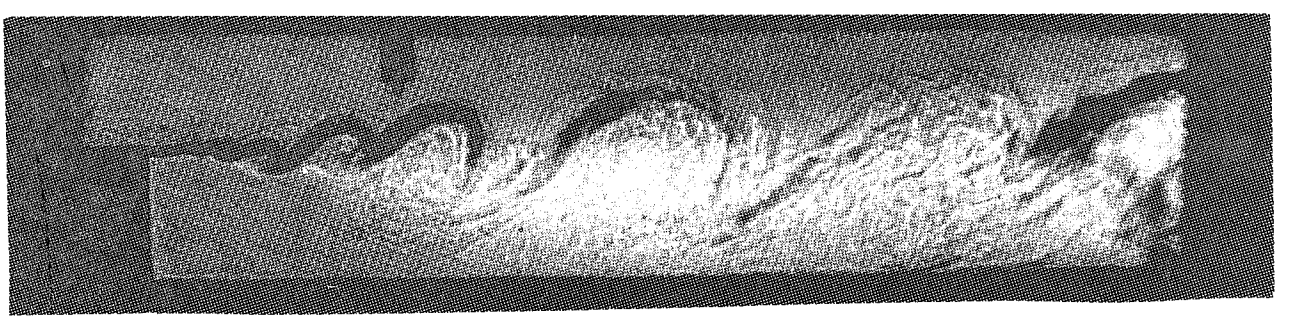

13.3 0.96 × 10⁴ 0.6 10⁻⁶

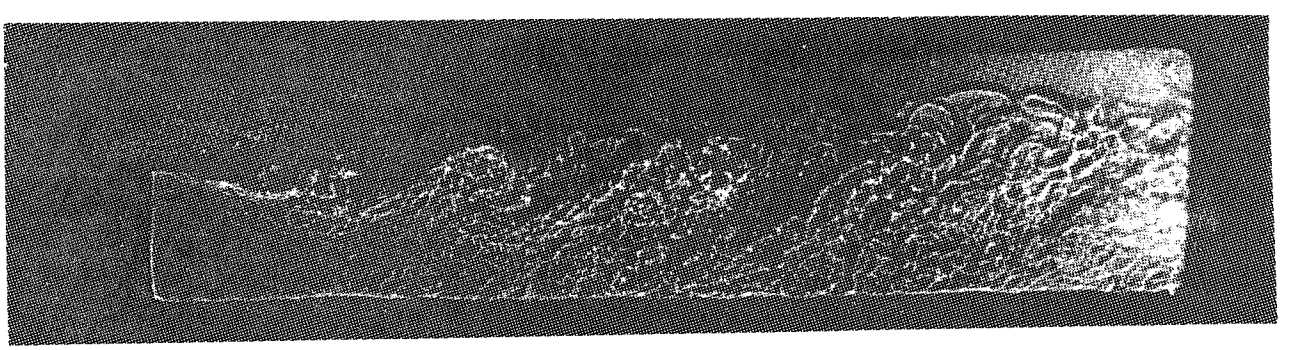

22.2 1.44 × 10⁴ 0.58 10⁻⁶

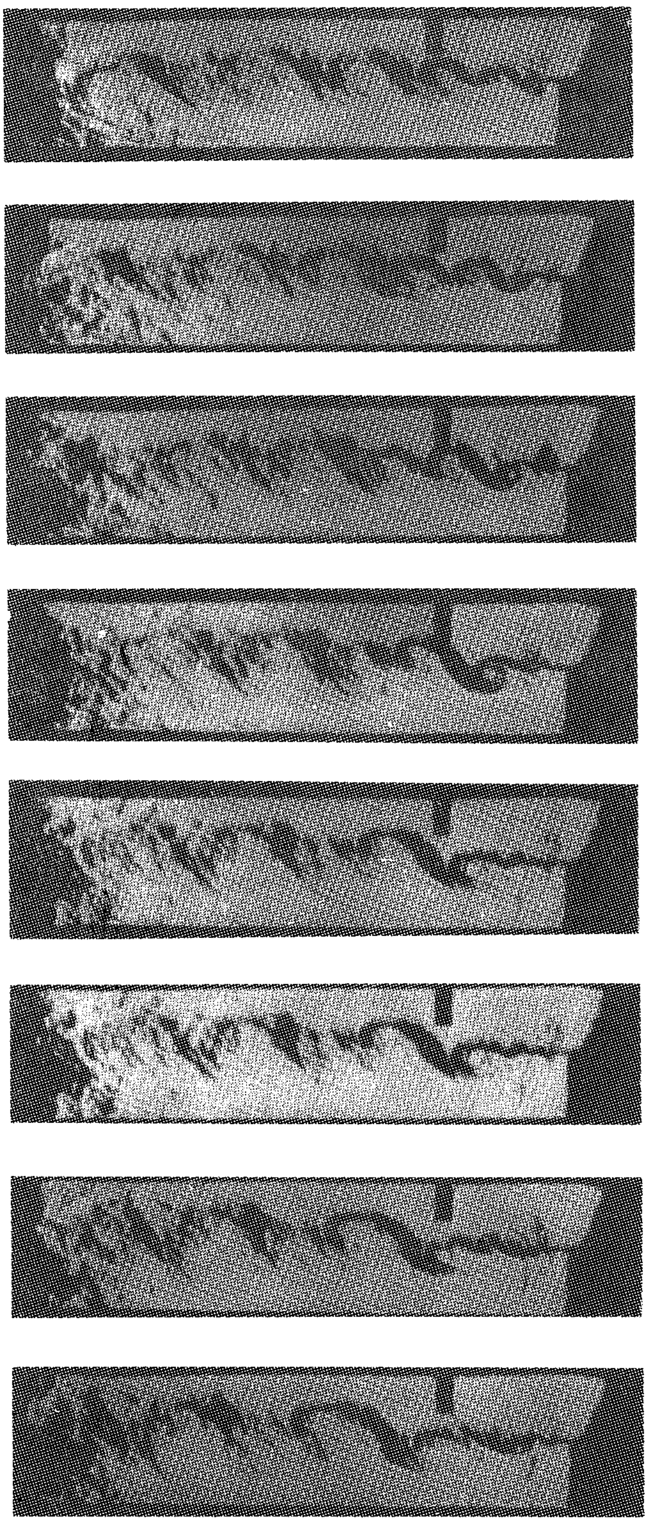

(а)

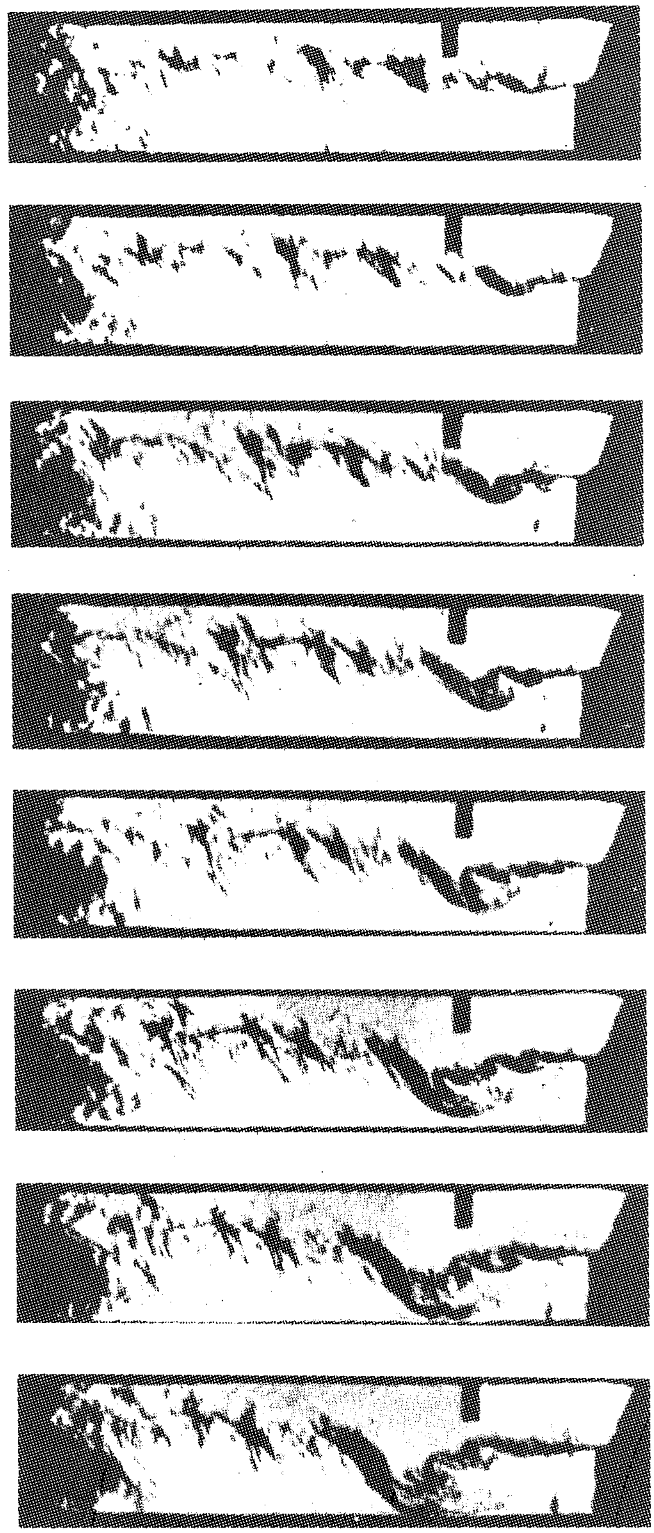

(б)

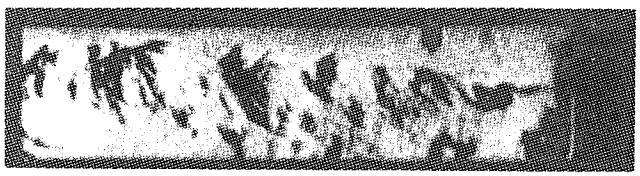
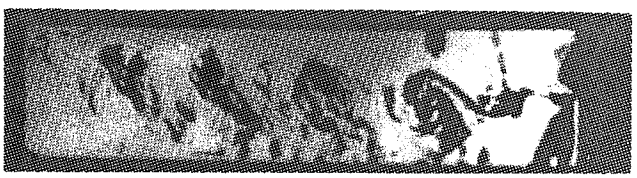
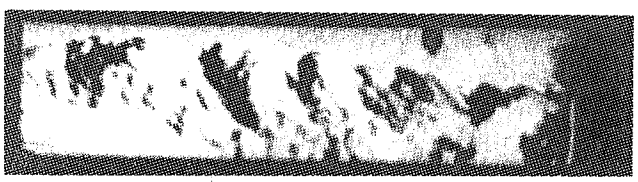
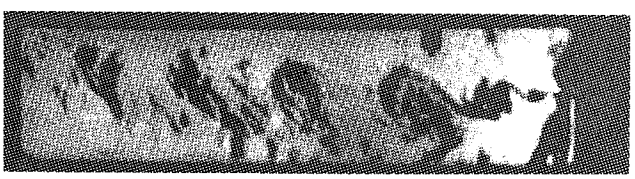
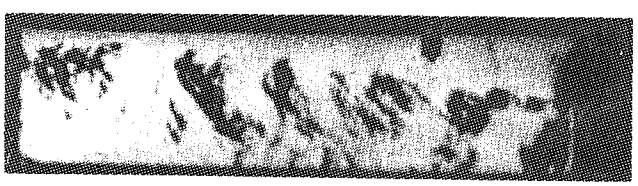

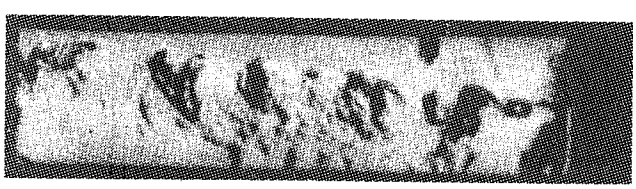
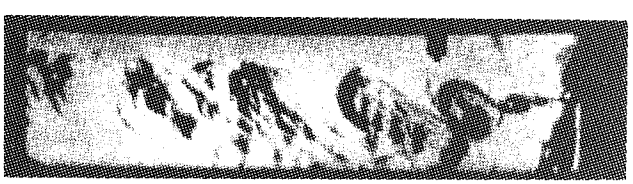
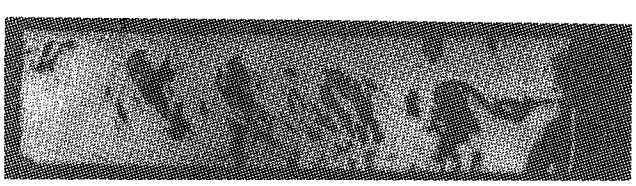







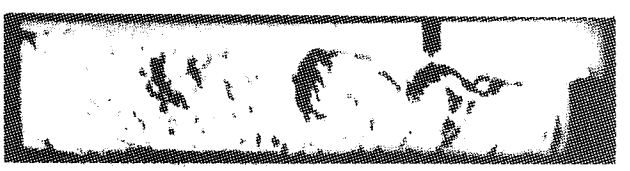
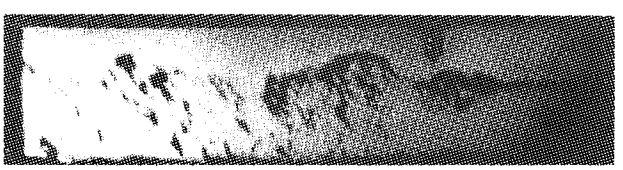
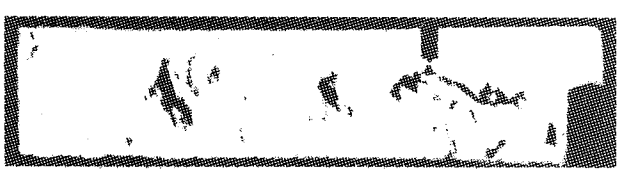
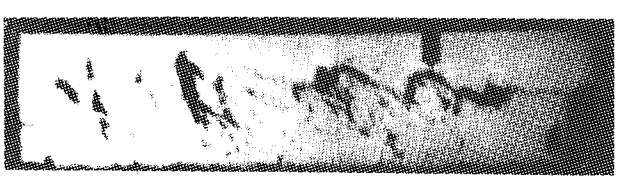
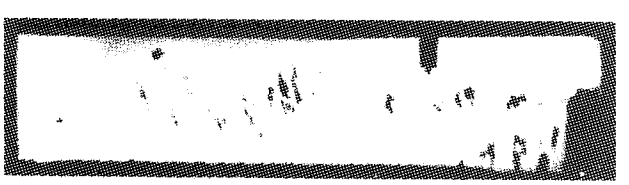




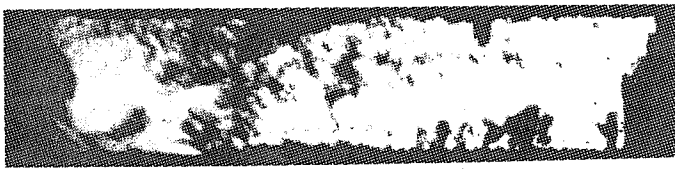
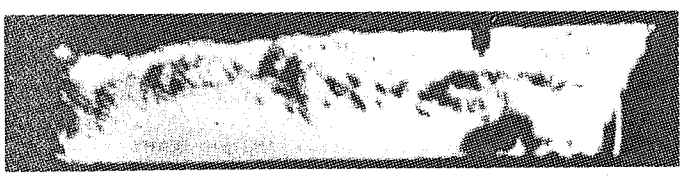
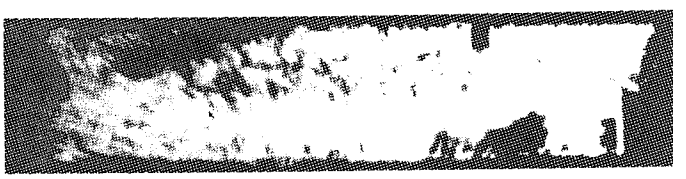


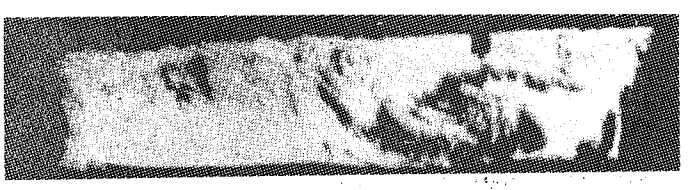


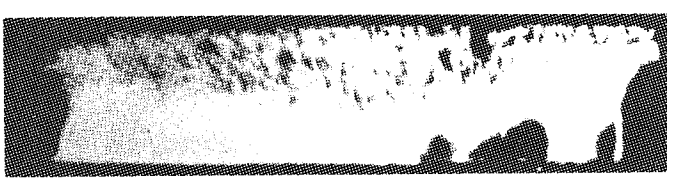
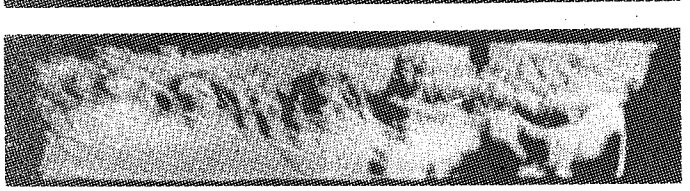


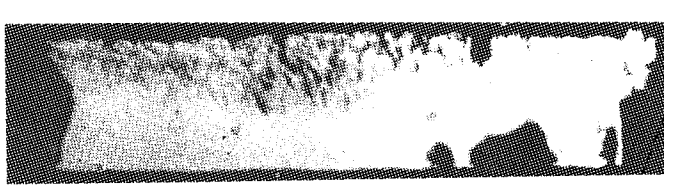


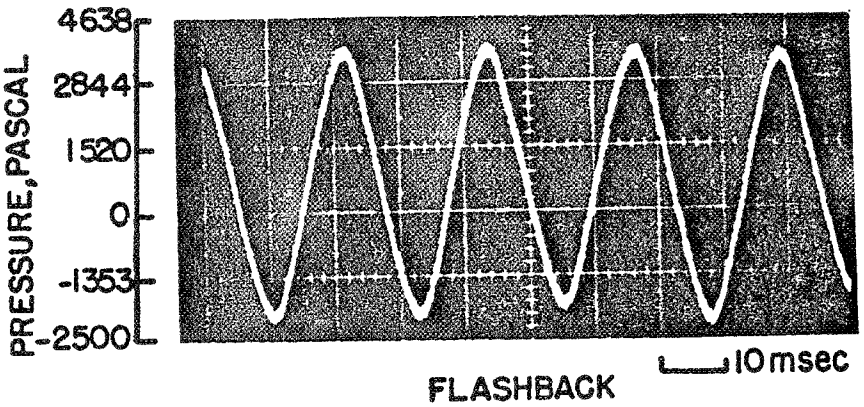
PRESSURE, PASCAL
4638
2844
1520
0
-1353
-2500
10 msec
FLASHBACK

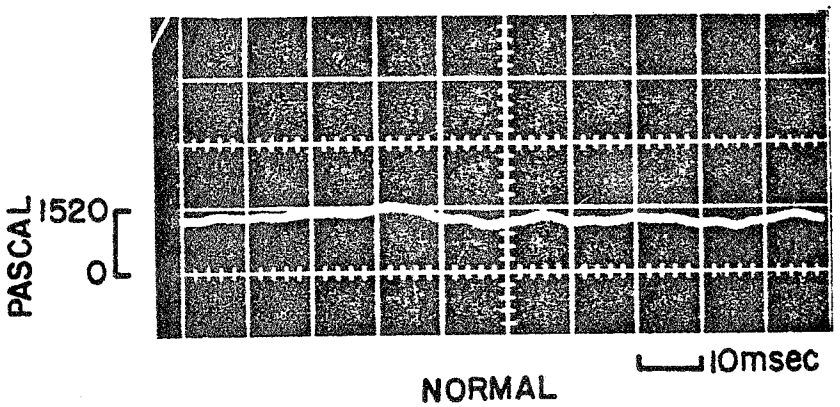
PASCAL
1520
0
10msec
NORMAL

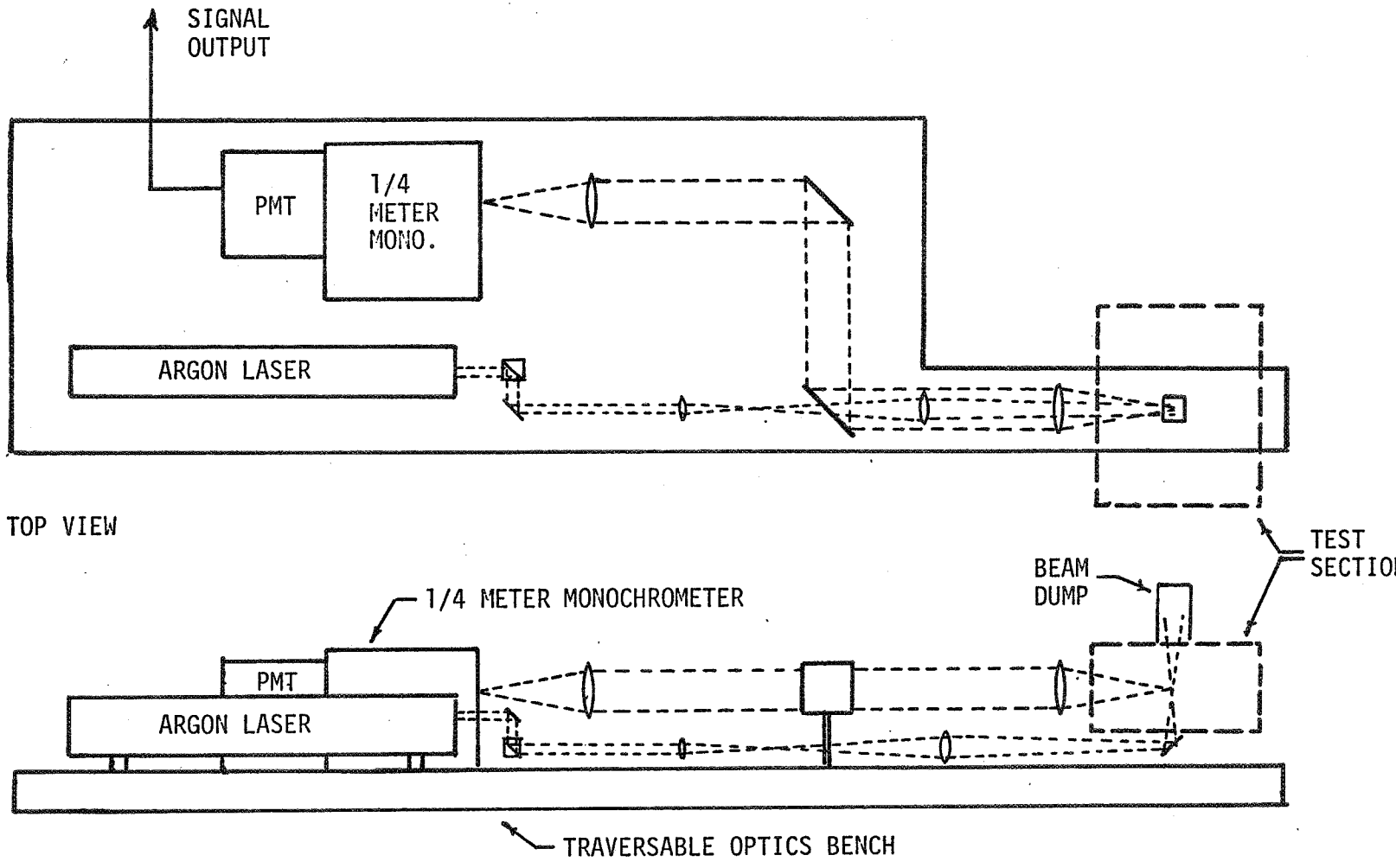
SIGNAL
OUTPUT
PMT
1/4
METER
MONO.
ARGON LASER
TOP VIEW
TEST
SECTION
BEAM
DUMP
1/4 METER MONOCHROMETER
PMT
ARGON LASER
TRAVERSABLE OPTICS BENCH
SIDE VIEW

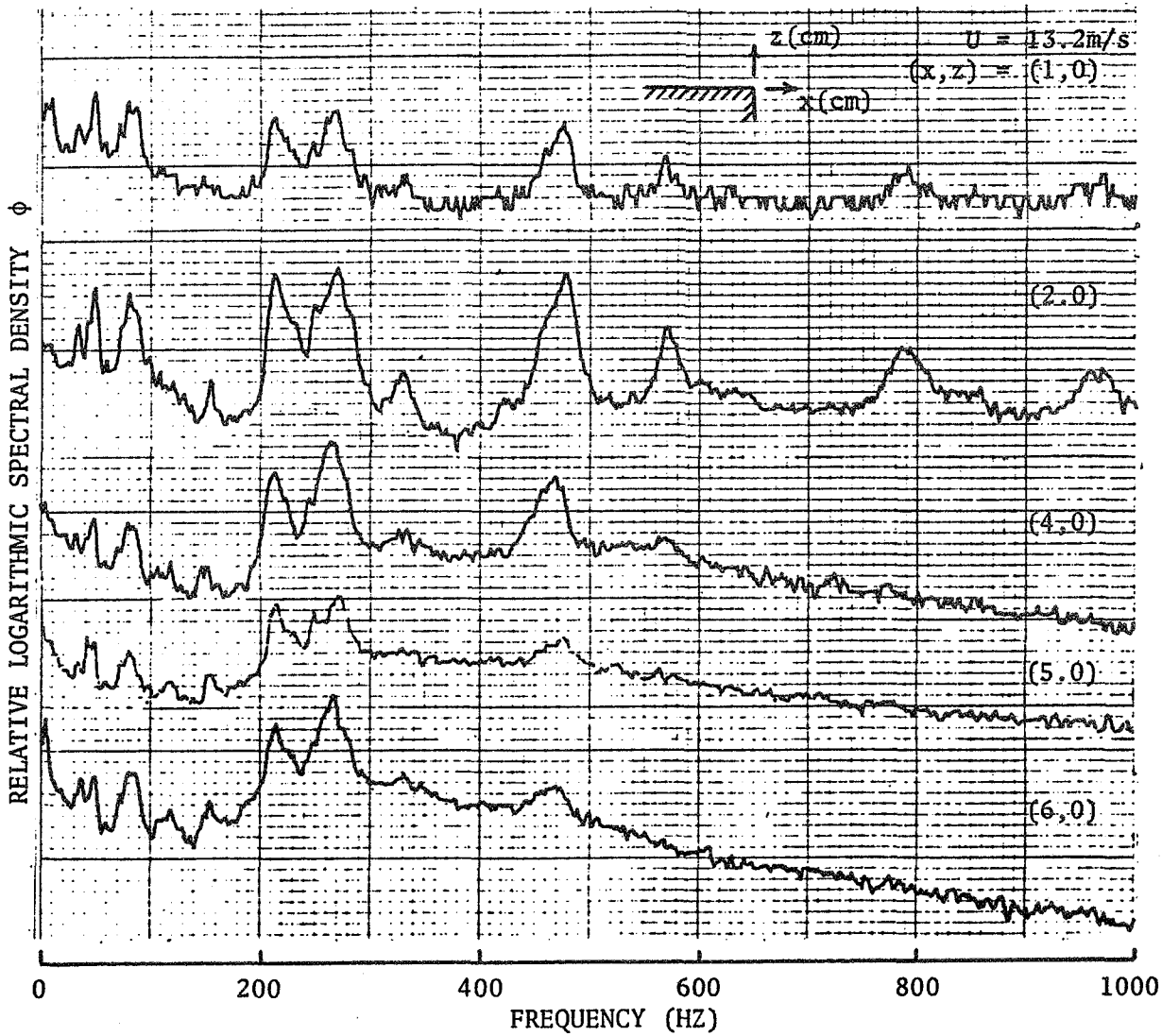
z(cm)
x(cm)
U = 13.2m/s
(x,z) = (1,0)
(2,0)
(4,0)
(5,0)
(6,0)
RELATIVE LOGARITHMIC SPECTRAL DENSITY φ
0
200
400
600
800
1000
FREQUENCY (HZ)

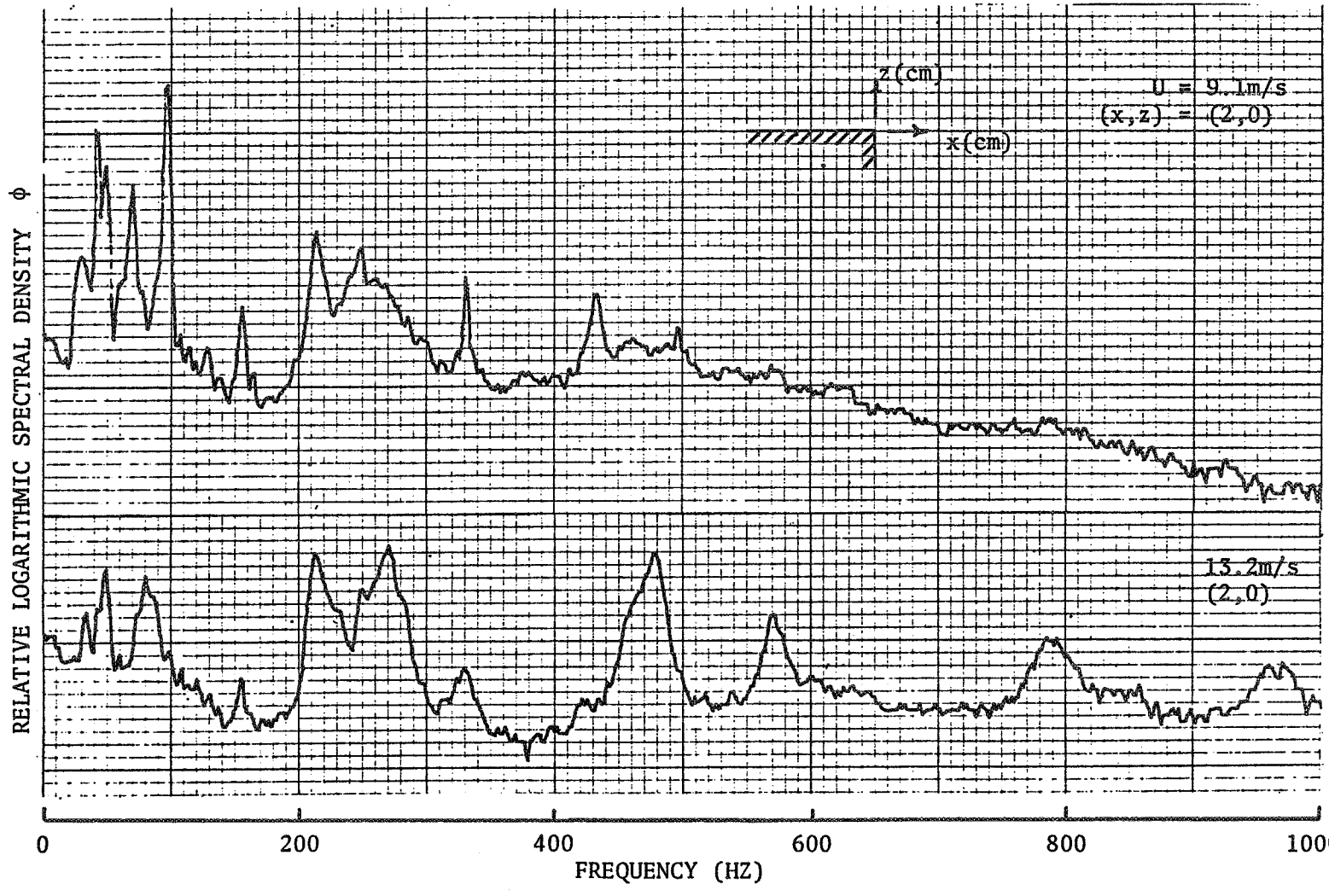
z(cm)
x(cm)
U = 9.1m/s
(x,z) = (2,0)
13.2m/s
(2,0)
RELATIVE LOGARITHMIC SPECTRAL DENSITY φ
0
200
400
600
800
1000
FREQUENCY (HZ)

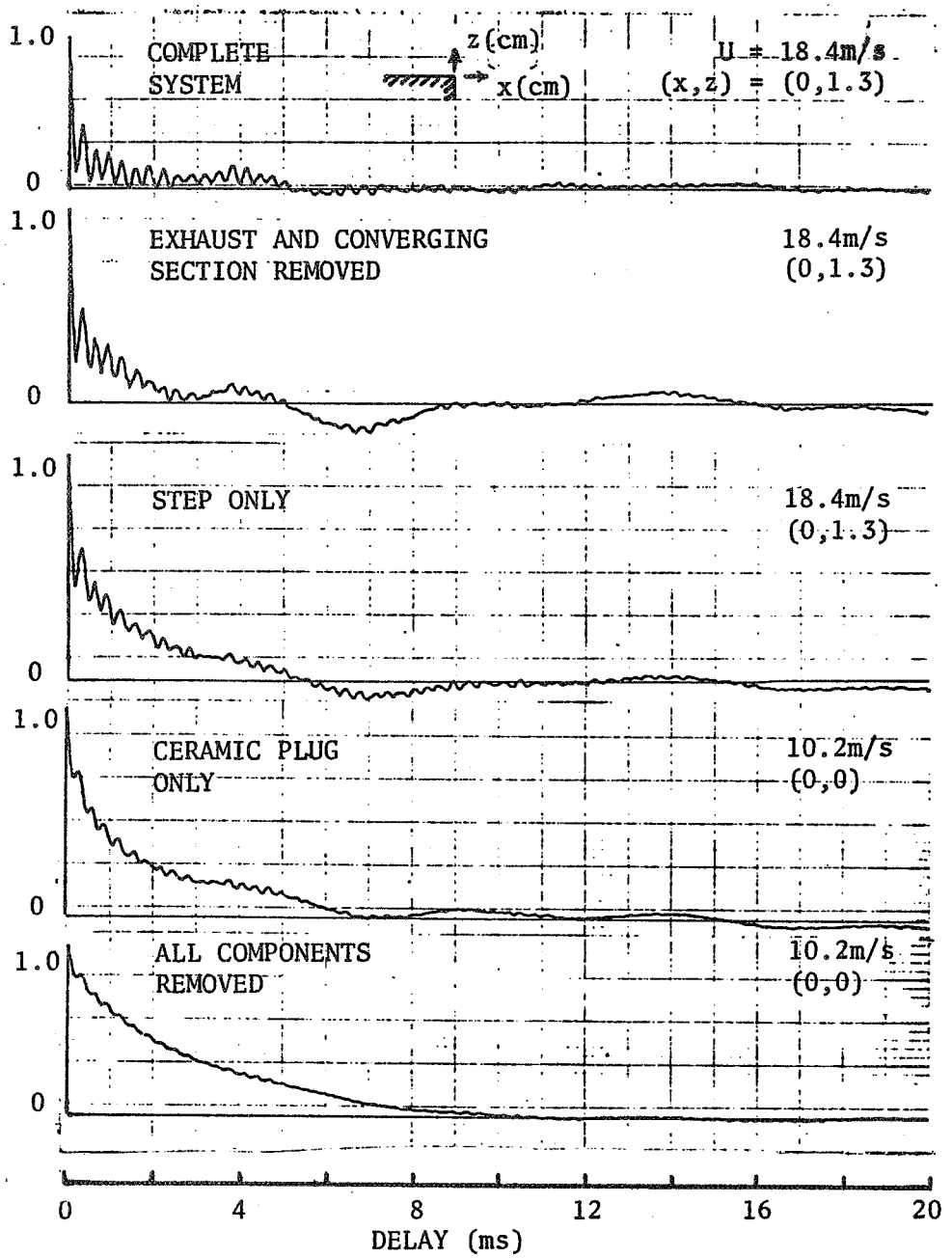
1.0
COMPLETE SYSTEM
z (cm)
x (cm)
U = 18.4m/s
(x,z) = (0,1.3)
0
1.0
EXHAUST AND CONVERGING SECTION REMOVED
18.4m/s
(0,1.3)
0
1.0
STEP ONLY
18.4m/s
(0,1.3)
0
1.0
CERAMIC PLUG ONLY
10.2m/s
(0,0)
0
1.0
ALL COMPONENTS REMOVED
10.2m/s
(0,0)
0
0
4
8
12
16
20
DELAY (ms)

DEVELOPMENT OF NUMERICAL TECHNIQUES

Phase 1 VISCOUS INCOMPRESSIBLE FLOW

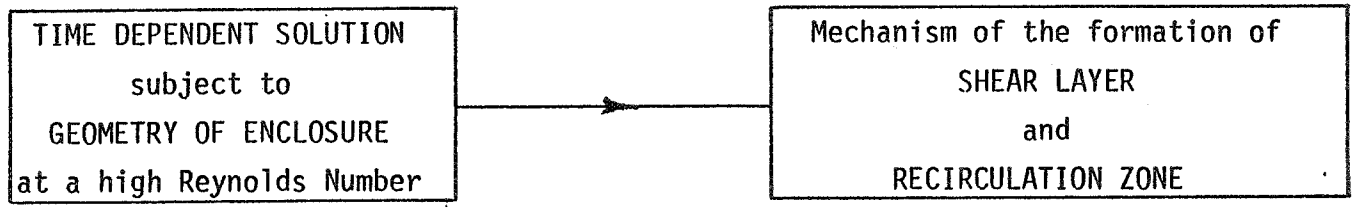

Phase 2 INFLUENCE OF COMPRESSIBILITY

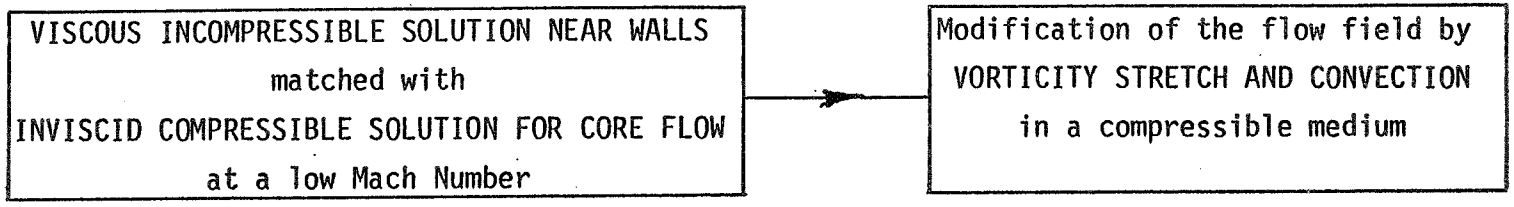

Phase 3 INFLUENCE OF COMBUSTION

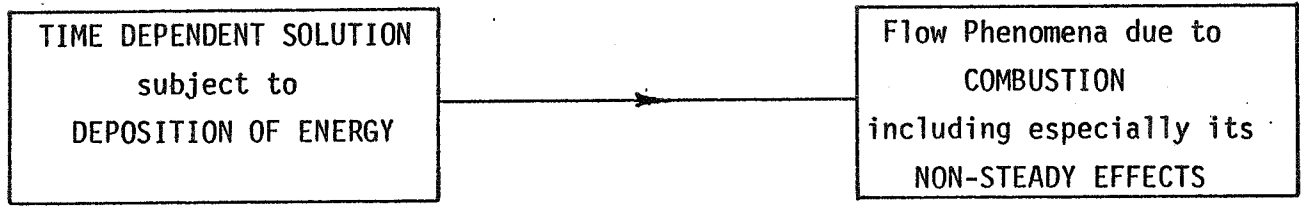

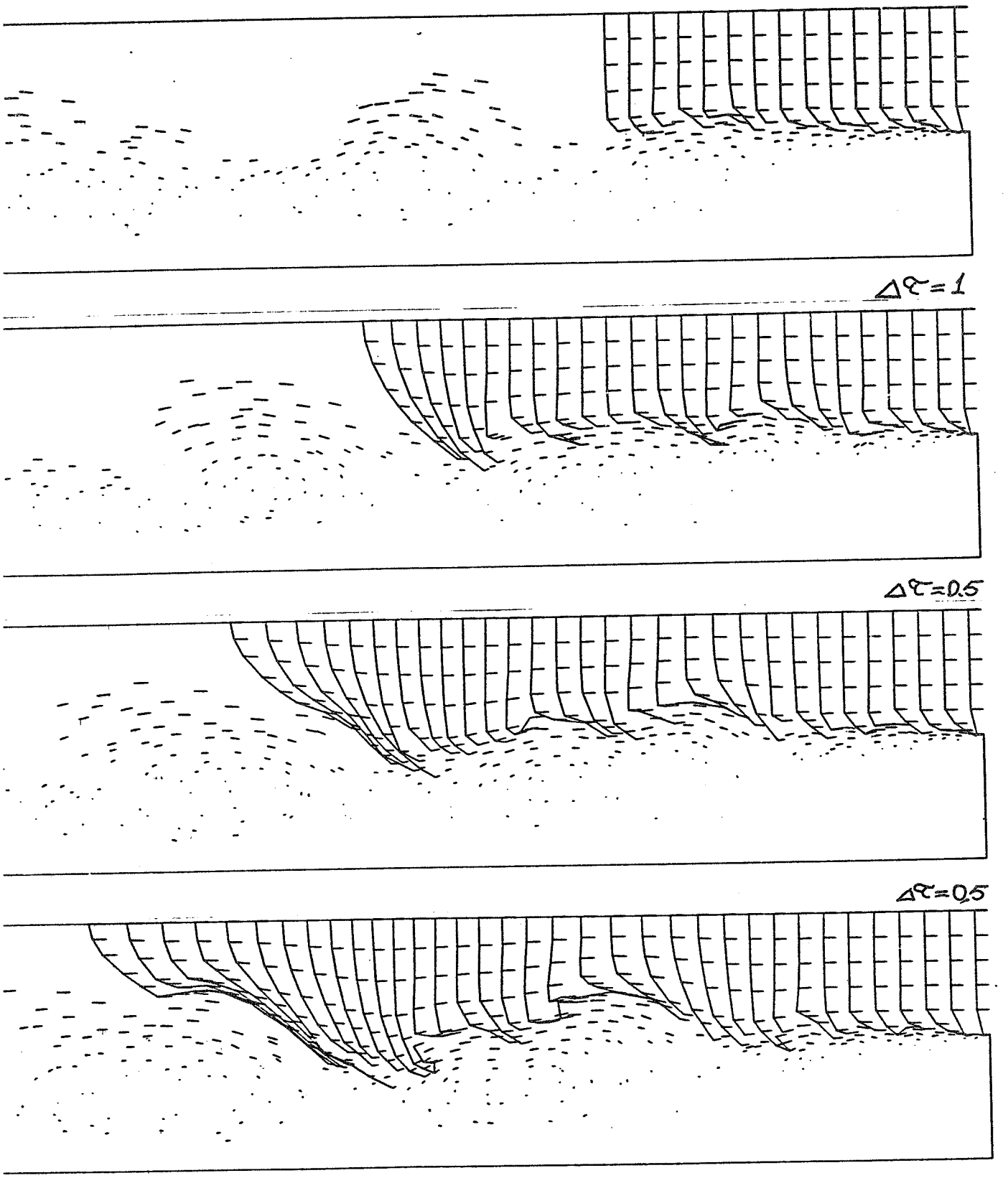
Δτ=1
Δτ=0.5
Δτ=0.5

EFFECT OF SWIRL ON PREMIXED COMBUSTION, by F. C. Gouldin and S. Leibovich

Many phenomena, including large scale flow recirculation, are observed in swirling flows. A particularly interesting set of flows, including closed recirculation zones, is often observed at sufficiently high Reynolds number and intermediate swirl levels. First observed in aerodynamic contexts, these phenomena have been referred to as vortex breakdown. The presence of a nearly stationary stagnation point on the axis and unsteady flow in the vortex core downstream of the front stagnation point are common characteristics of vortex breakdown. Experiments reveal a number of possible forms for vortex breakdown. Swirl flow combustors frequently exhibit similar flow features which we regard as additional examples of vortex breakdown. Such flow phenomena include central closed recirculation zones, and the "precessing vortex cores" reported by Syred and Beer.

Swirling flow and vortex breakdown have been studied at Cornell for over a decade. In recent years, attention has been focused on combustion in a premixed swirl combustor composed of confined concentric jets (5 cm and 10 cm diameter). The inner flow is fuel and air; the outer flow is air. Both flows may contain swirl either in the same (co-swirl) or opposite (counter-swirl) directions. The combustor operates at one atmosphere without preheat; methane and propane have been used as fuels. Related analyses and experiments have also been performed for water flows and isothermal air flows. In these studies a number of important concepts regarding premixed/prevaporized, swirl stabilized combustion have been developed. Some of the more significant will be discussed here.

Vortex breakdown exhibits a variety of forms. One of two forms, either the spiral form or the near axi-symmetric ("bubble") form, predominate, depending on inlet and boundary conditions. The occurrence of stagnation points in the vortex core, unsteady flow — usually containing a clear periodic disturbance — and the observed sensitivity to inlet and boundary conditions are all significant to the combustor designer. Not all vortex breakdowns provide a large central recirculation zone, but fortunately such recirculation zones may not be necessary for flame stabilization in premixed/prevaporized systems.

The adverse pressure gradient that can be produced in a vortex flow by dissipation of the swirling velocity component is frequently cited as the agent responsible for flow recirculation in the combustion literature. While adverse pressure gradients are involved in vortex breakdown, in cases of greatest interest they can be traced to kinematic effects in essentially inertia dominated flows, and are not produced by viscosity, or by inherently dissipative effects. The effect of an axial pressure gradient is, of course, magnified on the vortex core centerline by swirl.

Although vortex breakdowns are highly complex phenomena that still defy a completely satisfactory understanding, they have received considerable attention recently, and significant advances have been made. The development of a wave mechanism for breakdown by Squire, Benjamin and by Leibovich and his co-workers has enabled an explanation of many details of vortex breakdown flow. In this picture of vortex breakdown, inertial effects dominate. The wave model of Randall and Leibovich has been successful in predicting some features of the bubble form of vortex breakdown, such as the location and size of the recirculation zone. A major shortcoming of this theory is its restriction to axially symmetric flow. Thus the spiral form of breakdown is not accessible to the

theory. Furthermore, experiments convincingly show that the periodic oscillations present in both spiral and bubble forms of breakdowns are due to waves propagating in azimuth; thus the oscillations also fall outside the scope of an axisymmetric analysis. Oscillations observed in the recirculation zone and downstream subcritical flow have been traced by Garg and Leibovich to hydrodynamic instabilities. The emerging picture is of an inertia dominated flow sensitive to perturbation. If these perturbations can travel upstream, a vortex breakdown of some form will be present. Flow profiles and boundary conditions determine wave speed and type, hence, the sensitivity noted above.

A variety of experiments have been conducted in our combustor, including visual observations with a sodium tracer, blow-out measurements, and temperature and gas composition measurements throughout the combustor. A primary interest is in NO_x emissions for lean primary mixture operations. Expected reductions in emissions with leaner mixtures are observed. However, quenching of reaction in the mixing layer between the two jets causes reduced combustion efficiency and high CH_4 emissions. Most surprising is the observation of NO_2 in the exhaust. On the basis of these experiments a picture of the combustion process has been developed.

For liquid-fueled, diffusion flame combustors, two popular mechanisms, the stirred reactor recirculation zone model and the boundary layer ignition delay model, have been proposed for flame stabilization. Temperature and composition measurements and emission spectroscopy studies show that reaction is not uniformly distributed throughout the recirculation zone, and the stirred reactor model is therefore not appropriate for our combustor. The observation of reaction upstream of the recirculation zone and of insensitivity of the lean blow-out limits to recirculation zone size are difficult to explain in terms of the ignition delay model. In our combustor we believe that combustion takes place in a thick premixed turbulent flame-like structure. The flame is stabilized in the region of the forward stagnation point of the recirculation zone. Reaction propagates radially from this region while being convected downstream. Upstream convection of products in the recirculation zone is not essential to flame stability.

We believe that combustion in premixed/prevaporized combustors employing a free standing recirculation zone will be similar to what we observe. In these combustors, blow-out will depend on conditions in the forward stagnation region. Efficiency will depend on radial flame propagation. It is the low velocity region of flow upstream of the recirculation zone that makes combustion possible; upstream convection of hot products within the recirculation zone is not essential.

FIGURES

1. Photograph of typical axisymmetric vortex breakdown observed in water flow at approximately 2000 Reynolds number. For flow visualization, red dye is injected on the centerline; blue dye is injected off the centerline. Flow is left to right. The tube diverges slightly as is evident in the picture.

2. Mean Axial Velocity Profiles in Water Flow Containing Axisymmetric Vortex Breakdown as Measured by Laser Doppler Velocimetry. Re = 2560 based on flow rate and tube diameter. Axial positions of profiles are given by their distance from front stagnation point. Positive values denote positions downstream of the front stagnation point.

3. Time Mean Streamlines Inside Axisymmetric Vortex Breakdown for Flow of Figure 2. Note multicellular flow and multiple stagnation points.

4. Low Frequency Components of Energy Spectrum Measured by Laser Doppler Velocimetry at Three Radial Positions in the Recirculation Zone. Conditions are those of Figures 2 and 3. Fluctuations appear to be due to nonaxisymmetric waves.

5. Swirl combustor with pyrex test section in operation under co-swirl conditions (see Table 2). For ignition a continuous discharge spark ignitor is introduced through the port evident in the picture. During probe measurements a similar port in the stainless-steel test section was plugged to prevent flow distortion.

6. Swirl combustor in operation under counter-swirl conditions (see Table 2).

7. Schematic of swirl combustor showing swirl generators and test section. The approximate location of the recirculation zone is indicated. Axial measurement stations are noted by the letters a, b, c, etc.

8. Swirl combustor blow-off limits based on inner flow equivalence ratio for CH_4 firing. The combustion volume is estimated to $1.3 \times 10^{-3} m^3$ for all conditions.

9. Radial traverse for high co-swirl case. $S_o = 0.559$, $S_i = 0.523$, $\phi_i = 0.79$, $\phi_{oa} = 0.25$, $u_i/u_o = 1.5$, $u_{oa} \cong 23.3$ m/s.

10. Time mean isotherms (K) for co-swirl (a) and counter-swirl (b) conditions. R_o is the combustor radius and D_o its diameter.

11. Time mean isopleths of CH_4 (ppm) on a dry basis for co-swirl (a) and counter-swirl (b) conditions.

12. Radial profiles of line of sight CH and CO_2^+ emissions from combustor fired on methane (see Table 1). $X/D_o = 0.8$.

TABLE I. Combustor Operating Conditions

inner flow equivalence ratio (ϕ_i):	0.78
overall equivalence ratio (ϕ_{oa}):	0.23
overall average velocity (u_{oa}):	24.6 m/s
ratio of inner flow average velocity to outer flow average velocity:	1.4
inner flow swirl number (S_i):	0.493
outer flow swirl number, (S_o) co-swirl:	0.559
outer flow swirl number, counter-swirl:	-0.559*

*The minus sign is used to denote the counter-swirl condition, tangential velocities in the opposite direction for the two jet flows. As defined, the swirl number itself is positive.

$S = \int_{R_1}^{R_2} uvr^2 dr \Big/ R_2 \int^{R_2} u^2 r dr$. u and v are the axial and tangential velocities and R_1 and R_2 are the inner and outer radii of the jet in question.

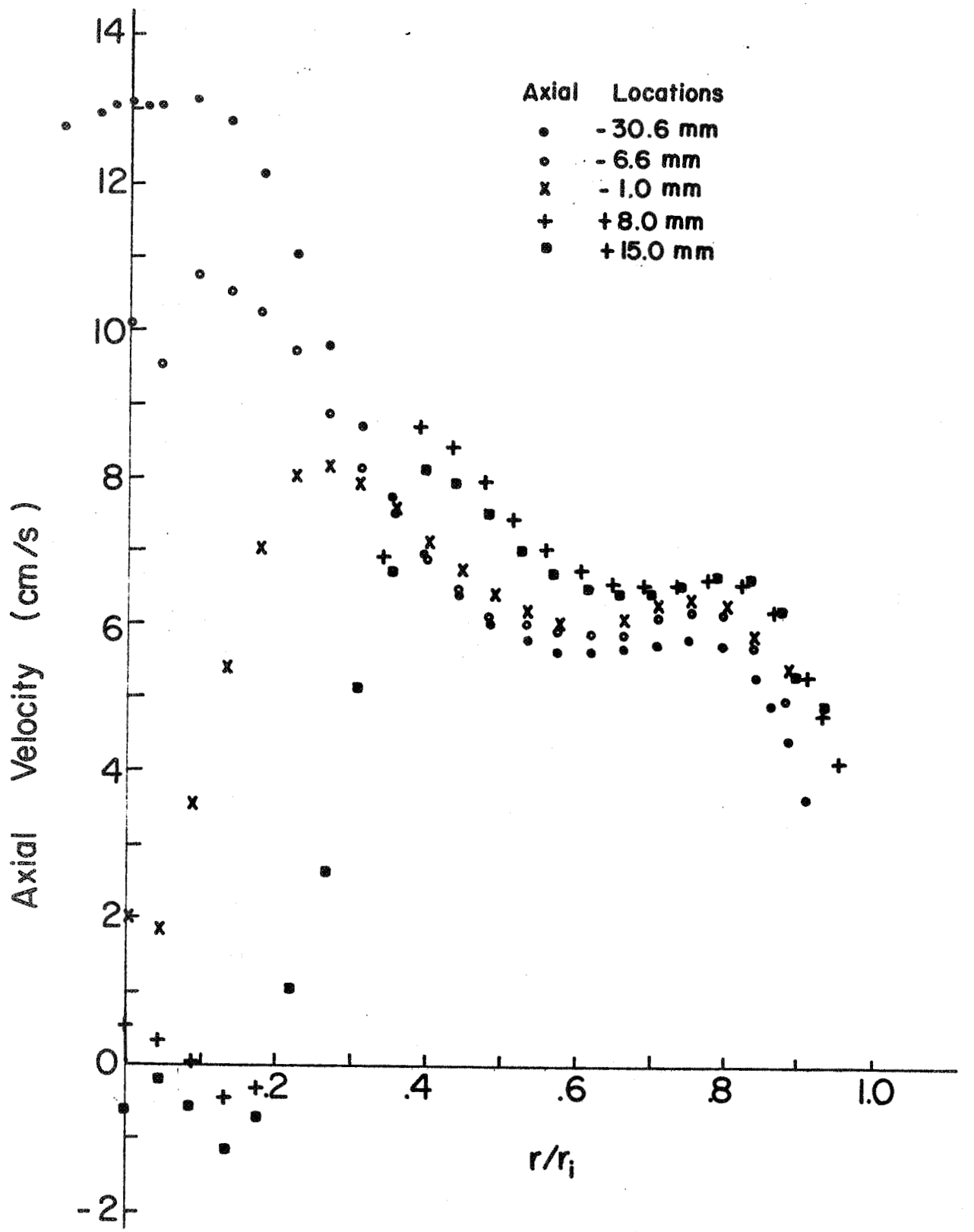
Axial Locations
- 30.6 mm
- 6.6 mm
- 1.0 mm
+ 8.0 mm
+ 15.0 mm
Axial Velocity (cm/s)
14
12
10
8
6
4
2
0
-2
+.2
.4
.6
.8
1.0
r/r_i

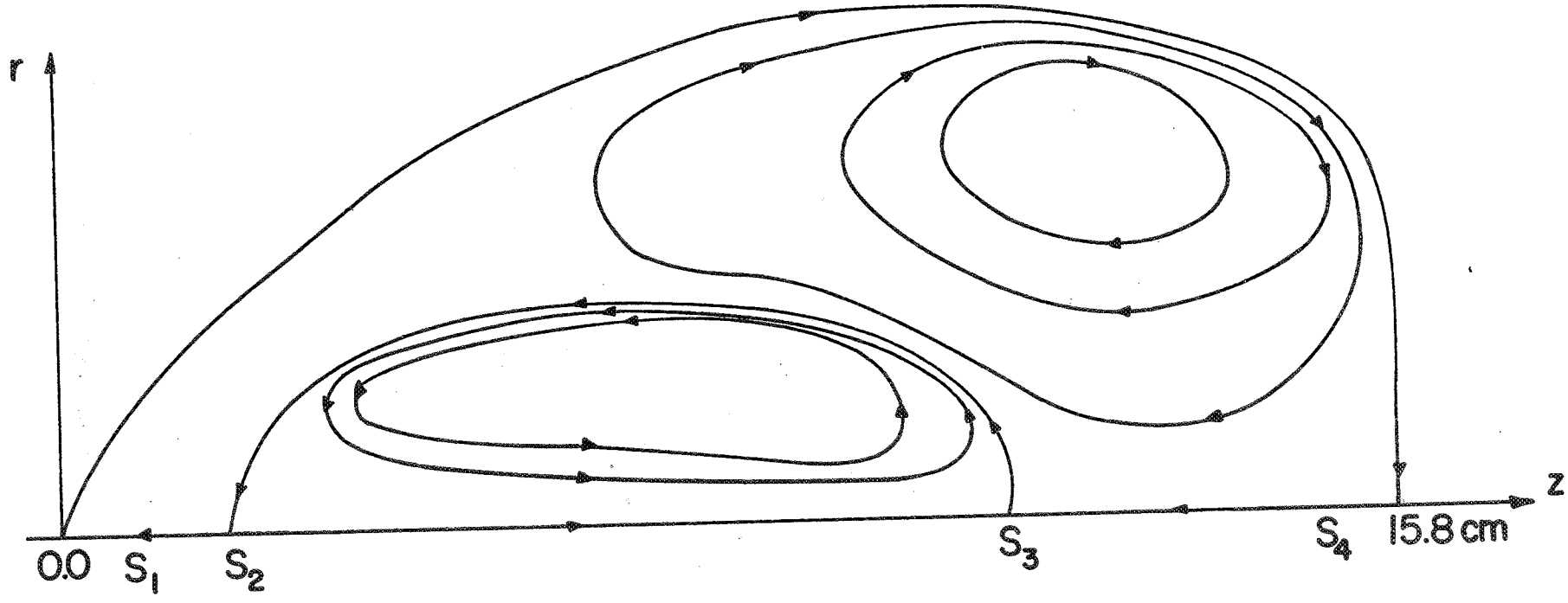

Time Averaged Streamlines

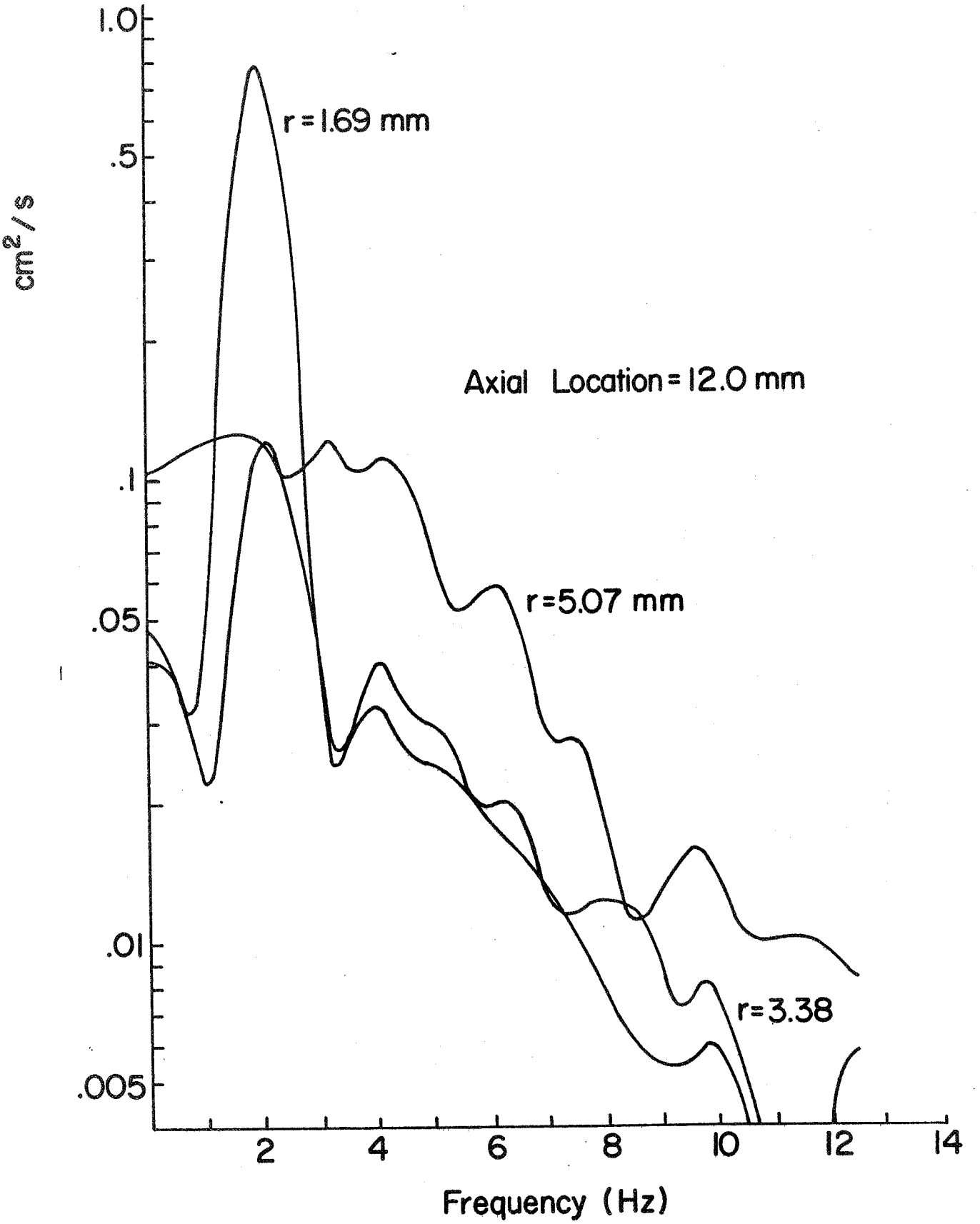
1.0
.5
.1
.05
.01
.005
cm²/s
r = 1.69 mm
Axial Location = 12.0 mm
r=5.07 mm
r=3.38
2
4
6
8
10
12
14
Frequency (Hz)

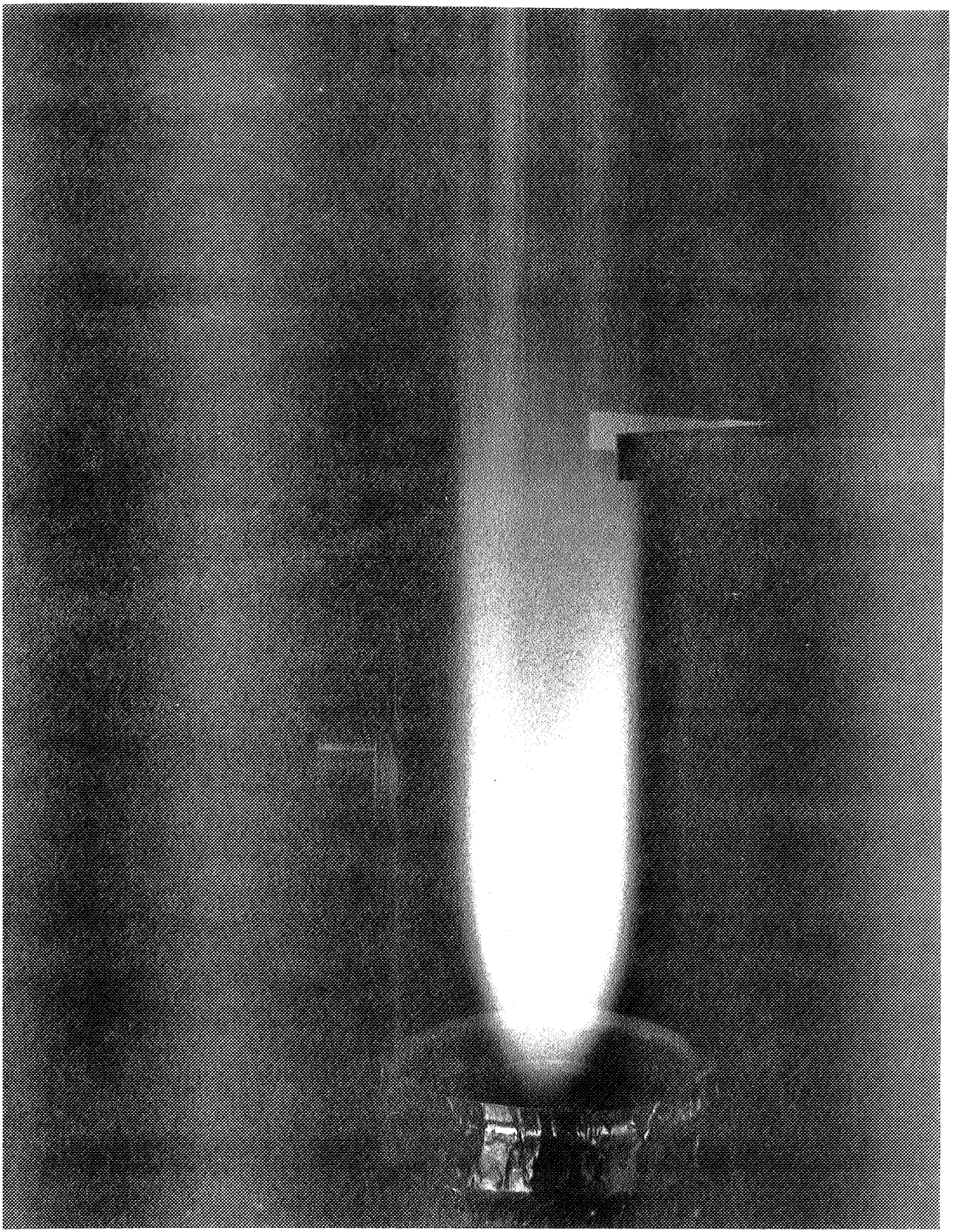

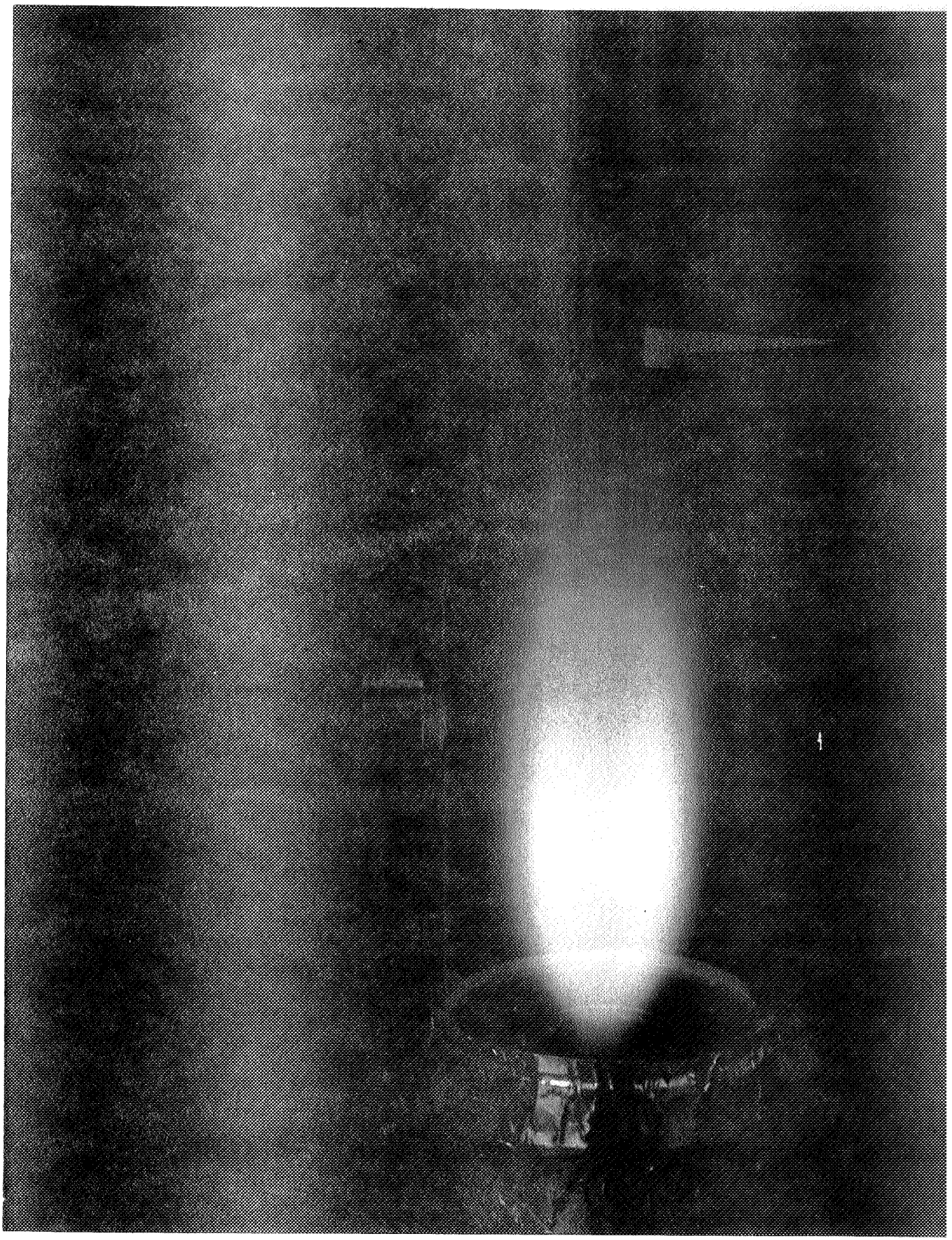

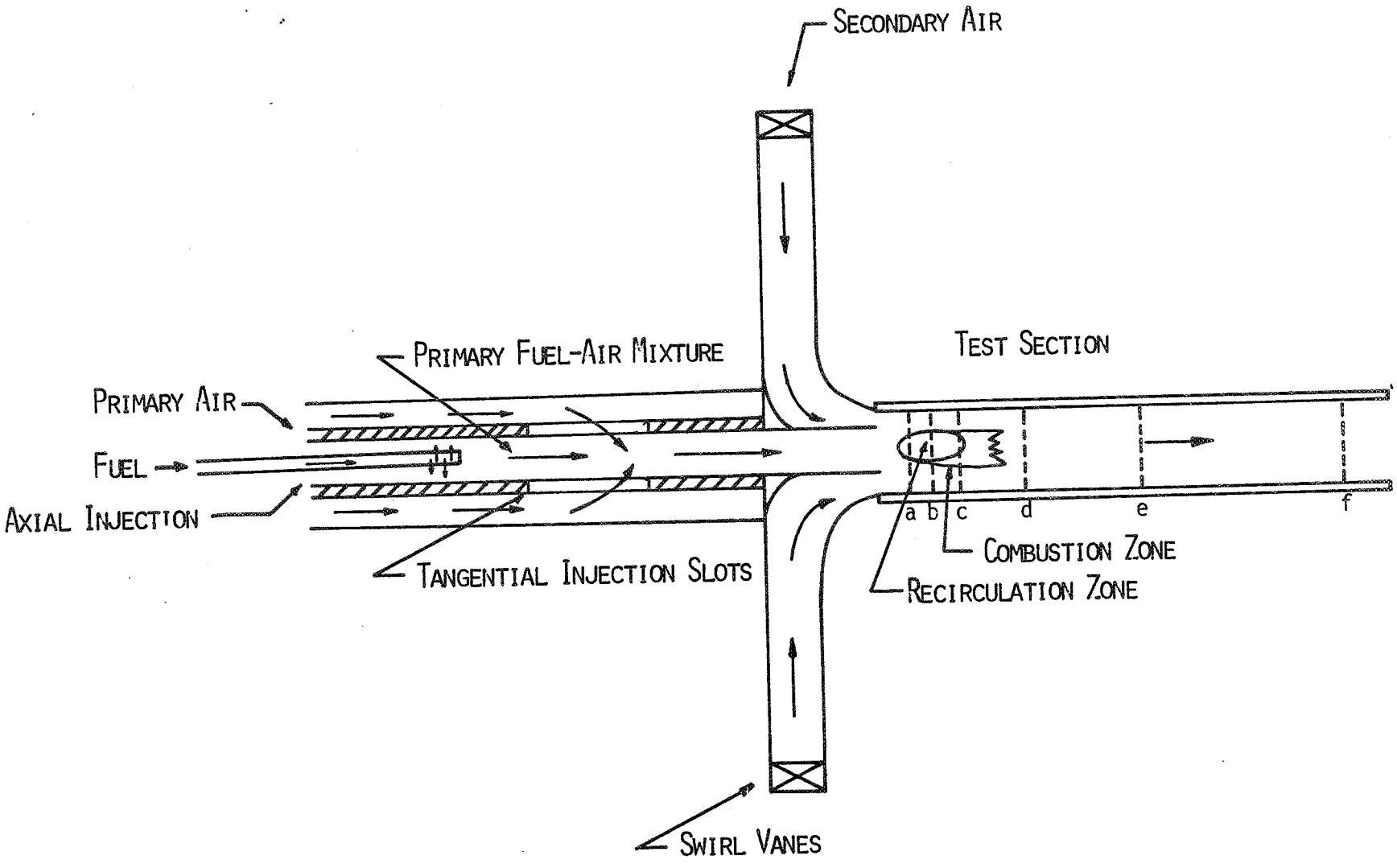
SECONDARY AIR
PRIMARY FUEL-AIR MIXTURE
TEST SECTION
PRIMARY AIR
FUEL
AXIAL INJECTION
TANGENTIAL INJECTION SLOTS
a b c d e f
COMBUSTION ZONE
RECIRCULATION ZONE
SWIRL VANES

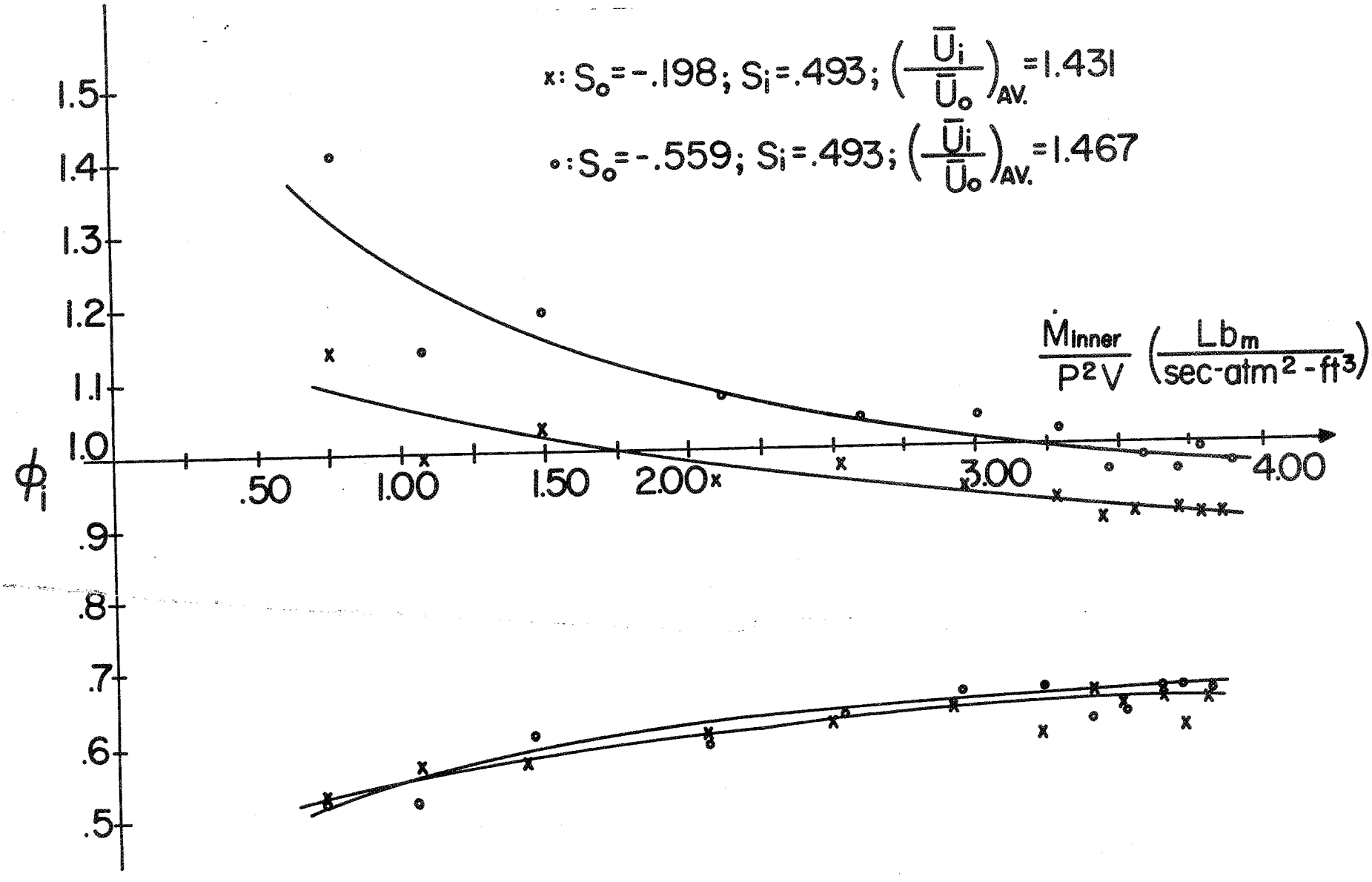
x: S_o = -.198; S_i = .493; $\left(\frac{\bar{U}_i}{\bar{U}_o}\right)_{AV.}$ = 1.431
o: S_o = -.559; S_i = .493; $\left(\frac{\bar{U}_i}{\bar{U}_o}\right)_{AV.}$ = 1.467
$\frac{\dot{M}_{inner}}{P^2V}$ $\left(\frac{Lb_m}{sec\text{-}atm^2\text{-}ft^3}\right)$
ϕ_1
1.5
1.4
1.3
1.2
1.1
1.0
.9
.8
.7
.6
.5
.50
1.00
1.50
2.00
3.00
4.00

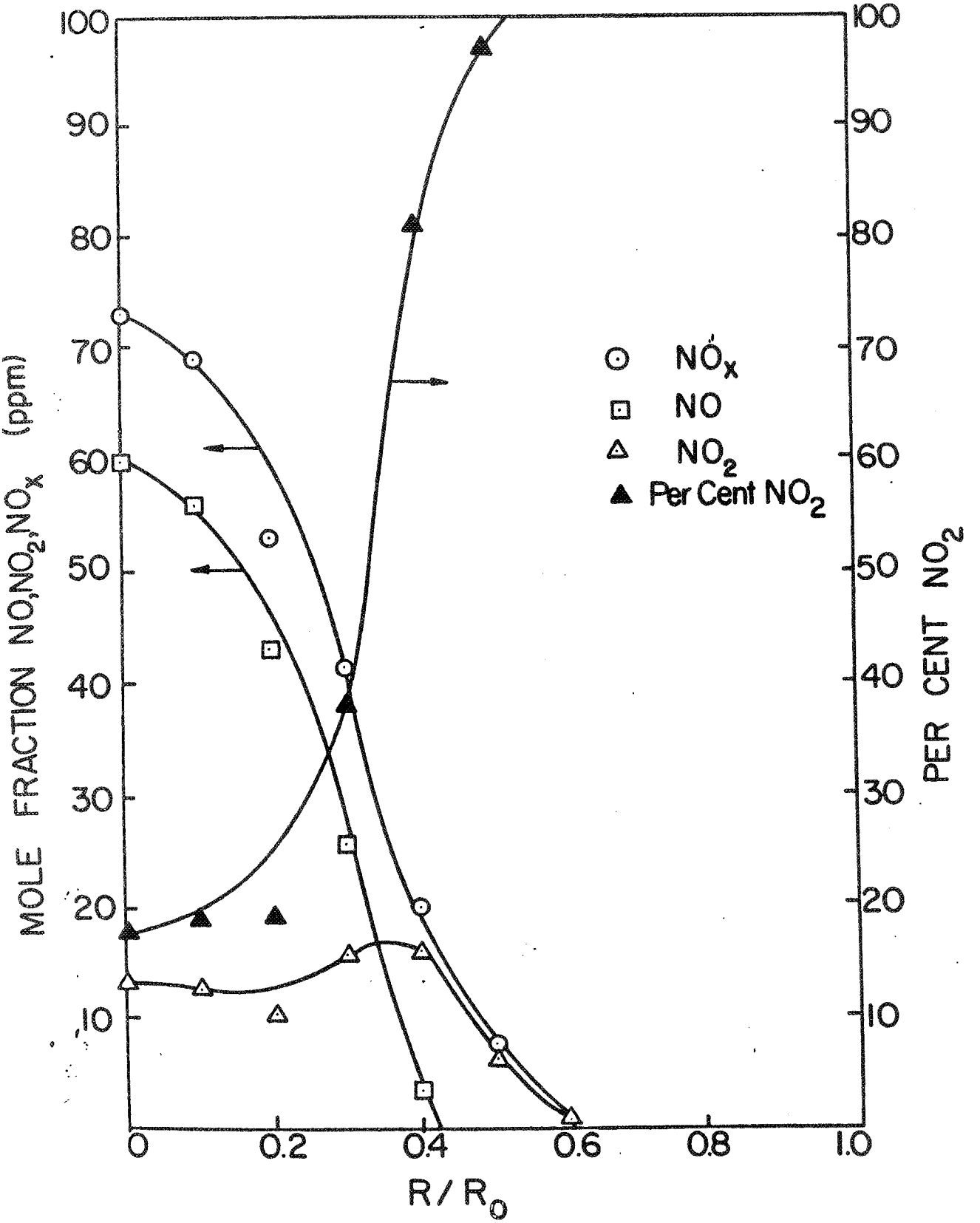
MOLE FRACTION NO, NO2, NOx (ppm)
PER CENT NO2
R / R0
NOx
NO
NO2
Per Cent NO2
100
90
80
70
60
50
40
30
20
10
0
0.2
0.4
0.6
0.8
1.0

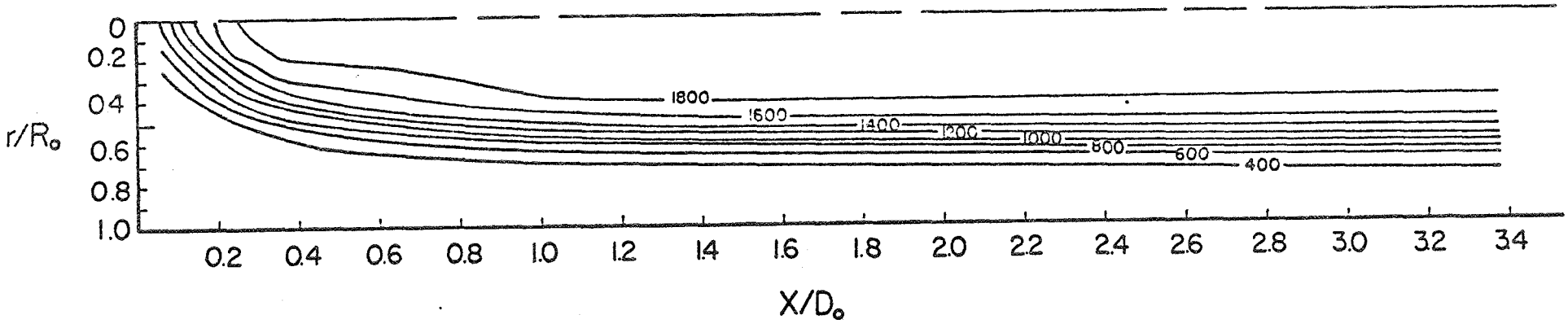
r/R₀
0
0.2
0.4
0.6
0.8
1.0
1800
1600
1400
1200
1000
800
600
400
0.2 0.4 0.6 0.8 1.0 1.2 1.4 1.6 1.8 2.0 2.2 2.4 2.6 2.8 3.0 3.2 3.4
X/D₀

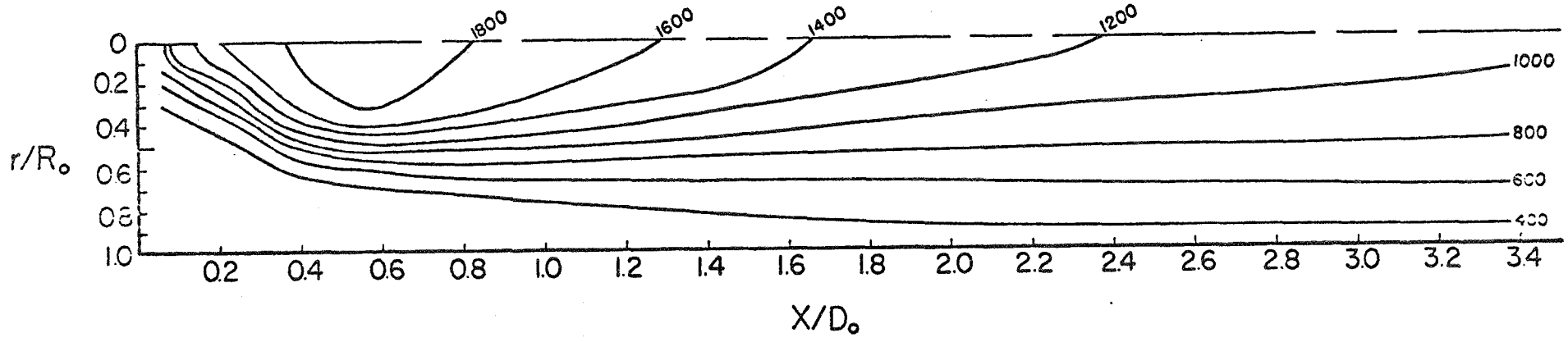
r/R₀
0
0.2
0.4
0.6
0.8
1.0
1800
1600
1400
1200
1000
800
600
400
0.2 0.4 0.6 0.8 1.0 1.2 1.4 1.6 1.8 2.0 2.2 2.4 2.6 2.8 3.0 3.2 3.4
X/D₀

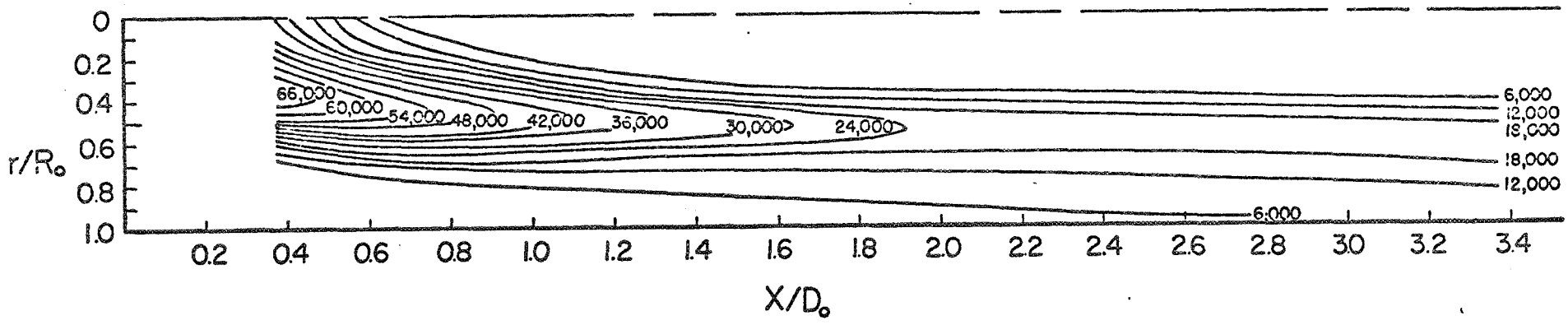
0
0.2
0.4
0.6
0.8
1.0
r/R₀
66,000
60,000
54,000
48,000
42,000
36,000
30,000
24,000
6,000
12,000
18,000
18,000
12,000
6,000
0.2 0.4 0.6 0.8 1.0 1.2 1.4 1.6 1.8 2.0 2.2 2.4 2.6 2.8 3.0 3.2 3.4
X/D₀

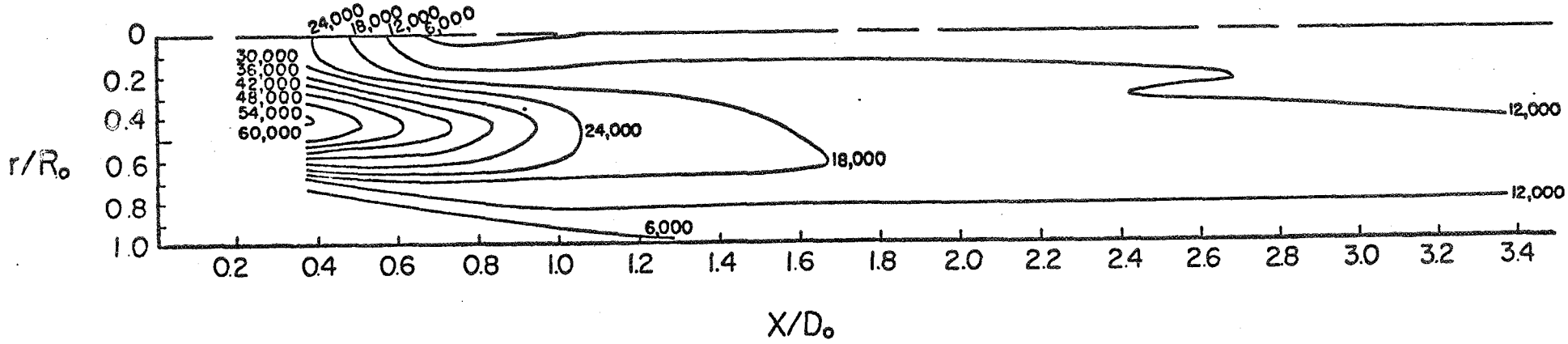
0
0.2
0.4
0.6
0.8
1.0
r/R₀
24,000
18,000
12,000
6,000
30,000
36,000
42,000
48,000
54,000
60,000
24,000
18,000
12,000
6,000
0.2 0.4 0.6 0.8 1.0 1.2 1.4 1.6 1.8 2.0 2.2 2.4 2.6 2.8 3.0 3.2 3.4
X/D₀

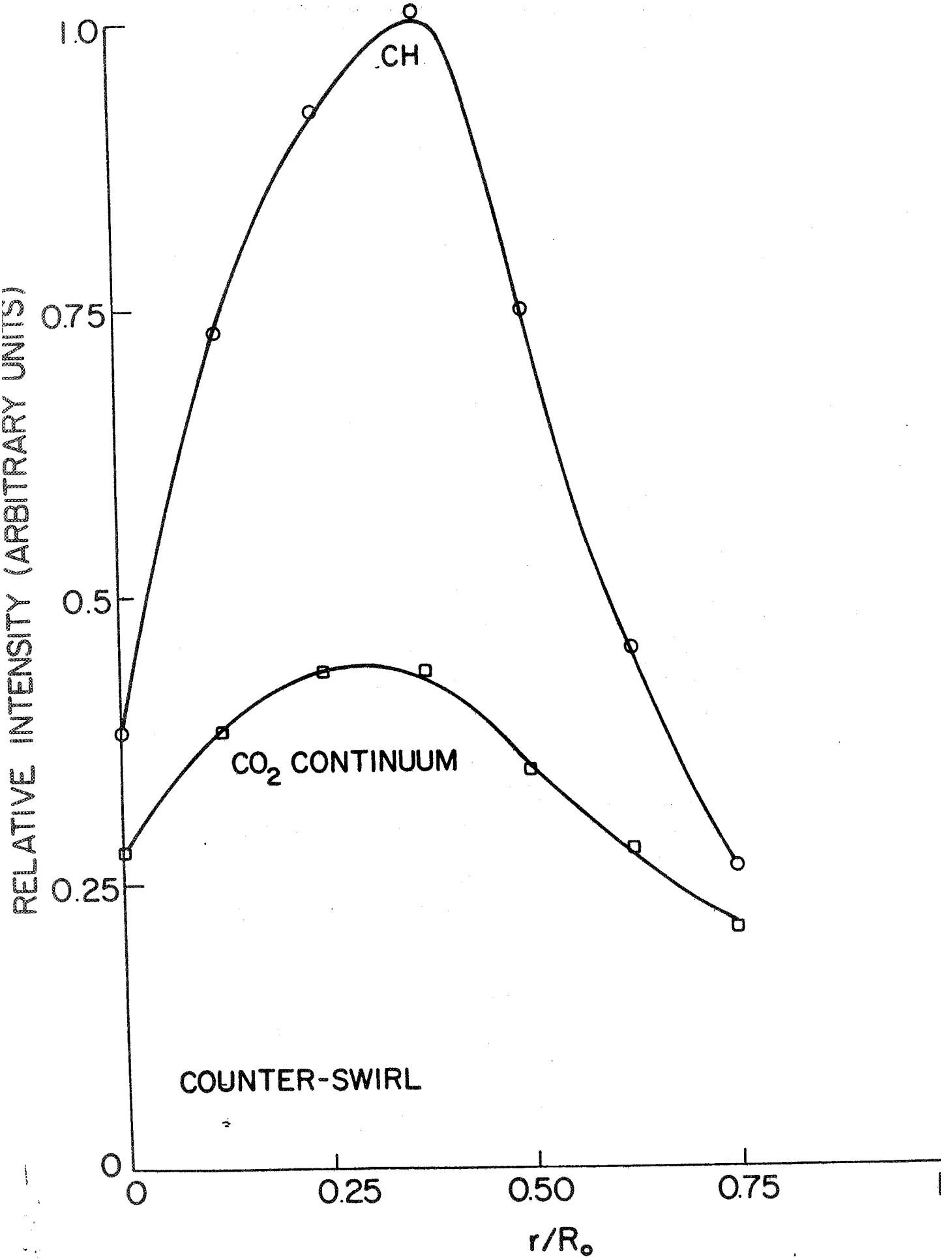
1.0
0.75
0.5
0.25
0
RELATIVE INTENSITY (ARBITRARY UNITS)
CH
CO_2 CONTINUUM
COUNTER-SWIRL
0
0.25
0.50
0.75
r/R_o

ADVANCED LOW EMISSIONS CATALYTIC COMBUSTOR PROGRAM (ALECC)

PHASE 1 - DESIGN STUDY

NASA PROGRAM MANAGER	-	A. J. SZANISZLO
GE PROGRAM MANAGER	-	A. L. MEYER
TECHNICAL PROGRAM MANAGER	-	D. W. BAHR
PRINCIPAL INVESTIGATOR	-	C. C. GLEASON
COMBUSTION ENGINEER	-	W. J. DODDS

INTRODUCTION

The Advanced Low Emissions Catalytic Combustor Program (ALECC) is being undertaken to evaluate the feasibility of employing catalytic combustion technology in aircraft gas turbine engines as a means to control emission of oxides of nitrogen during subsonic stratospheric cruise operation. The ALECC Program is being conducted in three phases, as illustrated in Table I. The first phase, which was completed in November, 1978, consisted of a design study to identify catalytic combustor designs having the greatest potential to meet the emissions and performance goals specified in Table II. The primary emissions goal of this program was to obtain cruise NO_x emissions of less than 1g/kg (compared with levels of 15 to 20 g/kg obtained with current designs). However, good overall performance and feasibility for engine development were heavily weighted in the evaluation of combustor designs. The General Electric design effort was supported by a subcontract with Engelhard Industries, specialists in the catalytic combustion field.

Catalytic Combustor Design Considerations

Reference Engine Operating requirements are compared with projected catalyst performance in Table III. Performance projections in this table were based on Engelhard Industries estimates of catalyst development over a 5 to 10 year period.

It is apparent that the catalyst cannot cover the entire range of operation. Specifically, idle inlet temperature is not high enough for catalyst ignition, and exit temperatures at the idle, approach, and minimum cruise conditions are too low to obtain high combustion efficiency.

Catalyst combustion efficiency characteristics as a function of fuel/air ratio(at constant inlet conditions) are shown in Figure 1. In order to obtain efficiency above 99.9%, the fuel/air ratio must be high enough to assure operation in the catalytically supported homogeneous combustion mode. Also shown in Figure 1 is the maximum fuel/air ratio corresponding to the catalyst maximum use temperature. In order to obtain high efficiency and avoid exceeding the catalyst maximum use temperature at the conditions shown, the mixture entering the catalyst must be between fuel/air ratios of about 24 and 35 g/kg. This provides for about +20% spacial variation in mixture uniformity if average fuel/air ratio is exactly 29.5 g/kg. However, in practice, mixture uniformity within about $\pm$10% will be required to allow some margin for fuel injector deterioration and control system inaccuracy.

Obtaining a uniform, fully evaporated fuel/air mixture is complicated by autoignition considerations. Autoignition delay times predicted based on References 1-3 are between 9.6 and 16.1 ms at the maximum cruise conditions, decreasing to between 2.2 and 3.1 ms at hot day takeoff. Within this period fuel must be injected, evaporated and thoroughly mixed with the air stream.

Principal catalytic combustor design considerations and possible design solutions are summarized in Table IV.

Combustor Conceptual Design

The six catalytic combustor conceptual designs are shown in Figures 2-7. All of these concepts incorporate (1) a conventional pilot stage designed specifically for relight and low idle emissions, and (2) a lean premixed catalytic stage sized specifically for ultralow NO_x emissions at cruise.

Concept 1(Figure 2) is a basic series staged combustor design. At power levels up to about 25% of rated thrust, only the pilot stage is fueled, and the catalyst is used as a cleanup device. At power levels above 25%, the pilot stage is cut back and fuel is injected through multiple point injectors located in the 90 main stage mixing chutes. This fuel is atomized by, and mixed with approximately 40% of combustor airflow which also passes through the chutes. During intermediate power operation, sector fueling is used to control catalyst inlet fuel/air ratio. Combustor pressure drop with this combustor is between 5 and 6% at all operating conditions.

The cross-sectional area of this combustor is reduced at the plane of the mixing chutes to accelerate the pilot stream, improving the velocity profile at the fuel injection plane and increasing the fuel/air mixing length, which is limited by autoignition requirements. Immediately upstream of the catalyst, the flow is rapidly diffused to the velocity required to obtain acceptable conversion and pressure drop.

This series staged design provides good emissions reduction potential because all fuel is reacted in the catalyst at all operating conditions. However, a major problem with this design is obtaining uniform fuel/air mixtures and avoiding autoignition with the main stage fuel injector system. This design also suffers because of increased system length and the difficulty of cooling the fuel injector chutes.

Concept 2(Figure 3)is a series staged combustor which incorporates (1) variable geometry, (2) a folded pilot burner, (3) external fuel/air mixing chutes, and (4) a third combustion stage downstream of the catalyst. At low power operating conditions, the variable geometry vanes are closed and all fuel is burned in the pilot stage. At intermediate and high power conditions, the variable vanes are opened, and fuel is injected through multiple point injectors located in the mixing ducts. At takeoff conditions and during transients, the third fuel injector stage may be fueled to avoid catalyst over temperature. As in the basic series staged design, circumferential fuel staging is utilized for catalyst fuel/air ratio control during intermediate power operation.

The use of variable geometry in this concept allows catalyst pressure drop to be increased relative to the basic series staged design, and

also increases the air flow admitted through the fuel injection chutes to about 70% of combustor air flow at cruise conditions. The use of external fuel injection chutes eliminates the chute cooling problem encountered with Concept 1, and the reverse flow pilot stage provides some length reduction relative to the basic series staged combustor. In the analysis of this design, it was determined that the takeoff stage shown in Figure 3 would not be required if combustor aft section film cooling flow was eliminated and used instead as catalyst air flow. Since the takeoff stage positioned at the catalyst exit was considered a high risk design feature, a revised design in which the takeoff stage was removed and the aft section was convectively cooled using turbine cooling air was considered in the final combustor evaluation.

The increased fuel injection chute air flow in this concept tends to decrease fuel/air mixing requirements relative to the basic series staged design. However, obtaining uniform catalyst inlet fuel/air mixtures without encountering autoignition still presents a difficult problem. Other problem areas with this design are increased idle pressure drop (10% vs. 5% at cruise), and additional mechanical design and operational complexity.

Concept 3 (Figure 4) is an annular, parallel-staged combustor. In this design, approximately 40% of the combustor air flow is used for pilot dome combustion and liner cooling air. The remaining 60% is used as catalyst air flow. Only the pilot stage is operated up to about 25% thrust. Above this level, pilot stage fuel flow is minimized and a majority of fuel flow is routed to the catalyst stage. At intermediate power levels, sector burning is utilized to control catalyst inlet fuel/air ratio. At higher power levels and during transients catalyst stage fuel flow is limited by catalyst maximum use temperature, and excess fuel is injected into the pilot stage. At the normal cruise condition, approximately 25% of the fuel is burned in the pilot stage.

Catalyst stage fuel flow is injected from orifices located in the central splitter vane of the inlet diffuser. A nominal flow velocity of 61 m/s is used in the premixing duct to provide adequate mixing length while meeting the 2 ms autoignition delay time requirement. Immediately upstream of the catalyst, the duct area is rapidly increased. The duct walls in this region are contoured to simulate the streamlines which would be observed in unconfined flow approaching the catalyst blockage.

Concept 4 (Figure 5) is a similar parallel staged design except that a cannular catalyst stage consisting of 30 cylindrical catalytic reactors is used. This catalyst stage has been relocated outboard of the pilot stage, and a reverse-flow configuration has been used to decrease combustor length. This cannular design provides advantages in fuel/air mixing duct velocity profile control and catalytic reactor access. Very uniform combustor exit temperature profiles are anticipated with this design because of improved mixing between the pilot and catalyst stages. Catalyst stage emissions and performance are also expected to be markedly improved during sector burning because individual reactors can be fueled, and the lean "fringe" area between fueled and unfueled

annular sectors is avoided.

A problem common to both Concepts 3 and 4 is the inability to meet cruise NO_x goals because a relatively large proportion of fuel (about 25%) must be burned in the pilot stage to avoid catalyst over temperature during cruise operation. In Concept 5(Figure 6), catalyst air flow at cruise condition is increased from 60 to about 80% by the use of variable geometry, thereby enabling approximately 95% of combustor fuel flow to be reacted in the catalyst. Within this concept, low power operations are conducted with the variable vanes closed. Under these conditions flow splits are similar to Concepts 3 and 4, but combustor pressure drop is increased to about 15%. Above the 25% thrust level, the variable geometry vanes are opened to increase catalyst flow to about 80% and reduce pressure drop to the 5% design level. As with Concept 2, the takeoff stage shown in this design was eliminated for the final evaluation.

Although NO_x emissions reduction potential is improved with this design, the use of variable geometry results in a significant increase in mechanical complexity and control requirements. Of concern is decreased compressor stall margin due to increased pressure drop during idle operation, which leads to an increased risk of stall during transient operation.

Concept 6(Figure 7) is essentially two complete combustors in parallel. All operations within the landing/takeoff cycle are conducted with the outer combustor, which is a piloted premixing design based on the radial/axial configuration investigated in the NASA/GE Experimental Clean Combustor Program (Reference 4). When this combustor is in operation, the catalytic combustor vanes are closed, and only about 10% leakage flow passes through the catalyst. At cruise conditions, the variable geometry vanes are rotated to direct as much as 90% of combustor air flow to the catalytic combustor located in the inner annulus. Instead of sector burning in this design, catalyst inlet fuel/air ratio is controlle by opening the main stage control vanes to bypass air flow around the catalytic combustor.

This design approach takes maximum advantage of conventional combustor design technology since the outboard mounted combustor used for landing/takeoff maneuvers can be of conventional design. The required range of operation of the catalytic combustor is thus limited to cruise range conditions, which results in less severe operating constraints for the catalytic reactor and fuel/air carburetion system. On the other hand, this system does not take advantage of the catalytic combustor emissions reduction potential during landing/takeoff maneuvers. Transition from main combustion to catalytic combustor operation also presents a major control challenge, and overall system length, weight, and complexity are increased with this design.

Concept Evaluation

A conceptual design evaluation summary is presented in Table V, where the six conceptual designs are ranked with respect to predicted emission and developmental risk in several areas of combustor performance. The

overall trend observed in the evaluation of these concepts is increased emissions reduction potential with increasing development risk. The parallel staged, non variable geometry concepts (BP and CRP) consistently rated highest in performance, but were lowest rated with respect to emissions. Therefore, the selection of the two most promising designs depended largely on the relative weighting of emissions and performance.

Predicted emissions for each of the combustor designs are presented in Table VI. As indicated in this figure, although cruise NO_x emissions for Concepts 3 and 4 were 2 to 3 times as high as those of the other concepts, absolute levels were an order of magnitude lower than emissions obtained with current technology combustors. These two concepts were therefore, selected for further study.

Preliminary Designs

Preliminary designs of the selected concepts are shown in Figure 8. In these designs, major emphasis was placed on reducing combustor length and increasing catalyst air flow. Features used to increase catalyst air flow include the reduction of film cooling in the pilot dome and combustor aft section. By incorporating these features, predicted cruise NO_x levels are decreased to about 1.2 to 1.4 g/kg, compared to about 2 g/kg in the conceptual designs.

Conclusions

Based on ALECC Phase I studies, catalytic combustion appears to be a promising means for obtaining ultra low NO_x emissions at aircraft cruise operating conditions. Levels below 2 g/kg appear to be obtainable without the use of variable geometry. Circumferential fuel staging appears to be a viable means for controlling catalyst inlet fuel/air ratio. Circumferentially non-uniform exit temperature patterns resulting from circumferential staging are expected to be acceptable because of the relatively low peak exit temperatures, which are catalyst limited.

Major challenges in the application of catalytic combustion to practical aircraft combustors include the following:

- Development of fuel/air carburetion systems to meet mixing and autoignition criteria.
- Development of catalyst, support, and mounting systems to obtain good high cycle performance (durability, thermal shock resistence).
- Development of advanced liner cooling techniques to reduce cooling flow requirements.
- Development of precise fuel/air ratio sensing and control techniques.

- Determination of the effects of circumferential staging on catalyst performance.

These will be major areas of study in the ALECC Phase II and III experimental programs.

REFERENCES

1. Marek, CJ; Papathakos, LC; and Verbulecz, PW: "Preliminary Studies of Autoignition and Flashback in a Premixing-Prevaporizing Flame Tube using Jet A Fuel at Lean Equivalence Ratios", NASA TM X-3526, May, 1977.

2. Stringer,FW; Clarke, AE; and Clarke, JS: "The Spontaneous Ignition of Hydrocarbon Fuels in a Flowing System", Paper No. 20, Symposium on Diesel Engine Combustion, Institution of Mech. Engineers, London, April, 1970, Proceedings Pages 198-221.

3. Spadaccini, LJ; "Autoignition Characteristics of Hydrocarbon Fuels at Elevated Temperatures and Pressures", ASME 76-GT-3, March, 1976.

4. Bahr, DW; and Gleason, CC: "Experimental Clean Combustor Program, Phase I Final Report", NASA-CR-134737,June 1975.

ALECC PROGRAM SCOPE

OVERALL PROGRAM

- PHASE I - DESIGN STUDY
- PHASE II - SCREENING TESTS
- PHASE III - COMBUSTOR REFINEMENT

PHASE I

- DESIGN STUDY (COMPLETED 11/20/78)
- DEFINE 6 CATALYTIC COMBUSTOR CONCEPTS
- ANALYZE AND EVALUATE CONCEPTS
- PERFORM PRELIMINARY DESIGN ON TWO MOST PROMISING CONCEPTS

TABLE I

ALECC DESIGN REQUIREMENTS AND GOALS

- DESIGNS BASED ON NASA/GE ENERGY EFFICIENT ENGINE CYCLE AND ENVELOPE
- EMISSIONS:
  - o $NO_X \leq 1$G/KG @ CRUISE
  - o MEET 1979 EPA EMISSIONS STANDARDS
- COMBUSTION EFFICIENCY
  - o $\geq$99.9% @ TAKEOFF
  - o $\geq$99.5% @ CRUISE
  - o $\geq$99% @ ALL OTHER
- PERFORMANCE COMPARABLE TO REFERENCE ENGINE
  - o PRESSURE DROP $\leq$5%
  - o PATTERN FACTOR $\leq$.35(TAKEOFF,CRUISE)
  - o RELIGHT
  - o LINER COOLING
- OPERATIONAL CHARACTERISTICS SUITABLE FOR USE ON REFERENCE ENGINE (WITH APPROPRIATE CONTROL MODIFICATIONS).

TABLE II

COMPARISON OF CATALYST PERFORMANCE WITH ENGINE OPERATING REQUIREMENTS

	ADVANCED CATALYST OPERATING RANGE	REFERENCE ENGINE CYCLE			
		IDLE	APPROACH	CRUISE	TAKEOFF (MAX.)
INLET TEMP, K	600-1100	485	633	677-782	864
PRESSURE, MPA	——	0.4	1.2	0.8-1.3	3.0
EXIT TEMP, K	1350-1811	940	1135	1289-1488	1693
PRESSURE LOSS, %	2-3	5.0	5.0	5.0	5.0
COMBUSTION EFFICIENCY, %	99.9	99.5	99	99	99.9
NO_X EMISSIONS	< 0.5G/KG	--	--	<1.0G/KG	--

TABLE III

ALECC DESIGN CONSIDERATIONS

DESIGN CONSIDERATION	POSSIBLE SOLUTION
IDLE INLET TEMPERATURE BELOW CATALYST IGNITION TEMPERATURE	– PREBURNER TO INCREASE CATALYST INLET TEMPERATURE – (SERIES STAGED) – PILOT BURNER FOR IDLE OPERATION (PARALLEL STAGED)
MID RANGE COMBUSTOR EXIT TEMPERATURE BELOW TEMPERATURE REQUIRED FOR COMPLETE CONVERSION	– FUEL STAGING (SECTOR OR PARTIAL ANNULAR BURNING) – AIRFLOW MODULATION (VARIABLE GEOMETRY)
MIXING/AUTOIGNITION	– AXIAL FUEL STAGING – INCREASED FUEL MIXING TUBE VELOCITY – MULTIPLE POINT INJECTION

TABLE IV

CATALYTIC COMBUSTOR ANALYSIS AND EVALUATION

	CONCEPT RANKING (BEST ← WORST)					
	1	2	3	4	5	6
EMISSIONS	VGS	BS	VGP	RAP	BP	CRP
OTHER CONSIDERATIONS						
AEROTHERMAL	CRP	BP	VGS	BS	VGP	RAP
OPERATIONAL	CRP	BP	BS	VGS	VGP	RAP
FUEL/AIR CARBURETION	RAP	BP	CRP	VGP	BS	VGS
MECHANICAL	BP	CRP	BS	VGP	RAP	VGS
OVERALL	CRP	BP	VGP	BS	RAP	VGS

BS - Basic Series Staged

VGS - Variable Geometry, Series Staged

BP - Basic Parallel Staged

CRP - Cannular Reverse-flow Parallel-staged

VGP - Variable Geometry Parallel-staged

RAP - Radial/Axial Parallel Staged

TABLE V

ALECC PREDICTED EMISSIONS

EMISSION PARAMETER	CONCEPT					
	BS	VGS	BP	CRP	VGP	RAP
CRUISE EMISSIONS, G/KG						
CO	2.9	3.0	2.5	2.4	3.0	3.0
HC	0.3	0.3	0.3	0.3	0.3	0.3
NO_X ($\leq$1)	0.7	0.6	1.9	2.1	0.7	0.6
EPAP , LB/1000 LB-HR						
CO($\leq$ 4.3)	2.06	1.99	1.97	1.96	1.88	2.32
HC($\leq$ 0.8)	0.08	0.08	0.07	0.07	0.07	0.04
NO_X($\leq$ 3.0)	0.59	0.59	1.17	1.25	0.71	3.04

TABLE VI

CATALYTIC COMBUSTOR DESIGN CONSIDERATIONS

CATALYST FUEL/AIR RATIO

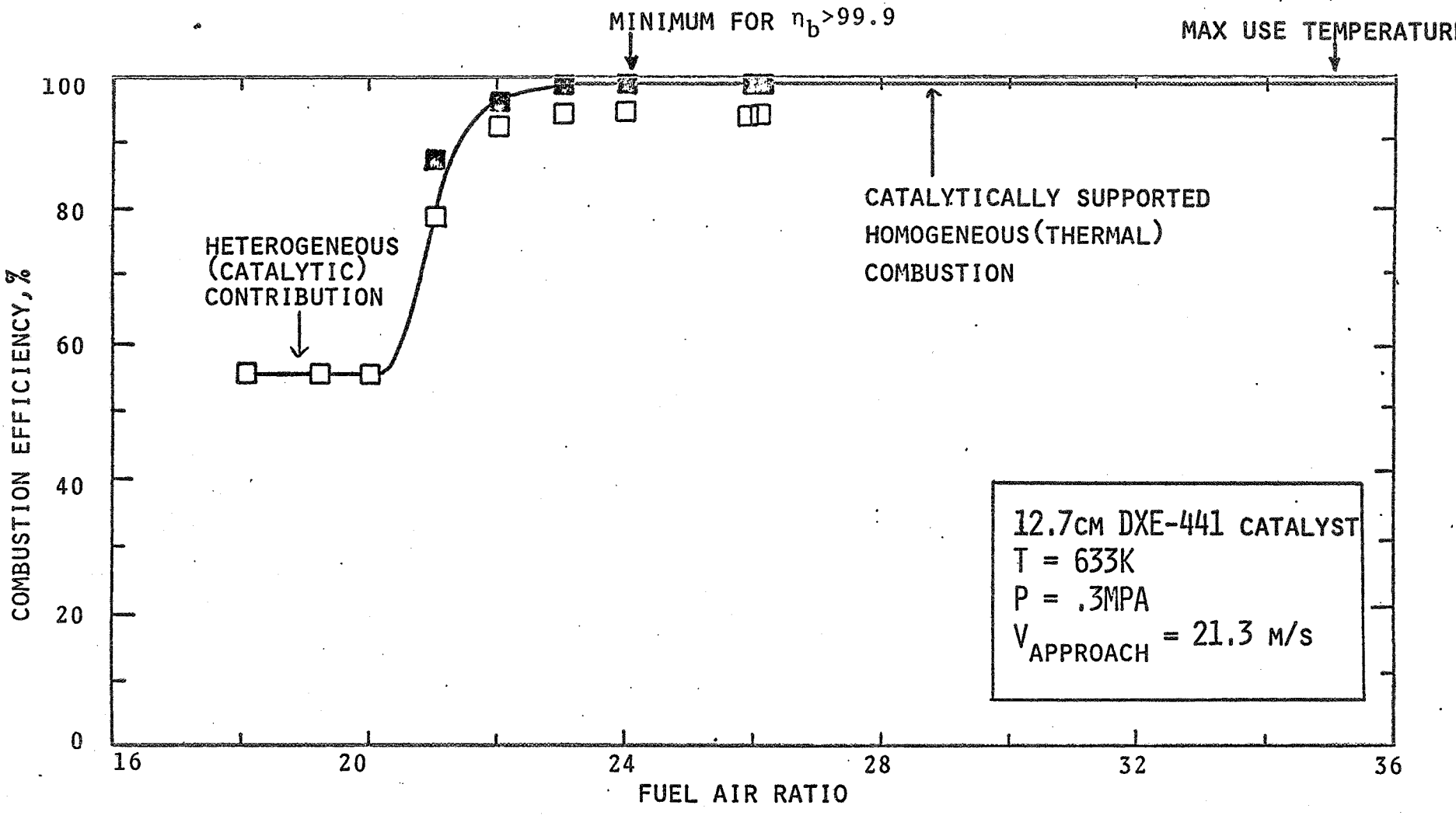

FIGURE I

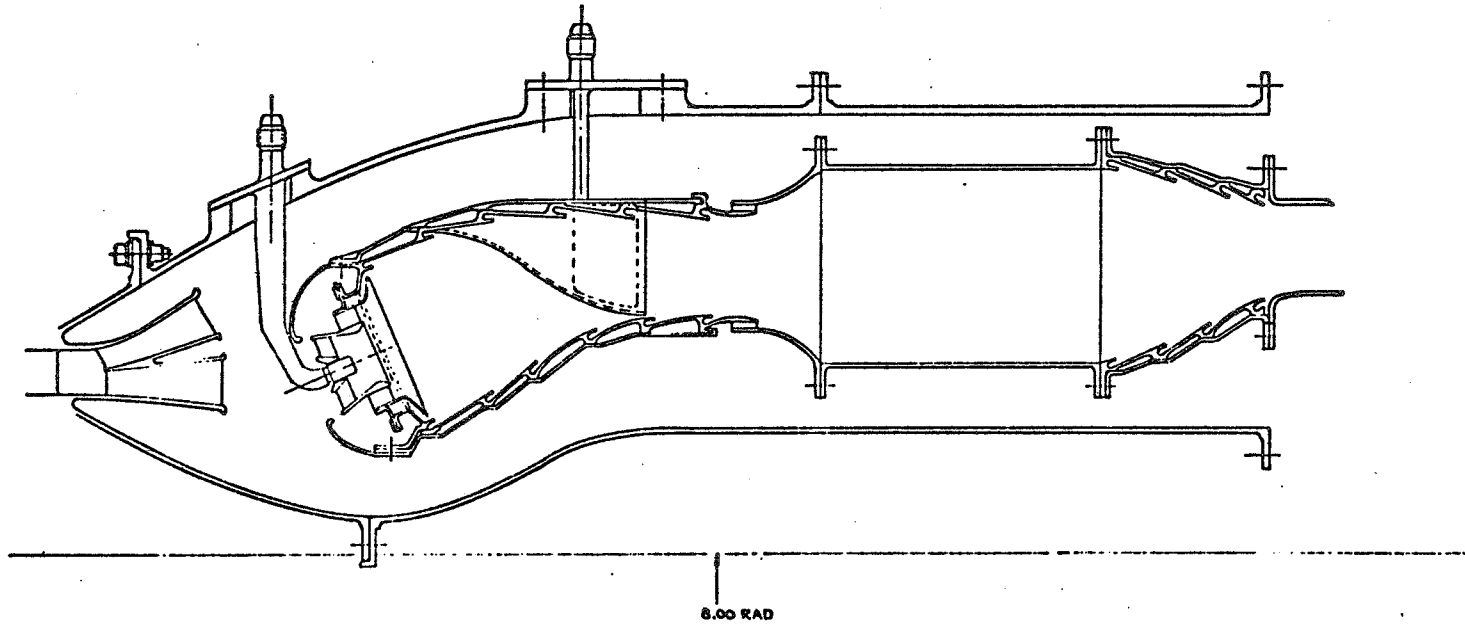

CONCEPT 1, BASIC SERIES STAGED CONFIGURATION (BS)

FIGURE 2

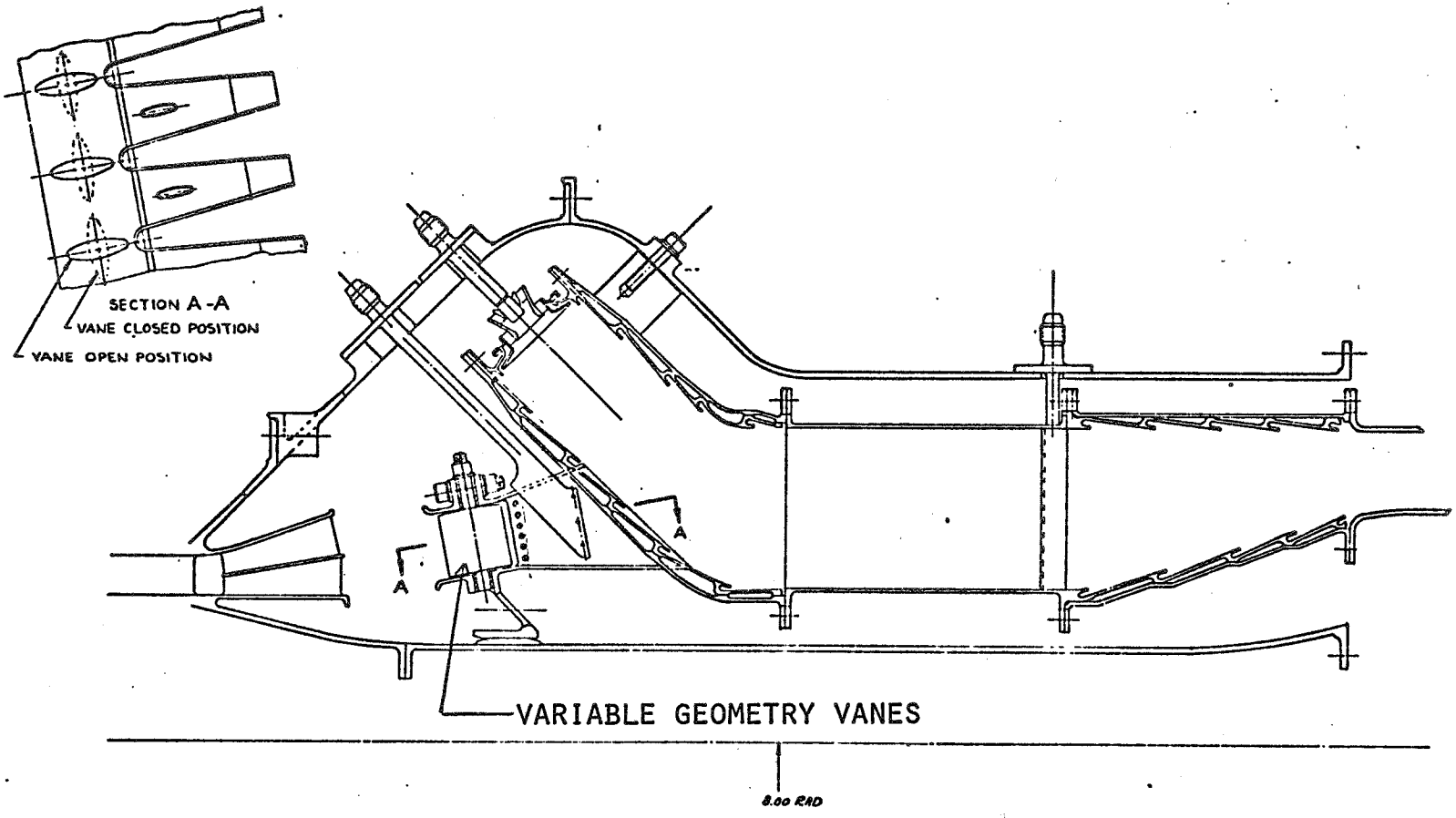

CONCEPT 2, SERIES STAGED CONFIGURATION WITH VARIABLE GEOMETRY (VGS)

FIGURE 3

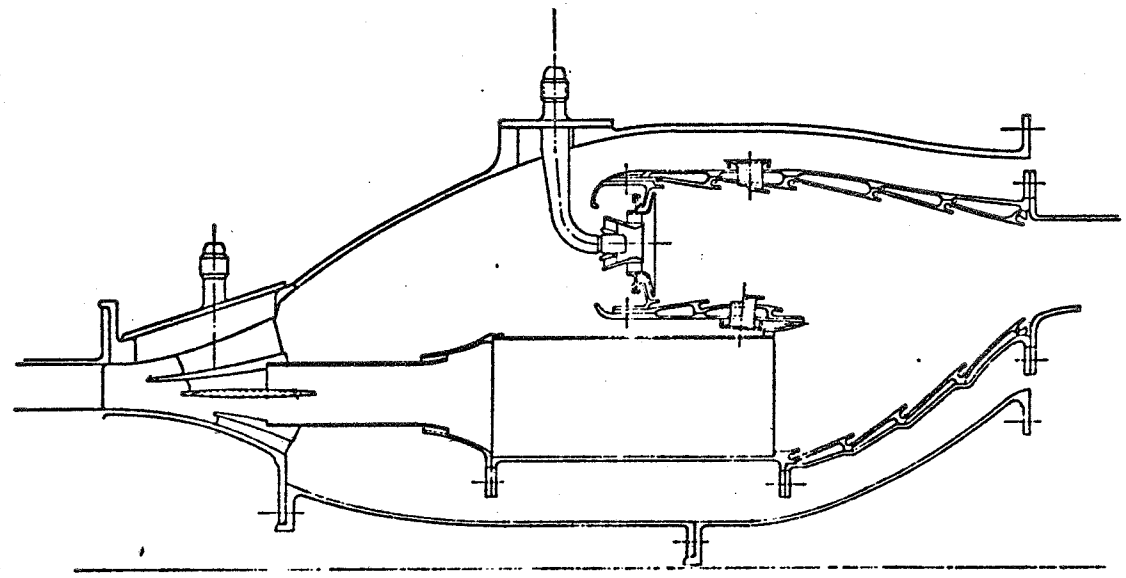

CONCEPT 3, BASIC PARALLEL STAGED CONFIGURATION (BP)

FIGURE 4

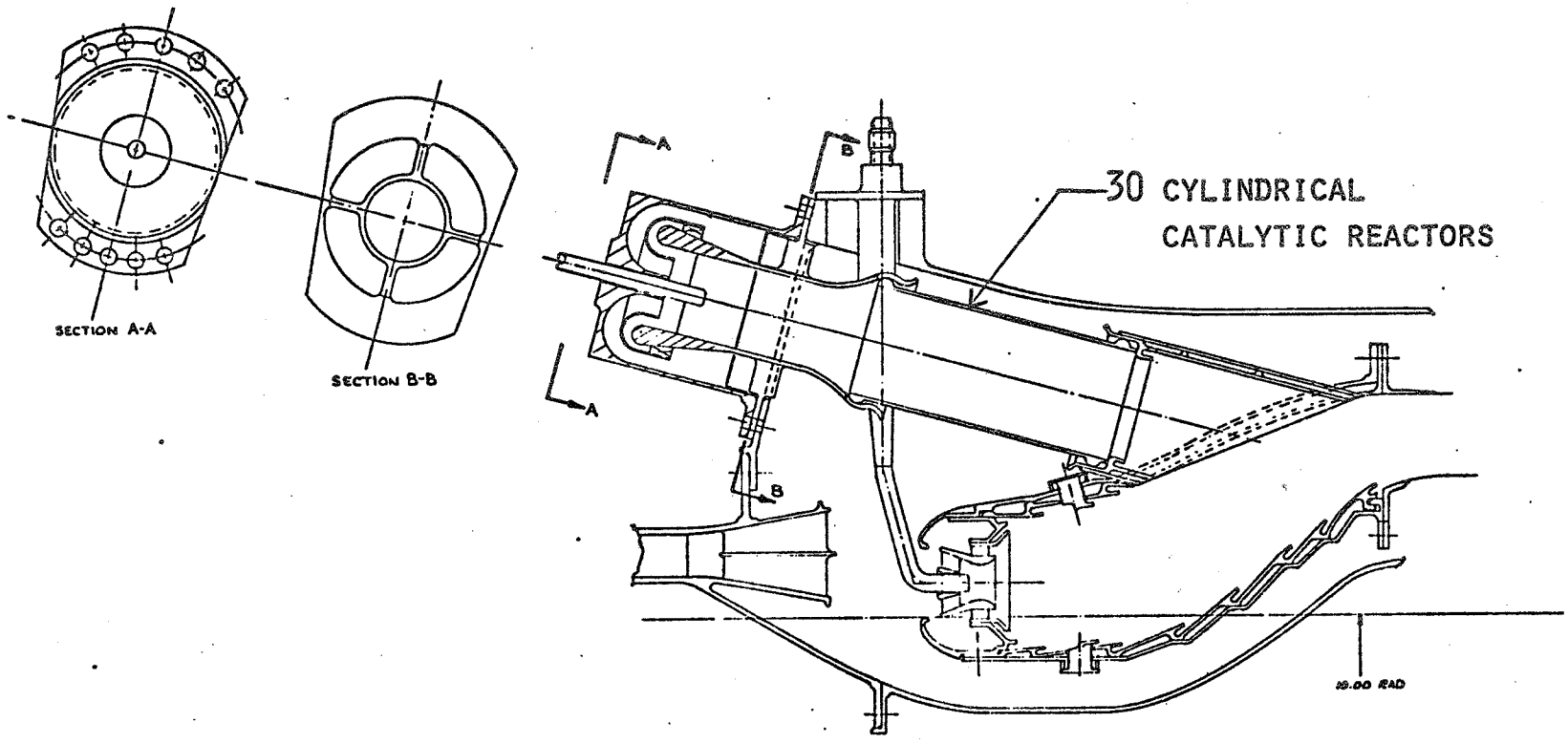

CONCEPT 4, CANNULAR REVERSE-FLOW PARALLEL STAGED CONFIGURATION (CRP)

FIGURE 5

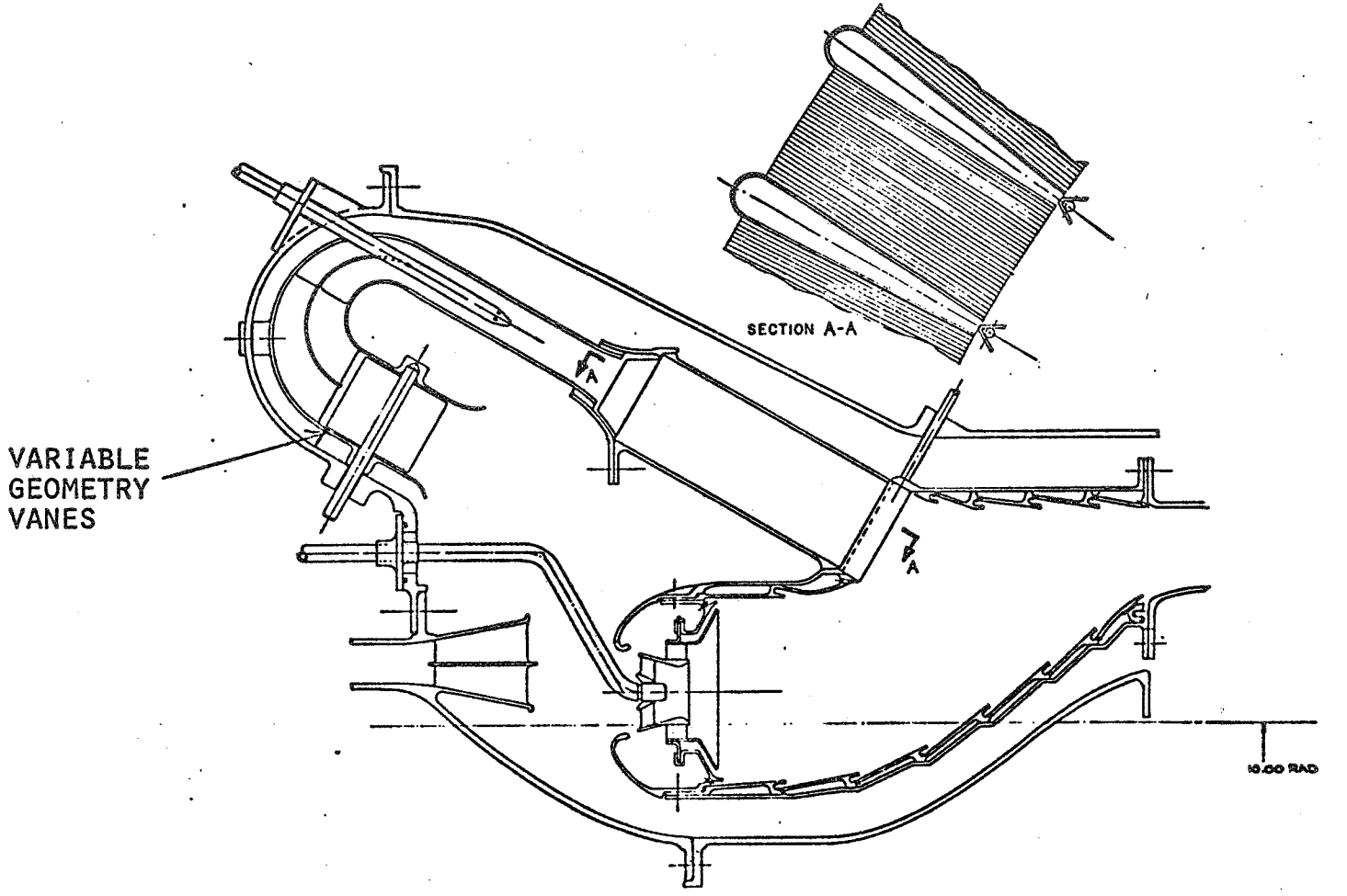

CONCEPT 5, REVERSE-FLOW PARALLEL STAGED CONFIGURATION WITH VARIABLE GEOMETRY (VGP)

FIGURE 6

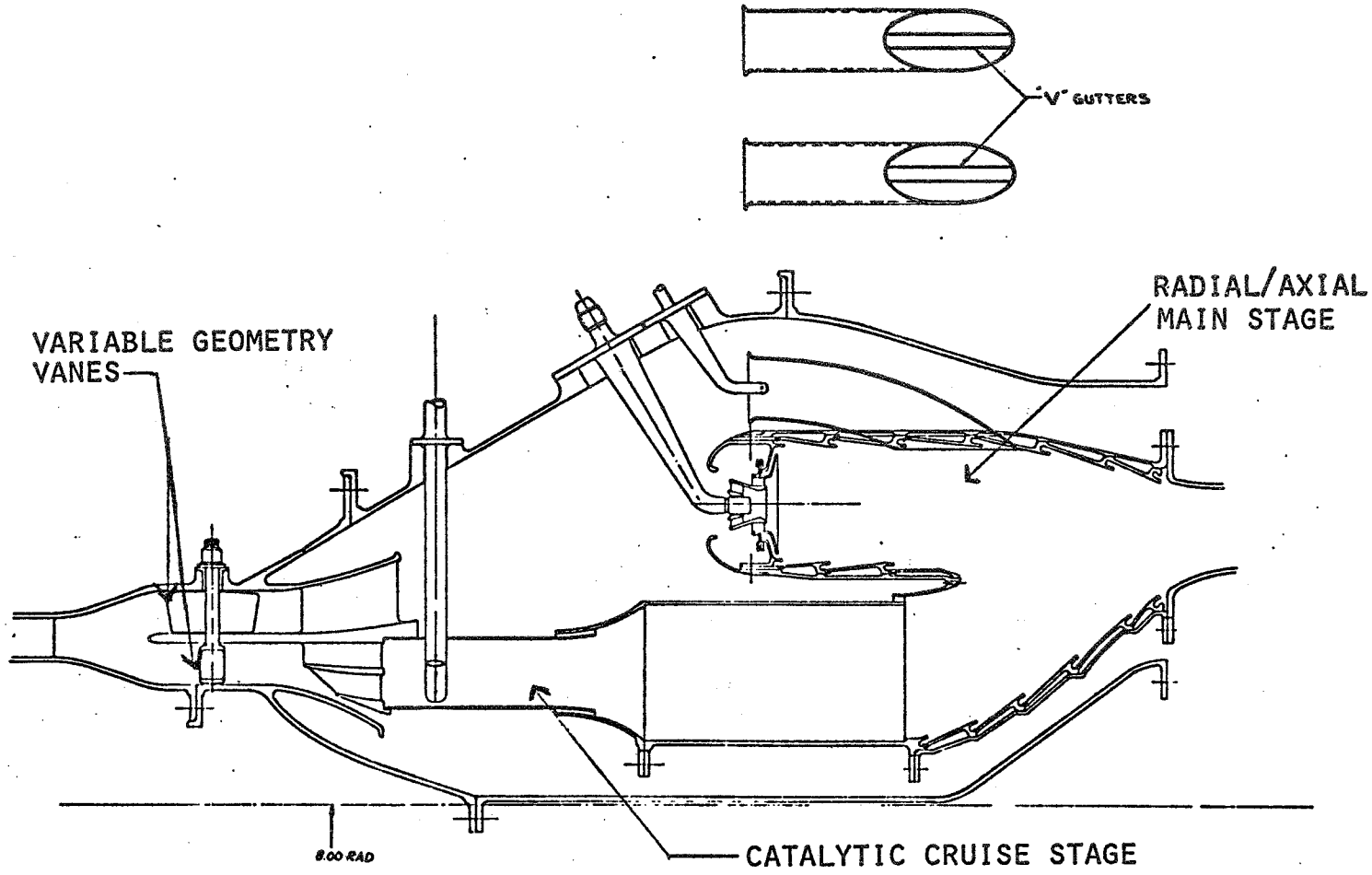

CONCEPT 6, RADIAL/AXIAL PARALLEL STAGED CONFIGURATION WITH VARIABLE GEOMETRY (RAP)

FIGURE 7

ALECC SELECTED CONCEPT PRELIMINARY DESIGN FEATURES

- O REDUCED SYSTEM LENGTH
- O ADVANCED COOLING TECHNIQUES IN COMBUSTOR DOME AND AFT LINERS
- O MULTIPLE POINT - CROSS STREAM INJECTORS
- O INCREASED FUEL/AIR MIXING DUCT VELOCITY
- O "COMPLIANT LAYER" CATALYST MOUNTING
- O IMPINGEMENT & FILM COOLED LINER CONSTRUCTION

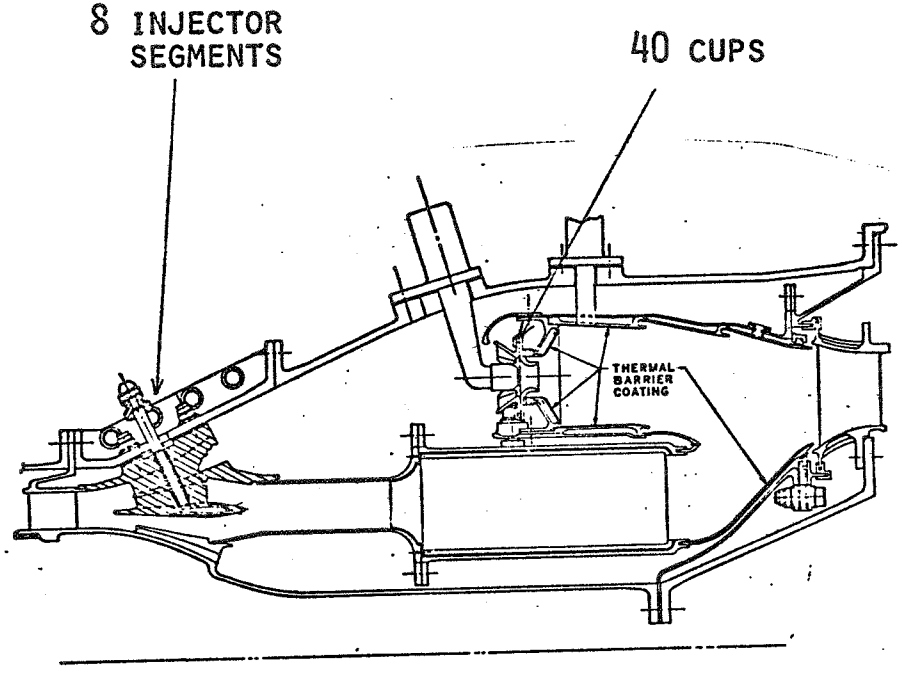

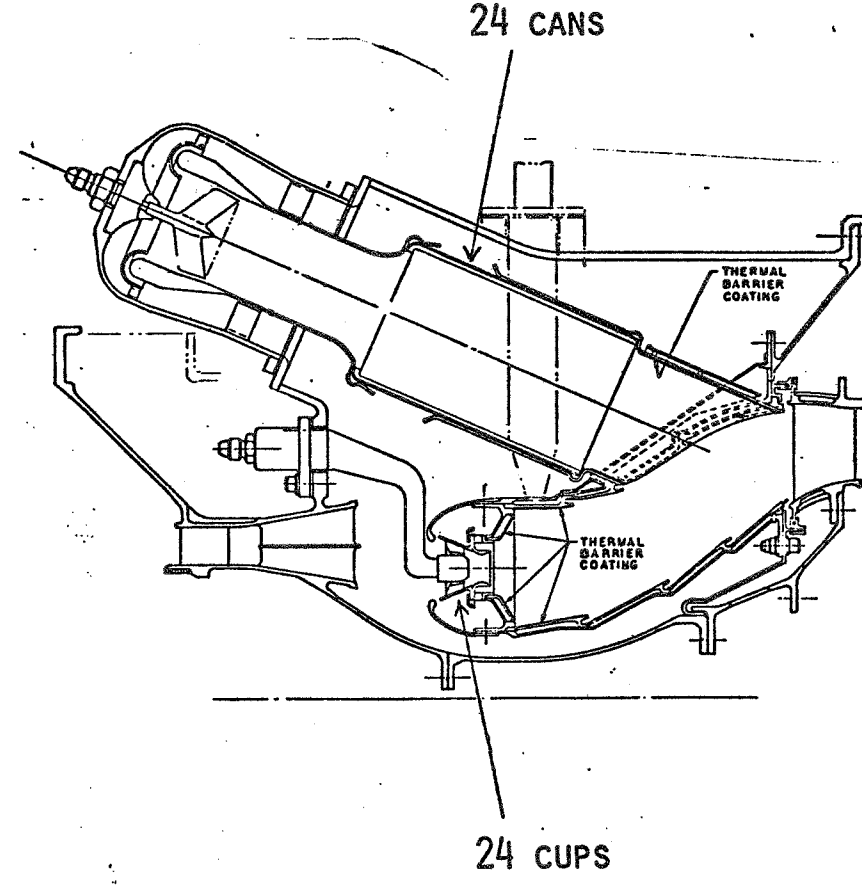

Advanced Low Emissions Catalytic Combustor Program (NAS3-20821)

G. J. Sturgess

Abstract and Introduction

The objective of the NASA contract is to evaluate the feasibility of employing catalytic combustion technology to control the emissions of oxides of nitrogen for subsonic, stratospheric cruise aircraft operation. The existing Environmental Protection Agency 1979 emissions standards for the landing and take-off cycle were also required to be satisfied. Work reported is for the first phase of a proposed three phase effort and is concerned with analytical design studies. The remaining two phases of the program structure are to cover screening testing and combustor refinement.

The analytical design studies of the initial phase involved conceptual definition of six different annular combustor concepts. Analysis and evaluation of these six concepts was to lead to the selection of the two most promising concepts. Refined analysis and design work was to result in preliminary layout drawings of the two selected concepts. The engine cycle selected for the study was a version of that for the Pratt & Whitney Energy Efficient Engine which is being designed under NASA contract. The original program plan called for completion of this first phase within seven months from go-ahead.

Consideration of the scope of the tasks, the general start-of-the-art in catalytic combustion, and the lack of experience in this area quickly indicated that the design tools necessary to implement the program in satisfactory fashion were not available. Such tools had to be developed in parallel with the program. Inevitably, the most immediate consequence of this was that the original schedule was found to be overly ambitious. Furthermore, design decisions which for more conventional combustors could have been taken on the basis of experience could not be agreed for these new concepts without analysis. This required that the nature of the tasks be changed to give fuller analysis of each of the concepts rather than concentrating on the two selected concepts as was originally intended. Indeed, rational selection of the two concepts could not be made without such analyses. This required change in approach implies an expanded workload, and such was found to be the case.

All of the necessary design tools could not be developed within the time-scale involved and this leaves serious gaps. As examples, no reliable flashback analyses could be conducted for the concepts involving premixing, and heterogeneous reaction rates of multi-component liquid hydrocarbon fuels remain uncertain. In addition, experimental verification of some of the design tools which were developed is lacking in sufficient depth for real confidence in the finished designs.

Six concepts were defined and these were as follows:

1. A "classical" catalytic combustor consisting of a partially premixed, partially vaporized fuel and air mixture being reacted catalytically at all operating conditions. This was not considered as a practical design for aircraft operations and served only as a base-line against which to compare the other concepts.

2. A so-called "rich-front-end" homogeneous combustor feeding a fully vaporized and partially-reacted fuel and air mixture into a bed for catalytic reaction of the majority of the fuel.

3. Separate homogeneous and heterogeneous reactors arranged as radial stages with the homogeneous reactor acting as a continuously operating pilot and the catalytic secondary combustor only being turned on when the compressor delivery air temperature is above the extinction temperature of the catalyst bed. Fuel staging is arranged such that both combustors operate at the same lean, equivalence ratio at take-off.

4. A variable geometry version of the second concept whereby the initial burning zone is at or near stoichiometric mixture strength at idle, but is made very lean at high power and where the downstream catalyst bed acts as a clean-up device rather than as a main reactor.

5. A variable geometry version of the third concept where fuel staging and pilot combustor air management are controlled to give equal equivalence ratios in the two combustors at all operating conditions and where most of the fuel at high power is reacted catalytically.

6. A design where a separate catalytic combustor is used in conjunction with a small pilot combustor at altitude cruise, and at all other operating points the catalytic combustor is non-functioning. Take-off emissions requirements are addressed with a version of the ECCP Vorbix I combustor designed by Pratt & Whitney Aircraft under NASA contract.

These concepts all offer low NO_x emissions at the design points, as was the design intent. Some uncertainty is associated with the estimates of emissions of carbon monoxide due to the difficulties associated with reaction rate constants. Satisfaction of the emissions goals is achieved with varying degrees of operational, control and mechanical complexity, which exact penalties in weight, reliability and first and continuing operating costs.

Lean, Premixed, Prevaporized

Combustor Conceptual Design Study

A. J. Fiorentino

Pratt & Whitney Aircraft Group
Division of United Technologies Corporation

The objective of this seven month study program is to identify and evaluate promising LPP combustor concepts utilizing variable geometry and/or other flow control techniques. The general approach taken to accomplish this objective is outlined on Figure 1 and consists of combustor design, design analysis and design ranking. The schedule being followed to achieve this program is shown in Figure 2.

Although the ultimate goal of this program is the significant reduction of cruise oxides of nitrogen, both the EPA emission standards and combustor performance levels outlined in Figure 3 are retained as goals as well. The combustor conceptual components are being designed for the cycle and performance characteristics for the Energy Efficient Engine (E^3), currently being developed under a contract with NASA. Representative operating conditions for this engine at the design points of the LTO cycle and for cruise are presented in Figure 4.

The basic design philosophy as listed in Figure 5 underlying all concepts in this program is that of lean, premixed, prevaporized (LPP) combustion utilizing axial-flow full annular designs constrained to the current E^3 configuration. The conclusion to be drawn from the numerous emission reduction programs so far completed, ours as well as others, is that substantial fuel prevaporization, fuel-air premixing, and controlled combustion over the entire engine operating envelope is the only way to reduce all critical emission levels while satisfying engine performance and operational requirements. Achieving the NOx emission goals will require equivalence ratios between 0.5 and 0.6 at reduced residence times while at low power a significantly high equivalence ratio must be maintained to ensure high combustion efficiency and low emissions of CO and THC. This stoichiometry must be controlled while maintaining acceptable combustor pressure drop, adequate cooling and structural integrity.

A variety of techniques were investigated to carry out the design goals of this program. Figure 6 outlines the more important approaches and considerations utilized in establishing the conceptual designs. Since the techniques for reducing low power emissions conflict with methods for reducing high power emissions, the apparent solutions are either a multi-stage combustor wherein each stage is employed and optimized for a particular flight condition or a variable geometry combustor to accommodate optimization of the stoichiometry by means of airflow modulation. The latter approach is more attractive since it can theoretically alleviate the off-design fall-off in performance and associated increase in emissions that has been experienced with previous attempts at employing premixed combustors. The utilization of variable geometry, though desirable from a combustor performance viewpoint, introduces significant complexity and difficulty with respect to combustor design. Reducing the equivalence ratio from 1.0 to 0.50 will require diverting approximately 50% of the combustor airflow. Because of the large change in area involved, the burner designs have to incorporate simultaneous control of front end and dilution zone areas in order to maintain a nearly constant burner section pressure loss. Fuel staging or the incorporation of a pilot stage is also being considered in conjunction with air modulation to optimize the performance of the combustor for starting, ground idle and altitude relight.

Serious consideration must be given to fuel-air preparation to avoid problems with mixedness and incomplete vaporization. Fuel atomization should be as

fine as practicable, and the fuel-air residence time must be less than the autoignition delay time.

In designing the premixing passages for the LPP system, precautions have to be taken to avoid potential flow problems, such as wakes behind variable geometry devices and fuel injectors, which could increase the residence time of fuel-air mixture in the premixing passage. Incomplete mixing/vaporization, hence, higher NOx emissions must be weighed against providing adequate margin to avoid autoigition and flashback.

The effect of utilizing large quantities of air in the front end of the combustor on cooling/dilution air requirements is shown in Figure 7a. The implication of this figure, evaluated in conjunction with Figure 7b which shows the effect of increasing combustor pressure on conventional (film-cooled) liner cooling requirements, clearly shows the need for advanced, more effective liner configurations. An additional design consideration is the cooling requirements of the flameholders. The additional cooling requirements of the lean premixed combustor may be alleviated by the reduction of flame radiation.

The four preliminary combustor concepts shown schematically in Figures 8 through 11 are currently being designed and analyzed. As shown, the concepts selected allow evaluation of three variable geometry techniques used in various combinations with advanced burner designs. The techniques include both primary and dilution zone area control as well as an aerodynamic method for varying combustor inlet velocity profile. Mechanical devices will be used to modulating combustor areas while diffuser wall bleed is being considered for the aerodynamic control.

Most of the design problems anticipated with variable geometry LPP systems, shown on Figure 12, have already been mentioned. A most important concern not yet discussed is the control, operation and durability of the variable geometry mechanism itself. The complex air staging techniques will require sophisticated control systems and sensors in order to keep the combustor stoichiometry at desired levels for various flight conditions. The influence of this control system on the overall operation of the engine will have to be evaluated.

Although variable geometry introduces significant complexity and difficulty with respect to combustor design for emissions reduction, it represents a new degree of freedom in turbine engine design. Future engine requirements of higher thrust/weight ratios, higher temperature rise, smaller combustor volume and extended flight envelopes will make it very difficult to achieve both emission and performance requirements. Air staging offers the unique potential of significant improvement in the areas of stability, altitude relight, ground starting and temperature distribution.

OVERALL PROGRAM APPROACH

Objective: Seven month study program to identify and evaluate promising LPP combustor concepts

Task I – Combustor design

- Design four concepts

Task II – Design analysis

- Evaluate for emission, performance, and operational requirements

Task III – Design ranking

- Rate design against requirements
- Rank designs by developmental risk

Task IV – Reporting

FIGURE 1

J20273-4
R782811

PROGRAM SCHEDULE

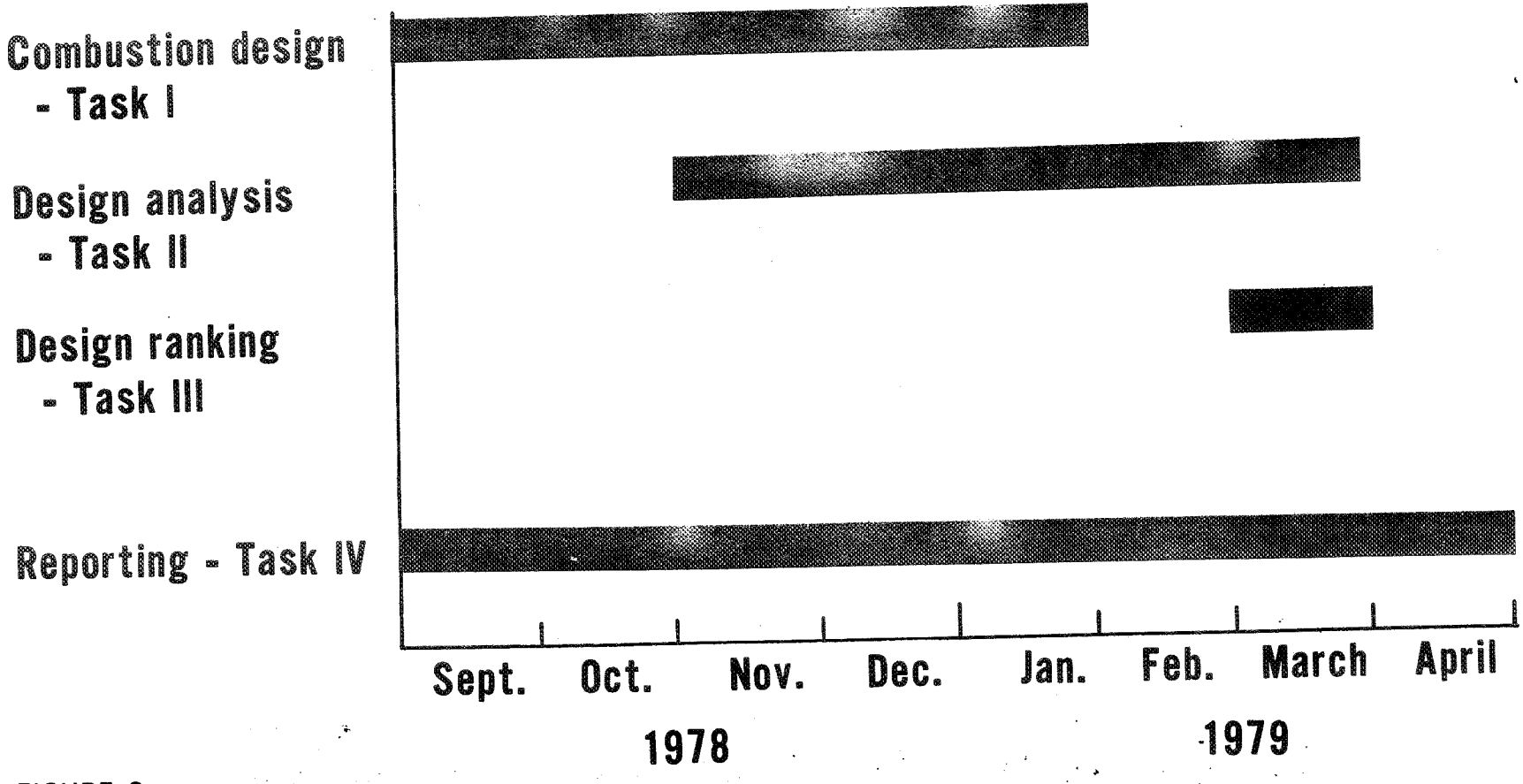

FIGURE 2

PROGRAM GOALS

Emission goals

- $NO_x \in I \leq 3g/kg$ at subsonic cruise
- Meet established standards for LTO cycle

  CO EPAP = 25g/kn

  THC EPAP = 3.3g/kn

  NO_x EPAP = 3 3g/kn

  SAE smoke no.= 20

Performance goals

- Combustion efficiency (η_c)

  η_c 99.9% at SLTO

  η_c 99.5% at idle

  η_c 99.0% at all other operating conditions
- Total pressure loss ($\frac{\Delta P}{P}$) = 5.5% (all conditions except idle)
- Altitude relight $\geq$ 10.7km

J20273-7
782011

FIGURE 3

PROGRAM DESIGN CONDITIONS

	Ground Idle (a)	Approach	Climb	Sea-level takeoff	Cruise (b)
Combustor inlet temperature (°K)	473	621	777	810	754
Combustor inlet pressure (atm)	4.4	11.7	27.0	31.2	13.8
Air flow rate (kg/sec)	14.0	31.6	62.4	70.2	31.7
Combustor exit temperature (°K)	815	1118	1522	1611	1533
Combustor exit pressure (atm)	4.1	11.0	25.5	29.5	13.1
Fuel flow rate (kg/sec)	0.13	0.43	1.38	1.68	0.74
Overall fuel-air ratio	0.009	0.0137	0.0221	0.0240	0.023

(a) Std day – uninstalled

(b) Alt = 10.7km, Mn=0.8

J20273-8
782011

FIGURE 4

DESIGN PHILOSOPHY

- Combustor designs shall be axial flow, full annular and constrained to current E^3 configuration and design conditions

- Burn lean ($\phi \cong .5 - .6$) at reduced residence times to achieve NO_x goals

- Burn richer($\phi \cong 1.0$) at idle and intermediate power levels to achieve THC, CO, and η_c goals

- Control combustion process over the entire engine operations envelope to meet required stability and transient capability

- Establish mechanical integrity

FIGURE 5

J20273-9
782011

DESIGN APPROACH

- Variable geometry and/or aerodynamic methods (diffuser bleeds, trips) to accommodate required air modulation
  - Simultaneous control of primary and dilution zone areas required to maintain pressure loss
- Fuel staging in conjunction with air modulation
- Fuel-air preparation
- Auto-ignition and flashback considerations
- Cooling and dilution air requirements

FIGURE 6

J20273-10
782011

COOLING AND DILUTION AIRFLOW REQUIREMENTS

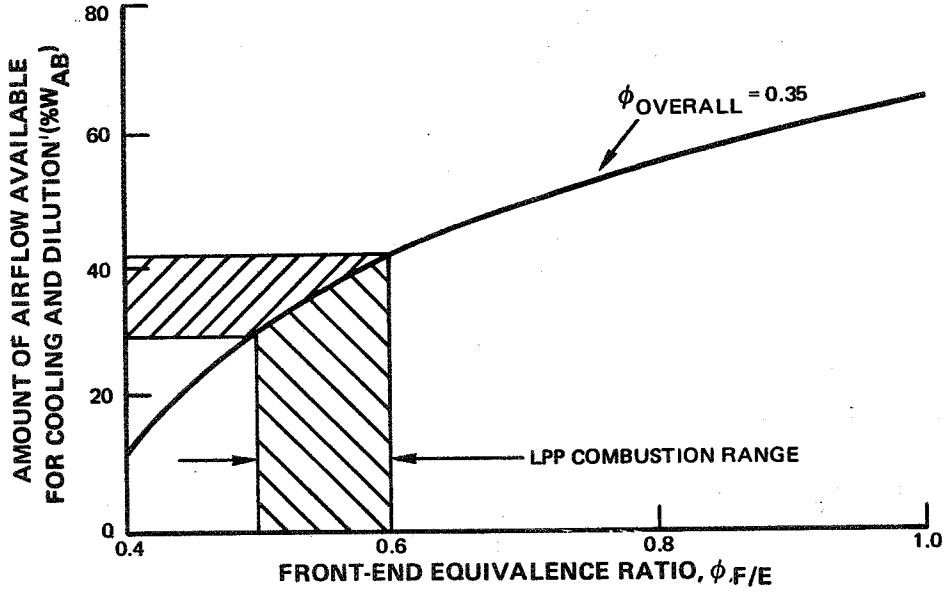

Cooling and dilution airflow requirements of lean combustion

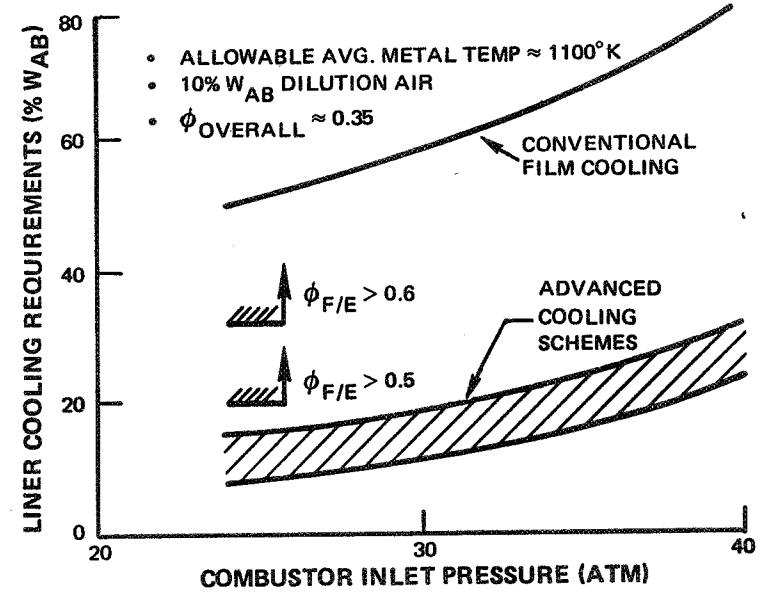

Comparison of conventional and advanced liner cooling requirements

FIGURE 7

J20273-11
782111

LPP VARIABLE GEOMETRY COMBUSTOR CONCEPT
TRANSLATING PREMIXING PASSAGE

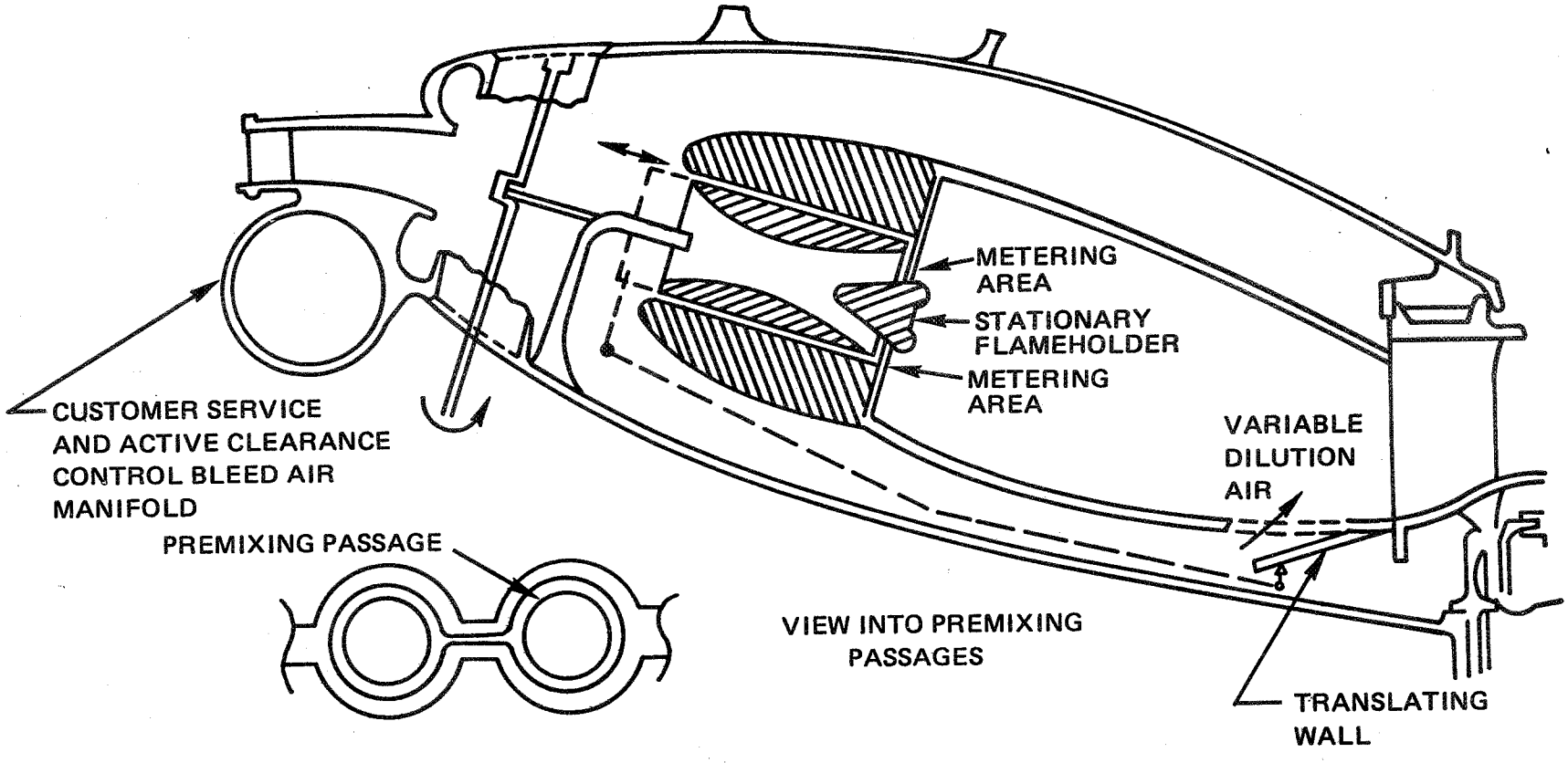

FIGURE 8

J20273-12
782111

LPP VARIABLE GEOMETRY COMBUSTOR CONCEPT
SWIRL PREMIX TUBES

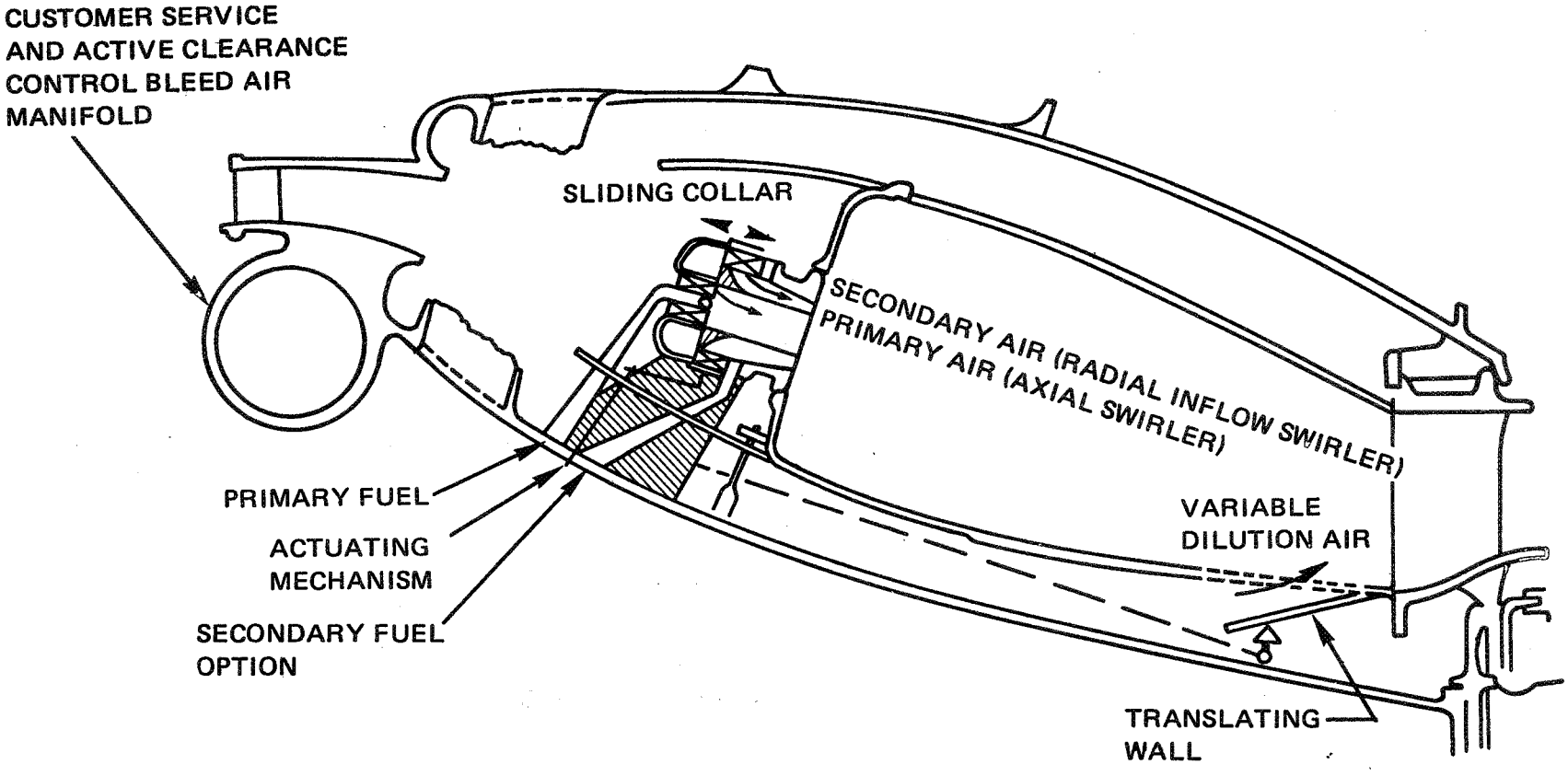

FIGURE 9

J20273-15
782111

LPP VARIABLE GEOMETRY COMBUSTOR CONCEPT
DUAL STAGE PREMIXED/PREVAPORIZED

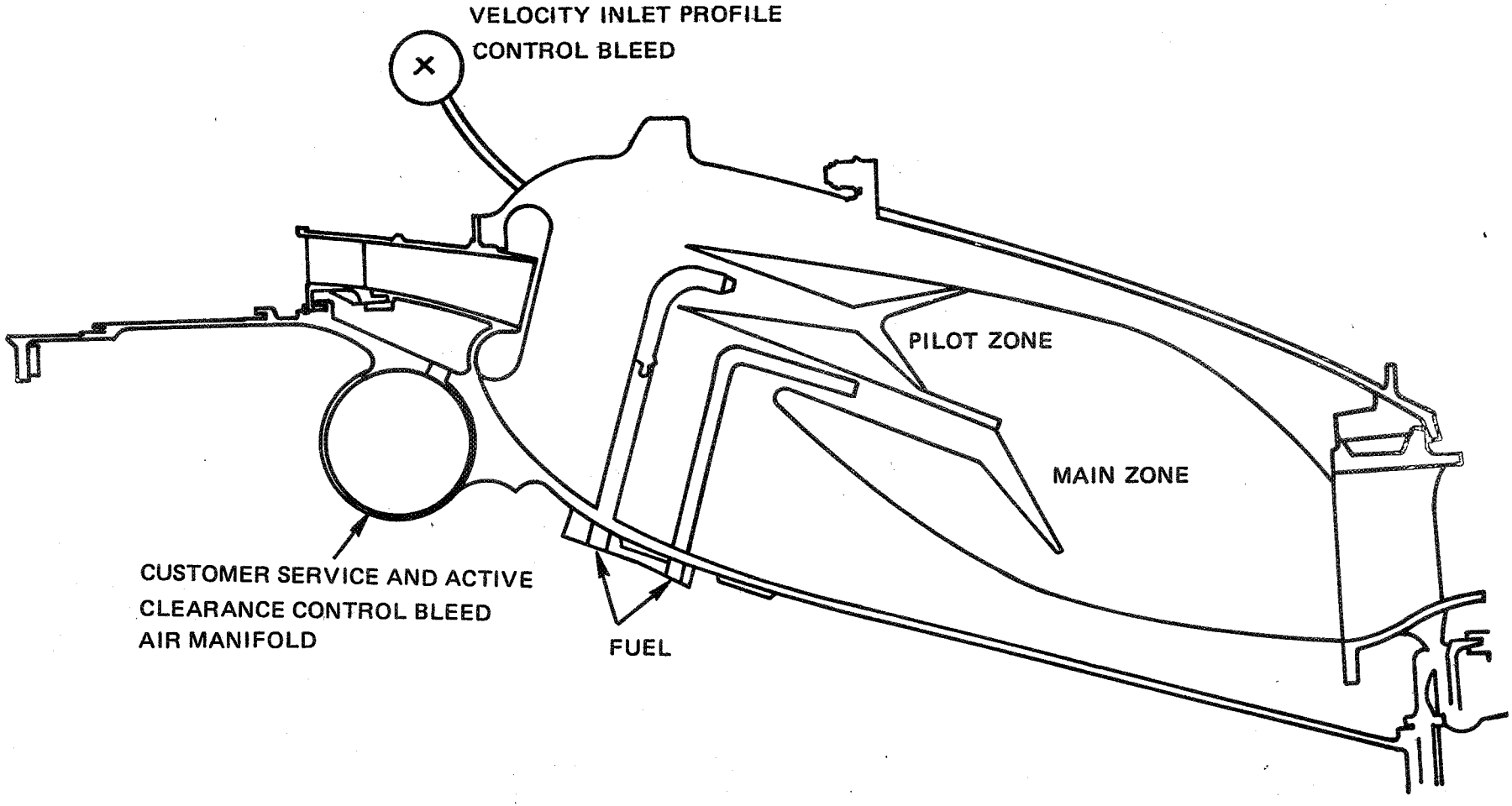

FIGURE 10

J20273-14
782111

LPP VARIABLE GEOMETRY COMBUSTOR/DILUTION AIR VALVE CONTROL

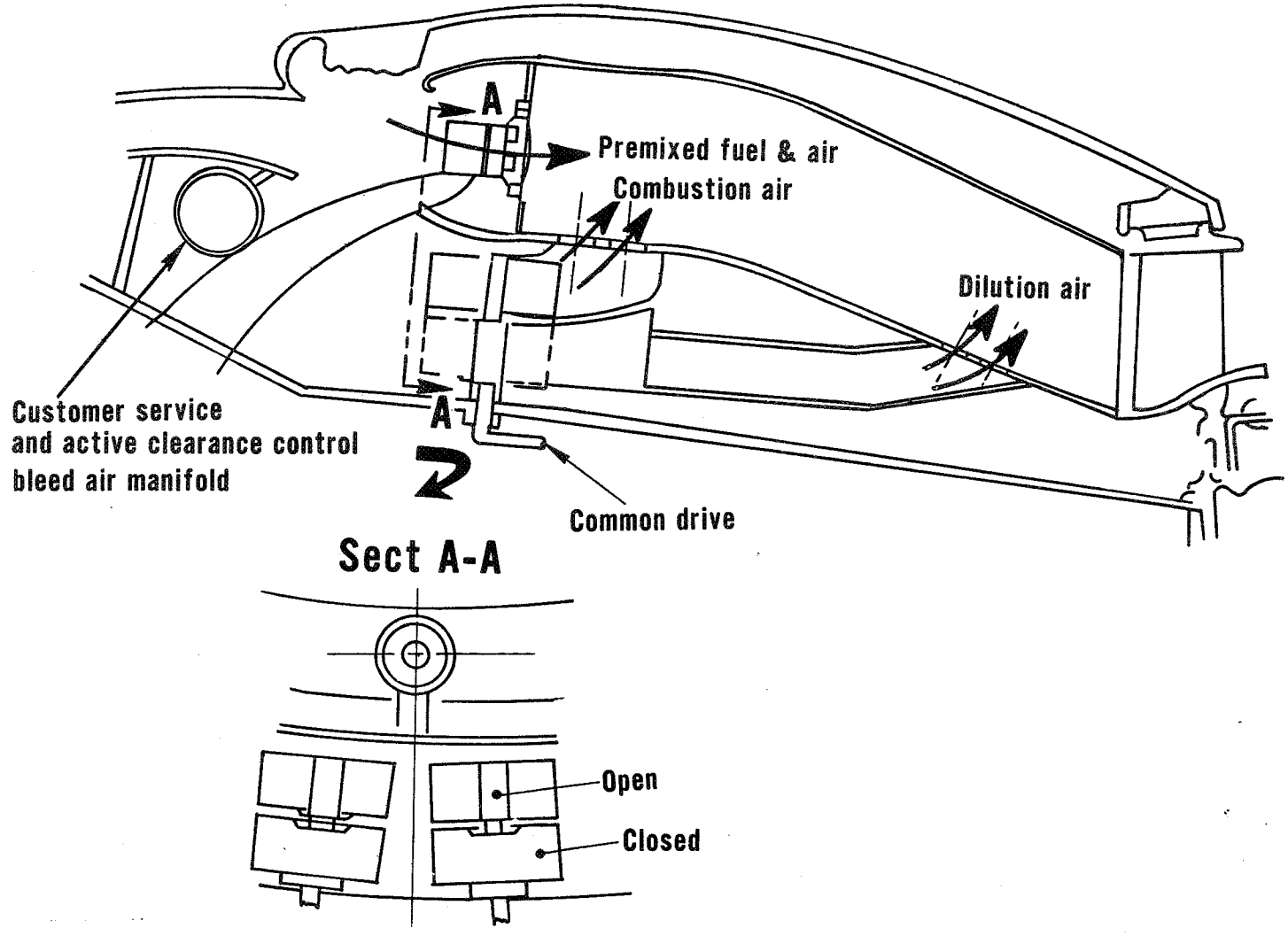

FIGURE 11

J20273-18
782711

DIFFICULTIES ENCOUNTERED IN APPLYING TECHNOLOGY

- The need to simultaneously control primary and dilution airflow
- Ability to adequately premix in residence time available limited by auto-ignition
- Flashback concerns
- Cooling requirements of combustor liners
- Flameholder durability
- Complex control system

FIGURE 12

J20273-17
782111

TECHNICAL ASSESSMENT

FIGURE 13

LEAN PREMIXED-PREVAPORIZED COMBUSTOR DESIGN STUDY

E. E. EKSTEDT - GENERAL ELECTRIC COMPANY

Phase I of the Lean Premixed-Prevaporized Combustor Design Study is a nine month analytical study effort with no experimental or testing activities included. The objective of this Program is to design and analyze advanced combustor concepts with features for fuel premixing and prevaporization upstream of the combustion zone for use in future subsonic aircraft engines. All of the designs also embody some form of variable geometry for combustor flow modulation. The primary criterion for these designs is low oxides of nitrogen (NO_x) emissions at stratospheric cruise conditions. The specific goal for these designs is an emissions index for NO_x of less than or equal to three grams per kilogram at the cruise condition. Additional criteria include meeting the ground level EPA emissions standards and all combustor performance requirements typical of advanced turbofan engines plus practicality of implementation.

In this study, four combustor concepts are being designed for the NASA/GE Energy Efficient Engine (E^3) envelope and cycle. The E^3 has a cycle pressure ratio of approximately thirty to one and a combustor exit temperature in excess of 1600K at sea level takeoff conditions. Table I shows combustor parameters at various operating conditions for the E^3. The combustor designs evolved are to be applicable to other high pressure ratio subsonic aircraft engines and one of the designs will also be designed and sized for the CF6 engine cycle and envelope.

Current status of the program is that the four concepts sized for the E^3 have been designed and are currently undergoing analysis and evaluation.

The four concepts are illustrated in Figures 2 thru 5. Table II presents design parameters. Concept 1 (Figure 2) features premixing-prevaporizing tubes with variable area primary swirlers. At cruise conditions approximately 53% of the combustor air flow is admitted through the swirlers so that the primary zone fuel air ratios are lean for low emissions of oxides of nitrogen. The equivalence ratio is approximately 0.55 at the exit of the secondary swirler. The combustor pressure drop at high power conditions is five percent. In order to obtain good low power combustion performance including low idle emissions, the primary swirler flow areas are reduced to admit approximately fifteen percent of the air flow. The equivalence ratio at the swirler exit was set at a little over 1.0 for idle. After addition of primary zone dilution and cooling air, the equivalence ratio is approximately 0.6 for good CO consumption. At idle conditions the combustor pressure drop is approximately 10 percent (versus 5 at hi power)because of the reduced dome flow. It has been shown in other experimental programs that idle emissions can be improved considerably by minimizing build up of film cooling air in the primary zone. Therefore, impingement cooling of the entire primary zone including the dome has been used to minimize the quantity of cooling required. Also the dome cooling air has been admitted in a manner to promote mixing with the primary zone gases as shown in Figure 6.

Two potential problem areas with this concept are high pressure drop at low power conditions and the possibility of flash back or auto-ignition in the premix tubes. Cycle studies have indicated that at steady state conditions (i.e. idle) there is adequate compressor stall margin for the selected pressure drop. During transient conditions (i.e. acceleration from idle) where stall margin is diminished by increased combustor temperature rise, it is anticipated that the primary swirler flows would be increased to counterbalance this effect. The premix duct residence times are set to avoid autoignition time and discontinuities are avoided to the max extent possible. At high power conditions the residence time in the duct is 1.4ms. This is believed to provide approximately a two to one safety margin for auto-ignition assuming reasonably uniform flow and no discontinuities.

Some features of this design are (1) only one stage of fuel injectors is employed, and (2) primary swirlers are continuously modulating for setting optimum local operating conditions at all times including transient operation.

Concept 2 shown in Figure 3 features a multiple annular duct main stage with variable inlet vanes and conventional swirlers in the pilot stage. At cruise conditions, the duct inlet vanes are full open for lean, low NO_x operation. The main stage has low pressure drop injectors for introduction of fuel into the annular passages. Each of the injectors spray fuel into both the upper and lower passages and from both sides of the injector. Uniform fuel distribution at the entrance to the dome is the main objective. The flow from the main stage enters the dome region through ports located between the pilot stage swirlers The main stage air stream is injected into the dome at an angle to the axial centerline and in a direction opposite to that of the pilot swirlers for good mixing. The dome is illustrated in Figure 7. At low power conditions, the primary zone air flow is reduced by closing the inlet vanes and all of the fuel is introduced through conventional pressure atomizing nozzles and fixed area swirlers.

Of prime importance in the design of this concept is achieving uniform fuel distribution in the main stage. A feature of this design is that the main stage may be operated at ultra lean fuel air ratios, because of the excellent piloting of the primary stage with the arrangement selected.

At idle, the inlet vanes will be closed so that the pressure drop will be 10 percent. During transients, the vanes may be modulated for reduced pressure drop, however, main stage fuel is not admitted until the vanes are opened. The high power pressure drop is five percent.

Concept 3 (Figure 4) is a series staged system with a fluidic flow control diffuser. This fluidic diffuser achieves variable flow split without the need for moveable geometry in the combustion cavity. At cruise conditions, a large portion of the flow is directed into the main stage for lean, low NO_x operation. The main stage is fueled with low pressure drop injectors and has a series of "V" shaped flame holders which permit flow of pilot zone gases to intermingle and mix with the main stage flow. Continuous ignition of the main stage is thereby

provided by the pilot stage. The pilot has conventional pressure atomizing injectors and fixed area counterrotating swirlers. This concept has the advantage that the pressure loss coefficient is comparable at all operating conditions. Fuel would not be admitted to the main stage until the flow is completely switched to the mode with high mainstage flow.

Concept 4 shown in Figure 5 is a parallel staged system with variable geometry and premixing. This system draws heavily from experience gained in the NASA/GE Experimental Clean Combustor Program, but has the advantage of variable geometry to meet the emission requirements over the required operating range. The main stage employs variable inlet vanes, sixty low pressure main stage injectors and a perforated plate main stage flame holder. Because the main stage operates only at high power conditions the perforated plate type flame holder has adequate stability. Further the low power stability of the main stage is extended by the piloting action of the pilot stage.

The pilot stage configuration and operation is similar to that of concepts 2 and 3. This configuration has the potential for the use of catalysts in the main stage flame holder.

These four designs have been established and are currently undergoing detailed analysis and performance prediction including both steady state and transient operation. The four designs will then be compared in detail for the purpose of ranking the designs and selecting the configuration that has the greatest potential for actual application. The selected design will also be designed for the CF6 cycle and envelope to demonstrate translation of the design concept to another engine.

Table I Reference Engine Cycle Parameters

Combustor Pressure Drop = 5%

Cycle Point	4% Idle	6% Idle	30% Approach	85% Climb	100% Takeoff	Hot Day Takeoff	Very Hot Day Takeoff	Max. Cruise	Normal Cruise	Min. Cruise
Ambient Conditions	Std Day	Std Day	Std Day	Std Day	Std Day	+27° F	+63° F	+18° F	+18° F	+18° F
h_o, Flight Altitude, k ft	0	0	0	0	0	0	0	35.0	35.0	35.0
M_o, Flight Mach No.	0	0	0	0	0	0	0	0.80	0.80	0.80
F_N, Installed Net Thrust, lb	1460	2190	10,948	31,032	36,501	36,506	30,864	8423	6740	3369
W_3 Compressor Exit Airflow, pps	19.1	23.6	63.4	121.7	136.0	132.4	114.0	59.5	52.8	39.1
W_{36}, Combustor Airflow, pps	17.0	21.0	56.4	108.3	121.1	117.9	101.5	53.0	47.0	34.8
P_{T3}, Compressor Exit Total Pressure, psia	46.5	58.2	171.5	380.9	438.0	436.1	375.5	189.4	162.6	112.2
T_{T3}, Compressor Exit Total Temperature, ° F	346	413	679	947	1005	1072	1096	948	881	759
T_{T4}, Combustor Exit Total Temperature, ° F	1154	1233	1584	2292	2452	2588	2585	2411	2219	1861
W_f, Fuel Flow, pph	711	902	2814	8689	10,634	11,006	9327	4672	3714	2177
f_{36}, Combustor Fuel-Air Ratio	0.0116	0.0119	0.0139	0.0223	0.0243	0.0259	0.0255	0.0245	0.0220	0.0174
M_3, Compressor Exit Mach No.(1)	0.273	0.281	0.296	0.286	0.283	0.282	0.285	0.281	0.282	0.289

(1) Assumes $A_{e3} = 48.7$ in.^{2}

TABLE II

COMBUSTOR DESIGN PARAMETERS

	CONCEPT 1	CONCEPT 2	CONCEPT 3	CONCEPT 4
COMBUSTOR OVERALL LENGTH, INCHES	14.5	14.5	14.5	14.5
COMBUSTION LENGTH	6.5	7.3	8.8	9.0
DOME HEIGHT	2.8	3.2	3.0	2.6
LENGTH/DOME HEIGHT	2.3	2.3	2.9	3.5
NUMBER OF INJECTORS(MAIN/PILOT)	28	60/30	60/30	60/30
NUMBER OF FUEL STAGES	1	2	2	2
VARIABLE GEOMETRY TYPE	CONTINUOUSLY VARIABLE VANES	VANES (OPEN/CLOSED)	FLUIDIC	VANES (OPEN/CLOSED)
PRESSURE LOSS, % (CRUISE/IDLE)	5/10	5/10	5/5	5/9
REFERENCE VELOCITY, FT/SEC.	78	69	60	67
DOME FLOW/COMBUSTOR FLOW, CRUISE	0.63	0.67	0.18	0.16
DOME FLOW/COMBUSTOR FLOW, IDLE	0.25	0.28	0.26	0.27
SPACE RATE, BTU/HR.-FT^3. ATM. (HI POWER)	9.0×10^6	7.0	6.1	5.7
PREMIX SWELL TIME - MS	1.4	1.2	2.0	1.9

LEAN PREMIXED-PREVAPORIZED (LPP) COMBUSTOR CONCEPTUAL DESIGN STUDY

OBJECTIVE:

- o DESIGN AND ANALYZE LEAN PREMIXED-PREVAPORIZED COMBUSTORS FOR ADVANCED SUBSONIC AIRCRAFT ENGINES.
- o DESIGNS INCLUDE VARIABLE GEOMETRY FOR FLOW CONTROL.
- o A PRIMARY GOAL IS LOW OXIDES OF NITROGEN AT SUBSONIC CRUISE ($\leq$3G/KG)

PHASE I

ELEMENT
- 1.0 COMBUSTOR DESIGN
- 2.0 DESIGN ANALYSIS
- 3.0 DESIGN RANKING
- 4.0 REPORTS & RECORDS

TIMING

9 MONTHS (EXCLUSIVE OF REPORTS)

COMPLETE 4/79

FIGURE I

CONCEPT 1-SWIRL TUBE LPP COMBUSTOR WITH VARIABLE SWIRL VANES

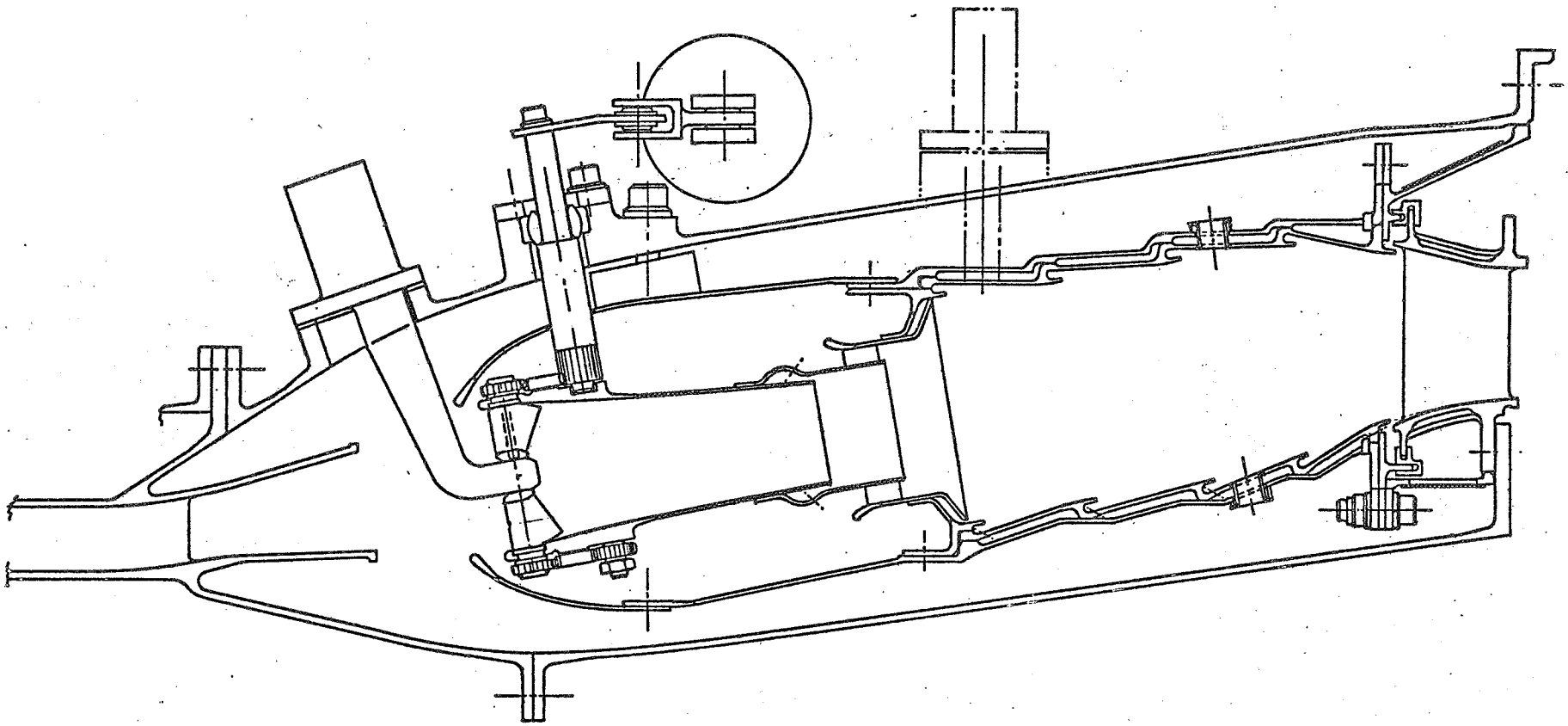

FIGURE 2

CONCEPT 2-MULTIPLE DUCT LPP COMBUSTOR WITH VARIABLE VANE ANNULAR PREMIXER

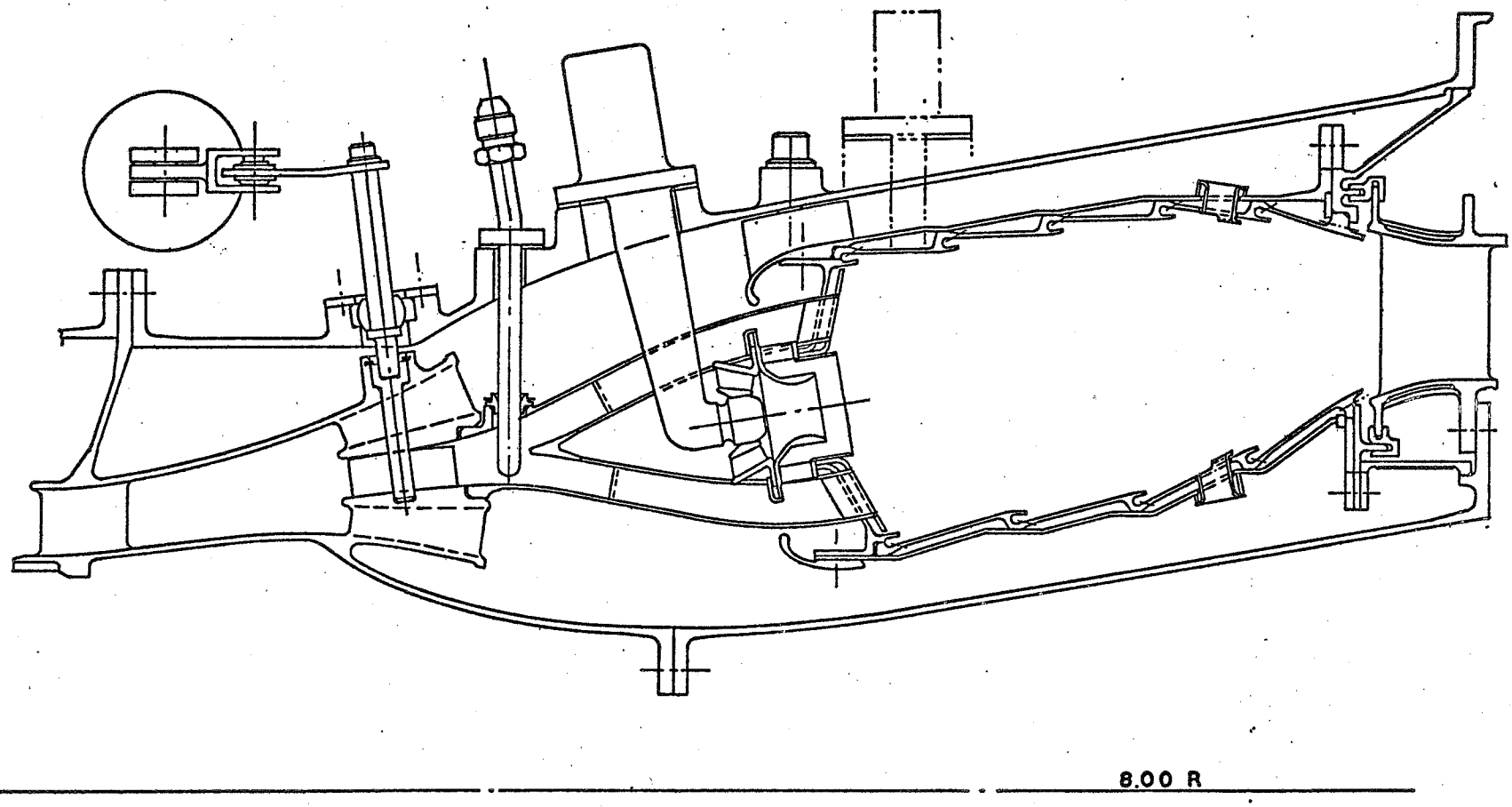

FIGURE 3

CONCEPT 3 - SERIES STAGED LPP COMBUSTOR WITH FLUIDIC FLOW CONTROL

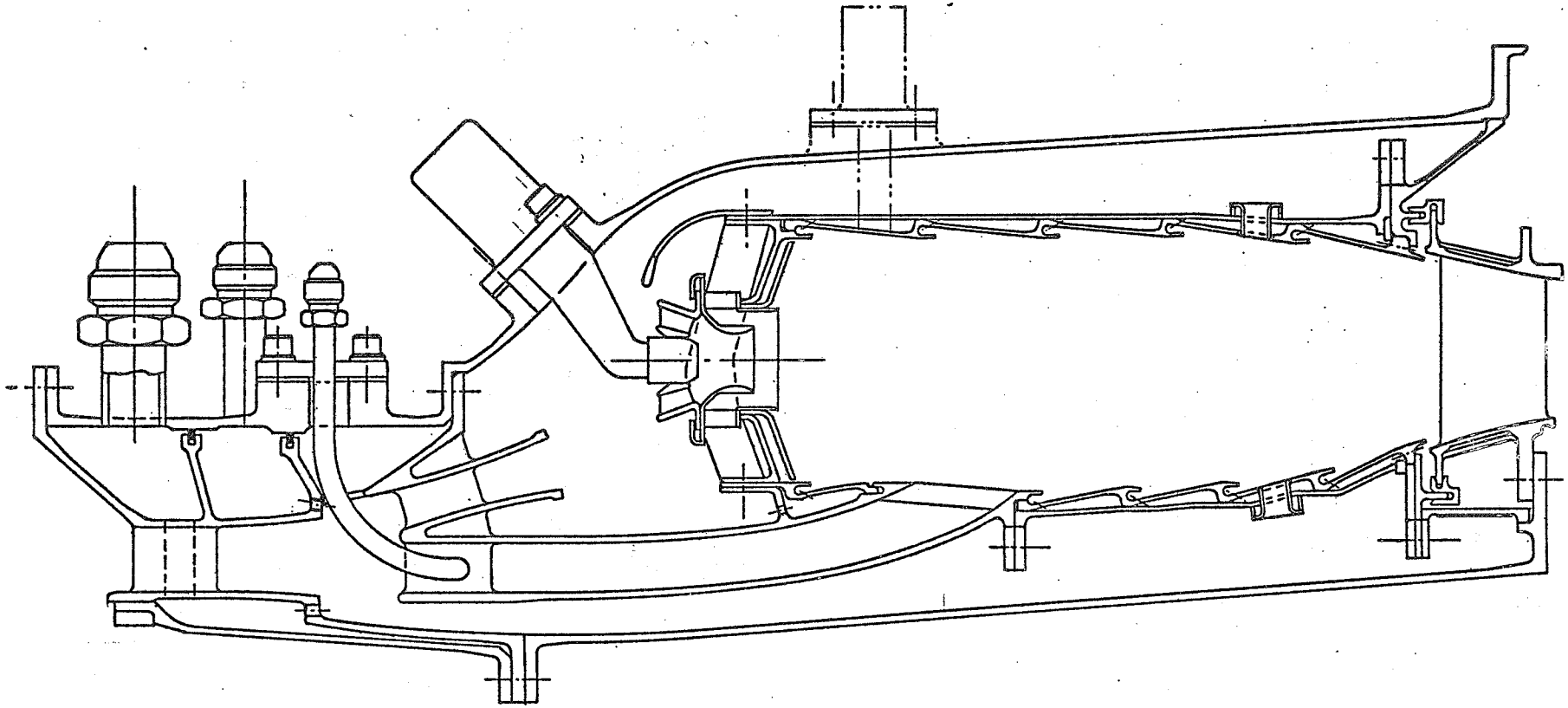

FIGURE 4

CONCEPT 4 - PARALLEL STAGED LPP COMBUSTOR WITH VARIABLE ANNULAR REMIXING DUCT

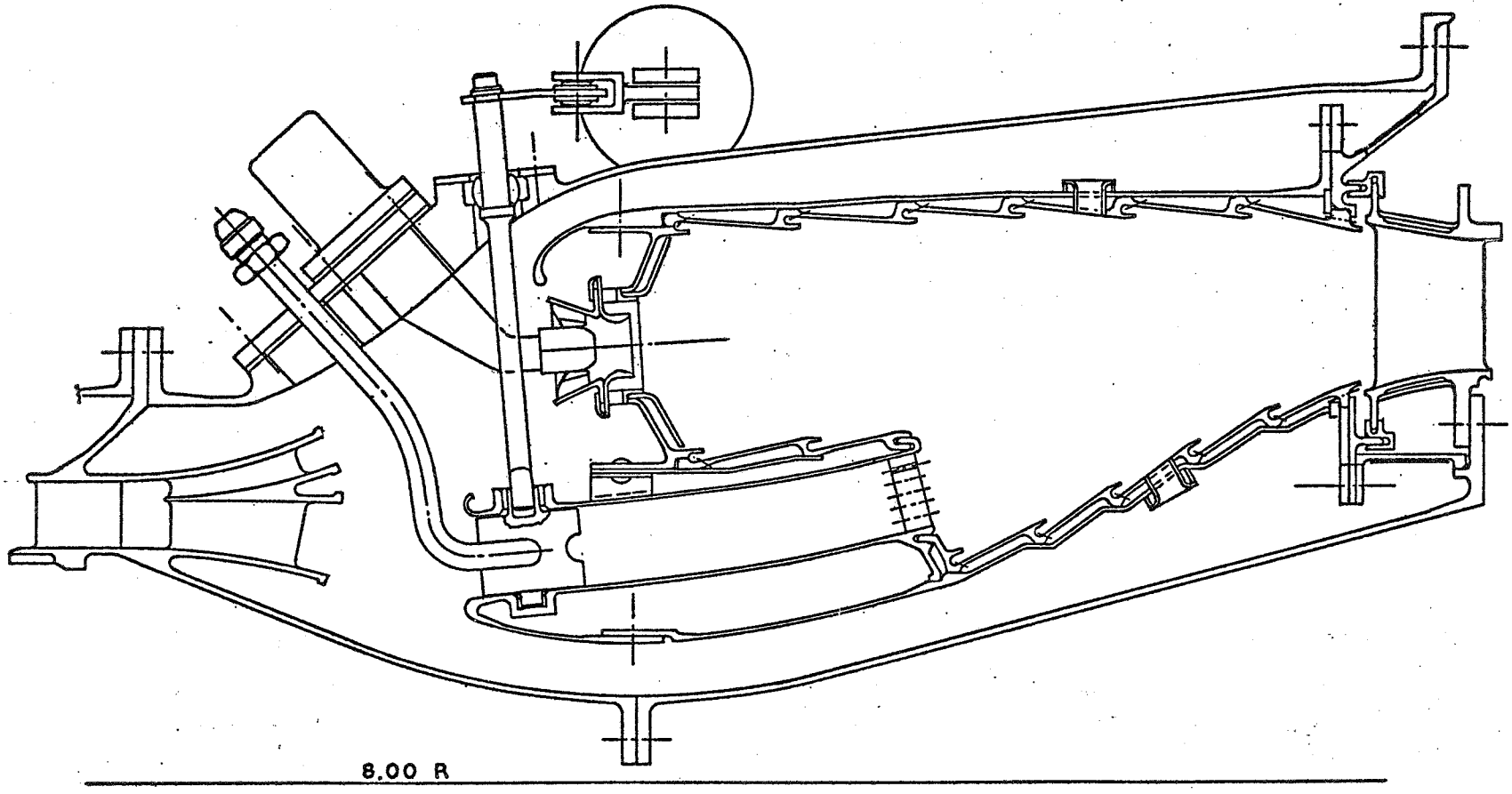

FIGURE 5

COMBUSTOR DOME ARRANGEMENT FOR IMPROVED MIXING OF DOME COOLING AIR IN PRIMARY ZONE

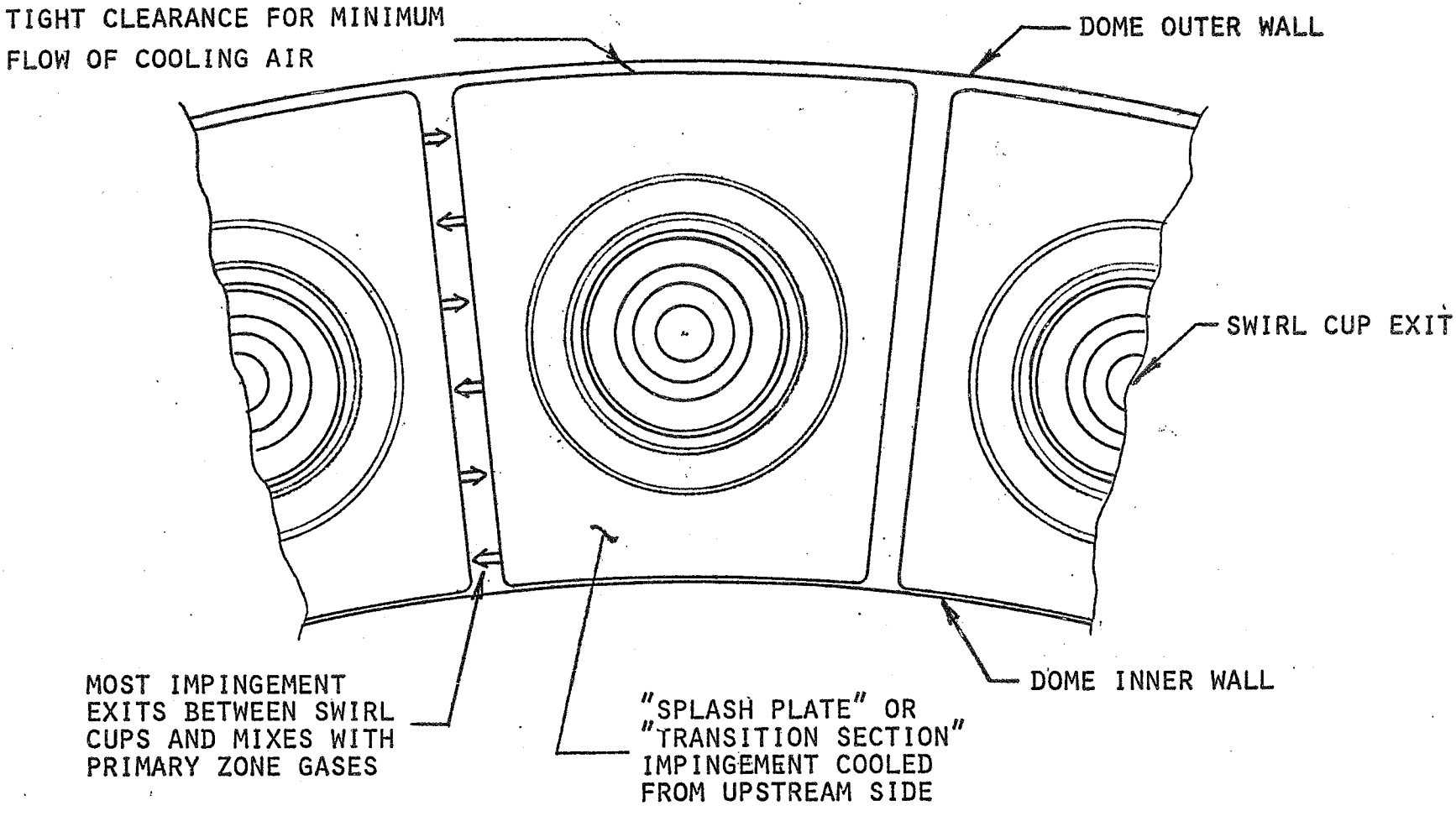

FIGURE 6

CONCEPT DOME ARRANGEMENT AND AIR FLOW PATTERNS

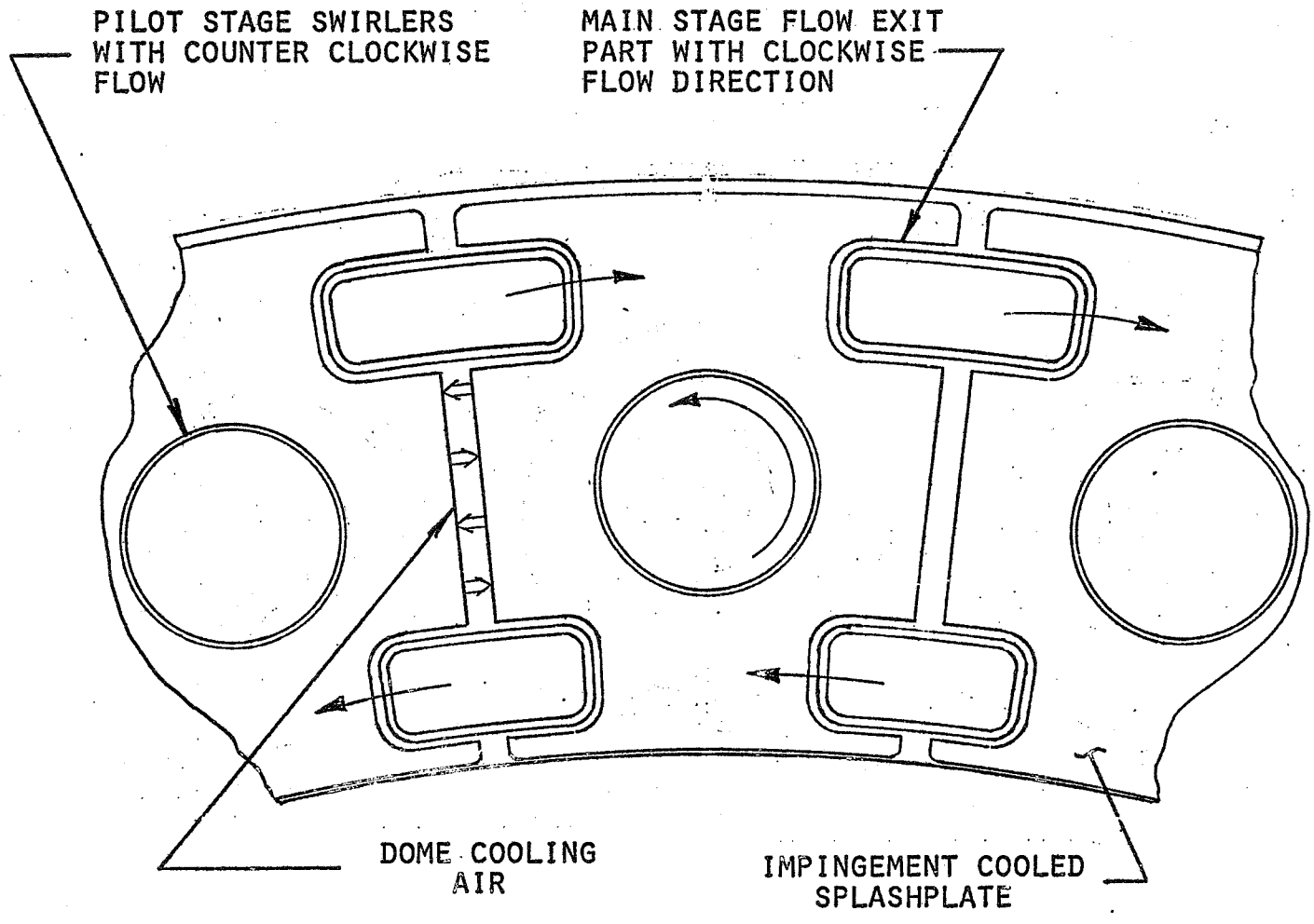

FIGURE 7